5-2010

MOBILITY OF PLUTONIUM IN ZEA MAYS (CORN): DETERMINATION OF TRANSPORT VELOCITIES, SPATIAL DISTRIBUTION AND CORRELATIONS WITH IRON.

Shannon Thompson
Clemson University, stfootprints@yahoo.com

MOBILITY OF PLUTONIUM IN ZEA MAYS (CORN): DETERMINATION OF TRANSPORT VELOCITIES, SPATIAL DISTRIBUTION AND CORRELATIONS WITH IRON.

A Dissertation
Presented to
the Graduate School of
Clemson University

In Partial Fulfillment
of the Requirements for the Degree
Doctor of Philosophy
Environmental Engineering and Science

By
Shannon W. Thompson
May 2010

Accepted by:
Dr. Robert A. Fjeld, Committee Chair
Dr. Timothy A. Devol
Dr. Daniel I. Kaplan
Dr. Haibo Liu
Dr. Fred J. Molz

ABSTRACT

Understanding the environmental behavior of plutonium (Pu) is essential for proper radioactive waste disposal or for remedial activities after an accidental release of Pu. The environmental behavior of Pu is influenced by physical, chemical, and biotic factors, such as the simultaneous existence of multiple Pu species, redox transformations at mineral surfaces, colloid formation, and the potential of microbes and plants to affect its sorption to soil. Plant Pu studies have been conducted for quantifying bioaccumulation or phytoremediation. Until now, experimental studies have not focused on the capacity of plants to affect the transport behavior and distribution of Pu in the subsurface.

This dissertation addressed the hypothesis that root uptake and transport in plants can influence the mobility of Pu in the vadose zone. The overarching goal was to provide experimental support for reactive transport modeling of root uptake and xylem transport and for a connection between Pu uptake and the plant's nutritional requirement for Fe. The objectives were to: (1) quantify complexed Pu retardation in graminaceous plants and to quantify complexed Pu sorption to plant xylem, (2) characterize the distribution and accumulation of complexed Pu in plants, and (3) compare correlations between plant uptake of complexed Pu and Fe. In addition, a couple of simple models for predicting Pu transport by roots were examined.

Bench scale experiments were conducted using corn (*Zea mays*) as a representative of the grass family. Corn was grown in 1L soil pots above 500 mL nutrient solution containers with the primary root inserted in solution. Growth conditions were 14/10 h day/night cycles (32/20 ℃), 30-50% RH, and a photosynthetic flux of 1300-1500 μmol/m^2s. To commence exposure, an aliquot of Pu(DFOB) or Pu_2DPTA_3 or both Pu and ^{59}Fe complexed with DFOB was added to the nutrient solution. Plants were 23 – 28 d old when sacrificed. Plutonium and ^{59}Fe contents were determined by liquid scintillation analysis and stable element contents were determined by ICP-MS. Sorption tests were conducted with Pu as Pu(IV), Pu(DFOB), or $Pu_2(DTPA)_3$ and cellulose or xylem excised from cotton stem tissue.

The Pu plant transport velocities were 174 – 348 cm/h and water velocities were 300 - 800 cm/h. Thus the retardation factor of Pu in live plants was measured to be 1-5 and estimated to be 1-10 due to water velocity uncertainty. With respect to the second objective, analysis of the spatial distribution of Pu in corn indicated that discrimination occurs at the exodermis and in root tissues, most of the Pu in the plant was retained in the roots, and the fraction of Pu that entered the xylem was rapidly transported upward to the rest of the plant. An overall average of greater than 97% of the Pu was found in the roots with the remainder in the shoots. The maximum shoot activity fraction was four per cent for plants exposed for 10 d however steady state translocation was not attained. Profiles of Pu concentration versus shoot length showed that Pu concentrated in the upper shoots. With respect to the third objective, several findings are of interest. The plant uptake of Pu remained unchanged for Fe: Pu ratios ranging from 0 - 2.2 x 10^5. Large changes in Fe concentrations did not inhibit or enhance plant uptake of Pu. Comparisons of the distribution profiles of Pu, ^{59}Fe, stable Fe, and several other nutrient elements showed that Pu was distributed very much like ^{59}Fe in the shoot. However six times as much Pu was found in the root than ^{59}Fe, and 40% more ^{59}Fe was found in the shoot than Pu. The shoot distribution data strongly suggest that upon entering the xylem, Pu and Fe are physiologically treated in a highly similar manner. Clearly, Pu is simultaneously taken up with Fe.

Using an instantaneous partitioning model, comparisons were remarkably consistent between the soil concentration data of the SRS lysimeters and predictions using concentration ratios derived from field studies involving different plants, soils, and experimental conditions. The steady-state advection model predicted K_d values for Pu and plant root zone soil that are much lower than batch sorption determinations. This is consistent with enhanced mobility of sorbed Pu by siderophores or other plant exudates.

ACKNOWLEDGMENTS

My parents, Ernest and Virginia Thompson, have made it possible for me to pursue my goals through their love, support, and dedication. I am grateful. My first date with my wife, Beth Farrar Thompson, happened on the day before I came to tour Clemson in 2005. Beth and I are delighted to have found each other and I truly appreciate her love, abundant energy, and support. Our teamwork, communications, and spirit of sharing have improved my life and buoyed my work.

I entered Clemson after several years working as a scientist and consultant. Before selecting a graduate program, I discussed my intentions with friends and colleagues. Dr. Chong Kim, Dean of the Business School at Marshall University, encouraged me to return to graduate school. I contacted Dr. Daniel Kaplan, who suggested that I investigate Clemson's Environmental Engineering and Science Program. On my acceptance and enrollment into the department, Dr. Kaplan became one of my committee members. I have benefited from his experience, especially as related to field work and environmental chemistry.

Multidisciplinary research benefits from the ideas and input of different people and this work is no exception. My advisor, Dr. Robert Fjeld provided guidance and funding for much of my time at Clemson. For my dissertation research however, Dr. Fred Molz has provided strong input in terms of both my funding and research direction. I have benefited greatly from having both Dr. Fjeld and Dr. Molz to stimulate questions, discuss and shape our research, and shed light on many aspects of this endeavor. I especially thank Dr. Molz for his time and energy in the laboratory, without which this research would have at best cast a much smaller shadow. Dr. Tim Devol has been important as my instructor and has provided energy, feedback, and motivation at critical stages of this work. Dr. Haibo Liu has been influential with respect to plant physiology, the experimental design, and the interpretation of results. Dr. Daniel Kaplan provided insightful suggestions and ideas to the research at many points along the way. The dissertation is a quest for knowledge and an assembly of both new and established information; this work is better defined and expressed with the guidance of my advisors and committee.

I appreciate Dr. Inci Demirkanli McLaughlin for sharing ideas, data, and information. I thank Dr. Brian Powell for his availability, insight, and for the use of the ICP-MS and his assistance in interpreting the ICP-MS data. Dr. Ian Stocks of the Entomology, Soils, and Plant Sciences Department assisted me in the use of their microscopy systems. Drs. Doug Bielenberg, Christina Wells, and Jeff Adelberg gave me initial ideas when my focus shifted from lysimeter projects to plant uptake of Pu.

This research was supported by the Office of Science (BER), U.S. Department of Energy, through Grant No. DE-FG02-07ER64401 and by Clemson University. Earlier research was funded by Radiochemistry Education Award Program (REAP) administered by the Medical University of South Carolina, Contract No. DE-FG07-05ID14692 / IDNE006.

TABLE OF CONTENTS

Table of Contents (Continued)

Page

LIST OF TABLES

List of Tables (Continued)

List of Tables (Continued)

Table Page

LIST OF FIGURES

List of Figures (Continued)

List of Figures (Continued)

List of Figures (Continued)

CHAPTER ONE

INTRODUCTION

Plutonium (Pu) is present in the environment as a result of global fallout from weapons testing and releases from nuclear power plants, nuclear materials production reactors, and research and development facilities. Trace concentrations of Pu from fallout are ubiquitous across the surface of the Earth. Higher concentrations may occur in the vicinity of nuclear facilities and radioactive waste disposal sites. Because of its toxicity, complex chemistry, and the long half-lives of several Pu isotopes, there is an interest in the long term behavior of Pu in the environment. In the context of waste disposal, there is a particular interest in identifying processes affecting Pu transport in the vadose zone and incorporating them quantitatively in reactive transport models.

The availability of data from four meso-scale field lysimeters at the Savannah River Site (SRS) has allowed significant progress to be made in quantifying Pu transport in the vadose zone in the last six years (Kaplan et al. 2006; Demirkanli et al. 2008). The data are depth-discrete normalized Pu soil concentrations above and below sources buried at 26 cm depth in each lysimeter. Three of the four lysimeters were exposed to Pu(III) or Pu(IV) for 11 years; a Pu(VI) lysimeter study was terminated after two years in the field. The observed concentration profiles below the source are consistent with predictions from a mathematical model formed from a conceptual model having two Pu species - a mobile oxidized form Pu_o [Pu(V) and Pu(VI)] and a much less mobile reduced form Pu_r

[Pu(III) and Pu(IV)] – and first-order kinetic transformations between the two (Fjeld et al. 2003). Experiments conducted to complement the field data and modeling efforts support the redox-driven conceptual/mathematical transport model. When upward transport through plants is included in the model, it yields predictions that are consistent with the concentration profiles above the sources as well (Demirkanli et al. 2009).

In field and laboratory settings, numerous researchers have shown that plant uptake can affect the environmental fate and transport of radionuclides. Elements studied in field settings include Se (Ashworth and Shaw 2006a); Cs and Sr (Sanford et al. 1998); Co, Cs, and Ra (Gerzabek et al. 1998); Cs, Sr, Pu and Am (Nisbet and Shaw 1994); Cl and I (Ashworth and Shaw 2006b); and Pu and Am (Sokolik et al. 2004). Wadey et al. (2001) noted that upward migration of Cs and Co was likely due to root uptake and translocation. Similarly, Sanford et al. (1998) attributed upward migration of Cs to plant transport. In the laboratory, Garland et al. (1981) studied Pu in soybeans and observed characteristics of xylem transport. Cataldo et al. (1988) suggested that Pu exists in plant xylem as soluble organic complexes. Although the mechanisms underlying the transport of Pu in plants have yet to be fully defined, it is known that Pu is more mobile in plants than in soil (Cataldo et al. 1988). Long-term reconnaissance studies of Pu in soils contaminated by the Chernobyl nuclear plant accident showed that native grasses affect the distribution of Pu in soil through concentration in plant tissues. Ultimately, this affects Pu mobility in near surface soils (Sokolik et al. 2001; Sokolik et al. 2004)

Isotopic ratios of SRS lysimeter surface sediments indicated that Pu uptake and translocation occurred through plants that grew on the lysimeters (Kaplan et al. (In press)). The weapons grade Pu sources emplaced in the lysimeters at the beginning of the study match the isotopic ratios found at the lysimeter surfaces. Those ratios distinctly differ from local and regional fallout Pu ratios. Transport modeling predicted that a Pu residue may be found at the lysimeter surfaces by moving upward through plants (Demirkanli et al. 2008).

The lysimeter soil data and isotope ratio analyses indicate that upward transport of Pu occurred at SRS. This upward migration appears to be due to Pu transport in plants. Predictions from a model require a plant uptake mechanism for upward transport to be consistent with the SRS field data. The model uses the retardation of Pu in plants and Pu-plant K_d values as fitting constants. Data for these parameters do not exist.

Plants have no known biological need for Pu, a manmade substance. Several studies suggest that Pu uptake in plants occurs based on the plant's requirement for Fe and the highly similar charge to size ratios of Fe(III) and Pu(IV) (Neu 2000, John et al. 2001, Ruggiero et al. 2004). Evidence for this also does not exist. The objectives of this research were to experimentally determine the retardation of Pu in plants and the Pu-plant K_d in order to build a quantitative knowledge base in support of transport modeling, and to examine plant uptake correlations between Fe and Pu.

CHAPTER TWO

BACKGROUND

2.1. The History and Characteristics of Plutonium

The element Pu is inexorably linked to uranium. Uranium was first found in mountainous regions of Germany in the mineral pitchblende. In 1872, the Russian chemist Dmitri Mendeleev published his second version of what would become the periodic table. He placed uranium as the heaviest element with an atomic mass of 240. Uranium remained the heaviest known element until World War II, although there were earlier predictions of “missing elements” (Bernstein 2007). The modern periodic table incorporates quantum theory and is thus arranged by atomic number. It includes two rows of heavy elements: the lanthanides and the actinides.

Following the discovery of the energy released from uranium undergoing nuclear fission, nations became interested in the military potential of such energy sources. In 1941 at the Lawrence Berkeley Laboratory, Glenn Seaborg and Arthur Wahl conducted experiments using neutrons generated by a cyclotron. They produced ^{239}Pu via neutron bombardment of ^{238}U with an intermediate ^{239}Np decay step, although their discovery remained unpublished until after the war. They also generated ^{238}Pu via deuteron collision with ^{238}U. They found that ^{239}Pu is a more fissile (neutron producing) energy source than ^{235}U. With this knowledge, the U.S. made Pu production an important objective (Bernstein 2007).

The development of Pu production facilities and separation processes was accomplished at great expense with a great deal of development. Although multiple schemes were tested for producing Pu, ultimately all methods to synthesize, isolate, and purify Pu were expensive, energy-intensive, and generated large quantities of hazardous wastes. This is because of the complex chemistry of Pu (discussed below) and the difficulty of separating Pu from U.

The first reactor to produce Pu was Hanford's 'B' reactor (Rhodes 1986). It was constructed in less than a year during the Manhattan project and operated from 1944 until 1968. The first nuclear bomb test at Alamogordo, New Mexico used Pu produced at Hanford. The first nuclear weapon deployed at Hiroshima, Japan used ^{235}U, and the second weapon deployed at Nagasaki, Japan contained ^{239}Pu.

Plutonium is a very dense metal with an atomic number of 94. It is nearly twice as dense as lead. It is an element in the actinide series, filling the 5f electron sub-shell (Huheey 1978). There are 15 isotopes of Pu (Walker et al. 1989). Of these, seven isotopes (mass numbers 236, 238, 239, 240, 241, 242, and 244) are well known to nuclear physicists and radiochemists.

Plutonium has several unique properties. It rarely occurs in nature and has an extremely low crustal abundance on Earth. It is found in ultra-trace quantities in a few uranium mineral deposits. Evidence of Pu formation was found in higher than normal concentrations at a uranium deposit called a "natural nuclear reactor" in Oklo, Gabon (Choppin et al. 2001). Since the discovery of the Oklo site, other natural Pu deposits have been identified (Hoffman, et. al. 1971; Curtis, et. al. 1991). Plutonium has four oxidation states (III, IV, V, VI) which may be simultaneously present in aquatic systems (Choppin et al. 1997). This fact is an aspect of Pu chemistry that challenges understanding and prediction of its environmental behavior. Plutonium can exist in six different crystal structures under environmental conditions, more than any other element (Hore-Lacey 2008).

2.2. Plutonium in the Environment

2.2.1. Sources

In terms of total mass, natural sources of Pu are insignificant on the earth's surface. Synthetic Pu comes from two activities: the production of high purity Pu for weapons or other purposes and the operation of nuclear reactors. Estimates of the global totals of Pu produced for weapons vary. The total mass of weapons-grade Pu has been estimated to be 3.0×10^6 kg (Cochran 1997). US quantities of weapons-grade Pu have been estimated at 100 metric tonnes, the former Soviet Union at 125 – 200 tonnes, and the rest of the world at less than 20 tonnes. Nuclear power reactors operating via thermal fission of ^{235}U produce ^{239}Pu through neutron capture reactions with ^{238}U. Plutonium-239, like ^{235}U, is a fissile material and is used as fuel. During the life cycle of fuel in reactors, several Pu isotopes are created. With 440 nuclear reactors operating worldwide, by the year 2000 an estimated 1,000 tonnes of Pu were produced in power plants. This quantity exceeds the mass of Pu produced purposely for weapons by a factor of three (Hecker 2000).

The production of nuclear weapons in the U. S. created 3.8×10^5 m^3 of high-level waste (50% of which is transuranic waste), 3.3×10^6 m^3 of low-level waste, and other waste streams (DOE 1996). Research and production processes have created significant environmental contamination. In 1996, the U. S. Department of Energy (DOE) estimated contaminated solids to be 7.9×10^7 m^3 and contaminated groundwater to be 1.8×10^9 m^3. Most of the Pu contamination is located at a few DOE facilities, with the highest inventories at Hanford (Washington), Savannah River (South Carolina), Idaho National Laboratory, Los Alamos National Laboratory (New Mexico), and the Waste Isolation Pilot Plant (New Mexico). In the past ten years, remedial actions have removed Pu from the Rocky Flats site in Colorado and from Mound Laboratories in Miamisburg, OH. Significant quantities of Pu contamination are present at the Nevada Test Site in the U. S. and other locations worldwide such as Tomsk in Russia and remote weapons testing locations in Siberia and Kazakhstan.

During the Cold War, the former Soviet Union undertook great efforts to produce Pu. Their waste management practices lagged those of the U.S. In the U. S., waste management practices underwent a long and expensive infrastructure development, whereas in the former Soviet Union states, nuclear waste disposition largely consisted of pumping wastes underground. Consequently, several of these areas have challenging environmental legacy issues.

Additional Pu sources are found in unmanned power applications, such as radioisotopic thermo-electric generators. These energy power stations were particularly common in remote settings. Plutonium energy sources have been used for powering deep space missions such as Cassini-Huygens and Voyager, undersea applications, and navigational beacons.

2.2.2. Distribution

The distribution of Pu in the environment is largely linked to nuclear weapons and nuclear power. The use of Pu for weapons has resulted in its distribution via:

- research, production, and waste facilities
- weapons deployment and
- weapons testing.

The U.S. development of nuclear weapons includes some of the most technologically challenging efforts ever undertaken. An assembly of scientists was recruited into the Manhattan Project to produce nuclear weapons. The Cold War ensued after World War II; during the 1950's and 1960's, focus shifted from research and production of small Pu quantities at a few locations to large scale production of nuclear warheads involving many locations.

Weapons research and production occurred at many locations in the U.S. This was by design so that critical research, production, and assembly facilities could not easily be eliminated (stopping weapons component supply) through enemy military action. With time, the U.S. weapons complex footprint grew to facilities located in 29 states (DOE 1997).

Historically, weapon manufacturing focused on technological development and production increases. The disposition of process waste streams and construction of waste handling facilities were not priorities at the time. As a consequence, at smaller sites or supplier sites, funds were not available for adequate waste handling techniques. At larger weapons complex sites, operators realized the need for more elaborate waste systems than dumps, storage pads, pits, trenches, and burial grounds, although the latter were still being created for waste streams deemed less hazardous. Underground tanks were built and installed at the Hanford Site, Savannah River Site, Idaho National Laboratory, and other facilities to store high-level waste streams. In the late 1940's and the 1950's, 142 single shell (single wall) tanks were buried in place at the Hanford Site. Later, 28 double shell tanks designed to contain larger volumes of high-level waste in a more structurally sound manner were installed. Although the single shelled tanks were expected to last 10 - 20 years, most are still in service. Greater than 50% of the Hanford single shell tanks have either been proven to have leaked or listed as probably leaking, with an estimated 4×10^6 L of tank waste emitted from the tanks to the vadose zone.

High level waste at DOE sites is in a state of flux, with wastes generated years ago not being placed in a long term repository. Similarly, transuranic wastes generated by power plants do not have a well designed permanent repository. Consequently, wastes are stored onsite at virtually all U. S. operating power reactors. One factor contributing to the delay in selecting a long term repository has been the provision of strong evidence that a repository could store long lived wastes without escape of radioactive contaminants for a period of 10,000 years. Since no previous man-made facilities have been designed with such long time criteria, the evidence for repository stability will rely heavily on radionuclide (including Pu) transport modeling.

The only military deployment of a Pu bomb occurred at Nagasaki, Japan on August 9, 1945 and resulted in the death of 78,000 Japanese citizens (Mahara and Kudo 1995; DOE 1997; Kudo 2001). The bomb was detonated 500 m above ground. Mahara and Kudo (1995) estimate that 1.2 kg of Pu fissioned from ~15 kg in the bomb. Surprisingly, only 0.3% of this deposited as local fallout, with greater than 99% transported into the atmosphere. Due to wind speed and direction and the shape of surrounding countryside, the maximum Pu concentrations were found 2.8 km east of the blast hypocenter.

Nuclear weapons tests were conducted in the atmosphere, on the earth's surface, underground, and in the ocean. Testing has resulted in the dispersion of Pu globally from atmospheric and surface detonations and locally from subsurface detonations. Tests were conducted at remote locations subject to access controls. Figure 2.1 shows nations known to have conducted nuclear weapons tests (in color highlights) and the locations of specific surface tests (circles, color indicates nation testing). Global fallout is the deposition of radioisotopes following their atmospheric dispersion, mixing, and transport from above ground testing. The U.S. and Russia conducted most above ground tests beginning in the 1940's and ceasing upon signing the Limited Test Ban Treaty in 1963. France and China continued above ground tests until 1982. The residence time of Pu in the atmosphere due to weapons testing is approximately

2 years (Buesseler 1997). Underground tests have contributed to localized surface contamination and substantial subsurface contamination.

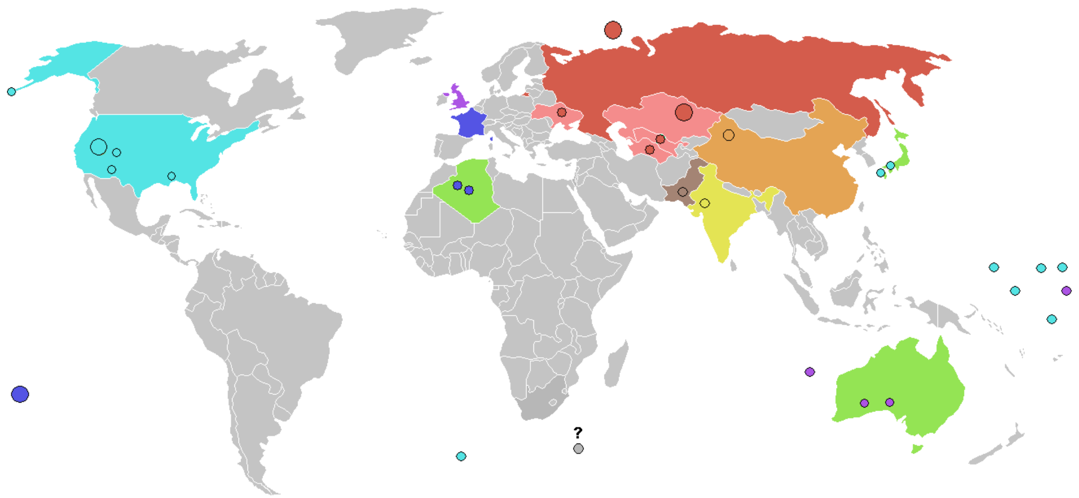

Figure 2.1 Nuclear weapons test map showing the locations of detonations and the nations that conducted the tests (by color). (WGBH, The American Experience, 1999)

Public perception of nuclear weapons and nuclear power ranges from acceptance and tolerance to outrage. Opponents of nuclear operations frequently point to concerns about the safe handling and storage of weapons and fuel and the disposition of nuclear waste. Since weapons tests were conducted for military purposes, direct sharing of weapons test data has been rare. Isotopic analysis is one of several methods employed to characterize weapon tests either remotely or as reconnaissance analysis.

The ratios of Pu isotopes are commonly used to distinguish source inputs. In studies conducted during the 1970's and early 1980's, ratios of ^{240}Pu to ^{239}Pu were assessed. Higher ^{240}Pu: ^{239}Pu ratios are generally based on higher neutron fluxes. The Pu ratios are influenced by blast intensity, height, test yield, and weapon design (Buesseler 1997). As detection sensitivity and accuracy have increased over time, isotopic signatures have led to much better source identification (Lee and Clark 2005; Smith and Williams 2005; Yoshida et al. 2007).

Due to its rare occurrence in nature and improved detection sensitivity, Pu isotopic ratios have also been used to examine anthropogenic inputs to phenomena such as sedimentation rates, water column concentrations and deposition onto coral in the ocean, and deposition onto soils, plant matter, and polar ice on land (Koide et al. 1975; Mahara and Kudo 1995; Pentreath 1995; Buesseler 1997; Jia et al. 2000; Lee and Clark 2005; Ohnuki et al. 2007). In addition to isotopic ratios, comparisons between Pu and other radionuclides permit examination of contaminant migration rates following a relatively short-term deposition event such as the Chernobyl accident (Holgye and Maly 2000). Ratios of different radionuclide activities may be more meaningful than activity values alone (Hulse et al. 1999).

Weapons development preceded the development of nuclear power. However, as noted previously, the amount of Pu produced by power production now exceeds weapons Pu. In the nuclear fuel cycle, Pu can be located in a reactor, in fuel storage, at reprocessing facilities, or stored as waste. It can also be consumed as fuel in a mixed-oxide fuel reactor. As nuclear fuel, Pu is in a ceramic metal oxide matrix. Barring a severe accident, it is likely to remain in the fuel matrix for a long time. Since Pu is dense, in an engineered environment, and non-volatile, the main pathways in which Pu is released from nuclear facilities are accidents or the inappropriate handling of wastes.

2.2.3 Environmental Chemistry

On the ground surface or in the subsurface, the simplest conceptual model of contaminant transport involves an aqueous phase and a solid phase. The aqueous phase can be pure water, rainwater, soil water, or groundwater. The solid phase consists of soil particles, minerals, rocks, or organic matter. For a contaminant to be transported, it must exist in a mobile phase. It can move with water, particles or microbes moving in pore water or groundwater, or inside plants upon passing the root tissues to the xylem. Few contaminants move freely with water because they sorb to solids. The solid-water distribution coefficient, K_d, is used to describe the tendency of a contaminant to sorb to solids and is expressed by Eqn. 2.1:

$$K_d = \frac{C_s}{C_l} \qquad \text{Eqn. 2.1}$$

where C_s is solid phase concentration and C_l is aqueous phase concentration of the contaminant. This form of expression simplifies the physical dynamics of sorption or processes that may remove a contaminant from the aqueous phase. For this reason K_d is considered a lumped parameter meaning it inherently can include other processes (discussed below). When sorption is linear, K_d represents an instantaneous, equilibrium, and reversible reaction. It is well understood that K_d may vary significantly depending on conditions, aqueous and solid phase chemistries, redox, and other conditions (EPA 1999). However, K_d is still of great utility, particularly in estimating contaminant transport.

The effect of sorption on contaminant mobility in the subsurface can be estimated quantitatively based on its retardation factor, R, defined as the ratio of water velocity to contaminant velocity. Retardation factor is related to distribution coefficient by

$$R = 1 + K_d \frac{\rho_b}{\theta} \qquad \text{Eqn. 2.2}$$

where ρ_b is bulk soil density and θ is volumetric water content in the vadose zone, which is equivalent to the porosity in the phreatic zone. Further inspection of the retardation factor shows that

$$R = 1 + K_d \frac{\rho_b}{\theta} = 1 + \left(\frac{C_s\left[\frac{mg_c}{g_s}\right]\times\rho_b\left[\frac{g_s}{cm^3}\right]}{C_l\left[\frac{mg_c}{mL}\right]\times\theta\left[\frac{mL}{cm^3}\right]}\right) \text{ which reduces to } R = 1 + \frac{Mass_s}{Mass_l}$$

So, as K_d increases, so does R. Also, if all of the contaminant stays in the aqueous phase, then R equals one and the contaminant moves at the same speed as the water. As seen in Eqn. 2.2, retardation may be calculated from the K_d or an apparent K_d may be inferred from the retardation.

Actinide aquatic chemistry processes include complexation, hydrolysis, precipitation/ dissolution, and colloid formation in addition to sorption (Choppin 2001). Plutonium speciation is complex because it has multiple oxidation states and its redox interactions are influenced by biogeochemical reactions at the surfaces of minerals, by varying oxygen content, through microbial interactions, and through combinations of these interactions (Nitsche and Silva 1996).

The sorption and retardation of Pu is strongly dependant on its oxidation state. Oxidation states +3 and +4 are favored under low pH conditions and +5 and +6 are favored under high pH conditions. Pu(IV) and Pu(V) are the most common oxidation states under vadose zone conditions. Oxidized species are more mobile than reduced species because they form less stable complexes and are therefore less likely to sorb to a solid or to form a precipitate and become immobile.

Since the 1960's, there has been an understanding that Pu oxidation state plays a key role in the mobility of Pu in the environment, i.e.,, that oxidized forms are more mobile than reduced forms (Cleveland 1970; Milyukova et al. 1969). The chemistry of Pu and its ability to exist in several redox states has led to seemingly contradictory research findings. For example, Fried et al. (1976) and Thompson (1989) observed fast fractions of non-sorbing Pu in the presence of strongly sorbing Pu. In column studies of radionuclide mobilities in groundwater in the Snake River plain aquifer, Fjeld et al. (2001) observed multiple mobilities of ^{239}Pu. Fjeld et al. (2003) developed a one-dimensional model for subsurface transport of Pu utilizing reduction of Pu(V) via surface mediated reactions and verified their conceptual model with column experiments. Similarly, Kaplan et al. (2004) conducted column studies on the effects of pH and oxidation states on the mobility of Pu in SRS sediments. These studies verified that Pu exists in more than one chemical species in the subsurface and that different species can have different mobilities. In the last few years, quantification of this using reactive transport modeling has been advanced significantly with field data from Pu lysimeters at the Savannah River Site and complementary laboratory data (Kaplan et al 2007; Demirkanli et al. 2008).

2.3 Vadose Zone Radionuclide Transport Studies

2.3.1. Background Information

The motivation for the research reported in this dissertation comes from lysimeter studies. A lysimeter is a well-defined container placed in the field and back-filled with soil. Online instruments and sampling portals permit monitoring of soil temperature and moisture, precipitation, and leachate concentrations. Lysimeters have been used in agronomy to monitor soil conditions, water fluxes, and nutrient utilization. During the 1970's and 1980's, long term lysimeter studies were initiated at Argonne National Laboratory, Oak Ridge National Laboratory, Savannah River Site, and other sites to examine the release and transport of radioactive contaminants from waste matrices (McConnell et al., 1988). Subsequent funding cuts terminated these projects before the end of their planned twenty year duration and significantly reduced the amount of information that was obtained.

Presented below are lysimeter study results related to radionuclide migration. The data are obtained from depth discrete soil samples collected at various distances from the source following closure of the lysimeter.

2.3.2. ORNL Lysimeters

The lysimeters at ORNL used Portland cement molded into cylindrical waste forms. The forms were prepared from Epicor-II prefilter waste materials from decontamination of Three Mile Island Unit-2. The highest activity radionuclides present in the wastes were ^{137}Cs, ^{134}Cs, and ^{90}Sr. The experiment consisted of five lysimeters, four of which were filled with local soils and the fifth was backfilled with silica sand and served as a control lysimeter. The waste forms were buried approximately 100 cm below the ground surface. Soil cores were collected and analyzed at the end of a seven year field exposure. Soil profile results are presented in Figure 2.2. The concentration profiles of the three radionuclides were similar in that they were relatively flat from 30 cm above the source all the way (another 70 cm) to the surface. The operation protocol for the ORNL lysimeters called for plants to be removed periodically; however plant roots were found in the soil core. The roots were analyzed for ^{137}Cs, and the ^{137}Cs concentration profile with depth was similar to that for the soil. Furthermore, the data in Figure 2.2 show that ^{137}Cs concentrations in the plant root are one to two orders of magnitude higher than in the surrounding soil, demonstrating the ability of plants to concentrate ^{137}Cs with respect to the surrounding soil. Another interesting attribute of the data is that there is a flat, relatively weak concentration gradient across this depth. Figure 2.2 contains no data collected within 30 cm of the source.

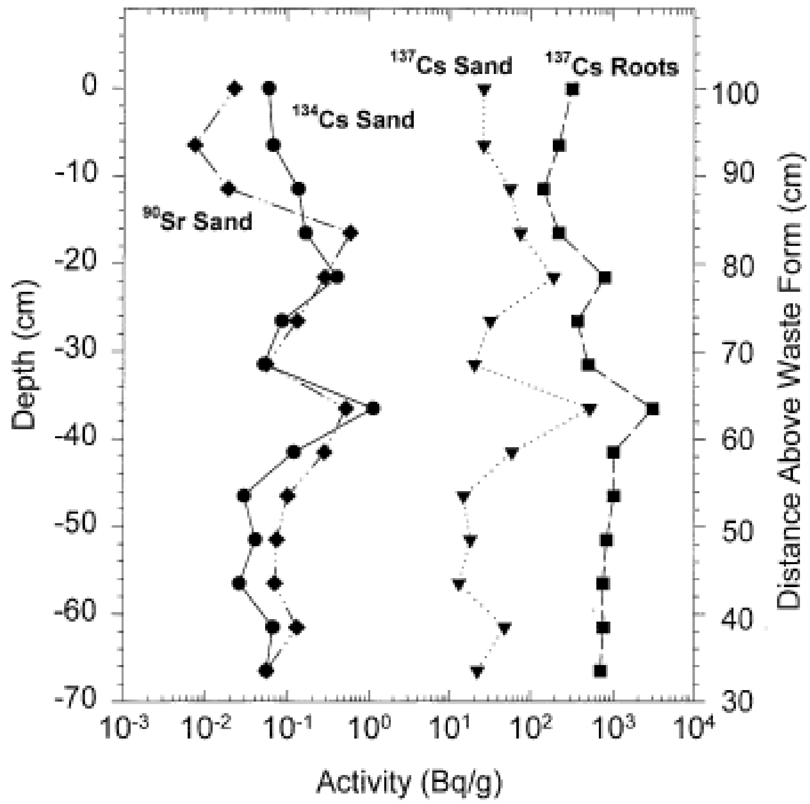

Figure 2.2 Cs and Sr concentrations versus depth in the ORNL control lysimeter soil. (Sanford et al. 1998)

2.3.3. Savannah River Site Pu Lysimeters

Approximately 150 lysimeters designed for various tests were used at the Savannah River Site (McIntyre 1987). Of interest here are three Pu lysimeter studies initiated in 1980. The lysimeters (Figure 2.3) were constructed of 52 L plastic carboys with bottoms removed. They were inverted, placed in an excavation in the ground, and backfilled to a depth of 51 cm. The sediment used for backfilling was a well-mixed sediment collected at 4 m depth from a nearby vadose zone excavation. Prior to backfilling the lysimeters, no biological materials were noticed in the sediment (Kaplan et al. 2007). During backfilling, a single filter paper spiked with $Pu(IV)(NO_3)_4$, $Pu(IV)(C_2O_4)_2$, or $Pu(III)Cl_3$ was sandwiched between two non-radioactive filters and then placed on the central axis of each lysimeter at ~ 26 cm below ground surface.

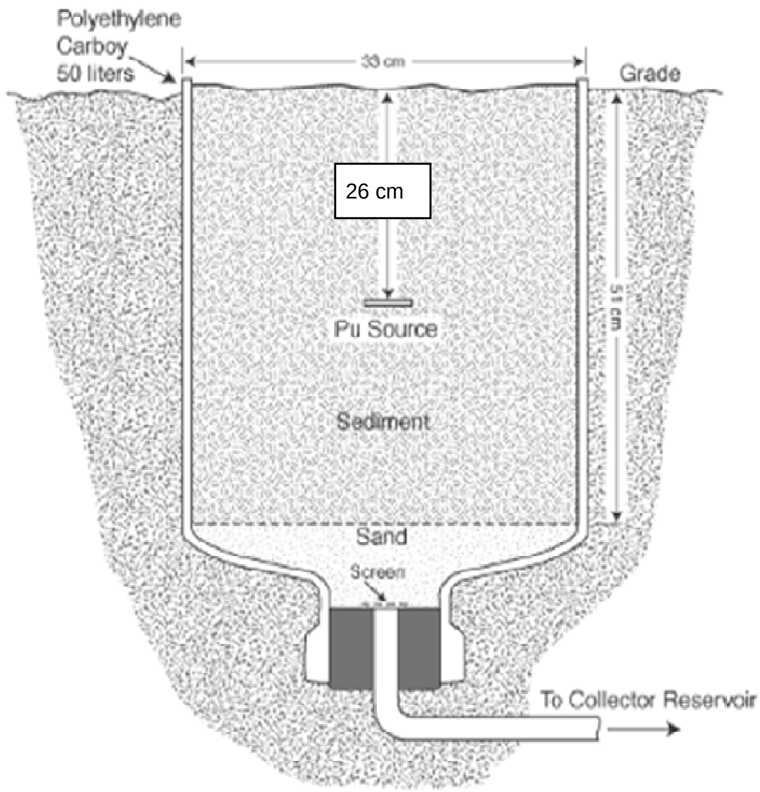

Figure 2.3 Schematic of an SRS Pu “mini-lysimeter”
(Kaplan, et. al. 2007)

At the SRS study area (Figure 2.4), the Pu lysimeters were undisturbed for eleven years. The lysimeters were subjected to natural precipitation and were not artificially watered. An important aspect of the operation was that plants, generally grasses, growing on the lysimeters were occasionally cut and left on the ground at the lysimeter surface. These opportunistic plants that grew in the lysimeters were identified from photographs of the study area and are presumed to be crabgrass (*Digitaria sanguinalis*), bahia grass (*Paspalum notatum*), and broomsedge (*Andropogon virginicus*). Even though plants were neither sampled nor identified during the study, it should be noted that roots likely penetrated the entire depth of the lysimeters over the 11 year study period, based on sampling of similar plants growing near the study site in similar soils. (Personal communication, Daniel Kaplan, Savannah River National Laboratory, Aiken SC). During the study period, leachate was collected initially on a monthly basis and from about six years into the project, on a quarterly basis. At the end of the field exposure, a 51 cm long by 7.6 cm diameter soil core was extracted from the central axis of each lysimeter. The soil cores were placed in cold storage for approximately ten years. In 2001 the cores were cut into 1.25 or 2.5 cm thick discrete sections and analyzed for $^{239+240}Pu$.

Figure 2.4 A photograph of the SRS lysimeter study area shows grass plants growing in and around the highlighted lysimeter surfaces.

The results of the field measurements and modeling efforts are presented in Figure 2.5, where relative Pu concentration is shown as a function of lysimeter depth. Focusing on the measurements below the source, the three data sets are consistent in showing (1) in the first four cm below the source, the Pu concentration declines by more than three orders of magnitude and (2) in the next 10 cm, the concentration declines by two orders of magnitude. Kaplan et al. (2006) and Demirkanli et al. (2007) showed that the observed Pu behavior can be replicated using a transport model which includes equilibrium partitioning of Pu_r (plutonium (IV)) and Pu_o (plutonium (V)) between the aqueous and solid phases and kinetic, surface-mediated redox reactions leading to transformations of Pu_r to Pu_o or vice versa, and time averaging of the transformation rate constants and percolation (mean water infiltration) rate. The distinctive shape was fit by assigning a K_d of 10000 to Pu_r, a K_d of 15 to Pu_o, a rate constant on the order of 7.0E-4/h for reduction of $Pu_{o,}$ and a rate constant on the order of 3.0E-7/h for oxidation of Pu_r.

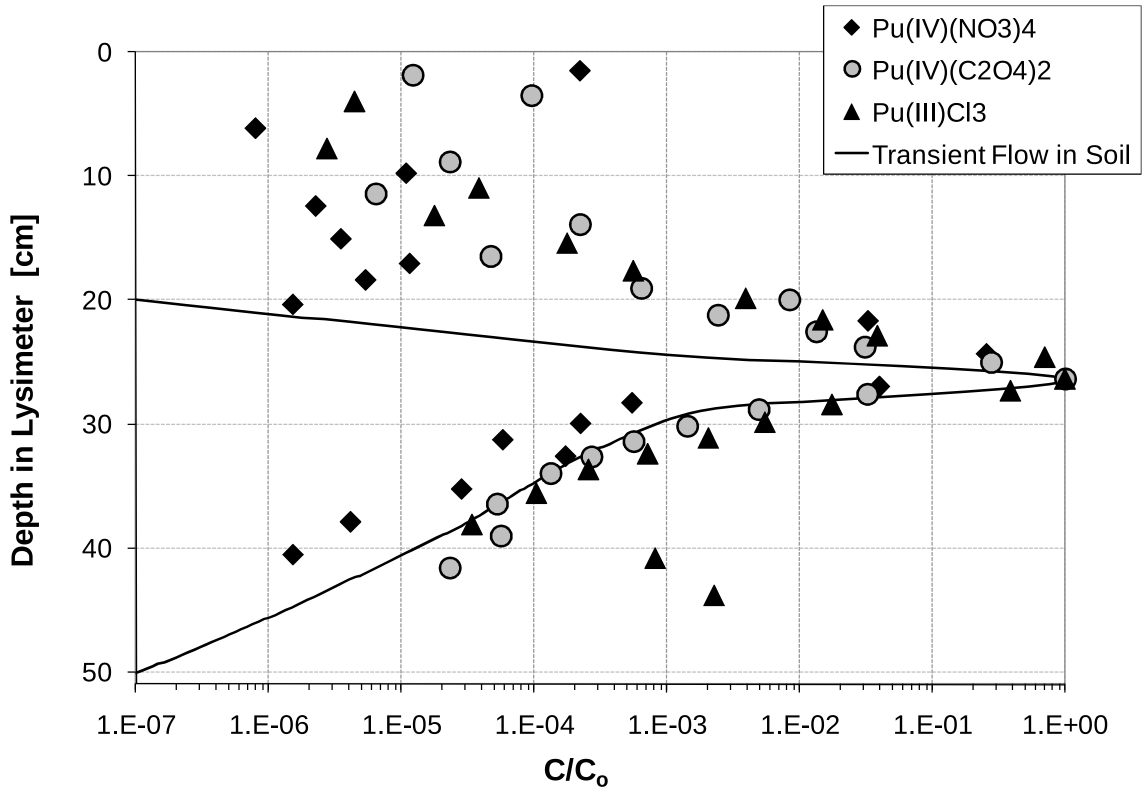

Figure 2.5 The ^{239}Pu relative concentrations in soil versus depth in three SRS lysimeters. The data are superimposed. The dashed line indicates the best fit modeling result from Demirkanli et al. (2008) without invoking plant uptake.

Focusing on the soil data above the source, it is found that Pu was transported upward all the way to the surface. From the source depth to 20 cm, the concentration data of the three lysimeters decrease from the source in a consistent manner and from ~20 cm to the surface, the relative concentration ratios range from 10^{-6} to 10^{-3}. Modeling efforts that utilized advection and dispersion equations to account for the equilibrium partitioning of Pu redox states and utilized both averaged water infiltration rates and transient water conditions could not simulate the upward transport observed in the lysimeters. The upward mobility of Pu could be explained only by estimating transport through plants. A key model parameter developed for plant transport is a distribution coefficient for

Pu sorption to plant xylem. Distribution coefficients of 1 - 10 L/kg are required for agreement with the near surface data.

2.3.4. SRS Surface Soil Analysis

Kaplan et al. (In press) conducted a study to test whether the Pu found at the SRS lysimeter surfaces was from the Pu sources or from fallout. Thermal ionization mass spectrometry (TIMS) was used to analyze lysimeter surface soils in addition to surface soil control samples from distant locations containing Pu from global fallout. TIMS is a very sensitive analysis with ^{239}Pu soil detection limits of ~0.5 μBq/g (~0.2 E-15g/g). It is used for Pu isotope ratio analyses. Isotope ratio analyses were performed on samples from the SRS lysimeter sediments, fallout surface soils, and a weapons grade control similar to the Pu in the lysimeter sources. The isotopic ratios of the surface lysimeter sediments were virtually identical to the weapons grade control sample whereas fallout surface soils have distinctly different ratios. This provided strong evidence that the Pu detected at the lysimeter surfaces originated from the Pu sources buried in each lysimeter at the beginning of the study and that the plants were behaving as a pump, virtually pumping the Pu at an accelerated rate from the source.

2.3.5 Basic Upward Transport Models

Presented in this section are two simple mathematical models for calculating Pu concentration in soil due to upward transport through roots. The first is an instantaneous partitioning model which utilizes the concentration ratio as the primary transport parameter. The second is a steady-state advection model which is a simplified version of the one-dimensional model of Demirkanli et al

(2009) with the same transport parameters. Both of the mathematical models are based on a conceptual model in which the lysimeter system consists of two homogeneous regions: a source zone and a root zone (Figure 2.6). The source zone is the contaminated region near the filter paper Pu source, and the root zone is the initially uncontaminated region between the source and the surface. Plutonium is taken up by roots of annual plants which penetrate both the root zone and source zone. Following the death of the plants at the end of the growing season, Pu in the roots becomes incorporated in the soil in the root zone. This process is repeated each year. The models provide a means of calculating the ratio of Pu concentration in root zone soil to concentration in source zone soil.

2.3.5.1 Instantaneous Partitioning

In this approximation, there is instantaneous partitioning of Pu between the soil in the source zone and the plant roots. The concentration in the roots is given by

$$C_r = CR_r \cdot C_0 \qquad \text{Eqn. 2.3}$$

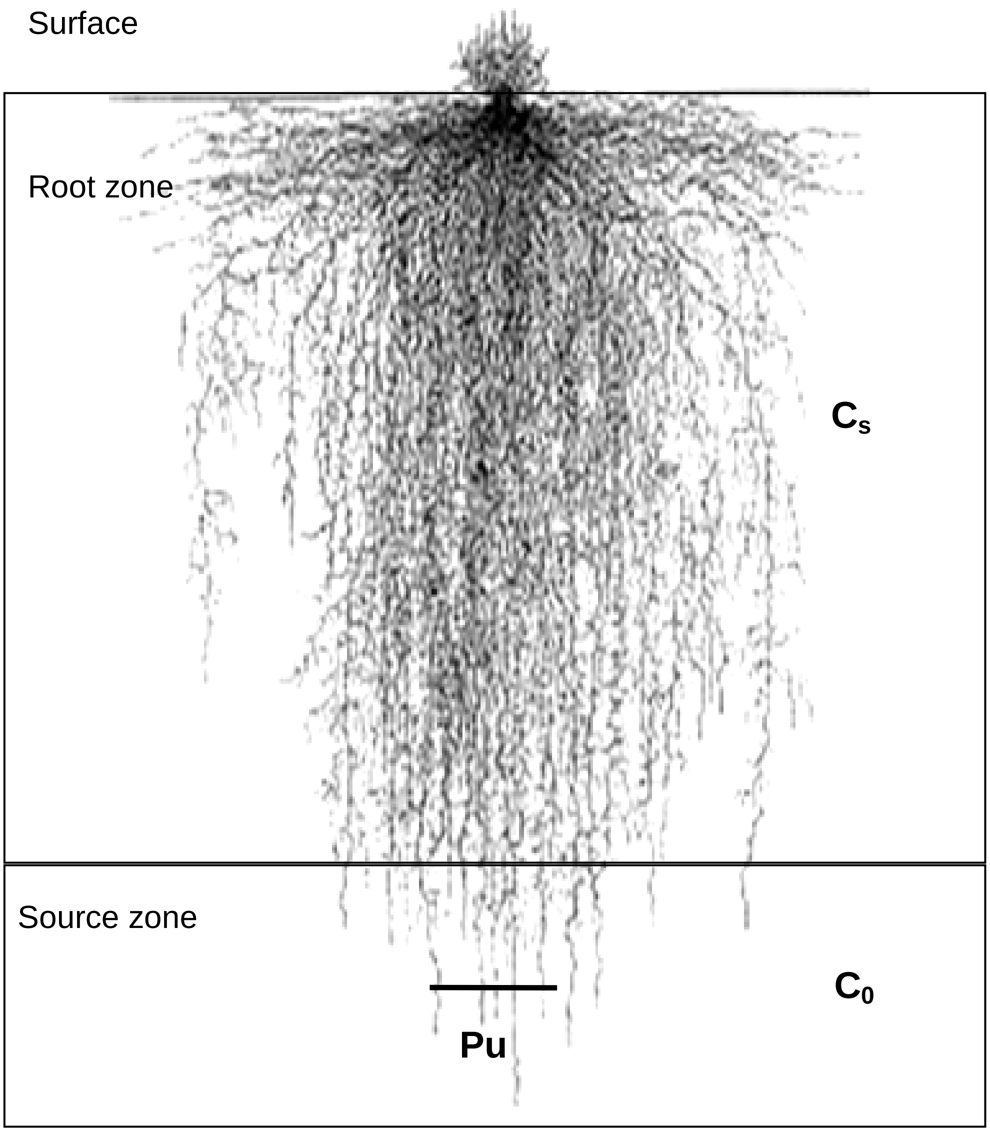

Figure 2.6 Conceptual model of the Savannah River Site Pu lysimeter system for the instantaneous partitioning and the steady-state advection models. (The rye grass root drawing shown is modified from Gregory 2006). In this conceptual model, the relative root density is not to scale. At the Pu source depth of ~26 cm, the root density is calculated to be 17% of that of the surface roots (Demirkanli et al. 2009). The key points of this conceptual drawing is that root density decreases rapidly with depth and that grasses have fibrous roots that tend to cover a lot of area with little mass

where C_r is Pu concentration in roots [Bq/kg$_r$], C_0 is Pu concentration in source zone soil [Bq/kg$_s$], and CR_r is concentration ratio for roots [kg$_s$/kg$_r$].

Concentration ratio is an empirical parameter used to quantify plant uptake data and is most commonly expressed as the ratio of contaminant concentration in the plant (or plant part) to the contaminant concentration in the soil (or solution, in hydroponic plant studies). Most concentration ratios reported in the literature apply either to the edible portions of the plant (e.g. seed, fruit or leaves) or to the entire above ground plant tissues. Root values are rare unless the root is edible (e.g., potatoes, turnips, etc). A table of Pu concentration ratios is presented in Section 2.4.4.

At the end of the growing season (year), Pu in the roots transfers to the soil uniformly throughout the root zone. Thus

$$C_r \rho_r V_T = C_s \rho_b V_T \text{ or } C_s = C_r \frac{\rho_r}{\rho_b} \qquad \text{Eqn. 2.4}$$

where ρ_r is bulk root density [kg_r/m_T^3], ρ_b is bulk soil density [kg_s/m_T^3], and V_T is total volume of the root zone [m_T^3]. Combining Eqns. (2.3) and (2.4) and taking into account N seasons of Pu accumulation in root zone soil yields

$$\frac{C_s}{C_0} = N \cdot CR_r \cdot \frac{\rho_r}{\rho_b} \qquad \text{Eqn. 2.5}$$

Eqn. 2.5 provides a means by which concentration ratio data, if available for roots, may be exploited for the root transport problem.

2.3.5.2 Steady-state Advection

In this approximation, the xylem tissues are conduits for the transpiration of water and dissolved constituents from the source zone to the above ground portion of the plant. In Demirkanli et al. (2009), the terms root and xylem were sometimes used synonymously. To be consistent with later chapters, a clear distinction is made here between xylem and the surrounding root tissue.

The conceptual model is shown in Figure 2.7. Advective flux of soluble Pu entering the root zone from the source zone, j_l [Bq/m_w^2s] is

$$j_l = C_l \cdot v_w \qquad \text{Eqn. 2.6}$$

where C_l is aqueous Pu concentration [Bq/m_w^3] and v_w is the mean velocity of water [m/s] entering the root zone. Aqueous Pu concentration is related to soil concentration in the source zone by

$$C_l = \frac{C_0}{K_{ds}} \qquad \text{Eqn. 2.7}$$

K_{ds} is distribution coefficient for Pu in soil [m_w^3/kg_s][1]. Combining Eqns. 2.6 and 2.7 yields

$$j_l = \frac{C_0}{K_{ds}} v_w \qquad \text{Eqn. 2.8}$$

Advective flux in the xylem, j_x, is

$$j_x = C_x v_{Pu} \qquad \text{Eqn. 2.9}$$

where C_x is Pu concentration in water flowing through the xylem [Bq/m_w^3] and v_{Pu} is Pu velocity in the xylem [m/s]. Advective transport of a dissolved species such as Pu through xylem is analogous to transport through a porous medium. Thus, the effect of sorption to the solid phase on Pu transport is calculated by

$$R_{Pu} = \frac{v_w}{v_{Pu}} \qquad \text{Eqn. 2.10}$$

[1] Elsewhere in this dissertation, the traditional units of L/kg (or cm^3/g) are used for distribution coefficient. The unit m^3/kg is used in this section to maintain consistent units throughout the derivation.

where R_{Pu} is Pu retardation factor for xylem [unitless],

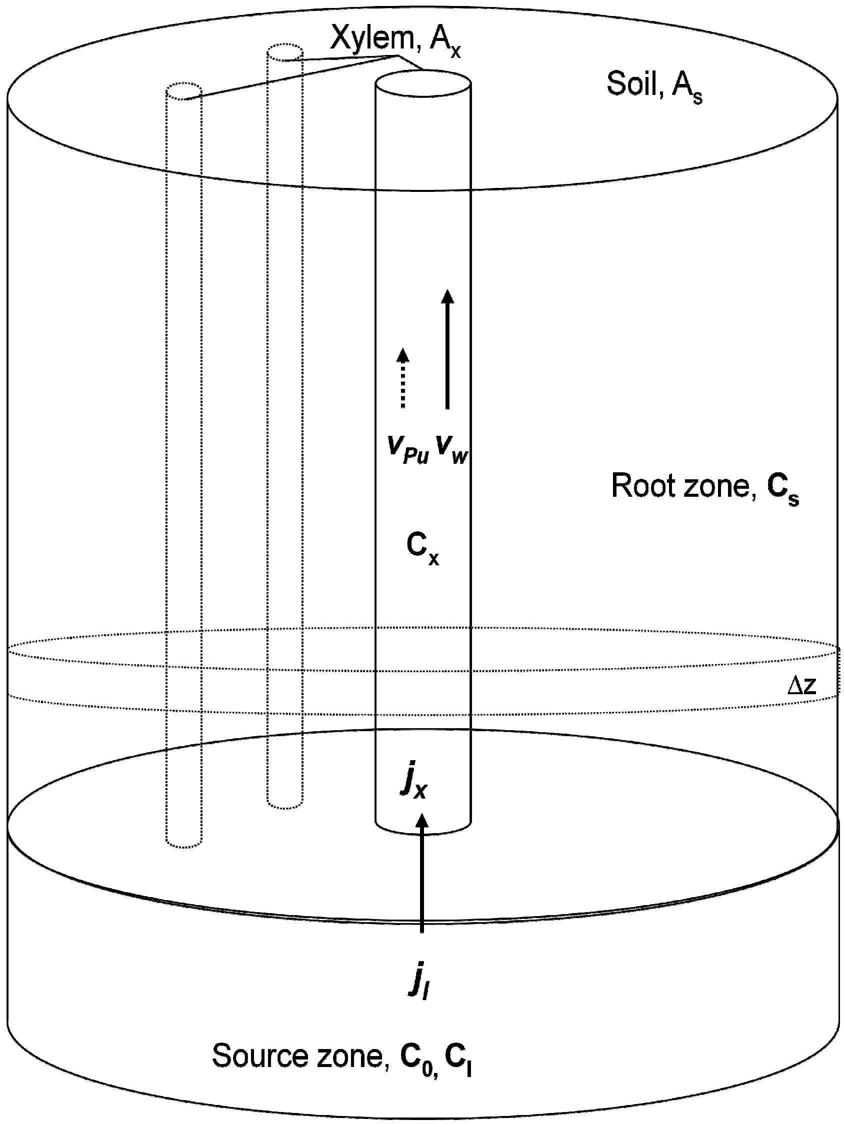

Figure 2.7 Steady-state advection model diagram illustrating upward Pu transport from the source zone to the soil zone in plant xylem.

$$R_{Pu} = 1 + \frac{\rho_x K_{dx}}{\eta_x} \qquad \text{Eqn. 2.11}$$

where ρ_x is xylem density [kg_x/m_x^3], K_{dx} is distribution coefficient for Pu in xylem [m_w^3/kg_x], and η_x is xylem porosity [m_w^3/m_x^3].

At the end of the growing season, Pu in the water contained within the xylem transfers to the root zone soil. For a thin section of the root zone, Δz,

$$C_x A_{wx} \Delta z = C_s \rho_b A_s \Delta z$$

where $A_{wx}\Delta z$ is volume of water occupied by water in the xylem. Thus, $A_{wx} = \eta_x A_x$ and

$$C_x \eta_x A_x \Delta z = C_s \rho_b A_s \Delta z$$

Simplifying and rearranging,

$$C_x = C_s \frac{\rho_b}{\eta_x} \frac{A_s}{A_x} \qquad \text{Eqn. 2.12}$$

Substituting Eqns. 2.11 and 2.12 into Eqn. 2.9 yields

$$j_x = C_s \frac{\rho_b}{\eta_x} \frac{A_s}{A_x} \frac{v_w}{R_{Pu}} \qquad \text{Eqn. 2.13}$$

At steady state, the flux entering the root zone (Eqn. 2.8) is equal to the flux through the xylem (Eqn. 2.13)

$$\frac{C_0}{K_{ds}} v_w = C_s \frac{\rho_b}{\eta_x} \frac{A_s}{A_x} \frac{v_w}{R_{Pu}}$$

Rearranging and simplifying,

$$\frac{C_s}{C_0} = \frac{R_{Pu}}{K_{ds}} \frac{\eta_x A_x}{\rho_b A_s} \qquad \text{Eqn. 2.14}$$

Finally, taking into account N years of Pu accumulation in the soil,

$$\frac{C_s}{C_0} = N \frac{R_{Pu}}{K_{ds}} \frac{\eta_x A_x}{\rho_b A_s} \qquad \text{Eqn. 2.15}$$

Figure 2.8 shows the SRS Pu lysimeter data above the source with plots of the rigorous advection-dispersion simulation results of Demirkanli et al. (2009) and the 1D steady state advection (SSA) model (Eqn. 2.15) results for 0 - 20 cm. SSA model C/C_0 results are plotted for Kd values of 5, 50, and 500 and constant parameters R_{Pu} = 3, N = 10.75 y, η_x = 0.6, ρ_b = 1.5 g/cm^3, and A_x/A_s = 6.24E-5. N and ρ_b are from the SRS lysimeter study. Xylem porosity η_x is from Demirkanli (PhD dissertation, Clemson University, Clemson, SC 2006). The xylem to soil ratio (A_x/A_s) is calculated from the geometric mean of the soil sample depths from 0 – 20 cm using the xylem area to soil area equation in Demirkanli et al. (2009). The Pu retardation factor is an approximate midpoint of R_{Pu} estimated and discussed in Chapters Five and Six.

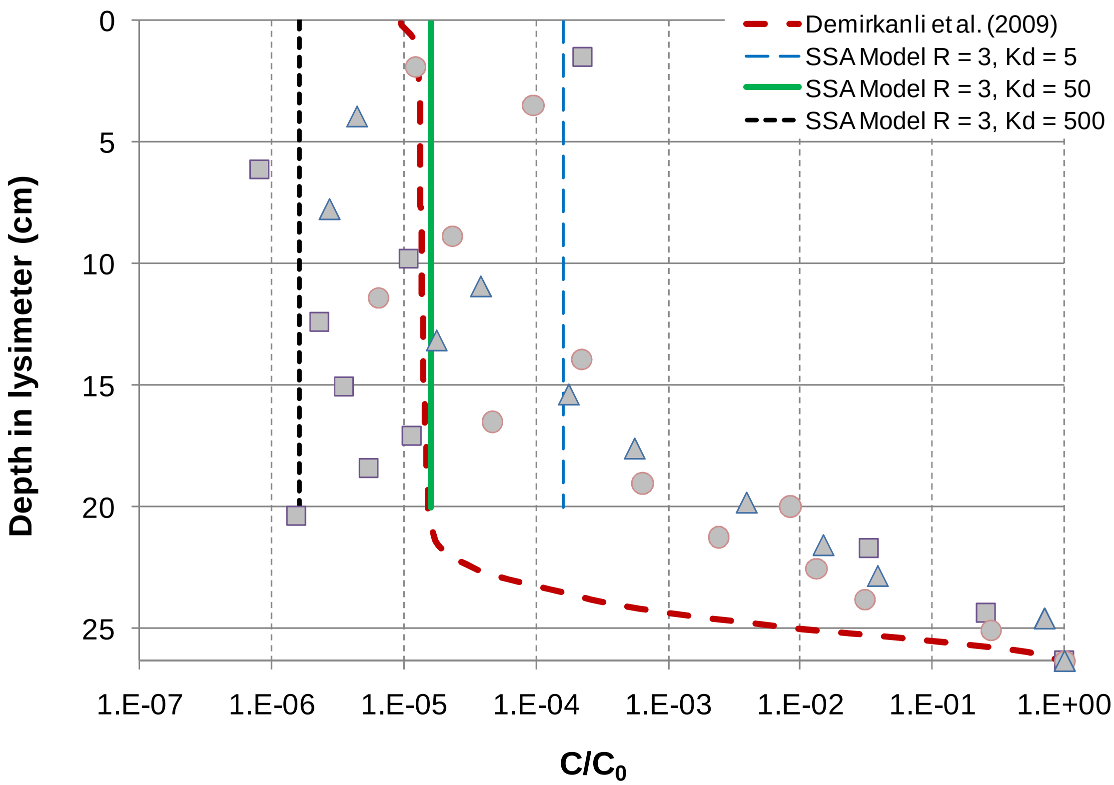

Figure 2.8 SRS Pu lysimeter soil concentration data above the source shown with Demirkanli et al. (2009) simulations (Pu plant K_d = 15) and steady state advection model where R_{Pu} = 3 and K_d values of 5, 50, and 500 respectively.

2.4 Plant Interactions

2.4.1 Plant Physiology Involved In Nutrient Metal Uptake And Transport

Vascular plants are divided into shoots (aerial) and roots (usually subterranean). Shoots consist of stem, branches, leaves and reproductive tissues. Roots consist of primary root(s), lateral roots, root caps, and root hairs (Gregory 2006). Clearly, root and shoot tissues are interdependent. For example, leaf fresh weight is dependent on root fresh weight for a particular species. Leaves capture light, photosynthesize, and provide metabolic energy to the plant. Roots provide most of the water and nutrients as well as anchor the plant. Roots interact dynamically with the soil and each influences the other (Jungk 2001; Pinton 2007).

In vascular plants, transmission of bulk water and nutrients occurs through the xylem. Sugars, amino acids, and other energy-rich compounds generally produced near photosynthesis sites are distributed via phloem. In cross sectional view of most mature woody plants, xylem and phloem are separated by significant distances and so there is little fluid exchange between them. In herbaceous plants however, especially in stem tissue where xylem and phloem are in close proximity, there is fluid exchange (Mori et al. 2000; Ohya et al. 2008).

Since the proposed research is concerned with metal transport within plants, it is important to note that:

- the architecture of vascular tissues in different plants is highly variable
- as plants undergo early stages of vegetative development, the size and positions of conductive tissues within the plant change
- positions of vascular tissues in the stem may change along its longitudinal axis.

These factors are important from the standpoint of measuring a simple velocity in plants. For example, if the xylem area (the combined diameters of xylem vessels at a particular height in the plant) changes, then the water velocity in one section of the plant will be different from that of a different part of the plant. The velocity at a particular position in the plant should be inversely proportional to the xylem area diameter.

It is essential to understand that for a plant to affect the distribution of elements in the soil roots must transect the volume of interest, i.e., the roots or root hairs must be in close proximity to the soil particles containing the elements. Figure 2.9 illustrates that root distribution of corn and rye grass are quite similar. Both root systems are fibrous, as opposed to a taproot system such as that of a carrot. For this research, the relative root zone distributions and densities of corn and grasses are quite similar within 40-50 cm depth, even though mature corn roots extend roughly 40% deeper. Since the total depth of the lysimeters was 51 cm, this factor is not significant.

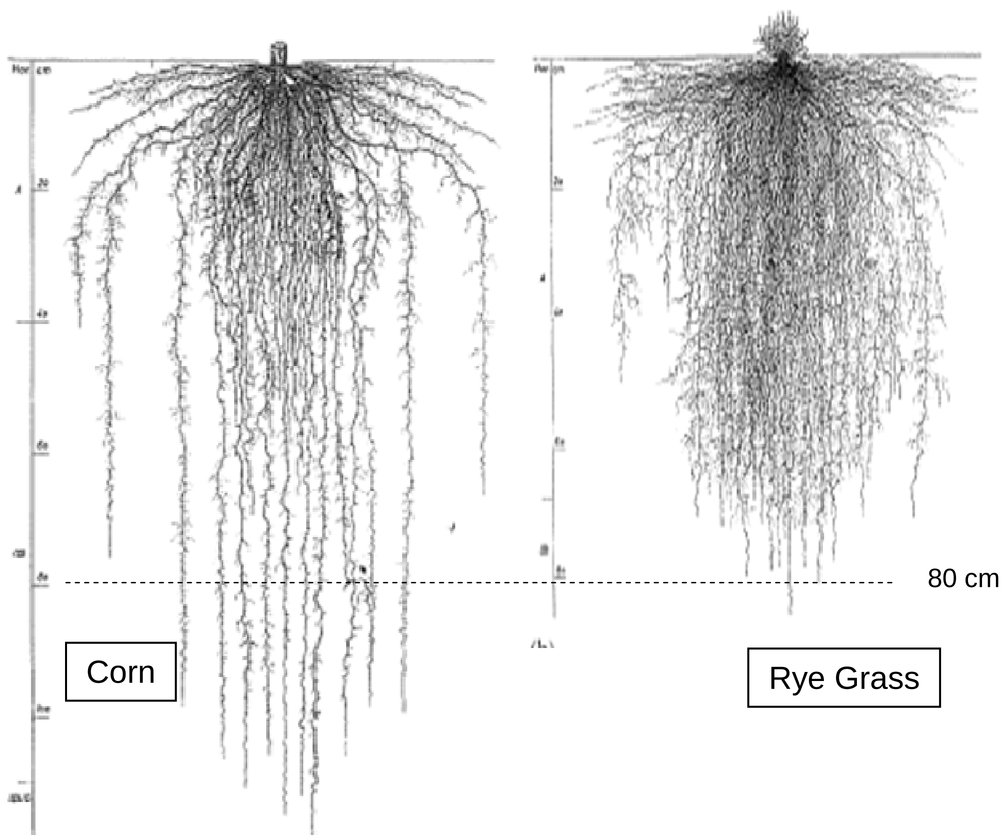

Figure 2.9 Drawings of corn and ryegrass roots shown with 80 cm depth (Gregory 2006)

Long distance transport in plants (from root to leaves) is commonly explained using the soil-plant-atmosphere continuum. With this concept, movement of water and nutrients through a plant is interconnected between environmental conditions in both the soil and the atmosphere. Water and nutrients are transported into plants in the transpiration stream, driven by negative pressure created through vapor loss at leaf surfaces (Sperry et al. 2003; Steudle 2000) and sometimes under very wet but low transpiration conditions by root pressure. Transport of a soluble nutrient or contaminant involves transport across the root boundary into root xylem and translocation from root xylem into shoot xylem (Lauchli et al. 1971). Non-volatile solutes may accumulate in the leaf and stem tissues as water transpires from stomatal cells.

Generally Pu would be transported to plant roots by advection and diffusion (Marschner 1995; Steudle 2000). When soil moisture is present, advective flow of soil solution occurs in response to the plant's transpiration stream (Sperry et. al. 2003; Hainsworth and Aylmore 1986). This is a dynamic process and if root uptake rates exceed mass flow rates, then a zone of depletion around the root can occur (Ehlken and Kirchner 2002). Root growth counteracts this situation in a dynamic manner. Through elongation and increasing fine root structure, roots improve access to nutrients.

Nutrient transport across the root boundary is slow relative to axial transport in the xylem (Maas and Ogata 1972; Epstein and Norlyn 1973). Using radiolabeled Rb^+ and Br^- ions and corn (*Zea mays*) roots, Epstein and Norlyn (1973) calculated radial transport velocities across the root of 1.8 and 1.4 cm/h versus axial transport velocities of 35 and 103 cm/h respectively. The dimension of primary importance in the effective upward transport in plants is the axial. In corn, the radial root is on the scale of 1-10 mm whereas the vertical scale of upward transport can be on the order of 1000 mm or more. Since the radial distances are quite small as compared to axial distances (e.g. from root to stem), the radial and axial transport rates may not be important in the measurement of an arrival time.

It is important to understand that solute movement from outside the root to inside the root and further into root xylem actually involves crossing several plant cell layers. An ion or molecule that crosses into root xylem moves first through outer dermal cells, then across cortical layers and the Donnan free space, and finally across the endodermis and the Casparian strip to xylem. In this document, movement or transport across the "root boundary" implies complete transmission across root tissues and into xylem wherein long distance transport within the xylem may occur. This distinction is also important because significant quantities of Pu or other elements may not cross all cell layers and reach xylem; so in effect, the root may accumulate Pu. For plant transport velocity experiments, the fraction of Pu in the xylem distributed upward is important. In other experiments, both Pu in the xylem and in the roots can be important.

Transport across the root boundary from root to xylem tissues is expected to be more difficult for multivalent ions. Hence, ratios of transport velocities of multivalent ions across the root versus within the root xylem may be expected to be smaller than the values for the monovalent ions listed above. For iron and Pu, transport across the root boundary is facilitated by specific plant transport molecules (referred to as active transport shuttles) and can not be characterized simply as an advective or diffusive process. Once across the root boundary and inside the plant xylem, transport is an advective process (Bollard 1960; Mori et al. 2000).

2.4.2 Uptake of Nutrients

Like all organisms, plants require nutrients to live and grow. Nutrient elements are often classified as macronutrients, micronutrients, and beneficial elements. Vascular plants need the following elements for adequate growth: N, P, K, Ca, Mg, S, Cl, B, Fe, Mn, Zn, Cu, Ni, and Mo. Other elements such as Na, Si, Co, I, and V are considered beneficial micronutrients (Marschner 1995). Certain essential nutrients (Mn, Cu, Zn, Ni, Mo, and B) need to be present at the proper concentration; too low is insufficient for growth yet too high is toxic (Gobran et al. 2001). Plants have sophisticated mechanisms to alter their environment to obtain nutrients and regulate internal concentrations. In general, plant uptake is characterized by three qualities:

- selectivity (finding and incorporating the nutrients they require)
- accumulation and regulation
- a degree of specificity according to plant genotype.

The rhizosphere is the zone in the immediate vicinity of a plant root in which roots, microbes, fungi, soil, and the soil solution interface (Pinton 2007). It is a dynamic environment in which many synergistic and competitive processes occur. Although interactions occurring in the rhizosphere are less well understood than many other factors governing plant growth, these interactions are critical in the biogeochemical cycling of elements. The rhizosphere is the zone of entry of a nutrient or contaminant going from the soil solution into a plant. Nutrients enter plants through their root systems and in turn root systems respond to environmental factors to access water and specific nutrients. Plants synthesize many organic compounds which can be exuded through their roots including sugars, amino acids, organic acids, fatty acids, sterols, enzymes, growth factors and other miscellaneous entities (Pinton 2007).

Plant root hairs protrude into pores, crevices, and void spaces of the surrounding soil. This way plants increase contact with soil and decrease distances between their root system and less mobile nutrients. Figure 2.10 is an electron micrograph of the root hairs of crabgrass (*Digitaria sanguinalis*) that shows the intimate contact between the root hairs and soil particles.

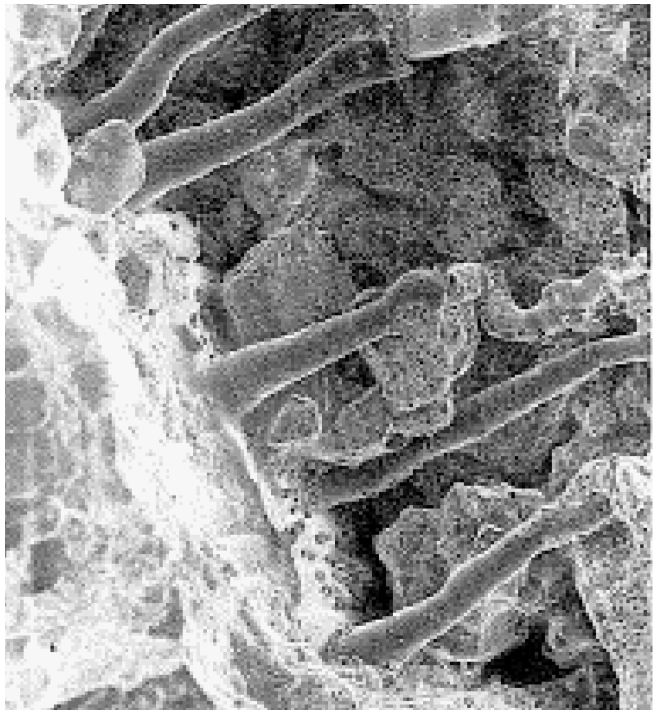

Figure 2.10 Electron microscopy image of crabgrass root hairs (*Digitaria sanguinalis*) at the root hair-soil interface (Gregory 2006)

Root exudates are primarily released through root hairs. Jungk (2001) notes that root hairs are variably developed. Their number and length depend upon environmental and genetic factors. For example, Ward (2008) found that root length is a function of iron and phosphorous content. Root length, root surface area, and total root volume increase in response to nutrient deficiency.

Plant members of the families Graminae, Chenopodiaceae, and Cruciferae are known to produce abundant root hairs. Several species of these families are hyperaccumulators and have been used in phytoremediation studies involving actinide elements (Thomas and Healy 1976; Hossner et al. 1998; Lee et al. 2002; Falck 2004; Ruggiero et al. 2004).

2.4.3 The Physiological Need for Iron

As plants grow, they require a continuous supply of iron because iron does not move from old cells to new cells during photosynthesis (Brown 1978). Since soluble iron is a metabolic requirement, plants express genes and commence a chain of activities in response to inadequate iron supply (Crowley 2006). Approximately 80% of the iron incorporated in gramminaceous plants is transported to the sites of new growth (Curie and Briat 2003). It is transported from the soil to chloroplasts during photosynthesis and used for its redox electron shuttle properties much like heme proteins are used in animal respiration. The translocation of iron from roots to shoots is vital.

2.4.3.1 Siderophores and the Soil-Microbe-Plant Environment

Iron is an abundant element on the Earth's surface and in soil. It is normally present in its oxidized state, Fe (III), which is insoluble under conditions favorable for plant growth. In neutral pH and alkaline soils, iron availability to plants is very low. Plants, microbes, and fungi have developed mechanisms to deal with the problem of iron acquisition. Plants accomplish selective acquisition of nutrients by exuding specific chemical compounds. Romheld and Marschner (1986) identified two strategies plants use to increase their intake of iron. In dicots and some monocots, enzymes, protons, organic acids and low molecular weight chelating compounds are released to acidify the rhizosphere, complex iron and other metals, and then reduce the metals prior to transmission across the root boundary. The metals are inducted into roots as reduced species. This process is termed Strategy I. Graminaceous plants (grasses and cereal crops) acquire metals using a Strategy II process. In this process, plants release phytosiderophores (PS) that are selective for iron and other metals, facilitate complexed-metal transport across the root boundary and may facilitate the long distance transport within plants. These PS functions have been termed "search and fetch" and "taxi shuttle" (Romheld and Marschner 1986; Von Wiren et al. 1993; Suzuki et al. 2006; Yehuda et al. 1996; Schaaf et al. 2004). Some plants exude PS on a diurnal rhythm. For example, Romheld and Marschner (1986) found that barley (*Hordeum vulgare*) exuded PS into the rhizosphere beginning shortly after sunrise and stopping a few hours after noon. The exudates are released against transpiration and are subsequently transported back into the plant in the high transpiration stream around noon. Although the siderophores have a short residence time in the rhizosphere, Reichard et al. (2007) and Loring et al. (2008) have demonstrated that plant organic acids and siderophores act synergistically to rapidly solubilize and complex iron from soil minerals and then induct it into the plant. This way, the siderophore molecules are not lost to microbes as energy sources.

Since iron solubility limits in soil are ubiquitous in the vadose zone, microbes and fungi are subject to its limited availability as well as plants and also release compounds to acquire nutrients. Bacteria produce siderophores. The degree with which plant exudates interact with other rhizosphere substances and benefit an individual species is not fully understood. It has been observed that siderophores are used by other organisms. Von Wiren et al. (1993) studied the influence of iron uptake in corn in the presence and absence of microorganisms. Corn plants responded to low iron by producing PS and rapidly adjusting their internal nutrient status. However, in the presence of a high microbial population density, it appeared that the microbes degraded PS and the plants suffered iron deficiency. Conversely, Bar-Ness et al. (1992) monitored iron uptake in cotton and corn with a fluorescent-labeled bacterial siderophore (NBD-DFOB). Iron uptake increased when iron was supplied as a Fe-DFOB complex. The labeled siderophore became fluorescent only when unferrated and thus served as a marker to follow iron removal. By studying iron uptake in the presence and absence of antibiotics, they suggest microbes facilitate DFOB-mediated iron uptake in plants. Ardon et al. (1998) have observed that fungi uptake DFOB-labeled iron at increased rates as well.

Highly detailed understanding of biochemical plant transport mechanisms across the root boundary is beyond the scope of this research. However, it is important to realize that plants, microbes, and fungi can compete or interact synergistically for limiting nutrients.

Different species produce differing types and amounts of PS. The collection and refinement of these entities is a difficult and time-consuming process (Suzuki et al. 2006). For this reason, plant siderophores are not commercially available but a bacterial siderophore, Desferrioxamine B (DFOB), is. DFOB (as Desferrioxamine Myselate) is a tri-hydroxamate ferrioxamine (Neu et al. 2000) with a formula of $C_{25}H_{48}N_6O_8CH_4O_3S$ and a molecular weight of 656.8 g. It is used for medical treatment of acute metal toxicity to complex and remove metals from the body (Bergeron et al. 2002).

Discussion of different siderophores is important for two reasons. First, due to the rigor and equipment involved in synthesizing, purifying, and characterizing plant-produced PS, DFOB has been selected as a proxy for PS. Second, Romheld and Marschner (1986) studied the uptake rates and fluxes of ^{59}Fe complexed with PS, DFOB, and synthetic chelates in barley (*Hordeum vulgare*). They observed that ^{59}Fe complexed with PS had 40 times the iron concentration in root tissue as did ^{59}Fe complexed with DFOB after 24 hours of exposure and also that ^{59}Fe-PS was incorporated faster than ^{59}Fe-DFOB.

2.4.3.2 Phytoremediation and Siderophore Research

Recently, several studies have attempted to exploit the metal-acquiring capabilities of siderophores or other complexing agents. At DOE sites, researchers have sought naturally-enhanced remediation strategies (Neu 2000; Lee et al. 2002; Ruggiero et al. 2004). The use of plants to transfer or remove contaminants is termed phytoremediation (Salt et al. 1995). One goal of phytoremediation is to eliminate digging contaminated soil, contaminant screening and removal by planting “hyperaccumulating” plant species which transfer contaminants from the soil into plants, and then translocate contaminants from root to shoot tissues. This way the above ground biomass can be easily collected and disposed at reduced volume and cost. This approach has several limitations. For Pu and transuranic contaminants, most of the activity accumulated in plants remains in root tissue (Price 1974; Wildung and Garland 1974; Hossner et al. 1998; Ruggiero et al. 2004). Removal of plants with their roots requires heavy equipment and characterization; thus remediation is a more expensive process.

Siderophores were originally believed to primarily acquire iron; however, they have been found to complex several metals, including Zn, Cu, Ni, among others (Neu 2000; Hill et al. 2002; Duckworth and Sposito 2005; Suzuki et al. 2006). Geochemical research has recently been conducted to examine the effect of DFOB on mineral dissolution. Duckworth and Sposito (2005) examined DFOB-enhanced dissolution rates of Mn minerals. Wolff-Boenisch and Traina (2007) investigated dissolution of U using DFOB. Their experiments were conducted at pH 6.0 and 25°C using U(VI) adsorbed to kaolinite. Under those conditions, they found that nearly all of the U was desorbed from the kaolinite by DFOB. They observed that the UO_2DFOBH complex was stable and unlikely to readsorb to soil particles and suggested a ligand-promoted dissolution process. Bouklalfa et al. (2007) determined DFOB-Pu stability constants and the ability for DFOB to promote Pu oxide and hydroxide mineral dissolution. They found DFOB to have a higher stability constant for Pu(4+) than for Fe(3+) (Figure 2.11).

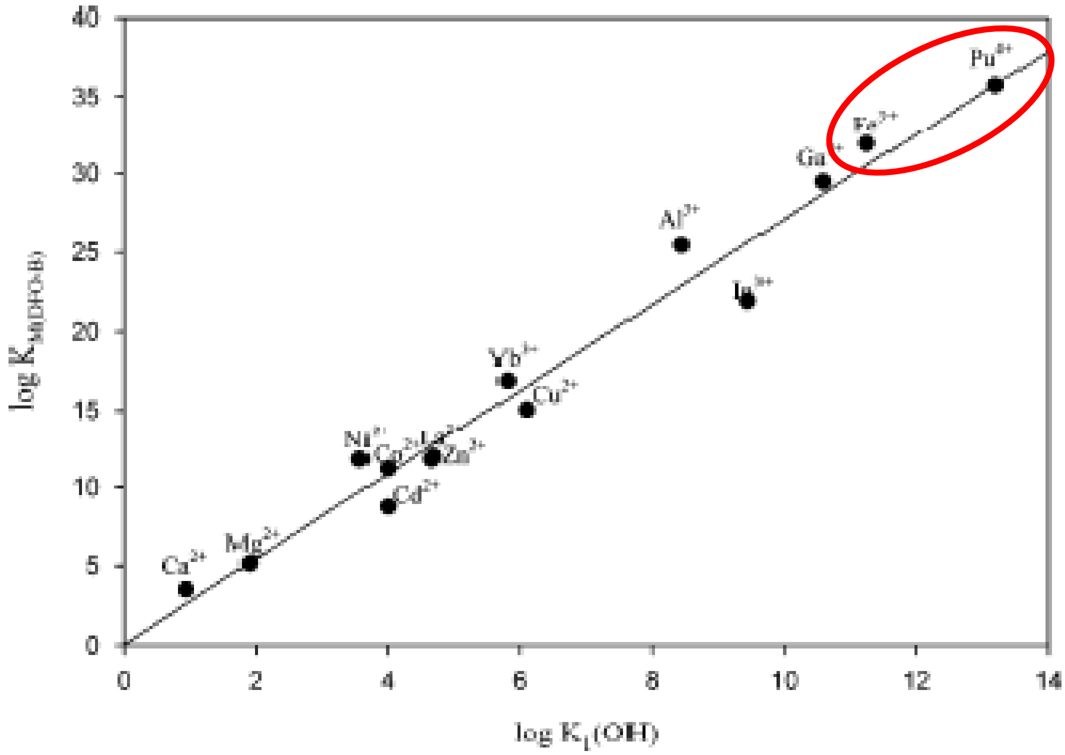

Figure 2.11 Plot of metal-DFOB stability constants versus metal hydrolysis constants (Boukhalfa et. al. 2007). The data of Fe^{3+} and Pu^{4+} are highlighted.

Complexation studies and geochemical modeling of Pu with siderophores (Ruggiero et al. 2004) under a range of environmental conditions show that siderophores exert control on the redox state of Pu. For example, Pu introduced to DFOB as Pu(VI), Pu(V), or Pu(III), will become a stable and soluble Pu(IV)$DFOB^{2+}$ complex. This aspect of their solution chemistry is reasonable since siderophores complex and transport insoluble or sparingly soluble iron to plants for immediate utilization. Conversely, adding Pu in an ionic form without sufficient complexing compounds into a dilute aqueous solution would likely cause Pu to undergo hydrolysis and precipitate.

As noted previously, plants require soluble iron for photosynthesis and once the iron is used in the process, it does not move from old to new cells. During rapid vegetative growth most of the iron taken into a plant is transported to new shoot tissues where both cellular development and photosynthesis occur. In corn and most grasses, shoot growth occurs at the top of the plant. The demands for water, iron, and other substances are high at locations of new growth, yet the plant demands for all substances are not necessarily highest at those locations (Marschner 1995). Therefore, the distributions of elements with dissimilar metabolic functions (e.g., Ca, Fe, and Mo - normally present in the nutrient solution) can be useful to qualitatively compare to the distribution of Pu. For example, if the relative concentrations of Pu and Fe in the shoot tissues follow similar distribution patterns in the shoots, then at least qualitatively the plants may be using Pu in substitution for Fe. Experimental evidence would be more sound should the distribution patterns of other elements differ distinctly. The primary reason for speculation that Pu is taken into plants in substitution for Fe, is the ionic charge to radius ratios which are (at coordination number 6) 0.47/nm for both Fe(III) and Pu(IV). This idea has been promoted in the literature, especially for phytoremediation studies and the design of actinide sequestering agents (Neu 2000; Gorden 2003; Ruggiero 2004). This possibility of Fe-Pu substitution during plant uptake has not been experimentally proven.

2.4.4 Plant Uptake of Pu

2.4.4.1 Field Studies

There is a considerable body of data on the uptake of Pu in plants due to the role of plants as a potential food ingestion pathway to humans. The results of contaminant uptake studies are quantified by a parameter historically called the concentration ratio (CR) and now given the name bioaccumulation factor. Bioaccumulation factors may be expressed either in terms of fresh weight or dry weight of vegetation. Since the primary application of bioaccumulation factors is in risk assessment, most of the studies focus on the edible portion of the plant and the data relevant to plant root uptake and transport are sparse.

Hossner et al. (1998) compiled Pu CR data from several sources and list values ranging from 10^{-2} - 10^{-9} (Bq/kg dry plant: Bq/kg dry soil). Some higher CR data have been reported since their review was published. Price (1974) evaluated field concentration ratios of actinides in food crops and other vegetation at the Hanford Site and CR data trended Am > Cm ~ Np >> Pu. Actinide chelation with EDTA, DPTA, or other organic complexants increased both plant uptake and translocation (Price 1974; Vyas and Mistry 1981; Lee et al. 2002). In early studies, Pu was often not detected in above ground portions of plants. In some of these studies, Pu observed in above ground portions of plants were not from plant uptake but from the resuspension of soil particles and deposition onto plant surfaces (Pinder et al. 1990). Plutonium does not translocate to other plant tissues after foliar deposition (Henner et al. 2005).

Plutonium concentration ratio data for various plants are presented in Table 2.1. The data for vegetables, cereal crop plants, and native species are presented together on a dry weight basis. In a multi-year greenhouse study, Adriano et al. (1986) observed that Pu CR for clover and Bahia grass increased over time. They suggested this could be the result of increased root contact with Pu, increased weathering, or increased plant metabolites in soil as the multi-year study progressed. In 1999, Whicker et al. (1999) studied actinide accumulation in *Brassica rapa* (turnips), *Phaseolus vulgaris* (bush beans) and *Zea mays* (corn) grown in sediments formerly covered by PAR Pond at the Savannah River Site. They observed CR trends: $^{244}Cm > ^{241}Am > ^{238}U > ^{232}Th > ^{239}Pu$ and noted that health risks of food consumption associated with all actinides was small in comparison with ^{137}Cs. This trend was remarkably similar to that noted in Hanford sediments, with markedly different sediments, climate, and plants (Price 1974).

Druteikiene et al. (1999) conducted one year field lysimeter tests using $Pu(IV)(NO_3)_4$, $Pu(IV)O_2$, and $Pu(III)Cl_3$ applied to forest and meadow grass soils. In each lysimeter, 30 Bq of Pu were added to the soil surface to initiate the study. Their objectives were to examine the migration rates into soil beneath the surface and to determine grass plant uptake. They reported dry weight CR data, calculating the ratio using the Pu observed in the uppermost 5 cm of soil (after the year in the field). The top 5 cm of soil contained 44 – 92 % of the applied Pu, depending on the chemical form of the Pu. It is not clear how the initial deposition of Pu was performed, since the meadow lysimeter sites are termed "undisturbed grassland". In approximately one year, from 2% (PuO_2) to 39% ($PuCl_3$) of the Pu spiked at the lysimeter surfaces was incorporated into grass plants.

When plant roots are near Pu in the soil, plant uptake can be substantial. These grass plant CR data are higher than most of the CR values in Table 2.1. However, this is not an isolated report of high Pu CR data. Lux et al. (1995) examined soil and plant samples from a 30 km zone around Chernobyl and found Pu CR values generally ranged from 0.001 – 0.02, noting an increase to 0.3 in berries. In a large scale study, Sokolik et al. (2004) sampled soils and plants from Belarusian grasslands at control sites 12 – 48 km from the Chernobyl nuclear power plant accident. They determined concentration ratios as a function of plant species and of soil type, and calculated the transport of ^{241}Am and $^{239+240}$Pu in soil between 1986 and 2001. Their Pu CR data ranged from 0.002 – 0.28. Lichens and mosses had the highest CR values. In summary, excluding differences in uptake by plant species, the dominant factors ultimately influencing Pu CR values are its sorption to soil and interaction with plant roots.

Table 2.1 Plutonium Concentration Ratio Data (Bq/kg dry plant: Bq/kg dry soil) from a Variety of Field and Greenhouse Studies

Reference	Condition	Plant (tissue)	Soil	CR
Nisbet & Shaw (1994)	to maturity in lysimeters (5y)	barley (straw) >15mm	loam	2.6E-4
			peat	3.0E-5
			sand	1.8E-4
	"	cabbage	loam	.3-2.5E-4
			peat	0-0.2E-4
			sand	.2-1.5E-4
	"	carrot	loam	0.3-4E-3
			peat	0-0.5E-3
			sand	.1-1.5E-3
Adriano et. al. (2000)	greenhouse study to maturity	beet	SRS H area sand (low CEC)	2.3E-3
	"	carrot	"	3.0E-3
	"	turnip	"	0.6E-3
Whicker et. al. (1999)	garden plot tilled to 23 cm and fertilized	bush bean	SRS PAR pond soil sandy acidic	3.6E-4
	"	corn husk	"	2.9E-4
	"	corn kernel	"	2.1E-5
	"	turnip green	"	2.3E-3
Druteikiene et. al. (1999)	Pu Oxide (in field lysimeter for 1 y)	meadow grass	Soddy podzolic, pH 4.3	2.0E-2
	Pu Nitrate	"	"	1.8E-1
	Pu Chloride	"	"	6.0E-1
Lux et al. (1995)	30 km of Chernobyl exclusion zone	all plants 1992	Organic forest soils	.003-.017
	"	all plants 1993	"	.013-0.39
Sokolik et. al. (2004)	Belarus 12-48 km downwind of CNPP (exposed ~15 y)	meadow grasses	Soddy-podzolic sand	3E-2
	"	"	Loamy sand	2E-2
	"	"	Organic soils	1E-2
	"	"	Peat-bog	5E-3

2.4.4.2 Laboratory Studies

An important series of laboratory studies of Pu uptake in plants were conducted by Wildung, Garland, and Cataldo at PNNL (Wildung and Garland

(1974); Garland et al. (1981); Cataldo et al. (1988)). They examined the uptake, fate, and transport of Pu, Np, and other metals in plants using barley as a monocot and soybean as a dicot. They investigated physiological processes that influence Pu distribution and gathered information about transport mechanisms inside plants. Wildung and Garland (1974) observed that Pu plant uptake was limited by soil type and that concentrations in plants increased linearly with time over the 60 day study period. Using Pu_2DTPA_3 in soybeans, Cataldo et al. (1988) observed a change in the chemical form of Pu upon absorption through roots. DTPA (Diethylenetriaminepentaacetic acid) is an organic chelator similar to EDTA. Garland (1981) found that, upon absorption, Pu_2DTPA_3 changed to a different organic chemical form once it crosses the root boundary into the plant. The Pu was associated with increasingly soluble fractions (roughly defined by the molecular weights of the associated organic constituents) as it went from root to stem to leaves. Through electrophoresis of xylem exudates from soybean stems, they determined that Pu supplied as $Pu(NO_3)_4$ was immobile whereas Pu supplied as Pu_2DTPA_3 accumulated in the plant. Chemical analysis performed on plant exudates indicated the presence of organic acids and sugars normally present in plant fluids. In five day old soybean plants, the fractions of Pu in the roots and shoot tissues were 0.84 and 0.16, respectively. In soil pot experiments, concentration ratios ranged from 10^{-4} to 10^{-5} depending on plant age. In 80 d experiments of soybean uptake from soil, the shoot Pu activity increases were linear for ~60 d, however in terms of shoot Pu concentration, the maximum value was observed when the plants were 10 d old.

Lee et al. (2002) studied the uptake, translocation, and distribution of Pu in Indian mustard *(Brassica juncea*) and sunflower (*Helianthus annuus*). They compared the uptake of Pu-DTPA, Pu-citrate and Pu-nitrate using both soils and hydroponic solutions. They varied DTPA concentrations both in soil and in solution. They found that DTPA increased the uptake of Pu in plants in both soil pot and solution experiments and that the maximum uptake was for DTPA concentrations between 10 and 50 mg/L. Uptake trended Pu-DTPA >> Pu-nitrate > Pu-citrate.

It was noted that the use of organic complexants greatly increased (in some cases > 1000-fold) uptake of Pu into plants. Previous studies comparing complexants to chelate Pu for maximal uptake report that Pu_2DTPA_3 increases uptake greater than all other complexants tested (Price 1974; Garland et al. 1981; Hoessner 1998). This trend is striking, especially for cases comparing organically complexed Pu with ionic Pu, such as observed by Lee et al. (2002). As discussed in the Plant Interactions sections involving siderophores, iron uptake is greatly increased through combining iron with siderophores. Since the literature indicates that Pu has low concentration ratios and this research is concerned with the transport phenomena of Pu in plants, Pu will be complexed with DTPA or DFOB in all live plant experiments conducted to determine uptake or transport phenomena.

CHAPTER THREE

RESEARCH OBJECTIVES

3.1 Objectives

Together, the lysimeter soil concentration data (Figure 2.5) and isotope ratio analyses of surface soils provide very strong evidence of the upward transport of Pu at SRS. It is hypothesized that this upward migration is due to Pu transport in plant roots. A model invoking plants as the dominant long distance (i.e., more than a few centimeters above the source) mechanism for upward transport through soils yields predictions which are consistent with the SRS lysimeter data. However, agreement between the model and the data requires that key transport parameters - the retardation of Pu in plants and Pu-plant K_d values - are used as fitting constants. Data for these parameters do not presently exist. It is also hypothesized that Pu uptake in plants occurs based on the plant's nutritional requirement for Fe. Laboratory evidence for this hypothesis is also lacking.

The overarching goal of this research was to provide experimental support for the modeling effort and for the plant uptake mechanisms. The objectives were:

1. To quantify Pu retardation in graminaceous plants and to quantify Pu sorption to plant xylem.
2. To characterize the distribution and accumulation of Pu in plants.
3. To compare the relationship between plant uptake of Pu and Fe.

The Pu retardation factor in xylem was a key parameter in the advective transport approximation (Eqn. 2.15) and was the focus of the first objective. To determine the retardation factor, two techniques were proposed. The first involves the measurement of Pu velocity in plants by measuring Pu in plant tissue at known distances from the source at known times following exposure to a nutrient solution containing Pu. The Pu was Pu(DFOB) as a proxy for Pu complexed with naturally-produced phytosiderophores. The second technique involves batch sorption experiments to determine the Pu distribution coefficient using aqueous Pu(DFOB) and ground plant xylem material. For the first technique, the retardation factor for Pu can then be calculated from the distribution coefficient using Eqn. 2.2. Comparison of these experimental data with the predictions will provide insight into the utility of the advective modeling approach.

The distribution of Pu between shoots and roots was needed for the instantaneous partitioning model (Eqn. 2.5) and was the focus of the second objective. Discrimination between shoot and root tissues was straightforward and the method of exposure allowed differentiation among root tissues in contact with the labeled solution and those that are not. Thus, this objective was accomplished by determining the total Pu in shoots and in exposed roots. These data enabled the estimation of root concentration ratios from the base of concentration ratio data (Table 2.1). The consistency between Pu retardation and root concentration ratios was determined using Eqn. 2.15.

Irrespective of the utility of either modeling approach, plant uptake of Pu may occur based on Pu substitution for Fe. The focus of the third objective was to examine Pu uptake at low, medium (optimal), and high Fe concentrations. The objective was accomplished by determining Pu and Fe concentrations in plant tissues and comparing both the total Pu under different Fe conditions and the relative distributions of Fe and Pu in plant shoot tissues. The total Pu uptake and translocation provided some insight into the substitution hypothesis. Comparison of the spatial distributions of Fe and Pu in shoots provided qualitative information about the internal transport mechanisms in plants. If relative concentrations versus shoot length (distance from the source) data trended similarly and data for other elements taken into the plant were dissimilar, then this implies that Pu and Fe were transported similarly and partially affirms the substitution hypothesis.

3.2 Overview of dissertation

The research objectives are described above; however the author's intention is to publish these studies. The publication process does not facilitate the objectives stated herein to be followed directly and sequentially therefore the subsequent chapters are delineated as follows:

- Chapter Four addresses the first part of the first objective: to quantify the retardation of Pu in plants for the first time. Chapter Four was published as Thompson, S. W.; Molz, F. J.; Fjeld, R. A.; Kaplan, D. I. (2009). "Plutonium uptake velocity in Zea mays (corn) and implications for plant uptake of Pu in the root zone." Journal of Radioanalytical and Nuclear Chemistry 282, 439-442. (http://www.springerlink.com/content/95451m6x63384vj8/)

- Chapter Five is an extended version of an article that has been submitted to Environmental Science & Technology as Thompson, S. W., Molz, F. J., Fjeld, R. A., and D. I. Kaplan. Xylem Velocity, Uptake, and Distribution of Complexed Plutonium in Corn (Zea mays). Chapter Five repeats and affirms quantification of the retardation of Pu in corn plants and addresses the second research objective: to characterize the spatial distribution and accumulation of Pu in plants.
- Chapter Six addresses the third objective: to compare the relationship between plant uptake of Pu and Fe. This research focus is intended for publication, but has not been prepared for submission at present.
- Chapter Seven is a combination of additional findings which are loosely related but are too brief to be complete chapters. It addresses:
    - the observed Pu discrimination at the root,
    - the evaluation of the basic upward transport models, and
    - the second part of the first objective: quantification of Pu sorption to plant xylem.
- Chapter Eight contains the conclusions of this research.

3.3 Overview of experiments

The corn plant velocity, uptake, and distribution experiments were conducted in batches with the maximum number of plants limited to 22 plants per batch due to the plant size, space required for lighting, and the arrangement of plants and equipment. Nine corn plant batches were grown and utilized; in the Appendix, they are called LRx where x is the sequential batch number with LR as an acronym for “Long Root” (a term for the growth arrangement with the corn proximal roots in soil and distal roots in labeled solutions). The earliest batches, LR1-4, were exploratory and were useful to develop plant growth, maintenance, and analytical techniques. Experimental protocols, plant treatment procedures, and the establishment of tissue matrix elimination, Pu analysis, and quantification of both the control activities and the quality control of the process were accomplished during this phase of the research. Data from those batches are not presented in this document however basic observations resulted from the initial work. First, the Pu plant velocities were much faster than initially expected. Second, in order to measure sensitively the Pu which moved into the plants, the activity levels applied to the plants would need to be increased and the control activities considered. Third, lacking an environmental chamber in which to conduct the experiments, the physical environment would need to be as controlled as practically achievable. Last and perhaps most importantly, there is a degree of natural variability in individual plant uptake, root size, root surface area, shoot size, etc. therefore in order to observe general trends such as uptake with time, plant replicates were essential. However, due to the effort required to grow, expose, monitor, process, and interpret the data of many plant tissues, the art of compromise was important in deciding how much emphasis to place on a particular experimental parameter. Overall, an accord was achieved, although some data might have been more robust with more plant replicates.

Batches LR5-LR9 are discussed in the text and their data are presented in the Appendices. For reference to the data, Table 3.1 lists the batch, objectives, plant conditions, and comments about experimental parameters as applicable.

Table 3.1 Corn Plant Batches and Brief Experimental Descriptions.

Batch	**Description**	**n (plants)**	**Comment**	**Age (d)**
LR9	Pu Fe Dual labeled	3	Discussed in Ch. 6	23
	Pu with 0x, 10x Fe	4	Discussed in Ch. 6	23
	Longer exposures	9	Discussed in Ch. 5,6, & 7	23
	Transpiration test	4	Not discussed	25
	Control	1		25
LR8	Pu Fe Dual labeled	2	Scoping test, not discussed	23
	Pu with 0x, 10x Fe	6	Discussed in Ch. 6	23
	Fe velocity	5	Not Discussed	23
	Control	1		23
LR7	2nd Pu velocity	6	Discussed in Ch. 5	23
	Accumulation	6	Discussed in Ch. 5 & 6	23
	Water velocity	2	Discussed in Ch. 5	23
	Control	3		23
LR6	1st Pu velocity	4	Discussed in Ch. 4 & 5	23
	Accumulation 1-4d	6	DTPA and DFOB	23
	Control	1	Obtain 23 d control data	23
	Control	2	Compare with 28 d control	28
LR5	DFOB Characterization	5	Single plants at 2,4,8,12,24 h	28
	DTPA Characterization	6	3 duplicates at 4, 8, 12 h	28
	Control	1		28

CHAPTER FOUR

PLUTONIUM VELOCITY IN *ZEA MAYS* (CORN) AND IMPLICATIONS FOR PLANT UPTAKE OF PU IN THE ROOT ZONE.

4.1 Abstract

A transport velocity of Pu complexed with the siderophore DFOB has been measured in corn to be at least 174 cm/h. Based on a calculated plant water velocity, a Pu retardation factor of 1 - 10 was estimated. Dominant Pu species retardation in soil is typically several orders of magnitude higher than this, implying that plants can be a vector for exceptionally rapid upward Pu mobility.

4.2 Introduction

To understand vadose zone transport, field lysimeter experiments were conducted at the Savannah River Site (SRS) near Aiken, SC, in the 1980's. Ionic forms of $^{239+240}$Pu were deposited on filters as sources and placed near the center of each lysimeter. Grasses and weeds grew in the lysimeter soils and were cut and deposited on the soil surfaces. After 11 years, soil cores were removed from the center of each lysimeter, sectioned and Pu activity concentrations measured and plotted as a function of elevation (Figure 4.1).

The resulting data have been the subject of intensive study, (Fjeld et al. 2003; Kaplan et al. 2006; Demirkanli et al. 2008; Demirkanli et al. 2009) which ultimately showed that the unexpected movement of Pu above the source was due to plant uptake and upward movement in the transpiration stream (Demirkanli et al. 2008; 2009). A secondary implication was that Pu should accumulate on the surface due to periodic cutting and annual die-back of grasses. Recently, this was proven to be the case when isotope ratio analysis indicated that Pu present in surface soils of each lysimeter originated from the sources, not from fallout (Kaplan et al. 2009). These results motivated this study of Pu uptake and translocation by corn, a member of the grass family.

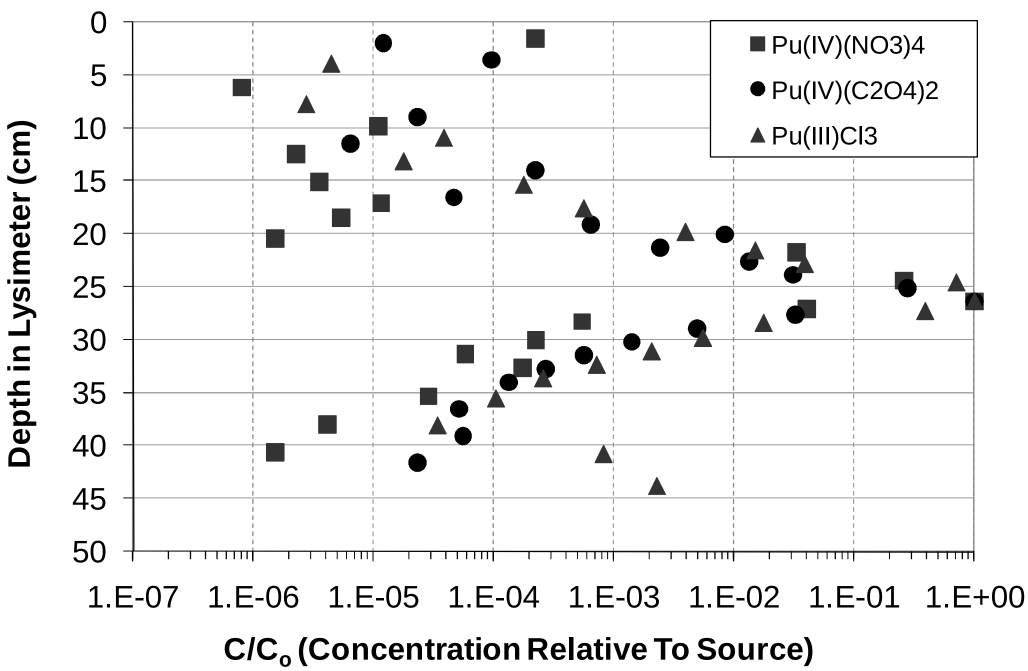

Figure 4.1 The $^{239+240}$Pu concentrations in soil versus depth in the SRS lysimeters. Data are superimposed from three lysimeters, each containing an ionic Pu complex. Note the Pu transport above the source.

In field and laboratory settings, numerous researchers (Nisbet and Shaw 1994; Ashworth and Shaw 1994; Gerzabek et al. 1998; Sokolik et al. 2004; Wadey et al. 2001; Sanford et al. 1998) have shown that plant uptake can affect environmental fate and transport of radionuclides. Elements studied include Se, Cs, Sr, Tc, Cl, I, Na, Co, Cd, Ra, Am, and Pu. Wadey (2001) noted that upward migration of Cs and Co was likely due to root uptake and translocation. Similarly, Sanford et al (1998) attributed upward migration of Cs to plant transport. Garland et al (1981) studied Pu in soybeans and observed characteristics of xylem transport. Cataldo et al (1988) suggested that Pu exists in xylem as soluble organic complexes. Although the mechanisms underlying the uptake and transport of Pu within plants have yet to be fully defined, it is known that Pu is much more mobile in plants than in soil (Cataldo et al. 1988).

The purpose of the present study was to build a quantitative knowledge base by measuring Pu transport velocities in plants. Plants identified from the SRS Lysimeter study area were crabgrass (*Digitaria sanguinalis*), bahia grass (*Paspalum notatum*), and broomsedge (*Andropogon virginicus*). Although corn (*Zea mays*) is a crop plant, its fibrous root system, stem, and parallel-veined leaf structure are quite similar to grasses, so it was selected for study.

For Pu to move from soil into a plant, the steps involved are:

1. movement from soil or mineral particles to the soil solution
2. movement of the soil solution to the plant root
3. transport into the root and across the casparian strip into root xylem
4. transport in root xylem upward into plant shoots.

4.3 Experimental

The focus on Pu velocity required a unique experimental design in that a first arrival over a known travel distance was measured or bounded. Several earlier studies (Garland et al. 1981; Price 1974; Lee et al. 2002a; Lee et al. 2002b) noted that organically-complexed Pu greatly increased plant uptake compared to ionic Pu. Therefore, plants were exposed to Pu as the complex Pu(IV)-DFOB. DFOB (Desferrioxamine B) is a commercially available bacterial siderophore.

The experiments were conducted using corn plants growing in soil pots placed above nutrient solution containers. Figure 4.2 is a photograph of plants in this arrangement. The primary root was inserted directly into nutrient solution through a hole at the bottom of the soil container. This eliminated the need to consider Pu sorption to soil and permitted rapid assessment of plant uptake.

Figure 4.2 Corn plants in soil over nutrient solution containers.

4.3.1 Materials

Uncoated corn seed (*Zea mays, cv. trucker's favorite*) and potting soil were procured. ^{238}Pu was purchased from Eckert & Zeigler Isotope Products Lab in Valencia, CA. DFOB (Desferrioxamine B) was obtained from Sigma-Aldrich Chemical Co, and the scintillation cocktail was Ultima Gold AB from Perkin-Elmer of Shelton, CT.

4.3.2 Plant Growth

Anchor paper was used for seed germination and initial growth. A plastic bag was placed over the plant seedlings and the container was placed under plant lights while roots elongated. After seven days seedlings were inserted into a tube under a stream of water. The tube allowed packing the plant into soil while keeping the root free. Soil pots were 1L amber containers, with a 3 cm hole in the bottom. Filter paper (with a hole for the root) prevented soil from falling into the nutrient solution. The plant was set on top of nutrient solution (pH 6.0) in a 500 mL aerated container. Solutions were changed twice per week to prevent nutrient depletion and reduce potential interference from microbes or algae. Soil was watered three times per week. Initially, one-half strength nutrient solution was utilized, prepared as described by Garland et al. (1981). After a few days, full strength nutrient solution was utilized. Growth conditions were 14/10 h day/night cycles (31/20 ℃ +/-2℃) with 35% (+/- 10%) RH. Plants grew at a photosynthetic flux of 1300-1500 μmol/m^{2}s using a 400 watt Sun Gro^{TM} system.

4.3.3 Plant Exposure, Measurement, and Analysis

To expose plants to ^{238}Pu, containers of pre-mixed Pu and nutrient solution (74000 Bq of ^{238}Pu and 9.7 x 10^{-5} M DFOB per plant) were exchanged quickly with non-radioactive nutrient solution. A series of four 23 day old plants were exposed for 10, 20, 40 or 80 minutes and sacrificed. To cease exposure, plant shoots were cut at 40 cm height and at the base. In total, Pu traveled through 18 cm of root and 40 cm of shoot for a distance of 58 cm before reaching the leaves at the top of the plant.

Plant tissue sections were cut, chopped, dried overnight at 75 ℃, weighed, and digested with concentrated HNO_3 and 30% H_2O_2. Digests were transferred into 20mL plastic scintillation vials as 8 mL of 0.1 M HNO_3 with 12 mL of Ultima Gold AB scintillation cocktail and shaken prior to counting. Samples were analyzed on a Wallac Model 1409 liquid scintillation counter. ^{238}Pu alpha energies are emitted as a single peak at 5.49 MeV. Sample digestion was a modification of a method described in Jones and Wallace (1992). Lee et al. (2002b) adapted this method to liquid scintillation. Pulse shape discrimination (Wallac PSA setting = 150) was adjusted to optimize for the Pu alpha signal.

4.3.4 Quality Control

Samples were counted for 10,000 seconds. The error of the >40 cm sample from the 20 minute plant including background and control activity was 9.7% at the one sigma confidence level. The overall error was 14% at one sigma. The average internal spike recovery was 94%. Sample duplicate analyses averaged 10% relative percent difference.

4.4 Results and Discussion

Figure 4.3 shows Pu concentration (Bq/g dry) versus time for 10, 20, 40, and 80 minute exposures. These experiments demonstrated that Pu-DFOB moved into the uppermost shoots within an elapsed time of 20 minutes. The minimum distance traveled through the plant is 58 cm, so the Pu velocity is ≥174 cm/h. The fluid velocity through the plant may vary across the stem, i.e., there may be high velocity pathways. Since we detect a first arrival time, the Pu velocity will be near the maximum, which may have varied between plants. This is illustrated by the 80 minute result, which evidently had a low transpiration rate. A small peak contribution was present in the ^{238}Pu alpha region of control (unexposed) plants from long lived progeny present in the soil (Ac, Ra, Po, Bi, Pb, etc.), so a mean control plant activity value has been subtracted from all Pu plant data.

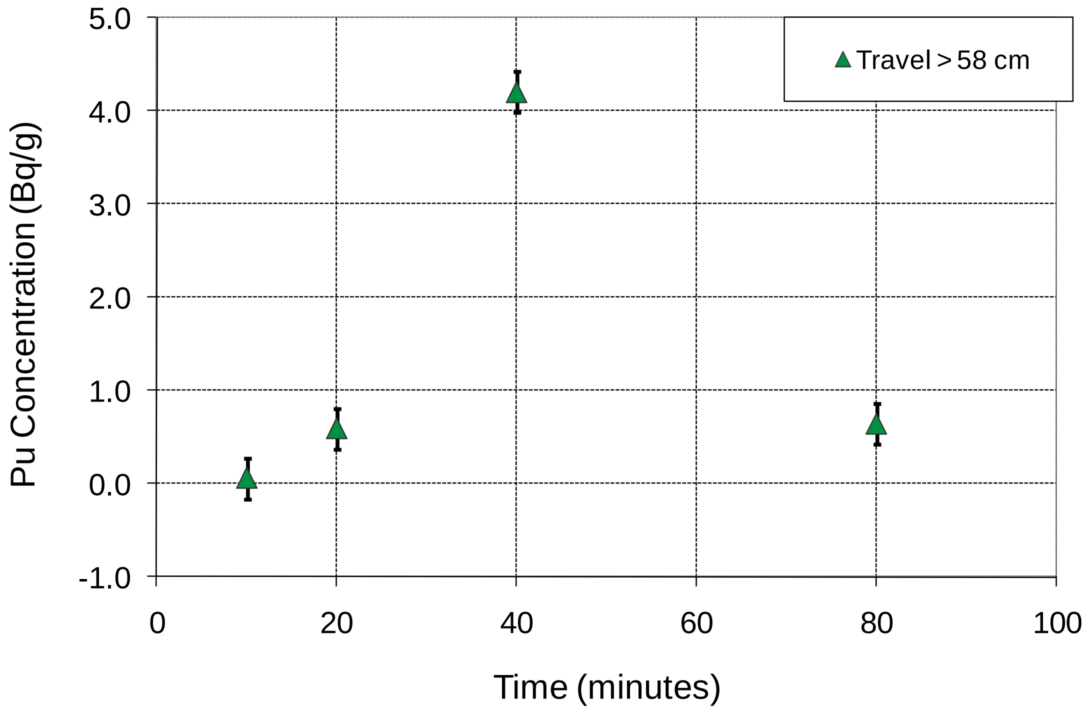

Figure 4.3 Net concentrations in upper shoot tissues versus time to travel 58 cm in corn. Data are singular results for each plant. Error bars represent 2 standard deviations of the control plant activity replicates.

4.4.1 Calculation of Pu Retardation in Corn Xylem

Corn transpiration rates averaged 5.75 g/hr (≈5.75 cm^3/hr) with 12 % relative percent difference for two 28 day old plants. Cross sections excised from these plants at six cm above the soil were examined by microscopy with dimensional software (Jenoptik ProgRes C5 digital camera with IMT iSolution Lite v. 7.7). Using tissue images enhanced with lignin pink and acid fusion stain, the stem area and vascular bundle size and number were determined. Figure 4.4 is a cross sectional view of a corn stem with vascular bundles visible. At the right of Figure 4.4, vascular bundles (oval "face-shaped" tissues) are clear.

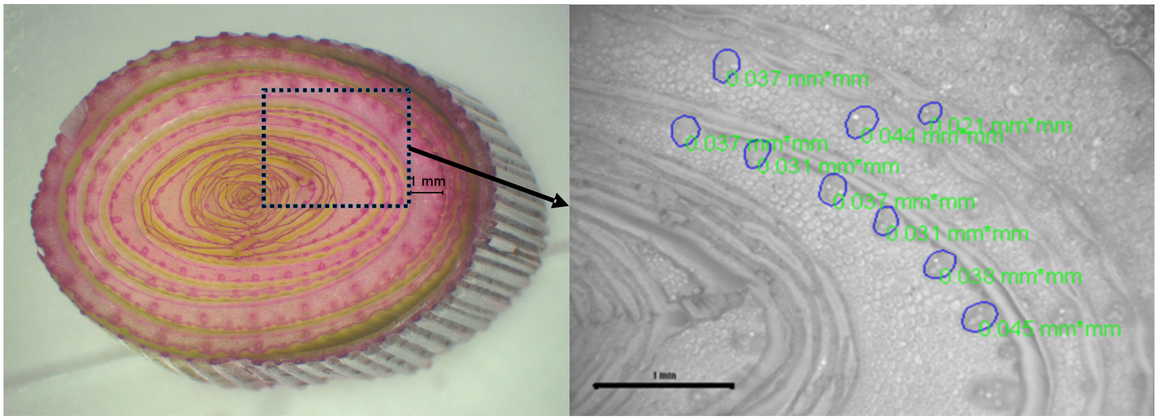

Figure 4.4 Photomicrographs of a corn stem cross section. At left, the entire stem is shown; at right, an enlarged image of the showing vascular bundles. Scale bars indicate 1 mm.

Calculation of xylem to total stem area was performed by counting vascular bundles in ¼ of the stem shown in Figure 4.4, measuring the areas of nine vascular bundles and the stem, and using a xylem to vascular bundle area ratio of 0.25. The xylem to total stem area ratio is 1.52% with a 21% error at 1 standard deviation. The total area in ¼ of the stem sampled was 32.32 mm^2. The total xylem area is $4 \bullet 32.32 \bullet 0.0152 = 1.97$ mm^2. Li et al. (2009) studied the xylem structure in two corn hybrids grown nearly to maturity. They determined ratios of vascular bundle to total stem area and reported 1.93% and 1.41%. Those data correspond to xylem to stem ratios of 0.48 and 0.35% respectively. Thus, the xylem to stem area ratio calculated (1.52 +/-0.32%) seems reasonable based on the idea that younger plants should have a proportionately higher vascular tissue area than more mature plants (Beck 2005).

The measured transpiration rate of 5.75 cm^3/hr included water lost through the soil by evapotranspiration, which should be negligible since the soil had not been watered for several days prior to the measurements. Thus, using an area of 1.97 mm^2 ($1.97x10^{-2}$ cm^2) yields an average water velocity of 292 cm/hr. If one assumed that average velocity and maximum velocity were equal, then the ratio of water velocity to Pu velocity would be 292/174 = 1.68. This ratio is the retardation factor, and as calculated 1.68 is a lower bound since the maximum velocity may be significantly higher than the average velocity. If the xylem area were halved to 0.0099 cm^2, then the implied retardation factor would double to 3.36. These retardation estimates are subject to uncertainty and need to be better defined experimentally. However, Pu-DFOB is much more mobile in corn than ionic Pu is in soils, where reduced Pu species can be essentially immobile with $R \approx 2,000 – 20,000$ at typical soil pH values and less common oxidized Pu species can be retarded by factors of 15 and often more.

4.5 Conclusions

The transport velocity of Pu-DFOB has been measured in corn plants for the first time to be at least 174 cm/hr. Mean water velocities of control plants were 292 cm/hr. If the xylem flow exhibited plug flow, then the retardation factor would be 1.68. Given the uncertainty of xylem area estimates and of fluid velocity in the xylem, the actual retardation could be up to 10 or more. Future research may narrow this range. However, since reduced Pu species are essentially immobile in soil at typical pH values, our data imply clearly that plants can serve as a conduit for transporting Pu rapidly from the subsurface to the surface.

CHAPTER FIVE

XYLEM VELOCITY, UPTAKE, AND DISTRIBUTION OF COMPLEXED PLUTONIUM IN CORN (*ZEA MAYS*)

5.1 Abstract

The uptake, distribution, and velocity of Pu complexed with the bacterial siderophore (DFOB) were studied in corn (*Zea mays*) to experimentally validate the hypothesized rapid transport of Pu in grass xylem. Plants were exposed to nutrient solutions containing Pu for time periods ranging from 10 min to 10 d. Pu(DFOB) entered root xylem and moved upward at a velocity of at least 174 cm/h. Based on water velocity calculations, the Pu(DFOB) xylem retardation factor was estimated to be in the range of 1 – 10. Pu concentrations in xylem were two to three orders of magnitude smaller than those in the nutrient solution, because Pu(DFOB) in solution was impeded by the root. Most (97%) of the plant Pu activity remained in the root external to the xylem; however, once Pu reached the xylem it moved rapidly upward and accumulated in the upper shoots. Overall, these results provide strong support for the hypothesis that grass plants can be a vector for extremely rapid upward transport of Pu in the vadose zone.

5.2 Introduction

Most, if not all, prior experimental studies of Pu uptake by plants have been in the context of either the contamination of food (Adriano et al. 1986; Whicker et al. 1999) or phytoremediation (Hossner et al. 1998; Lee et al. 2002). Results indicated that Pu was incorporated in above ground plant tissue within a growing season. In general, plant concentrations were very small relative to soil concentrations, but the transport distance was relatively large considering that Pu normally has very low mobility (< 1 cm/y). It has recently been hypothesized by Kaplan et al. (2006) and Demirkanli et al. (2008) that plant roots can be an important vector for the upward migration of Pu in the vadose zone. This hypothesis emerged from attempts to model data from field lysimeters at the Savannah River National Laboratory (Demirkanli et al. 2008). The upward migration observed in the data was only simulated by the model when Pu uptake by plant roots and subsequent transport in the xylem were included. Further, reasonable fits to the data were obtained only by either assuming values for transport parameters (retardation of Pu in plants, Pu-xylem K_d, root Pu uptake efficiency) or using them as fitting parameters due to the absence of transport related information in the literature. The transport of reduced Pu in soil is highly retarded (Demirkanli et al. 2008; Choppin et al. 2001), with a soil distribution coefficient of 1800 cm^3/g ($Retardation_{soil} \approx 12{,}000$). The simulation results (Demirkanli et al. 2009) suggest a 15 cm^3/g Pu-xylem distribution coefficient ($Retardation_{plants} \approx 10$). This distribution coefficient implies that Pu is moving upward in the xylem as a mobile complex. Presented here are the results of laboratory experiments focused on Pu transport in plants.

Plants regulate their internal nutrient concentrations by homeostasis (Marschner 1995) and have specific transport pathways for water, K^+, Fe^{2+}, Fe^{3+}, and other materials. Transport in plants occurs within the context of the soil-plant-atmosphere continuum. Water and some soluble nutrients move across root cell layers into the root xylem in the transpiration stream, driven by vapor loss at leaf surfaces (Sperry et al. 2003). Once inside the xylem, transport of soluble constituents is mainly an advective process (Bollard 1960; Mori et al. 2000) subject to applicable retardation. The use of complexants to increase the plant uptake of Pu is believed to enhance transport through the root tissues (Garland et al. 1987). Rapid siderophore-facilitated root transport pathways have been demonstrated with Fe (Romheld and Marschner 1986; Yehuda et al. 1996; Schaaf et al. 2004) and with Zn (Suzuki et al. 2006). However the mechanisms of root uptake of Pu are poorly understood.

Garland et al. (1981) and Cataldo et al. (1988) characterized the Pu fluids inside soybeans by analyzing xylem exudates collected by cutting the stem below the first leaf node. Garland et al. (1981) demonstrated that after passing through the roots, Pu_2DTPA_3 changed to a plant-complexed Pu species not subject to rapid hydrolysis. Cataldo et al. (1988) compared the behavior of organo-complexed Pu^{4+}, Fe^{3+}, Ni^{2+}, and Cd^{2+} by gel electrophoresis and found that Pu^{4+} and Fe^{3+} exhibited similar behavior. Research has quantified the partitioning of Pu between shoot and root tissues after long time intervals (weeks to years) (Garland et al. 1981; Nisbet and Shaw 1994, Adriano et al. 2000; Lee et al. 2002), however a fundamental understanding of the movement of Pu into living plants is lacking.

The objectives of this study are to estimate the velocity and retardation with respect to water of organically complexed Pu in corn (*Zea mays*) and to characterize the spatial and short term temporal uptake of Pu in plants. Spatial distributions were determined by discrete analysis of root and shoot tissues. The uptake and accumulation of Pu were characterized using activity in relation to time, transpiration, and the relative amount excluded from the plant xylem. The experiments were conducted with an organic complex of Pu because that is the form found in plants (Garland et al. 1981). Corn was selected due to the structural and physiological its similarities to annual grasses (*Poaceae*) of the type found in the Savannah River Site lysimeters and because its size and growth rate facilitate laboratory experiments.

5.3 Experimental

5.3.1 Materials

Corn seed (*Zea mays, cv. Trucker's Favorite*) and potting soil (pH 6.0) were locally purchased. ^{238}Pu was procured from Eckert & Zeigler Isotope Products Lab in Valencia, CA. DTPA was purchased from Aldrich Chemical Company of Milwaukee, WI. Desferrioxamine B was purchased from Sigma-Aldrich Chemical Co. Ultima Gold AB scintillation cocktail was purchased from Perkin-Elmer Biosciences of Shelton, CT. The soil pots were 1.0 L amber HDPE containers with the necks cut to be vertically straight-sided and cut at the bottom with 3 cm holes for the roots. Solution containers were Nalgene 500 mL straight sided jars with holes cut for the roots and for small aeration portals.

5.3.2 Plant Growth Conditions

Plants were grown in soil pots resting on nutrient solution containers shown in the left photograph in Figure 5.1. This permitted proximal roots of the plant to be anchored in the soil for stability and to provide for more natural growth than a purely hydroponic system. The distal roots grew in the nutrient solution container where complexed Pu could be introduced in a controlled manner. The photograph at right in Figure 5.1 reveals the primary root with the soil and nutrient containers removed and the roots spread apart. Plant growth and tissue preparation are presented in greater detail in Thompson et al. (2009; Chapter 4). Briefly, seeds were germinated in seed paper for seven days until their primary roots were long enough to exit the bottom of the soil pot and contact the nutrient solution. Each seedling in a soil pot was placed on top of a container (with matching holes for the root) containing 500 mL of aerated nutrient solution. Plants were grown at 14/10 h day/night cycles at 34/20 ℃ (+/-2℃) and 35% (+/-15%) relative humidity. A 400 watt Sun Gro™ light system was suspended above the corn plants and was raised as the corn grew. The initial photosynthetic flux to the plants was ~700 μmol/m^2s as measured at the upper leaves. Plant height increased until the upper leaves reached a flux of 1300-1500 μmol/m^2s, which was the daytime light flux for the remainder of the experiments.

The nutrient solution, was described by Garland et al. (1981), and contained (in mg/L): 946 $Ca(NO_3)_2$●$4H_20$, 150 KCl, 120 $MgSO_4$, 68 KH_2PO_4, 0.69 H_3BO_3, 0.06 $ZnSO_4$●$7H_20$, 0.024 Na_2MoO_4●$2H_20$, 0.022 $MnCl_2$●$4H_20$, 0.017 $CuCl_2$●$2H_20$, and 0.60 $FeCl_3$. Solutions were adjusted to pH 6.0 (+/- 0.05), the same pH as the Savannah River Site lysimeter soil. To prevent Pu from precipitating and to maximize uptake (Lee et al. 2002), Pu was introduced to plants as the organic complexes, either Pu_2DTPA_3 or Pu(DFOB).

Figure 5.1 Corn plants growing in soil pots with the primary root inserted in nutrient solution. On the left, corn grown under plant lights; on the right, with the soil and nutrient pots removed, the primary root is exposed. To initiate an experiment, complexed Pu was added to the hydroponic solution.

5.3.3 Plant exposure and handling

Plutonium isotopes are not amenable to rapid autoradiography since their alpha particles are embedded in tissues and do not have the penetrating power to be rapidly detected through plant cells (the radiographic process requires times which are too long for the velocity measurement). Plutonium-241 is a very weak beta emitter with less penetration than the Pu alpha particles (Walker et al. 1989). Measuring the first arrival of Pu in plants required high detection sensitivity; therefore destructive analysis was required to measure Pu in plant tissues. Plutonium-238 isotope was selected for study due to its high specific activity, 633 GBq/g.

Experiments were conducted with Pu concentrations of 0.9–9.7 x 10^{-10} M. Complexant concentrations were 9.8 x 10^{-5} M. Plants were exposed by rapidly exchanging non-radioactive nutrient solutions with Pu-labeled nutrient solutions. The shoot distribution experiments were conducted using 28 day old plants with DFOB or DTPA and ^{238}Pu activities of ~37 KBq/plant. To end exposure, plants were cut at the soil surface and then the shoot lengths were recorded. The shoot stem and leaves were straightened, measured, and cut into 10 cm tissue sections. Velocity experiments were conducted using 23 day old plants and ^{238}Pu(DFOB) at ~74 KBq/plant. Exposure times were monitored using a digital stopwatch. To end exposure, shoots were cut 40 cm above the soil height and then at the soil surface. Since velocity experiments were conducted rapidly, root tissues were not collected. The accumulation experiments were conducted with 23 day old plants and ^{238}Pu(DFOB) activities of 8.28 KBq/plant. The exposure times were 3, 7, and 10 days for three replicate plants. Three day plants were exposed once for three days. Because of nutrient solution consumption, the seven day plant solutions were replaced once and the ten day plant solutions were replaced twice during their respective exposure times. Thus, seven day plants were exposed to a total of 1000 mL and ten day plants were exposed to a total of 1500 mL of labeled solution. This way, the plants did not consume sufficient solution to restrict transpiration. Accumulation plant shoots were processed as in the distribution experiments.

Following exposure, shoot sections of test plants were cut into specific lengths, chopped finely, dried overnight at 75 °C, we ighed, and digested with concentrated HNO_3 and 30% H_2O_2. Roots removed from solution were allowed to drip on blotter paper, rinsed in water for one minute, dried, chopped, and processed like the shoot tissues. Digests were transferred into 20 mL plastic scintillation vials as 8 mL of 0.1 M HNO_3 with 12 mL of Ultima Gold AB liquid scintillation cocktail and shaken for 15 s prior to counting. Tissue digestion was done as described in Jones and Wallace (1992). Lee et al. (2002) adapted this method to liquid scintillation. Samples were counted using a Wallac Model 1409 liquid scintillation counter. Plutonium-238 alpha energies were detected at 5.49 MeV. Pulse shape discrimination (PSA = 150) was adjusted to optimize for the ^{238}Pu signal. The Pu recovery was 94% and data were not adjusted for recovery. Sample counting errors were < 10% at the 1 σ level.

Control plants were treated identically to those exposed to Pu. They were found to contain low levels of alpha activity, presumably from the uptake of naturally occurring radionuclides in the potting soil. Gamma spectrometry of both the soil and control plant shoots indicated the presence of the following natural radionuclides: ^{228}Ac, ^{226}Ra, ^{214}Po, ^{214}Bi, ^{210}Pb, and ^{40}K. Since the natural radionuclides contribute to the Pu signal recorded for the exposed plants, it was necessary to subtract this contribution from exposed plant raw data.

5.3.4 Water Velocity and the Retardation of Complexed-Pu in Corn

Maximum Pu velocity was measured directly, and average water velocity was estimated by transpiration and flow area measurements. Water velocity in two 23-day-old control plants was determined from the volume of water lost due to transpiration over a 24 hour period and the xylem cross sectional area. Transpiration volume was inferred from the change in total mass of their nutrient solutions. Tissue cross sections of these controls were excised from the root and the stem at 5 cm, were stained with toluidene blue to increase vascular cell contrast, and were photographed with a Jenoptik ProgRes C5 digital camera under magnification. Image & Microscope Technology iSolution Lite software (version 7.7) was used to measure dimensions.

5.4 Results and discussion

5.4.1 Spatial Distribution of Complexed-Pu in Corn Shoots

Figure 5.2 shows shoot section concentrations versus distance traveled in plants exposed to $Pu_2(DTPA)_3$ or Pu(DFOB) for 4 and 8 h or data from controls. The distances are from the bottom of the soil to the midpoint of each section. The important observations are as follows. First, the mean control concentrations are approximately constant as a function of height, indicating the activity taken up from the soil is uniformly distributed in the shoots. Second, Pu concentrations in exposed plants are significantly larger than equivalent concentrations in the controls. Third, Pu concentration increases with shoot height. This occurs because the Pu, which is carried up through the plant by the water, is left behind in the stomates when the water evaporates. Finally, the Pu concentrations in plants exposed to Pu(DFOB) (closed symbols) exceed the concentrations in plants exposed to $Pu_2(DTPA)_3$ (open symbols) by factors of 2-4. Price (1974) ranked the enhancement of plant uptake of Pu complexed with different ligands as: DTPA > EDTA > citrate > oxalate > glycolate > acetate > nitrate. Our data show that Pu uptake in corn is greater for the siderophore DFOB than for DTPA.

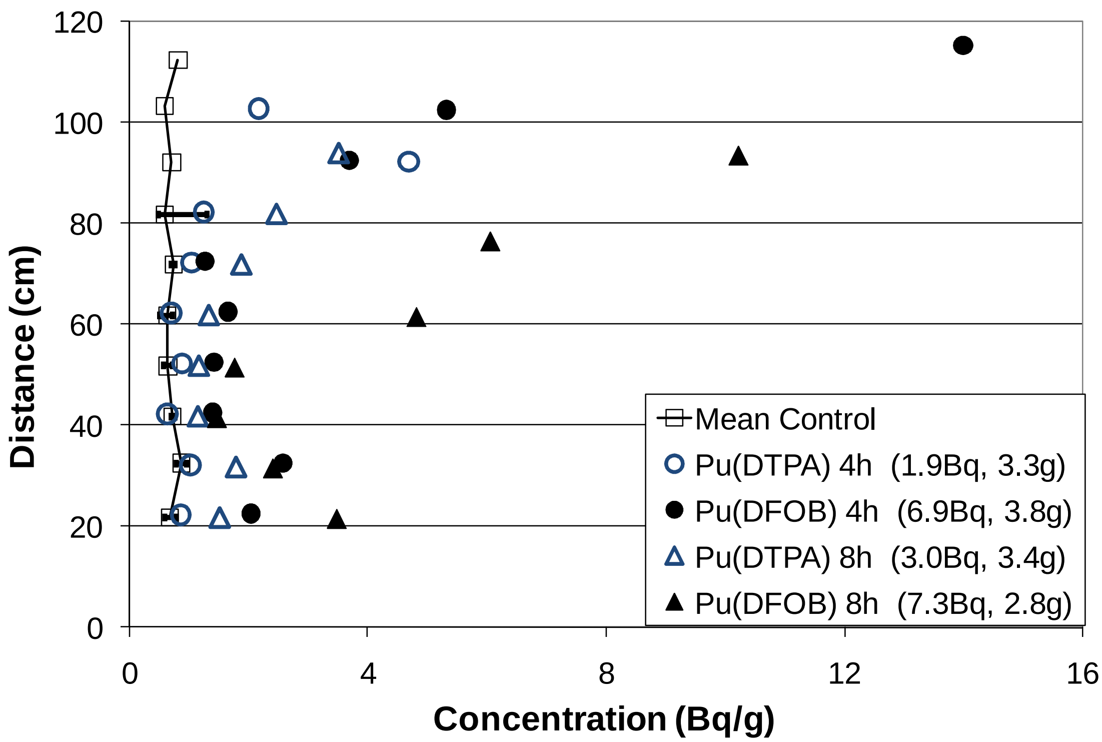

Figure 5.2 Concentration in corn shoot sections versus distance in 28 d old plants exposed to ^{238}Pu and non-labeled (control) solutions. The data are obtained from plants exposed to solutions with equal activities of either $Pu_2(DTPA)_3$ or Pu(DFOB) for 4 and 8 hours. The legend contains shoot Pu activities and shoot masses. Mean control data originate from two control plants; relatively small error bars (shown with the square markers) are available for the two plants up to about 85 cm. However only one control plant grew taller than this distance, thus there are no error bars for the top three control data.

5.4.2 Velocity of Complexed-Pu in Corn

Velocity experiment shoot section concentration and distance data are presented in Figure 5.3. The data are mean concentration values (three replicate plants for each exposure time) of 23 day old plant shoots exposed to Pu(DFOB) for 10, 20 and 40 minutes. Following exposure, the shoots were cut at 0, 10, 20, 30, and 40 cm heights. The distance data are midpoint shoot section distances from the bottom of the soil just above the solution container. The tissues >40 cm from the soil level (thus >58 cm from the soil bottom) are combined into one sample referred to as the top shoot. Mean top shoot distances were ~69 cm for 10, 20, and 40 minute plants. The top shoot data indicate the presence of Pu in plants exposed for 20 and 40 min whereas no or very little Pu is detected in plants exposed for 10 min. The solid oval highlights that top shoot concentrations of 10 min exposure plants are near the control concentration. The dashed oval highlights that top shoot concentrations of 20 and 40 minute exposure plants are significantly greater than the 10 min and control plants. Although concentrations in lower shoot sections of exposed plants exceed control concentrations, the differences are less than for the top shoots. This is due to the preferential accumulation of Pu in the top shoots with evaporation as noted above.

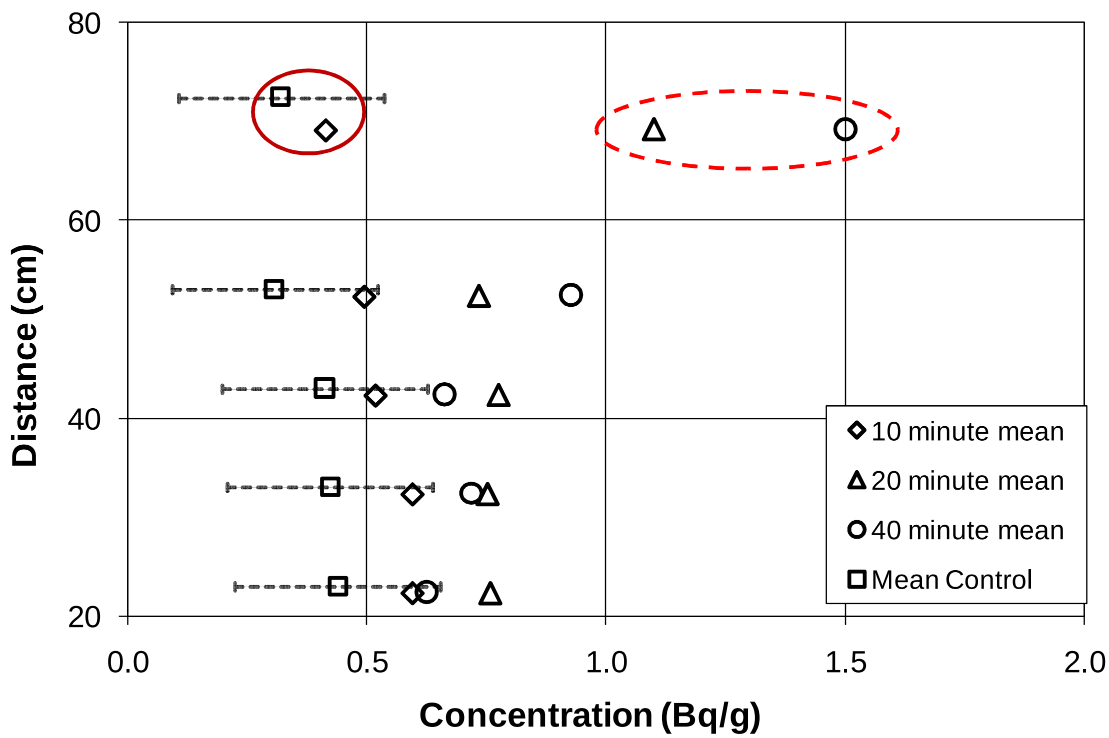

Figure 5.3 The data are mean concentrations of shoot tissue sections from plants (n=3) with 10, 20, and 40 minute exposures to Pu(DFOB). Control data have error bars showing two standard deviations from the mean concentrations. For clarity, error bars of exposed plants have been omitted, but were approximately the same as those of the control. Concentration data from 10 min plants are within two standard deviations of the control concentrations, whereas 20 and 40 min plant concentrations are greater than the control and 10 min plant data. The top section data from 20 and 40 min plants (dashed circle) are distinct from the control and 10 min plants (closed circle), indicating the presence of Pu.

The top shoot data from Figure 5.4 for control, 10 min, and 20 min plants are plotted as a function of exposure time in Figure 5.4. This more clearly depicts the presence of Pu in the top shoots of 20 min exposure plants and its absence in the controls (i.e., zero exposure time) and 10 min exposure plants. The solid line is the mean concentration of three control plants and the dashed line is the control mean plus two standard deviations above the mean.

Plutonium velocity, v_{Pu}, is calculated from the Pu travel distance and the exposure time. The minimum travel distance to the top shoots is 58 cm (18 cm through the primary root in the soil and 40 cm in the shoot). From Figs. 5.3 and 5.4, the bounds on travel time to 58 cm are 10 and 20 min, thus yielding the Pu velocity range as 174 cm/h $\leq v_{Pu} <$ 348 cm/h.

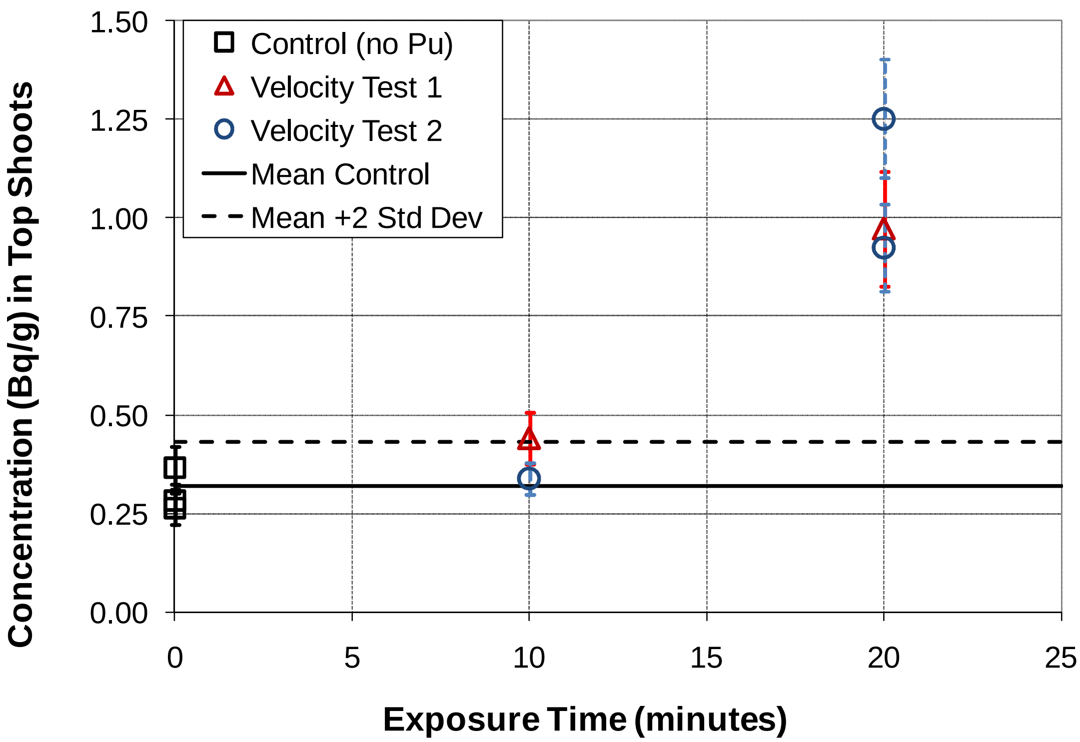

Figure 5.4 A plot of Pu concentration versus exposure time in top shoots (58 cm travel distance). The solid line indicates mean control activity and the dashed line is mean control activity plus two standard deviations. Pu concentrations in plants exposed for 20 min clearly exceed the Pu concentrations of the controls and 10 min plant samples.

5.4.3 Water Velocity and the Retardation of Complexed-Pu in Corn

In corn and grasses, vascular bundles contain xylem, phloem, and bundle sheath cells (Jones 1985). The xylem carries water and nutrients upward to the above ground tissues and the sites of photosynthesis. Phloem transports the products of photosynthesis downward to all plant parts. For short time periods with high transpiration rates, nearly all water moving into the plant is lost to the atmosphere; only very small amounts of water contribute to plant growth. The average water velocity was calculated using measured transpiration rates and estimated total xylem area. Figure 5.5 is a photomicrograph of a stem cross section at 5 cm height. Dimension measurements were made using image outlines and computer calculated distances based on calibration to microscopic settings using iSolution Lite software v. 7.7 (Image & Microscope Technology, Daejeon, South Korea). The average stem area of two control plants was 1.0780 cm^2 and the xylem area/stem area ratio was 0.0115 thus, the stem xylem area, A_x, at 5 cm above the soil is 0.0124 cm^2. The average transpiration rate, Q, (solution flow rate) of two control plants was 9.98 cm^3/h during 24 h under continuous lighting. Thus, the average xylem water velocity at 5 cm is:

$$v_w = \frac{Q}{A_x} = \frac{9.98\ cm^3 / h}{0.0124\ cm^2} = 800\, cm / h \qquad \text{Eqn. 5.1}$$

The calculated xylem water velocity has a 20% error estimate based on the standard deviation of the bundle areas. The Pu velocity was measured to be at least 174 cm/h, so a first estimate of the Pu retardation factor. R_{Pu}, in corn is:

$$R_{Pu} \approx \frac{v_w}{v_{Pu}} = \frac{800\ cm / h}{174\ cm / h} = 4.6 \qquad \text{Eqn. 5.2}$$

Equation (5.2) must be viewed as an approximate estimate for R_{Pu}. First, v_w was estimated at a fixed location in the stem, while v_{Pu} was measured over a 58 cm distance. It is doubtful that v_w is constant with elevation, although one would not expect it to be highly variable (Jones 1985). Second, v_w is an average velocity over the xylem cross sectional area, while v_{Pu} is a lower bound estimate for the maximum Pu velocity. To be consistent, v_w should also be a maximum water velocity (v_w could vary with the radial position in the stem). All things considered, our measurements suggest that R_{Pu} for corn xylem falls between 1 and 10.

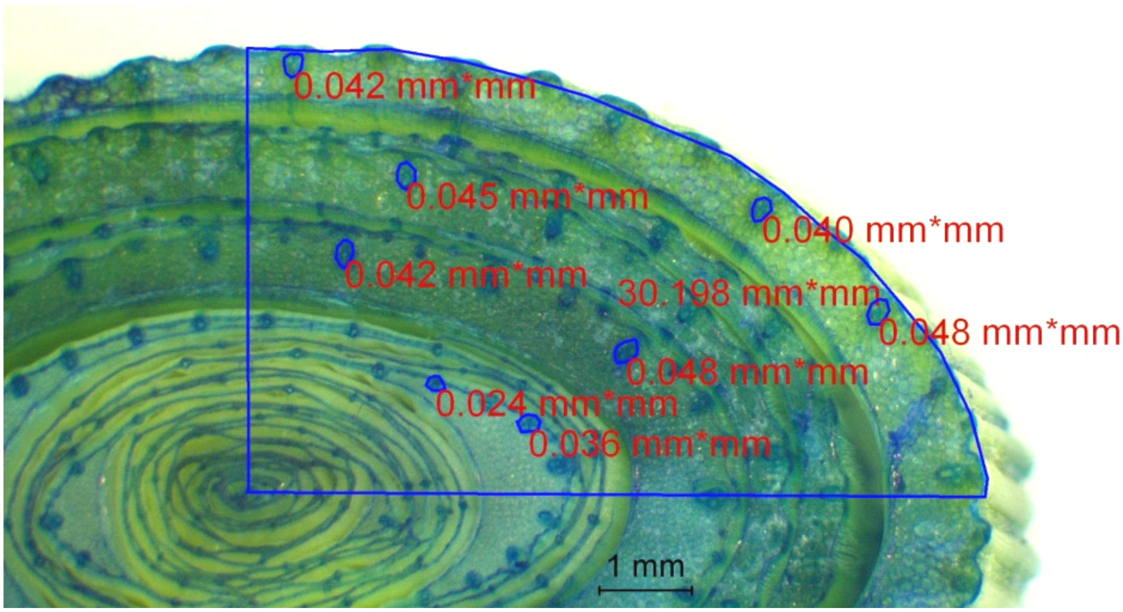

Figure 5.5 Photomicrograph of the cross section of a control plant stem cut 5cm above the soil. The tissue is stained to increase contrast of the vascular bundles, which are the dark oval structures. Dimension measurements were made for the vascular bundle areas shown in the upper right quadrant of the stem.

5.4.4 Accumulation of Complexed-Pu in Corn Shoots and Roots

The Pu velocity test data and figures discussed above focus on short term exposures of 0 – 40 minutes. Additional experiments were conducted in which plants were exposed to Pu(DFOB) for longer time intervals. Figure 5.6 is a plot of total shoot activity as a function of light exposure time (i.e., the cumulative time of active light). The data in Figure 5.6 originate from several experiments and include the data in Figs. 5.3 – 5.4. For convenience the data are divided into two sets. Set 1 data are from single plants exposed for 10, 20, 40, 80, 840, 1680, and 3290 minutes. Set 2 data are from duplicate plants exposed for 10, 20, 40, 100, 360, and 1440 minutes. Since the total amount of Pu in the nutrient solutions varied (~74 KBKq/plant for plants exposed for 40 min or less and ~37 KBq/plant for plants exposed for longer times) the ~37 KBq/plant data have been doubled to normalize their shoot activities.

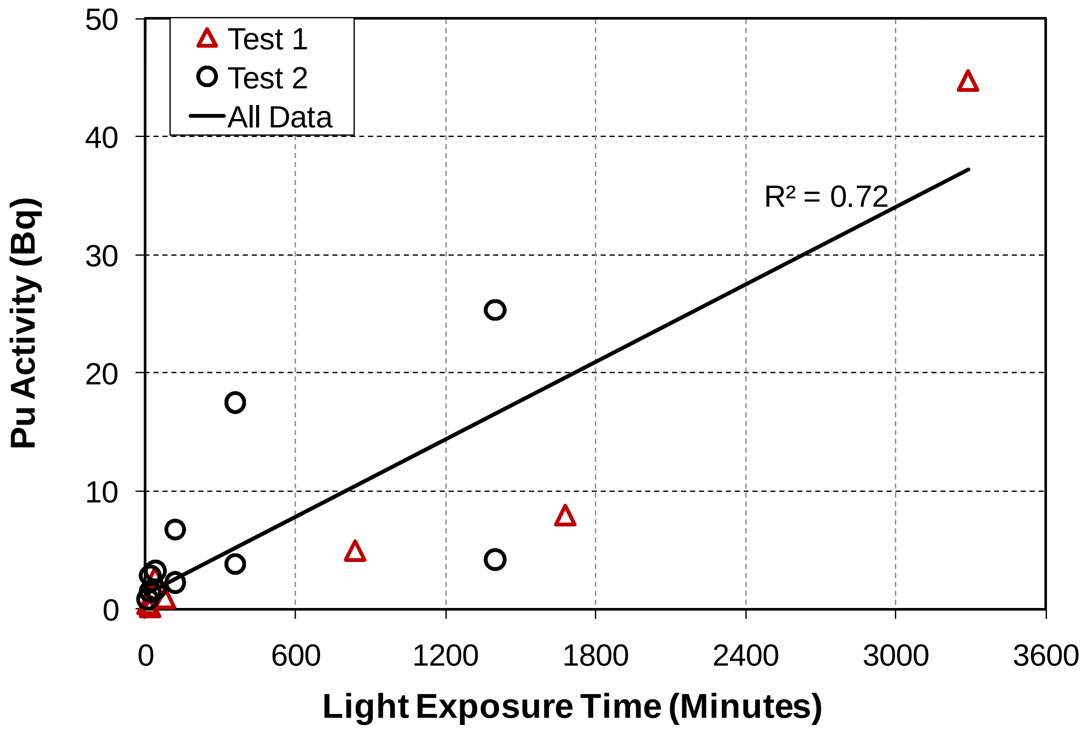

Figure 5.6 Pu activities in shoots are plotted as a function of time for 18 plants exposed to Pu(DFOB). Set 1 data (triangles) are from an experiment with single plants exposed for 10, 20, 40, 80, 840, 1660, and 3290 minutes. In set 2 (circles), duplicate plants are exposed for 10, 20, 40, 120, 360, and 1440 minute periods. The X-axis is expressed as light exposure time since those plants exposed for times in excess of 840 minutes (14 hours) are combined time periods during which those plants were illuminated.

There are two principal observations from Figure 5.6. The first is that Pu activity increased with light exposure time up to the maximum exposure time of

3290 minutes. This is consistent with observations for transition metals complexed with chelants in solution (Nowack et al. 2006) and for Pu uptake from soil (Garland et al. 1981) over much longer time intervals. The second observation is the large variability; for example, shoot activities of the 360 and 1400 min duplicate plants which vary by up to a factor of four. Plant uptake variability in both roots and shoots of equivalent plants was observed in the data of all experiments. There are many factors which may contribute to this variability including natural variability in root size and surface area, transpiration rate, overall plant size, etc.

To examine the uptake, accumulation, and distribution trends over longer term exposures and to account for plant variability, 3 sets of 3 replicate plants each were exposed to Pu(DFOB) for 3, 7 or 10 days respectively. Figure 5.7 shows that the mean shoot Pu activity increased linearly with time (correlation coefficient of 0.98). Figure 5.8 however shows a comparison of shoot activity versus transpiration volume (solution consumed) at each exposure time and indicates little or no correlation.

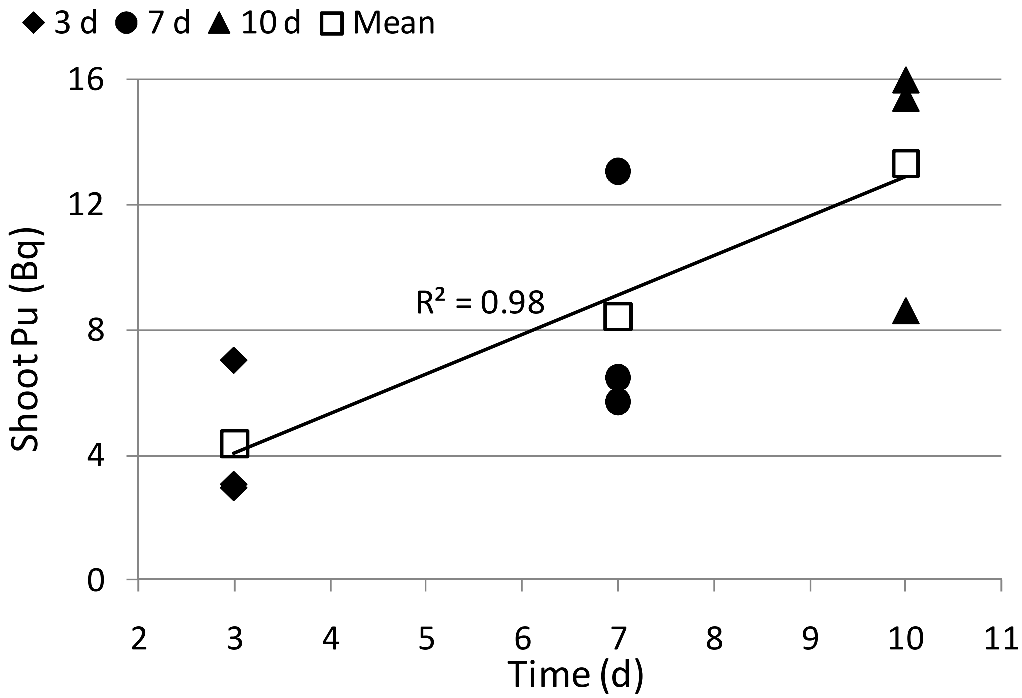

Figure 5.7 Total shoot Pu activity versus time of plants exposed to Pu(DFOB) for 3, 7, and 10 days (three replicate plants at each time).

Clearly, a better defined relationship exists between Pu uptake and translocation into the shoot versus time than versus transpiration volume. Figure 5.8 shows that for the 3 and 7 day exposures, there is practically no correlation between total shoot activity and transpiration volume, while only one data point leads to some correlation for the 10 day exposure. The Pu transport across the root is not proportional to water transport.

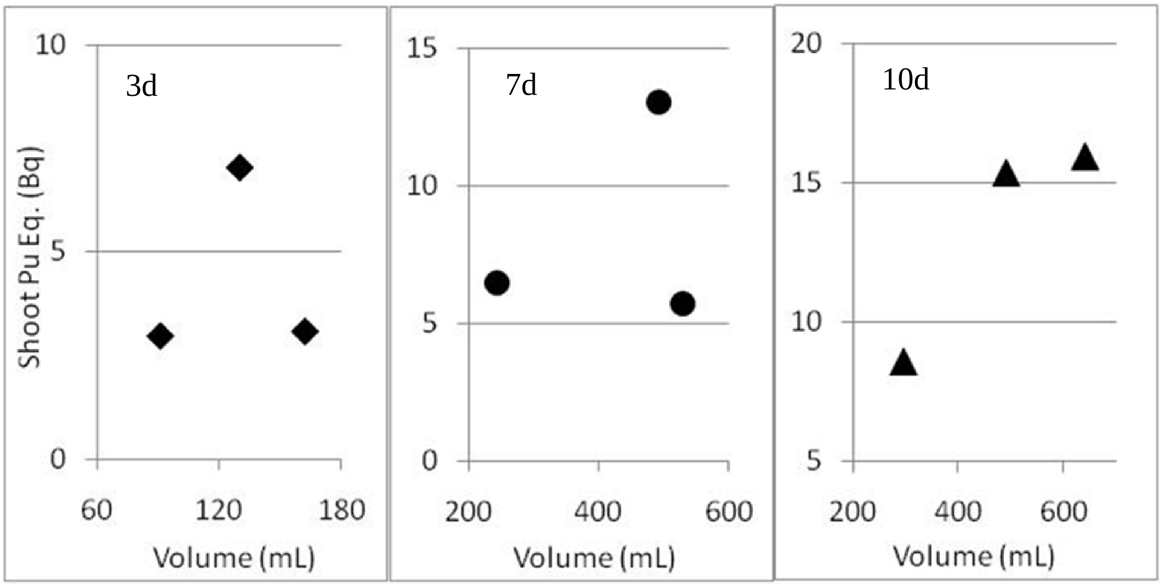

Figure 5.8 Total shoot Pu activity versus transpiration volume of plants exposed to Pu(DFOB) for 3, 7, and 10 days (three replicate plants at each time).

If soluble Pu moves across the root tissues precisely with the water, then the xylem fluid concentration would be the same as the solution concentration. The Pu in the shoots must enter in the transpiration volume V_t. Since the transpiration volumes (100 – 600 mL) are large compared to the small root xylem volume (< 1mL), it is reasonable to assume that very little Pu remains in the root xylem at the end of the experiment compared to the Pu in the shoot. If the shoot activity is A_t, then one can calculate the concentration of Pu that crossed into the xylem in the transpiration volume as A_t/V_t. If this calculated concentration is less than the solution concentration, then Pu is either retained by the roots outside of the xylem or excluded at the root surface.

The ratio of A_t/V_t for the 3, 7 and 10 day plants is plotted for 3 different times in Figure 5.9. The overall mean value of A_t/V_t is 0.028 Bq/cm^3. The nutrient solution Pu concentration is 16.5 Bq/cm^3, which is greater than the shoot activity divided by transpiration volume by a factor of 580. This quantity differs from the concentration ratio which is the ratio of concentration in the plant divided by the concentration in the water (or soil) (Lee et al. 2002). Clearly Pu is excluded from the xylem. The activity distribution of the whole plants shows that an average of 97% of the Pu activity is in the solution roots outside of the xylem. Research quantifying Pu transport through the root and examining correlations between the uptake of iron and Pu is reported in Chapters 6 & 7.

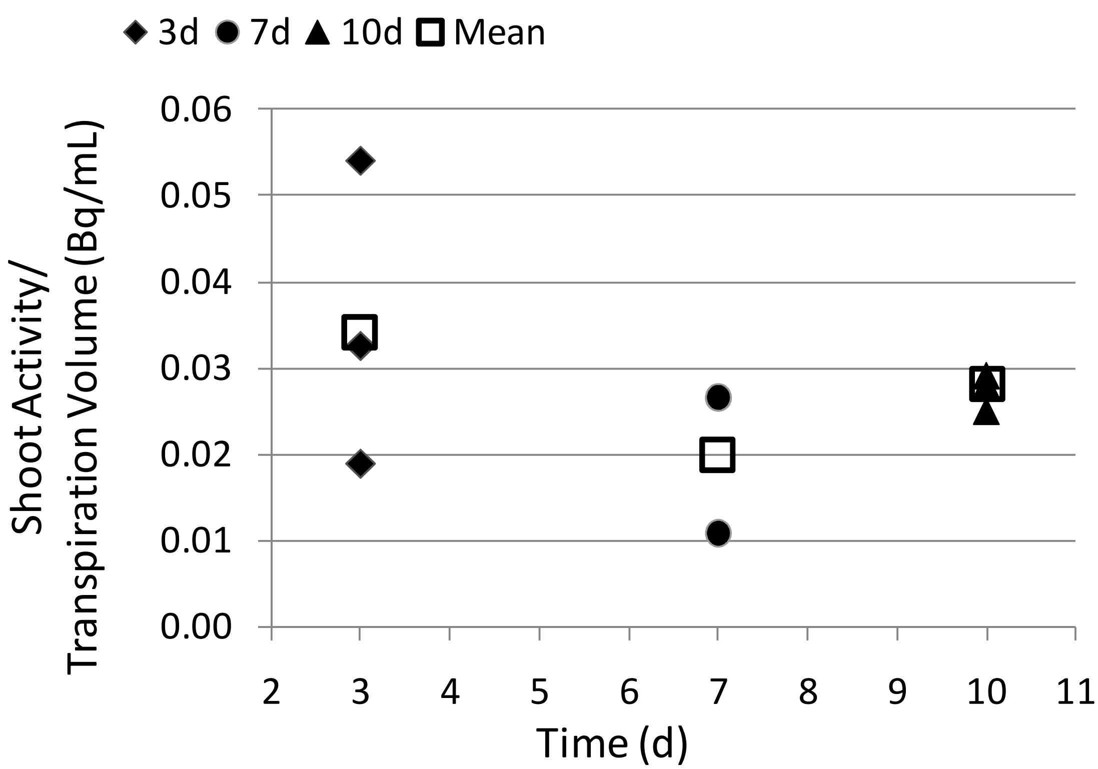

Figure 5.9 The shoot activity divided by the transpiration volume of 3, 7, and 10 d plants along with the mean for each exposure time. The nutrient solution Pu concentration is 16.5 Bq/cm^3 and the overall mean shoot activity/ transpiration volume is 0.028 Bq/cm^3 indicating that 1/580th of the Pu entered the xylem.

5.5 Conclusion

In summary, the retardation of Pu complexed with the siderophore DFOB is estimated to range between 1 and 10. This is the first plant study involving the use of DFOB and Pu. Using discrete sampling, we have shown a concentration distribution in corn shoots, examined shoot activity as a function of time and transpiration, and demonstrated that most of the Pu remains in the root tissues. Our work is focused on the initial movement of Pu into plants, hence it does not represent steady-state uptake. The effect of plant uptake on Pu transport in soil is influenced by the density of roots and other factors, such as soil type, type of deposition, and Pu species; however these results suggest that plant transport can be a conduit of rapid upward Pu movement that can be a million times more rapid than reduced Pu transport in soil. This research is consistent with the Pu transport modeling results of Demirkanli et al. (2009) because our estimated Pu retardation is in the order-of-magnitude range of their simulated values for the Savannah River Site lysimeter grass plants. These results may have implications on the Pu pathways assumed for calculated risks associated with Pu in near surface and surface soils.

CHAPTER SIX

RELATIONSHIP BETWEEN CORN UPTAKE OF PU(DFOB) AND FE(DFOB)

6.1 Abstract

Two types of experiments were conducted to study the plant uptake of Pu(DFOB) in relation to Fe(DFOB) and to test the hypothesis that Pu uptake may occur based on plant requirement for Fe. Both experiments were performed using *Zea mays* (corn) grown with its distal roots in solution and proximal roots in soil. In the first, plants were grown in unlabeled nutrient solutions from day 7 to day 21, at which time plants were exposed for two days to ~37KBq each of ^{238}Pu and ^{59}Fe complexed with DFOB, a bacterial siderophore. The complexed Pu and complexed ^{59}Fe were transported into the roots and the shoots of the plants. About 40% more ^{59}Fe activity than Pu activity was found in the shoots, whereas 600% more Pu activity than ^{59}Fe activity was found in the roots. Concentration profiles with shoot length indicated that the distribution trends of complexed ^{59}Fe and Pu were quite similar and were generally distinct from the shoot concentration profiles of stable elements. This suggests that once inside the xylem Fe and Pu are physiologically treated in a similar manner. In the second experiment, plants were exposed to complexed Pu at day 21 with stable Fe concentrations of 0 or 10 times the normal nutrient solution Fe concentration (1.07×10^{-5} M). The Pu uptake was not affected by changes in the nutrient solution Fe concentration. It is possible that the Fe contained in intracellular root tissues (inside the root but outside the xylem) from earlier plant exposure to

relatively large stable Fe concentrations in solution did not result in a zero Fe condition in the root, even though Fe was not present in solution containers.

6.2 Introduction

Iron is an essential nutrient required by plants, animals, fungi, and most microbes. It is commonly metabolized in activities that make use of its redox potential as an energy source. In plants, a primary function of iron is in the development of chloroplasts which are essential for photosynthesis; approximately 80% of the plant iron is used in this process (Marschner 1995). Chlorosis is a fairly common condition in which a plant's leaves have discolored or necrotic spots caused by an insufficient production of chlorophyll. Chlorosis can be caused by an iron deficiency. Photosynthesis occurs in the leaves therefore iron must be transported from the soil to developing chloroplasts in new leaf tissues. Once the iron is metabolized in this process, it becomes incorporated in the leaf cell structure and cannot be recycled (Brown 1978). Due to its vital role in photosynthesis, plants have evolved physiological mechanisms to maintain a steady supply of iron from the soil. Importantly, while iron is an abundant element, it has a very low solubility at pH values favorable for plant growth. So plants must perform two critical tasks to attain their required iron; first they must solubilize iron from the soil and second they must maintain high affinity transport pathways in order to incorporate iron rapidly when it is needed.

Upon entering the xylem, Fe is transported as soluble Fe(III) complexes until it is metabolized. Different plants, however, use different methods to incorporate Fe (Romheld and Marschner 1986). Strategy I plants, dicots and many monocots, exude protons and simple low-molecular weight entities to solubilize iron. In this strategy, Fe(III) is reduced to Fe(II) during induction through the root cells, and then it is re-complexed with molecules such as citrate and transported in xylem as an Fe(III) complex. Strategy II plants, monocots of the Poaceae family (grasses), exude higher molecular weight complexes called siderophores (Greek for "iron bearers") to both obtain and transport complexed Fe(III) through the root (Romheld and Marschner 1986, Yehuda et al. 1996, Schaaf et al. 2004, Suzuki et al. 2006). The form in which Fe is transported in the xylem of strategy II plants after induction through the root is not clear. Although it is known that uptake of Fe is enhanced by complexation with siderophores, it is not known if the transport of Fe in xylem of strategy II plants occurs as a Fe-siderophore complex. Curie et al. (2009) indicates that in xylem transport Fe reacts with poorly characterized organic ligands, including precursors of phytosiderophores (nicotianamine) and known oligopeptides of plant transporters.

A good review of how siderophores affect iron uptake in plants is found in Crowley (2006). Several studies have demonstrated that plant and fungal metal uptake is enhanced in the presence of bacterial siderophores (Bar-Ness et al. 1992, Ardon et al.1998). However there is also clear evidence that Fe uptake in grass plants is faster and up to 40 times more efficient when it is complexed with native phytosiderophore versus bacterial siderophores or synthetic chelates (Romheld and Marschner 1986; Walter et al. 1994). Experiments with this degree of physiological detail are not available for plant uptake of Pu.

Studies of the dissolution rates of Fe and other metals with the siderophore DFOB have shown that the solution complexation properties alone may or may not liberate a significant quantity of actinides from a soil or mineral matrix (Ruggiero et al. 2001; Wolf-Boenisch and Traina 2007). Recent desorption studies have demonstrated that the process of liberating metals from a solid matrix may occur faster and much more effectively in the presence of both siderophores and oxalate or citrate (Reichard et al. 2005; Loring et al. 2008). The synthesis of high molecular weight siderophore molecules has a high metabolic cost for plants, hence it is not efficient for plants to produce and exude siderophores unless they obtain iron in the process. Although questions remain about the mechanisms which siderophores use to increase metal solubility, research has demonstrated that once the metals are in solution, siderophores are very strong complexants and keep metals soluble under many conditions. In fact, recent research by Xu et al. (2008) demonstrated that organic siderophore decomposition products significantly increased the mobility of Pu in soil.

Since plants have no known need for Pu, its uptake may occur in response to a nutrient requirement for iron (Neu et al. 2002). Fe(III) and Pu(IV) are similar in that they have: 1) identical charge/ionic radius ratios of 47 nm^{-1}; 2) similar first hydrolysis constants (Fe^{3+} LogK = 11.1, Pu^{4+} LogK = 12.2); and 3) nearly identical complexation constants with DFOB (Fe^{3+} LogK = 30.6, Pu^{4+} LogK= 30.8). Thus, it has been suggested that bacterial and plant siderophores that incorporate Fe may complex Pu, thereby enhancing its availability to and mobility in plants (Neu et al. 2002; Ruggiero et al. 2002; John et al. 2001). Although John et al. (2001) found that siderophores enhance Pu accumulation in a bacterium (*Microbacterium flavescens*), similar observations have not been made in plants. Ruggiero et al. (2002) studied the structural properties and complexation of Fe and Pu with several siderophores including DFOB. Figure 6.1 is a reproduction of spatial models showing the metal free DFOE (denoted as DFE in John et al. (2001)) and DFOE complexed with Fe and with Pu. The siderophores DFOB and DFOE have a tri-hydroxamate molecular structure and have one different functional group. DFOE has a cyclic ring structure whereas DFOB is linear.

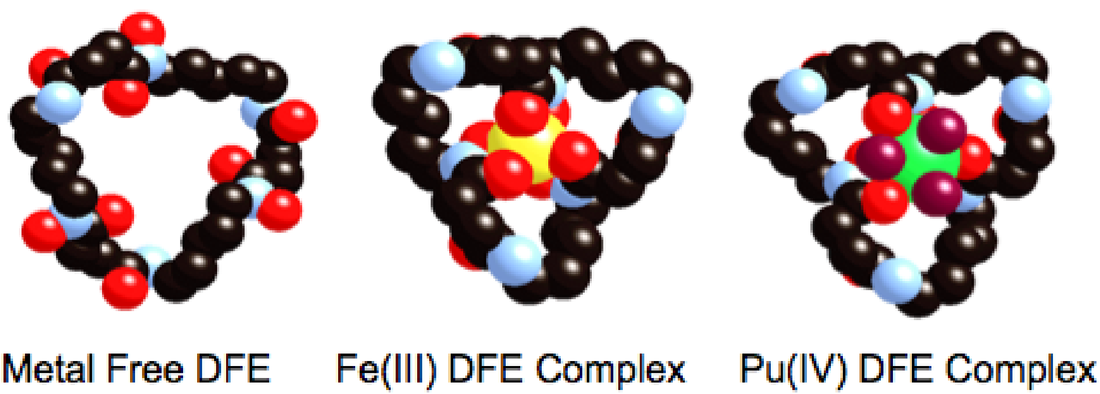

Figure 6.1 Spatial models of the microbial siderophore DFOE: at left the tri-hydroxamate molecule is uncomplexed, at the center it is complexed with Fe(III), and at right it is complexed with Pu(IV). In this illustration, subtle differences in the Fe and Pu complexes may be significant with respect to their uptake and incorporation across cell membranes. The Fe in the complex is 6-coordinate and the Pu is 9-coordinate (with 3 bound waters), so while the complex structures are approximately the same size, differences exist. (Figure from John et al. 2001)

John et al. (2001) studied the uptake amounts and rates of Fe and Pu complexed with DFOB (at 80 μM of metal complexed with 400 μM DFOB) with the bacterium (*Microbacter flavesence*). They tested the effects of competition between the complexes and demonstrated that both Fe and Pu are taken into the bacterium when added singly or together and that the complexed metals were recognized by the same proteins associated with transport channels and competed for the same sites of entry into bacteria. However, important differences were observed:

- Bacterial uptake of Pu was one quarter of that of Fe
- Fe incorporation into the cell was ~7 times faster than Pu
- In displacement tests, the Fe could generally displace some Pu however the longer the Pu was in contact with the bacteria, the smaller the degree of displacement. This was attributed to the slow Pu rate of entry into the cell wall, yet once inside Pu was more difficult to remove.
- Based on the slower incorporation of Pu and cell lysing tests (designed to gain information about the location of Pu and Fe), much less Pu than Fe passed through the cell wall.

The research described here was motivated by evidence of microbial uptake, competition, and recognition by the transport channels of complexed Pu and Fe (John et al. 2001) and earlier plant research (Garland et al. 1981; Cataldo et al. 1988) which demonstrated that Pu behavior in soybean xylem exudates was quite similar to that of Fe. The hypothesis was that Pu is transported into plants in substitution for Fe due to similarities between the metal chemistry, the siderophore-complexed metals, and possibly passage into the plant roots via high affinity uptake pathways. Our experimental design has been proven useful for the sensitive examination of Pu distribution and uptake required to measure Pu velocities in corn plants (Thompson et al. 2009; Chapter 5). This same plant growth and exposure method has been adapted to study Pu and Fe plant uptake.

The research objectives are to characterize and compare the distributions of Pu, ^{59}Fe, and several stable elements, including stable Fe, in corn plants which were simultaneously exposed to approximately equal activities (not equal molar quantities) of Pu and ^{59}Fe, to perform an activity distribution analysis, and, in separate experiments, to examine for potential enhancement or interference effects of varying the stable Fe nutrient solution concentration on Pu uptake.

6.3 Experimental

6.3.1 Conditions

The plant growth, exposure, and tissue processing steps were conducted as described in Thompson et al. (in press); Chapter 5. An important aspect of this work was our plant growth and exposure system in which plants were grown in soil pots resting on top of nutrient solutions. The distal plant roots were in direct contact with the solution and the more proximal roots were in the soil. This system provided a way to expose plants to radioactivity without concern of metal sorption to soil.

Two plant treatments are described below; the corn plants were 23 days old at the end of their respective exposures in both treatments. In tests designed to compare the uptake and distributions of Pu and Fe in corn, three plants were exposed for two days to ~37KBq of ^{238}Pu (4.71×10^{-10} M) and ~37KBq of ^{59}Fe (6.68×10^{-13} M) complexed with 9.8×10^{-5} M DFOB in nutrient solution. Importantly, the DFOB existed at 5 to 8 orders of magnitude greater concentrations than the ^{238}Pu and ^{59}Fe and both metals form extremely strong complexes with DFOB, insuring both radionuclides existed as complexed moieties during the experiments. The pH 6.0 solutions contained 1.07 x 10^{-5} M (0.60 mg/L) stable iron and (in mg/L): 946 $Ca(NO_3)_2 \bullet 4H_20$, 150 KCl, 120 $MgSO_4$, 68 KH_2PO_4, 0.69 H_3BO_3, 0.06 $ZnSO_4 \bullet 7H_20$, 0.024 $Na_2MoO_4 \bullet 2H_20$, 0.022 $MnCl_2 \bullet 4H_20$, and 0.017 $CuCl_2 \bullet 2H_20$. The analysis of the dual labeled plant tissues was performed via liquid scintillation and ICP-MS. In the second treatment, plants were grown in soil pots and usual nutrient solutions until 2-3 days prior to exposure. At which time, the nutrient solution concentrations of Fe were changed to contain either zero or 1.07 x 10^{-4} M Fe(III) (termed 0x Fe and 10x Fe) while the concentrations of other nutrients were prepared as described above. Five plants each were exposed to ^{238}Pu(DFOB) at ~37KBq/plant in solutions containing zero or 1.07 x 10^{-4} M Fe(III). In these latter plant treatments, the plant tissue analysis of Pu was performed as described previously in Thompson et al. (in press); Chapter 5.

6.3.2 Analysis of plants labeled with ^{238}Pu and ^{59}Fe

Plant tissues were digested with concentrated HNO_3 and 30% H_2O_2. The resulting digests, 8 mL of sample in 0.1 M HNO_3, were split: 7 mL were diluted to 8 mL and combined with 12 mL of Ultima Gold AB cocktail for liquid scintillation analysis, and 1 mL was diluted to 10 mL and analyzed for Mg, K, Ca, Fe, and Mo via Inductively Coupled Plasma-Mass Spectrometry (ICP-MS). The tissue samples consisted of roots in solution, roots in soil, and measured shoot sections. In general, the roots in the soil (Figure 5.1) include two types of roots: the adventitious roots and the primary root. The primary root connects the roots in solution with the rest of the plant, thus it is the conduit for upward xylem transport of Pu. Adventitious roots in the soil were not in direct contact with Pu. All root samples were analyzed, however the terms root and root tissue used in the discussion below apply only to the roots in solution. The roots in soil had negligible radioactivity and are not reported. This is most likely due to two factors. First, the primary root in the soil had very small masses in comparison with both the solution roots and the shoot sections. Second, these experiments were relatively short term exposures therefore little to no redistribution was observed into the other root tissues.

The liquid scintillation analysis of ^{238}Pu and ^{59}Fe was performed using a Wallac Model 1409 counter. ^{238}Pu was detected as an alpha peak at 5.49 MeV and ^{59}Fe was detected as a relatively broad beta spectrum with a maximum energy of 1.57 MeV and average beta energy of 0.46 MeV. Nuclides were analyzed simultaneously using pulse shape discrimination (PSA = 100) which was optimized to detect both the ^{238}Pu alpha and ^{59}Fe beta signals with minimal interferences. Examples of the spectra of ^{238}Pu and ^{59}Fe are shown in Appendix A for reference. The solution internal spike ^{238}Pu recovery was 103%, ^{59}Fe recovery was 87%, and plant tissue data were not adjusted for recovery. The nutrient solutions were amended with ^{238}Pu and ^{59}Fe complexed with DFOB, such that the respective activities presented to the plants were equal at the time of their exposure based on the stock ^{238}Pu and ^{59}Fe solution reference dates. However, ^{238}Pu has an 88 y half-life whereas ^{59}Fe has a 44.5 d half-life, hence the amount of Fe decay between plant exposure and sample counting must be taken into consideration. Tissue samples were counted 7 d after exposure so data were decay-corrected by multiplying the measured ^{59}Fe by a factor of 1.115. The majority of sample counting errors of ^{238}Pu and ^{59}Fe were less than 10% at the 1 σ level. Relatively very small alpha and beta activities were observed in control plant tissues. The control plants were not exposed to ^{238}Pu, ^{59}Fe, or DFOB, but had detectable activities in both the ^{238}Pu alpha and ^{59}Fe beta spectra which were from uptake of naturally occurring radionuclides in the potting soil. All plant radioactivity data were corrected for these contributions by subtracting the control activity.

The concentrations of Mg, K, Ca, Fe, and Mo in the plant sample digests were measured using a Thermo X-Series II Inductively Coupled Plasma Mass Spectrometer. An internal standard solution containing Sc, Ga, Y, and In was simultaneously aspirated with the samples. To reduce interferences, the instrument was operated using collision cell technology employing an 8% H_2 / 92% He gas mixture. Calibration standards were prepared using single and multi isotope standards (High Purity Standards, Charleston, SC). All samples and standards were prepared in 2% ultrapure HNO3 (BDH Aristar Ultra) in distilled-deionized water. Sample concentrations were obtained by accounting for the digest fraction and then dividing by dry tissue mass. The ICP-MS analyte concentration results had <5% respective errors except for Ca which had roughly 20% analytical errors.

Table 6.1 shows the relevant molar solution concentrations of the conditions for both dual labeled and 0x and 10x Fe plant uptake experiments. Although the ^{238}Pu and ^{59}Fe activities were approximately equal, due their respective decay rates the molar quantities are quite different. With the exception of the 0x Fe condition, the concentrations of Fe in the solutions are much greater than that of ^{238}Pu or ^{59}Fe. The DFOB concentration was selected based on the success and database of earlier uptake and velocity experiments (Chapters 4 & 5), and the complexant concentrations utilized in similar Pu uptake research (Lee et al. 2002).

Table 6.1 Solution Concentrations of Complexant, Fe, Pu, and ^{59}Fe

Experimental Condition	**DFOB**	**(Molar Solution Concentration)** **Fe**	**Pu**	**^{59}Fe**
Pu and ^{59}Fe	9.8×10^{-5}	1.07×10^{-5}	4.7×10^{-10}	6.7×10^{-13}
0x Fe	9.8×10^{-5}	0	4.8×10^{-10}	0
10x Fe	9.8×10^{-5}	1.07×10^{-4}	4.8×10^{-10}	0

6.4 Results and Discussion

For clarity in the Chapter 6 discussion, the terms Pu and ^{59}Fe refer to radioisotopes which were complexed with DFOB prior to introduction to the nutrient solution and exposure to the plants. Pu denotes ^{238}Pu, the only isotope of Pu used in this research. Fe denotes stable iron, whereas ^{59}Fe indicates the radioisotope which was used only in the dual labeled experiments. One can infer from Table 6.1, in nutrient solution the metals are entirely complexed with the siderophore. To enter the shoots these metals must enter the xylem and since the metals are complexed in xylem but it is not clear if they remain complexed with DFOB and analyses were not performed to determine metal complexation in the shoots, Pu and ^{59}Fe denote the activities or concentrations observed. To clearly designate the use of complexed metals, when stable isotope and radioisotope results are presented together the dual labeled data will be denoted as Pu(DFOB) or ^{59}Fe(DFOB).

6.4.1 Dual Labeled Plant Shoot Distribution Profiles

The concentration profiles of Pu and ^{59}Fe of the three dual labeled plants are shown in Figure 6.2. The concentration data are Bq per dry gram of shoot tissue and the shoot length data are at the midpoint of each shoot section, with zero distance at the soil surface (e.g., 5 cm data represents the 0-10 cm shoot section). The corn shoot tissues were processed by measuring and cutting the stem and leaves with the leaves straightened by elongation, thus shoot length is more accurate than shoot height because the leaves do not naturally extend vertically. Examining the Pu and ^{59}Fe data in each plant, the concentration profiles with shoot length are similar although their magnitudes differ. The main point of this plot is to demonstrate that concentration trends of both Pu and ^{59}Fe are similar within each plant although they differ somewhat between plants. Due to the total number of data on a given plot, the individual plant data are especially difficult to visualize with additional distribution data for comparison therefore averaged dual labeled experiment data will be discussed from this point forward.

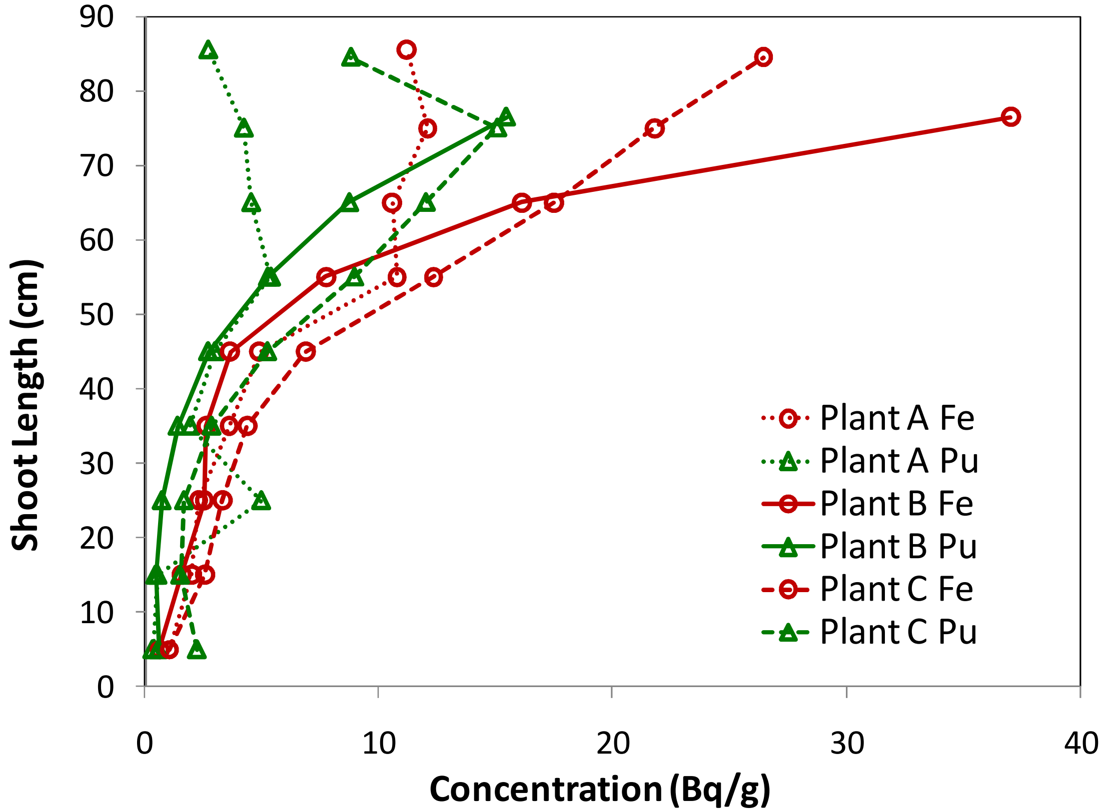

Figure 6.2 Tissue section concentrations of Pu and ^{59}Fe versus shoot length. The Pu data are open triangles, the ^{59}Fe data are open circles, and the lines linking both Pu and ^{59}Fe shoot data are consistent for each plant (e. g., the narrow dashed line is plant A and the solid line is plant B, etc.).

Shoot tissue mass and activity fraction data for the dual labeled plants are shown in Figure 6.3. The fraction data are obtained by dividing averaged data at a particular shoot length by the averaged total of the entire shoot. At the bottom left of Figure 6.3, about 7% of the averaged shoot Pu activity (open triangle) is contained in the bottom tissue section. From this plot, one can see that the distribution of the relative activity fraction data does not follow the shoot mass fraction distribution. If the activity fraction data were distributed uniformly with respect to the shoot mass, then those data would overlay the mass fraction data.

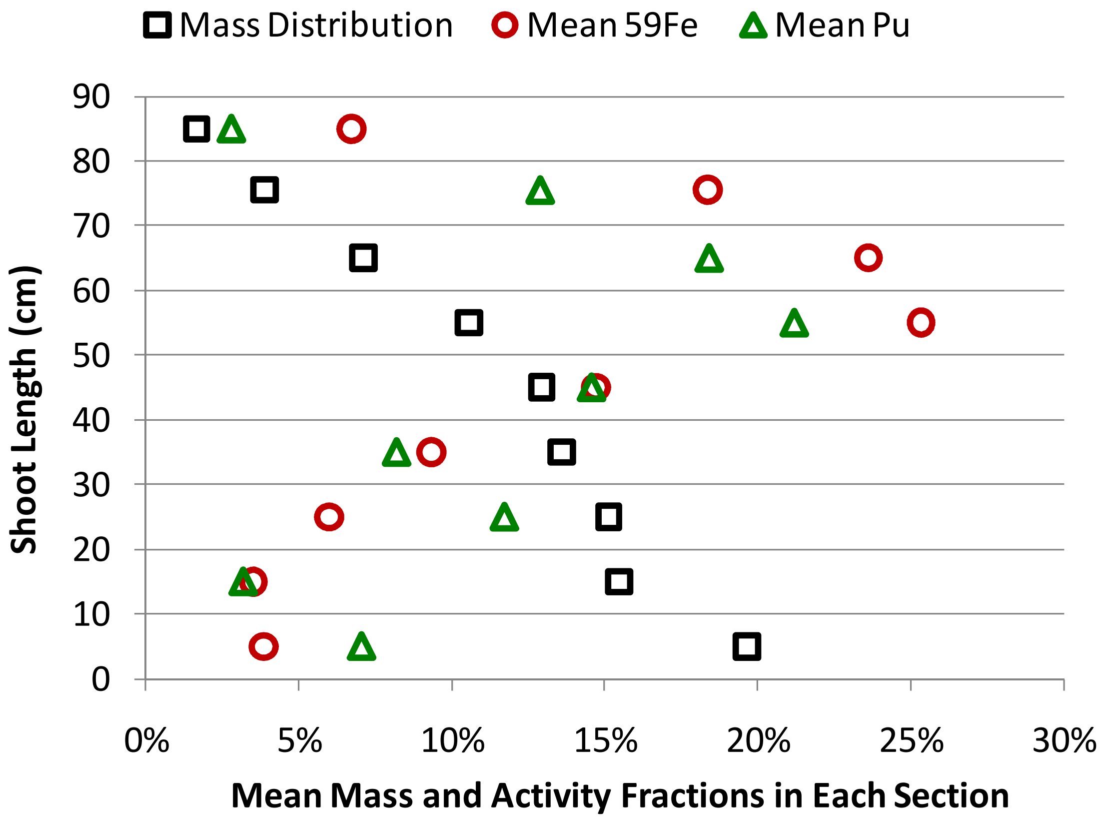

Figure 6.3 Mass and activity fraction data for dry shoot section masses and activities of ^{59}Fe and Pu averaged over the three dual labeled plants. Data are obtained by dividing each section value by the respective totals. For example, nearly 20% of the total shoot mass is contained in the bottom shoot section (the open square at bottom right) and about 2% of the total shoot mass is in the top tissue sample. Both ^{59}Fe and Pu activity fractions are less than the mass fractions below 40 cm, and above this shoot length, the activity fractions exceed the equivalent mass fractions.

Figure 6.4 is a combination of two plots showing the averaged concentrations versus shoot length on the left and at right the Pu and ^{59}Fe data have been transformed (non-dimensionalized) by dividing the averaged concentration of a particular stem section by the mean concentration of all the stem sections. The data are presented in this manner so that the concentration distribution profiles of different analytes (with greatly differing molar concentrations) can be viewed together as variations about their respective mean values. The concentration and relative concentration of an element that is uniformly distributed with respect to mass would plot as a straight line as a function of length. Comparing the left and the right plots, even though ^{59}Fe concentrations are generally greater than Pu, by transforming the data one can see that their shoot concentration distributions about their respective means are quite similar. The transformed concentration data of both Pu and ^{59}Fe are nearly identical from the bottom of the shoot up to the 45 cm section. Concentration minima are found in the bottom two sections for ^{59}Fe and Pu respectively and maxima are found in the 75 cm sections. (Top section tissue data were occasionally noisy, due to a relatively small amount of dry mass and due partly to unhealthy tissue near the uppermost leaves.) Beginning at 55 cm and moving upward, the ^{59}Fe concentration data exceed those of Pu showing that Fe is somewhat more concentrated in the upper shoot tissues than Pu.

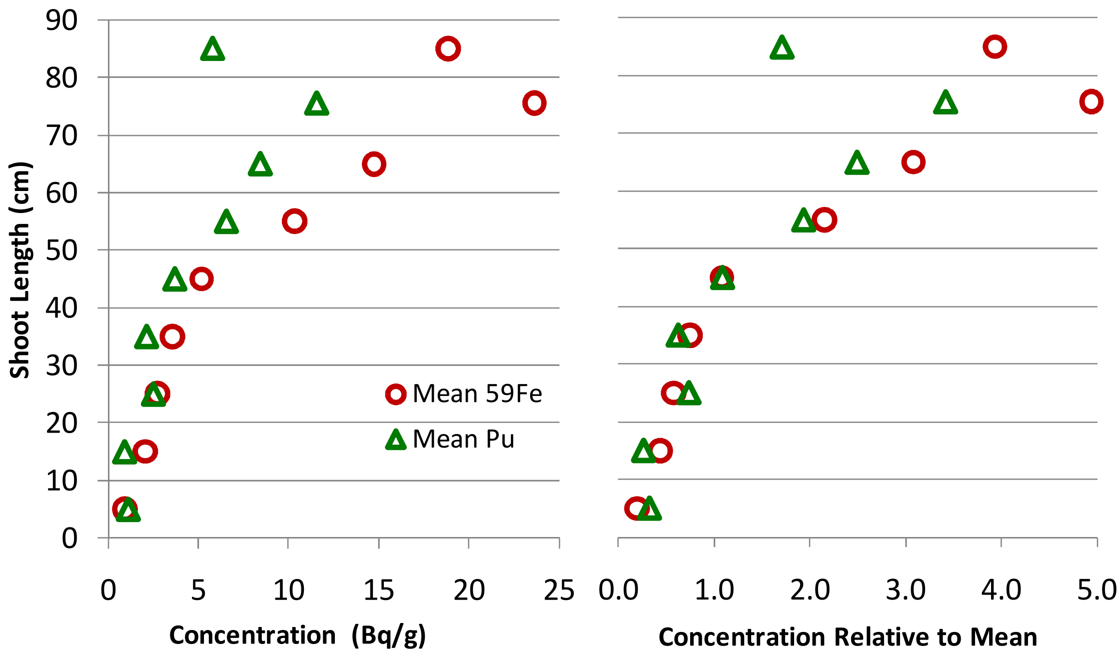

Figure 6.4 Combination plots of averaged and dimensionless ^{59}Fe and Pu concentrations versus shoot length. At left, the averaged data of concentrations versus length are shown. On the right, data have been transformed by dividing the individual concentration data by the mean shoot concentration resulting in dimensionless ((Bq/g) / (Bq/g)) “concentration relative to the mean” data plotted on the same length scale.

In Figure 6.5, we compare shoot radiological data with shoot chemical data using the shoot concentrations divided by their mean values. The averaged total shoot quantities are (moles): 7.2×10^{-4} Mg, 1.1×10^{-2} K, 1.3×10^{-3} Ca, 2.2×10^{-5} Fe, 1.6×10^{-15} ^{59}Fe, 5.6×10^{-7} Mo, and 6.6×10^{-12} Pu. Figure 6.5 shows the relative concentration data versus shoot length of Mg, K, Ca, Fe, ^{59}Fe(DFOB), Mo and Pu(DFOB) from ICP-MS and liquid scintillation analyses. The concentration trends of Mg, K, and Ca are dissimilar to those of Fe, ^{59}Fe(DFOB), Mo or Pu(DFOB). Magnesium has the highest concentration in the lowest section and the most uniform distribution with length, excluding the bottom section. Potassium has the next most uniform concentration distribution profile and is fairly constant in the upper sections. Calcium has the third highest relative concentration in the lowest shoot tissues but increases in the higher sections. Molybdenum and Fe both have relatively low concentrations in low shoot sections and their concentrations increase smoothly with length. The relative concentration profiles of ^{59}Fe(DFOB) and Pu(DFOB) are very similar with low concentrations at the lower heights, increasing concentrations with elevation, and the highest values at or near the top sections as described previously. At 45 cm, the concentration data of Fe, ^{59}Fe(DFOB), and Pu(DFOB) nearly overlap, however above this length Pu(DFOB) and ^{59}Fe(DFOB) are distinct from Fe, which indicates that Pu(DFOB) and ^{59}Fe(DFOB) are more similarly distributed than are ^{59}Fe(DFOB) and stable Fe. The stable elements were distributed in the shoots over 23 days whereas the radionuclide ^{59}Fe(DFOB) and Pu(DFOB) distributions resulted from relatively short term exposure from day 21 to day 23. As mentioned previously, once Fe is incorporated into the cells during chloroplast development it is bound. The position of most active growth increases as young plants grow because the leaves grow out of the apical meristem (which is located near the top of the corn plants). Because the Fe which was bound to cells during earlier growth cannot move, it is logical that Fe introduced to a 21 day old plant is less in demand at the lower stem structures and relatively more in demand at higher elevations. The data for Fe and ^{59}Fe at 75 cm have the largest relative concentration difference with Fe at ~1.5 and ^{59}Fe at ~5. This is clearly the highest concentration of ^{59}Fe (and Pu), so it is reasonable to suggest that the tissues with the most active growth and demand for chloroplasts during exposure were in this section, however no other plant data were collected to support this suggestion. The concentration data in this research consistently show that the highest Pu concentrations are found at or near the top shoot sections where they are likely deposited as the transpiration stream evaporates.

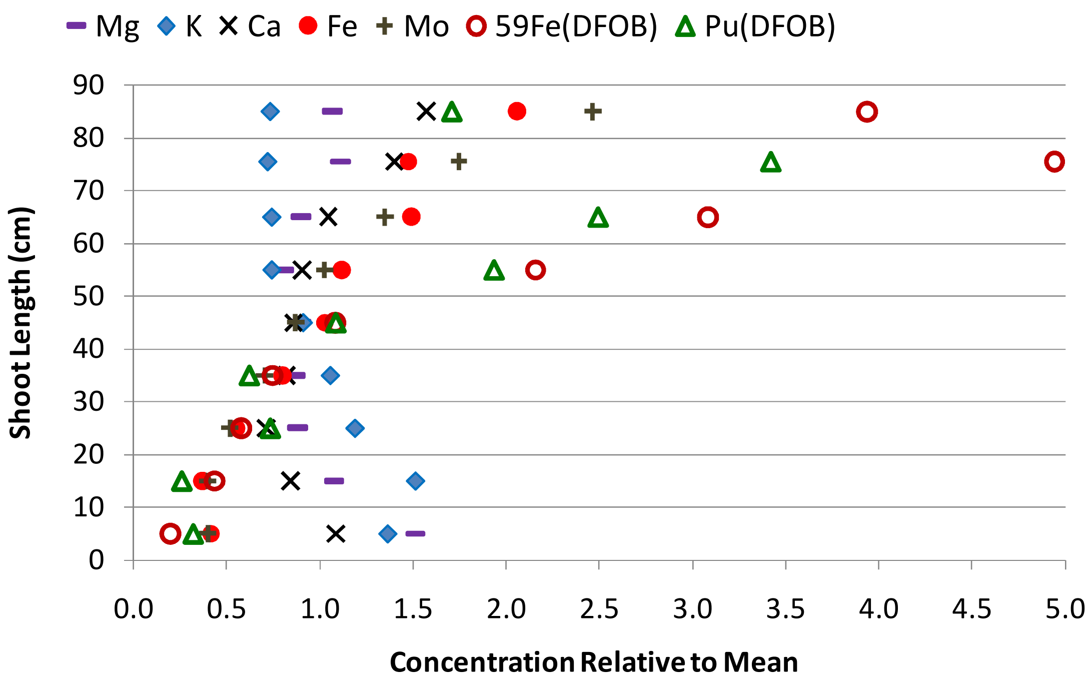

Figure 6.5 The concentrations relative to the mean data are plotted as a function of shoot length for Mg, K, Ca, Fe, ^{59}Fe, Mo, and Pu. The plants were exposed to complexes of ^{59}Fe(DFOB) and Pu(DFOB) from day 21 to day 23, whereas stable shot concentration result from uptake of uncomplexed elements over 16 days. Fe, ^{59}Fe(DFOB), Mo and Pu(DFOB) have somewhat similar profiles with low concentrations at lower elevations and greater concentrations at higher elevations. Mg, Ca and K have much different shoot concentration distribution profiles than the other elements. The Fe, ^{59}Fe(DFOB), and Pu(DFOB) data are similar in the lower shoot sections, but from 55 cm to 75 cm ^{59}Fe(DFOB) and Pu(DFOB) far exceed the relative concentration data of Fe. This pattern of distribution not only highlights the similar trends of complexed ^{59}Fe and Pu but also the differences in plant physiology of the two different exposure periods.

As mentioned above, the plants had different exposure times to the nutrient elements and radioactive compounds in solution (16 d for stable elements versus 2 d for ^{59}Fe(DFOB) and Pu(DFOB)), so these concentration relative to the mean data must be viewed with this in mind. The general trends of concentrations at a particular location in the shoot are directly comparable. However, the final concentration data integrate both the plant physiology and the exposure times, i.e., the short-term exposures are somewhat different and occur in more mature vascular pathways relative to the longer stable element exposures. Given this difference, Fe, Mo, ^{59}Fe(DFOB), and Pu(DFOB) all have similar concentration profiles in the shoot.

The degree of similarity in the relative concentration profiles of Pu(DFOB) and ^{59}Fe(DFOB) suggests that once Pu enters the plant xylem, the two compounds are physiologically treated similarly. For example, both Pu and ^{59}Fe maximum concentrations are observed in the same shoot section and the respective minimum concentrations are observed in the two adjacent sections at the bottom. Clearly the Pu and ^{59}Fe concentration profiles are distinct from most of the other data shown in 6.5. The shoot activity distributions are an important part of this study, because they reflect how elements are distributed after entering the xylem. The effectiveness with which complexed Pu and ^{59}Fe enter the xylem through the roots is the focus of the next section.

6.3.2 Comparison of complexed Pu and ^{59}Fe distributions in the roots and shoots

Table 6.2 contains the basic distribution analysis of plant-averaged data from the dual labeled plants. It has the average root and shoot activities of Pu and ^{59}Fe, the fractions of total plant activity of each metal found in the root and in the shoot, and the Pu/^{59}Fe activity ratios of the root and shoot tissue data. The plant activities are the sum of the root and shoot activities. For Pu, nearly 99% of the total plant activity was in the roots with 1% in the shoots whereas for ^{59}Fe, ~90% of the plant activity was in the roots with ~9% in the shoots. Of interest, the root Pu activity is ~6 times the ^{59}Fe root activity, yet > 40% more ^{59}Fe was transported into the shoots than Pu.

Table 6.2 The Pu and ^{59}Fe Activity Distribution and Activity Ratios of Pu/ ^{59}Fe in the Root and the Shoot

Metal	**Root (Bq.)**	**Shoot (Bq.)**	**Total (Bq.)**	**Root Fraction**	**Shoot Fraction**	**Pu/ ^{59}Fe Root**	**Pu/ ^{59}Fe Shoot**
Pu	979.2	10.3	989.6	0.989	0.010	5.97	0.69
^{59}Fe	164.0	14.9	179.0	0.903	0.089		

All data are plant-averaged values of the three dual-labeled plants.

Table 6.3 shows the fractions of the total plant activity divided by the activity contained in the average solution volume transpired by the plants, the root activity divided by the average plant root volume, and the average root concentrations divided by the solution concentrations. The solution transpiration volume activities represent the total activities which could have been transported into the plant in the fluid; they are obtained by multiplying the solution concentrations by the mean transpiration volumes. The plant activities divided by the activities in the transpiration volume activities [Plant (Bq)/ T. Vol. (Bq)] indicate that about 15% of the Pu in solution was taken up but only 3% of the ^{59}Fe was taken up by the plants. Following Table 6.3 to the right, the root activities have been divided by the root volume (calculated from the plant-averaged root mass to be 3.02 cm^3). The root volume concentrations of Pu and ^{59}Fe are compared to the respective solution concentrations presented to the plants. From this, Pu was concentrated in the roots relative to the solution by a factor of 4.4, but the ^{59}Fe root concentration was slightly less than the solution ^{59}Fe concentration. The ^{59}Fe decay has been taken into account in all these calculations.

Table 6.3 The Pu and ^{59}Fe Activity Distribution, the Total Plant Activity Fraction Relative to the Activity in the Average Transpiration Volume, the Root Activity Per Root Volume, and the Average Root Concentration Compared to the Solution Concentration

Metal	**Root (Bq.)**	**Shoot (Bq.)**	**Total (Bq.)**	**Plant (Bq) / T. Vol. (Bq)**	**Bq/root volume (3.02 cm^3)**	**Solution Bq/cm3**	**Root / Solution**
Pu	979.2	10.3	989.6	0.146	324.4	73.7	4.40
^{59}Fe	164.0	14.9	179.0	0.031	54.3	64.0	0.85

We now present the dual labeled plant data focused on molar proportions rather than activities. Table 6.4 contains the plant-averaged Pu and ^{59}Fe data converted from activities to moles, the *molar ratios* of Pu/ ^{59}Fe in the roots, the shoots, and the solutions. Using Eqns. 1 and 2 we find that equal ^{238}Pu and ^{59}Fe activities result in a *molar ratio* of 705: 1 due to their respective decay rates.

$$\frac{Activity}{\lambda(decay)} = Atoms \qquad \text{Eqn. 6.1}$$

$$\frac{Atoms}{6.023x10^{23}} = Moles \qquad \text{Eqn. 6.2}$$

Thus, the solution concentrations presented to the plants were 6.68 x 10^{-13} M ^{59}Fe and 4.71 x 10^{-10} M ^{238}Pu. Following Table 6.4 to the right, the Pu/^{59}Fe molar ratios are 4289, 498, and 705 in the root, shoot, and solution respectively. The respective activity ratios of the root, shoot, and solution are 5.97, 0.69, and

1.00. The molar ratios are in proportion to the activity ratios since they are derived from the activity data. The molar solution concentrations of both Pu and ^{59}Fe are small as compared to the stable Fe concentration 1.07×10^{-5} M.

Table 6.4 Molar Data for the Pu and ^{59}Fe Labeled Plants

Metal	**Root (Bq.)**	**Shoot (Bq.)**	**Decay λ (s^{-1})**	**Root (Moles)**	**Shoot (Moles)**	**Solution Molarity**	**Molar Ratio Pu/Fe**		
							Root	**Shoot**	**Solution**
Pu	979.2	10.3	2.51E-10	6.48E-12	6.83E-14	4.71E-10	4289	498	705
^{59}Fe	164.0	14.9	1.80E-07	1.51E-15	1.37E-16	6.68E-13	Activity Ratio Pu/Fe		
							5.97	0.69	1.00
							Molar/Activity Ratio		
							719	**719**	**705**

6.4.3 Pu uptake and distribution at varied stable Fe solution concentrations

Five plants each were exposed to Pu(DFOB) in nutrient solutions containing either zero or ten times the stable Fe concentration in the nutrient solution. These Fe concentrations were presented to the plants beginning two to three days prior to exposure and were again presented to the plants at the time of their exposure to Pu. The logic for altering the solution Fe concentration a few days prior to exposure was to allow time for the plants to respond to the Fe solution conditions and potentially produce phytosiderophores before exposure. The experiments were designed to examine Pu uptake in relation to the nutrient solution Fe concentrations which may have the following potential outcomes: first, lacking sufficient Fe, the plants may produce phytosiderophores which would be expected to increase Pu uptake, and second, by providing an overabundance of Fe (which exceeded the DFOB concentration, 10.7×10^{-5} M Fe versus 9.8×10^{-5} M DFOB), the plants may show an inhibitory Pu and ^{59}Fe uptake effect due to stable Fe saturation.

Figure 6.6 is a plot showing all Pu shoot concentration versus height data at both Fe concentrations. The Pu concentrations are greatest at or near the top shoots of both sets. The Pu concentration data of plant 10x Fe8C, particularly at 65 cm, greatly exceeded those of the rest of both plant treatments (plant 10x Fe8C data are sown with the heavy dashed line. Plant 10x Fe8C had the largest transpiration and second largest root mass of the ten plants. The mean 0x and 10x Fe concentration profiles (with and without plant 10x Fe8C) are presented in Figure 6.7 which indicates small differences between the plant Fe treatments when the data of plant 10x Fe8C are excluded. Since the plants had roots in solution and in soil, it is probable that the 0x plants obtained Fe from the soil roots. With their rapid growth rate during age 18 to 23 days, the corn plants would be expected to have chlorotic leaves and no signs of this condition were observed during any of the experiments.

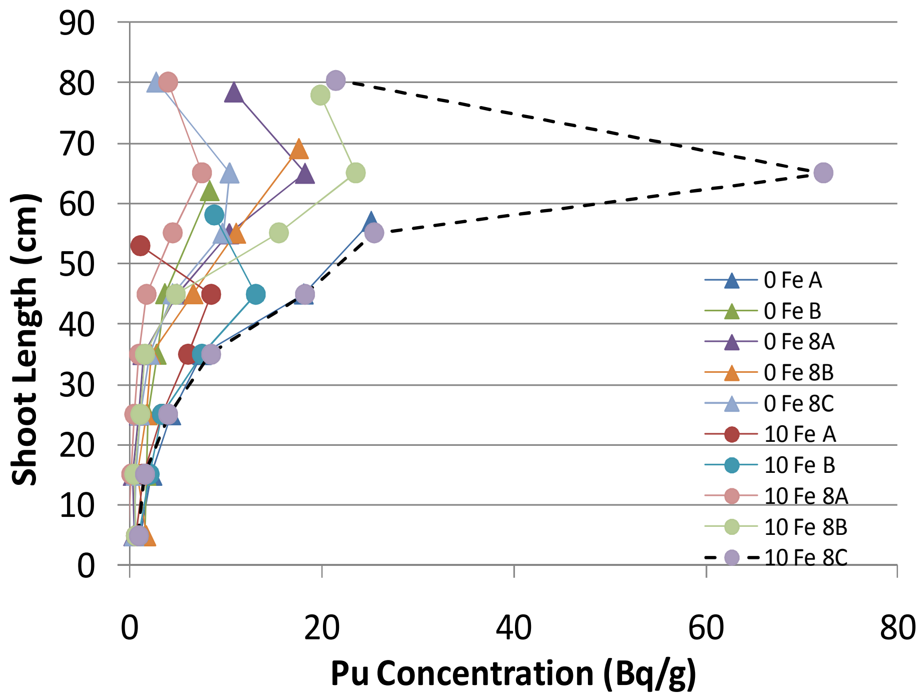

Figure 6.6 Plots of plant shoot concentration versus corn shoot length for the 0x & 10x Fe solution concentrations. Data symbols are 0x Fe (triangles) and 10x Fe (circles). Pu tissue concentrations tended to increase with shoot length.

From the shoot distribution data shown in Figure 6.7, two implied results can be described: comparing the 10X data without the single extraordinarily high concentration Pu data point at 65 cm for experiment 10X Fe 8C, little to no differences are seen in the data of the plant treatments, and comparing the 0x and 10x data with plant 8C, the 10x shoot concentrations exceed that of the 0x treatment. In either case, the potential outcomes mentioned above were not observed which suggests that phytosiderophore production did not occur (possibly due to the plant's obtaining iron from their soil pots) nor did higher Fe solution concentrations inhibit Pu translocation into the shoots.

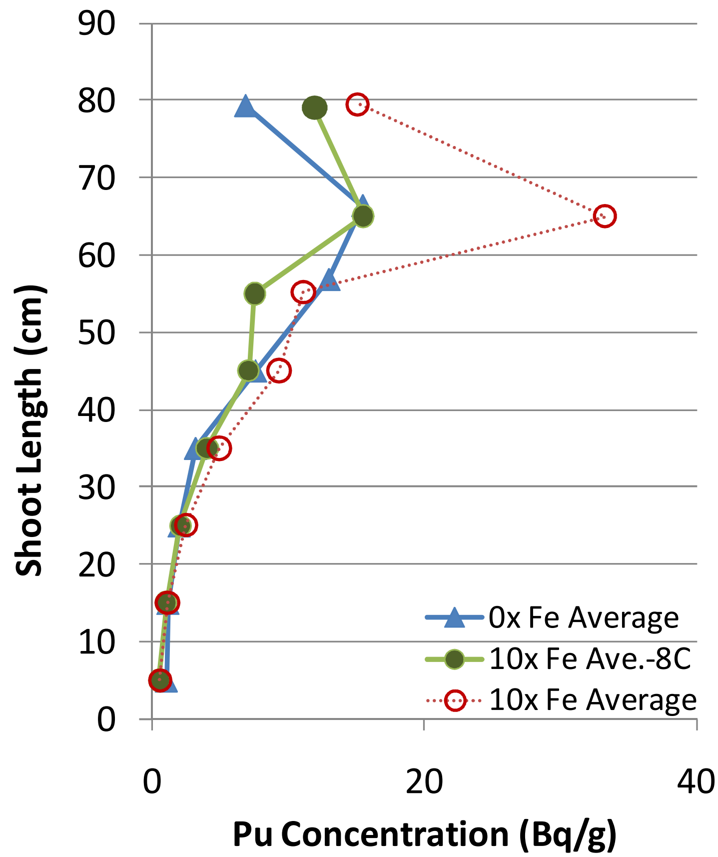

Figure 6.7 A plot depicts mean shoot versus length data for the 0x and the 10x plants with and without plant 10x Fe8C. For all 10x plant data, at 65 cm height the standard deviation /mean is greater than twice that of the 10x plants excluding 10x Fe8C. Comparing the 0x Fe with the 10x Fe without plant 8C, the mean concentration profiles are very similar.

Table 6.5 summarizes the averaged activity distribution data for the 0x plants, the 10x plants with and without plant 8C, and the dual labeled plant data. As discussed above the mean shoot activity data of the 10x plants is strongly affected by the data of plant 10x Fe8C. First, focusing on comparisons between the 0x plants and the 10x plants without plant 8C, the root and shoot activities, root and shoot fractions, and the ratio of the plant activity/ the averaged transpiration volume activity are similar regardless of the Fe concentration. Inclusion of the 10x Fe8C data changes the data comparisons by increasing the fraction in the shoots from 0.014 to 0.030 and by increasing the averaged root volume. The averaged Pu plant activity divided by activity contained in the averaged transpiration volumes are similar under all conditions and also compare well with Pu data of the dual labeled plants. The Pu activity divided by the root volume is obtained from the averaged values of the individual plant calculations. The two columns at the right of Table 6.5 show that the Pu root concentration and root concentration relative to the solution concentrations are all quite similar for Pu. The Pu data differ from the ^{59}Fe data in terms of the shoot activity distribution and the root concentrations relative to the solution concentration.

Table 6.5 Summary Activity Distribution Data for Both the Varied Fe Solution Concentration Plants and the Dual Pu and ^{59}Fe labeled Plants

	Root (Bq)	Shoot (Bq)	Root Fraction	Shoot Fraction	Plant (Bq) / T. Vol. (Bq)	Root Vol (cm3)	Pu Act (Bq) / root (cm3)	Root / Solution
0x Fe	632.8	11.6	0.982	0.018	0.120	3.62	300	4.12
10x Fe	671.0	20.6	0.970	0.030	0.150	3.61	284	3.91
10x Fe*	585.2	8.2	0.986	0.014	0.173	2.76	319	4.39
Pu	979.2	10.3	0.989	0.010	0.146	3.02	324	4.40
Fe	164.0	14.9	0.903	0.089	0.031	3.02	54	0.85

Under experimental conditions in which the Fe/ Pu solution concentration ratios are 0 – 2.2 x 10^5, there is no significant difference in the Pu uptake. Thus from these results, Fe does not interfere with Pu uptake. It is worth noting that the plants grew in nutrient solution for several days prior to removal of Fe completely from the solution and due to the xylem arrangement in the root tissue, therefore some Fe could have remained in the root but outside the xylem. There was no way to determine this extra-xylem cellular Fe content in these experiments.

In Chapter 5 and in Table 6.3 the tissue activities found in the root and shoot were divided by the total activity contained in the volume of solution transpired. The concentration (i.e., activity/ solution volume) in tissues can be directly compared with the fluid concentration as a way to understand the exclusion or concentration of Pu. Table 6.6 shows the activity ratios of the container solution concentrations divided by the average concentrations in the root and shoot. The ratios of the solution concentration to the root concentration of Pu are about 7 comparing the Fe solution concentration experiment and the dual labeled experiment. An average of about 1/7th of the Pu contained in the measured transpiration stream transited into the root interior. Similar comparisons show that less than 1/500th of the Pu in the transpiration volume was translocated into the shoots. If one imagines following the transpiration stream from the solution, into the root tissues, and then upward to the shoots, the observation that 1/7th of the Pu transpired crosses into the roots and only <1/500th of it enters the xylem means that Pu must accumulate in the roots. This is evidenced by the data in Table 6.5 showing that (on the basis of root volume and not transpiration volume) the root Pu concentration is about 4 times the solution concentration. For ^{59}Fe, the equivalent ratio is 36, indicating that only 1/36th of the ^{59}Fe in solution crossed into the root and about 1/400th of the Fe traveled further into the shoots.

Table 6.6 Activity Ratios of Pu and ^{59}Fe Concentrations in Solution Compared to the Concentrations of Calculated Averaged Root and Shoot Concentrations

	Solution (Bq/cm^3) **Root /T.Vol. (Bq/cm^3)**	**Solution (Bq/cm^3)** **Shoot /T.Vol. (Bq/cm^3)**
Pu (0x Fe)	8.4	680
Pu (10x Fe)	6.7	550
Pu (10x Fe*)	5.8	760
Pu	6.9	660
^{59}Fe	36.0	400

In the introduction, the research by John et al. (2001) involving Pu and Fe uptake in the bacterium (*Microbacter flavesence*) was cited as a motivation for this research. Comparing these results with those of John et al. (2001), several experimental factors must be considered. First, they used equal molar Fe and Pu concentration whereas these tests were conducted with equal activities of Fe and Pu in the dual labeled tests or much different ambient concentrations of stable Fe and Pu in the other tests. These differences made assessing uptake competition between the metals problematic in this study. Second, basic physiological differences in size and complexity of bacterial cells and plants roots must be understood to compare the studies. John et al. (2001) observed that bacterial uptake of Pu was ¼ that of Fe whereas in this study the Pu plant uptake was six times greater than that of Fe. Overall two observations are consistent between the studies. John et al. (2001) found that much less Pu passed through the bacterial cell wall than Fe. Similarly, less Pu passed into the xylem of corn plants than Fe and much more Pu was localized in the root tissues than was Fe. The fact that more Fe was transported into the shoot and much more Pu was found in the root shows that the complexed Pu is much less effective than complexed Fe at entering the xylem. It also suggests that, although most of the Pu was excluded at the exodermis, what fraction did enter the root may have become trapped in the root tissue which is somewhat similar to the displacement test results of John et al. (2001) wherein they found that once the Pu was inside the cell wall, it was difficult to remove.

6.5 Conclusions

This research has resulted in several findings pertaining to the plant uptake and distribution of Pu and Fe. First, once Pu enters the xylem, it is distributed and hence physiologically treated quite similarly to Fe. The shoot ^{59}Fe and ^{238}Pu concentration distributions are highly similar as compared to those of Mg, K, Ca, Mo, and even stable Fe. The observation that ^{59}Fe has slightly higher relative concentrations in the upper shoot tissue sections may suggest that it has a lower retardation in xylem than does Pu (conversely Pu undergoes slightly greater sorption in the shoot tissues than Fe). Second, proportionally more Fe transits through the root than does Pu since ~ 9% of the total plant Fe activity was in the shoot versus ~1% of the Pu. This plant tissue activity distribution is complicated by the observation that overall ~6 times more Pu activity was found in the root than ^{59}Fe activity. Since both the ^{59}Fe and the Pu were excluded from the xylem and the root, it is difficult to interpret this observation. Perhaps the Fe moves much more freely through the root and a significant portion of the Fe was removed during the root sample processing step by rinsing the roots in water. It is possible that the Pu was either immobilized or so much less mobile in the root tissues that it was preferentially retained in the plant root. Irrespective of the meaning of the relative activities found in the roots, in a gross sense, Fe does not appear to interfere with the uptake of Pu. Under Fe/Pu solution molar ratios ranging from 0-2.2 x 10^5, the proportion of Pu concentrated in the roots relative to the solution concentrations remained nearly constant. Potential interference between plant uptake of Fe and Pu deserves further study due to the uncertainty about the actual Fe content in the root tissue discussed earlier. Since plants have no known biological need for Pu, it appears that Pu is taken into plants based on similarities between Pu and Fe. However, Pu is less effective than Fe at crossing through the root which suggests that a portion of it may be localized in the root tissues. This root localization could be a contributing factor (among several other factors) in the wide range of plant bioaccumulation factors reported in the literature.

CHAPTER SEVEN

ADDITIONAL FINDINGS

7.1 Introduction

The broad objective of the research reported in this dissertation was to provide experimental support for the hypothesis that plants can play a significant role in the upward transport of Pu in the vadose zone. The major findings are reported in Chapters 4-6, which are complete or longer versions of publication-formatted articles. Presented in this chapter are three additional findings that provide important insights into certain aspects of plant transport. They are only loosely related to of one another but are too short to be separate chapters. Rather, they are presented as independent sections in this chapter.

The first section is an analysis of the discrimination of Pu by the root. The data come from these experiments and from the literature. The second section is focused on the basic upward transport models described in Chapter 2 and their transport parameters. The third section contains the results of batch sorption tests with xylem and cellulose.

7.2 Pu Discrimination by Roots

7.2.1 Data from this research

This work has been focused on the movement of Pu into and through plants by studying velocity, retardation, and discrete spatial distribution from a transport perspective. As mentioned previously, the principal focus of related research by others on phytoremediation and bioaccumulation focused primarily on the concentration or accumulation of contaminants in the above ground plant tissues. No studies exist which can be directly compared to our root exclusion data, therefore the analysis below is conducted by presenting our data in both a straightforward manner and in such a way that comparisons can be made with data of other studies. In particular, the translocation data of phytoremediation studies conducted with plants in solution media and the bioaccumulation data of Pu in root vegetables may be helpful to better understand the nature of Pu movement through plant roots.

Evidence of root exclusion is seen in Table 6.4, which contains a comparison of the activities in the root and shoot and the activities contained in each plant's transpiration volume. These data show Pu is excluded from the root at the exodermis and then some of the Pu which enters the exodermis does not transit all the way through the root cortex to enter the xylem. Figure 7.1 is a diagram of a corn plant root with a single root magnified to illustrate that the soluble Pu must cross through the exodermis (1) and the root cortical cells (2) to enter the xylem wherein upward transport may occur.

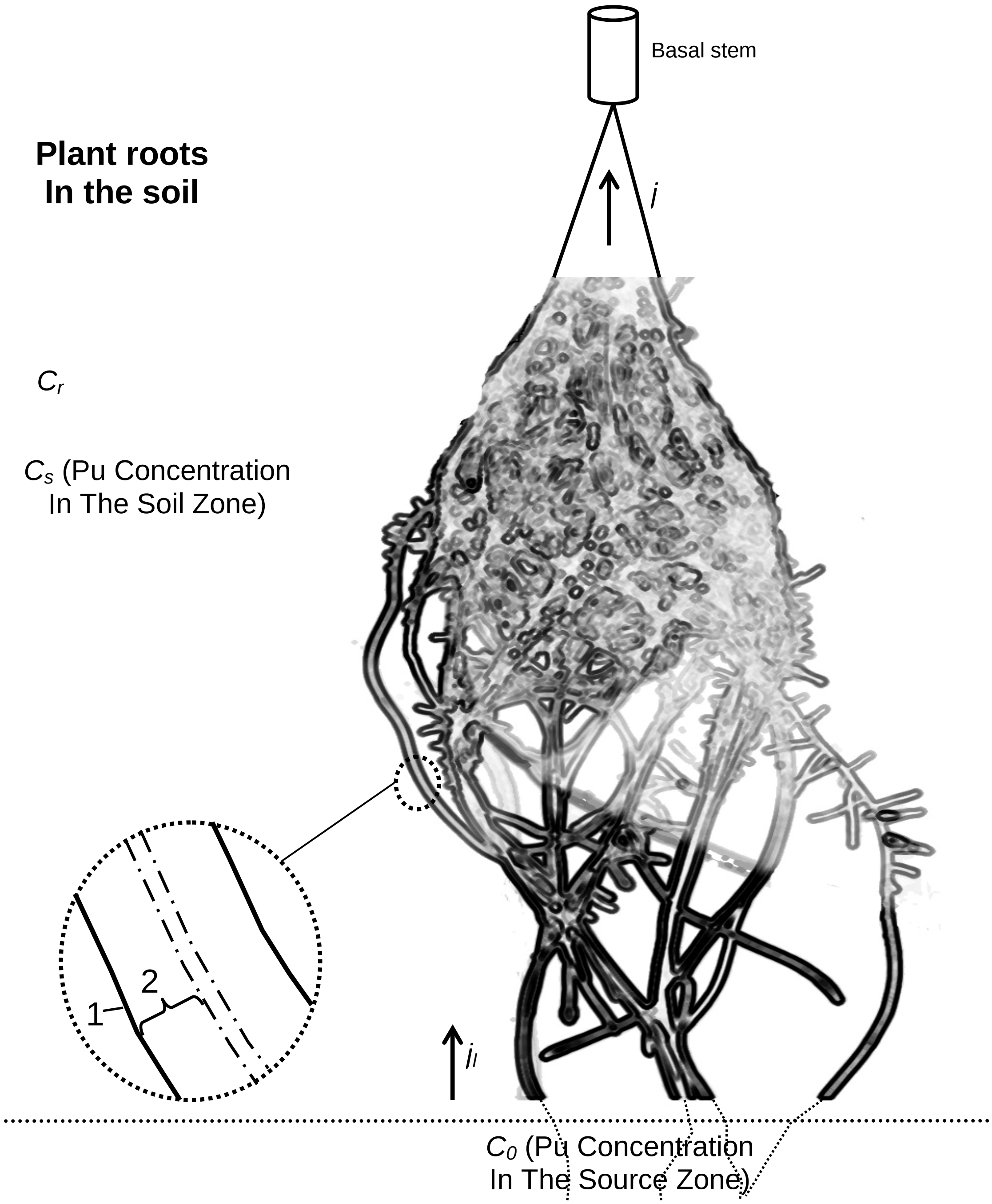

Figure 7.1 A diagram depicts the uptake and upward transport process in detail. The main object is a corn plant root. For upward transport in plants to occur, the roots must nearly intercept the soil containing Pu, and the Pu in the soil water must cross the epidermis (1) and root cortical tissues (2) to reach xylem for long distance upward transport in plants in the root zone. (Corn root xylem is not arranged exactly as illustrated in the enlargement; it has been simplified for clarity.) (Corn root image adapted from photograph taken by Craig Mehaffy of Clemson University, Clemson, SC 2009)

Table 7.1 contains the results of several experiments in which the root and total shoot activities were carefully determined. It includes the number of plants in an experimental set, plant age at the end of exposure, exposure time, mean transpiration volume, mean shoot and root masses, mean shoot and root activity fractions and the standard deviation associated with each plant set, and the ratio of shoot concentration to root concentration. The data are from experiments with 23 to 25 d old plants (26 total plants) arranged by increasing exposure time. These data show that irrespective of the experimental conditions, the Pu activity distribution was about 2.4% in the shoots and 97.6% in the roots. Unfortunately, due to the paucity of similar Pu shoot-root activity distribution data in the literature, the only data available for comparison are from the hydroponic study of Lee et al. (2002), who report the ratio of shoot to root concentration. Consequently, this ratio is also presented in Table 7.1 and comparisons with Lee et al. are made in a subsequent section. The ratios vary between 0.0009 – 0.0038 and are roughly an order of magnitude lower than activity fractions due to the differences in shoot and root masses.

Table 7.1 The Partitioning of Pu In the Roots and Shoots of Corn Plants
.

LR9 Experimental Set Mean Plant Data	n	Age d	Time d	Trans mL	mass g	Activity Fraction	1SD	CR_s / CR_r
1d Shoot (Transpiration)	4	25	1	142	4.869	0.0298	0.0175	**0.0020**
1d Root					0.372	0.9702	0.0175	
2d Shoot (Dual labeled)	3	23	2	92	3.127	0.0104	0.0048	**0.0009**
2d Root					0.266	0.9889	0.1826	
2d Shoot (0x, 10x Fe)	10	23	2	128	3.619	0.0241	0.0298	**0.0012**
2d Root					0.318	0.9759	0.6247	
3d Shoot (Shoot-Root)	3	23	3	128	2.364	0.0171	0.0048	**0.0014**
3d Root					0.198	0.9829	0.0028	
7d Shoot (Shoot-Root)	3	23	7	421	2.223	0.0234	0.0102	**0.0019**
7d Root					0.291	0.9766	0.0134	
10d Shoot (Shoot-Root)	3	23	10	475	3.063	0.0407	0.0168	**0.0038**
10d Root					0.301	0.9593	0.0169	
				Overall mean		**0.0243**	**shoot**	
				Overall mean		**0.9756**	**root**	

CR_s/CR_r is concentration ratio in the shoot divided by concentration ratio in the root which reduces to the shoot concentration divided by the root concentration.

The mean xylem, shoot, and root solution concentration ratios (CR_s = (Bq/g)/ (Bq/cm^3) solution) are presented as plots versus time in Figures 7.2, 7.3, and 7.4 respectively. The xylem concentration is calculated by dividing the shoot activity by the transpiration volume. The shoot and root concentration ratios are calculated by dividing the shoot or root concentration by the solution concentration, respectively. In general, both shoot and root concentrations are expected to increase with time. In Figure 7.2, the xylem concentration ratios show no clear trend with time. This may be an indication that there is no time trend or that the data represent the fluctuations in transpiration of a particular set of plants. The xylem CR at 1d is considerably lower than at later times. Since the xylem CR is calculated by dividing the shoot activities by the transpiration volumes, the 1d data are likely to be lower because of the relatively larger transpiration volume. The utility of the 1d data will be seen in Figures 7.3 and 7.4.

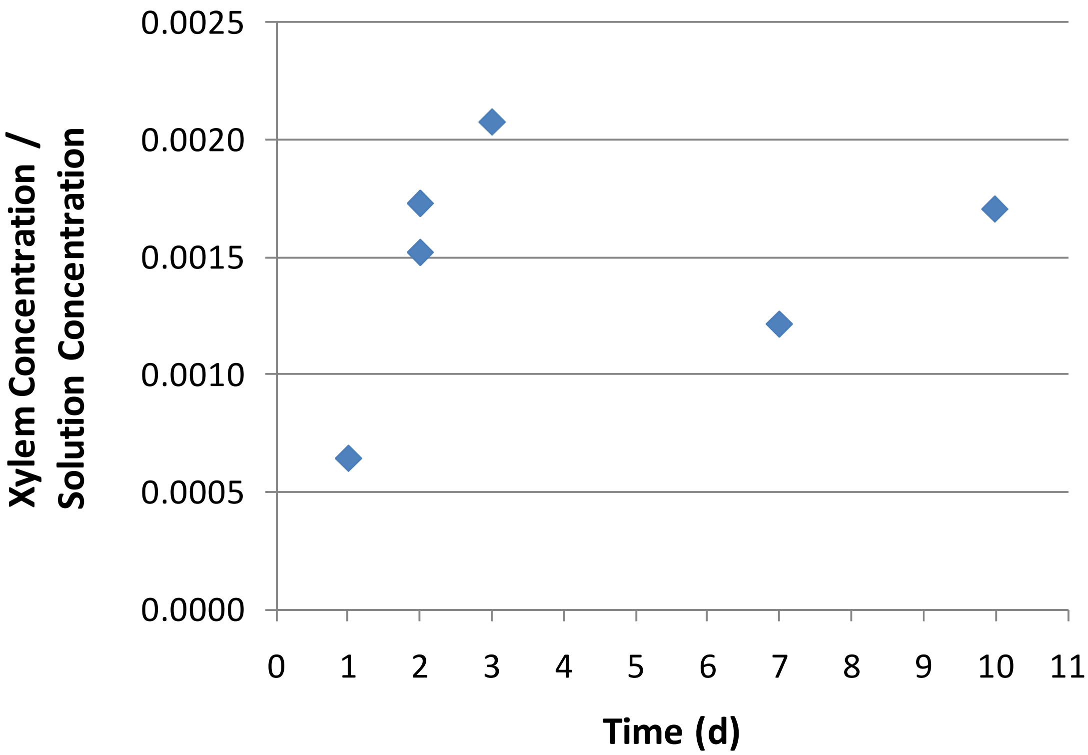

Figure 7.2 The ratios of xylem concentration to solution concentration are plotted as a function of exposure time. No trend is evident with time and the data are scattered about the mean value of 0.00148.

Figure 7.3 shows the shoot CR_s data as a function of time. As expected from prior discussion, the shoot CR_s values increase with increasing exposure time. The CR_s data of days 1 – 3 increase in a fairly linear fashion, but by 7d and to a greater extent by 10d the rate of increase in the shoot CR_s values is lower.

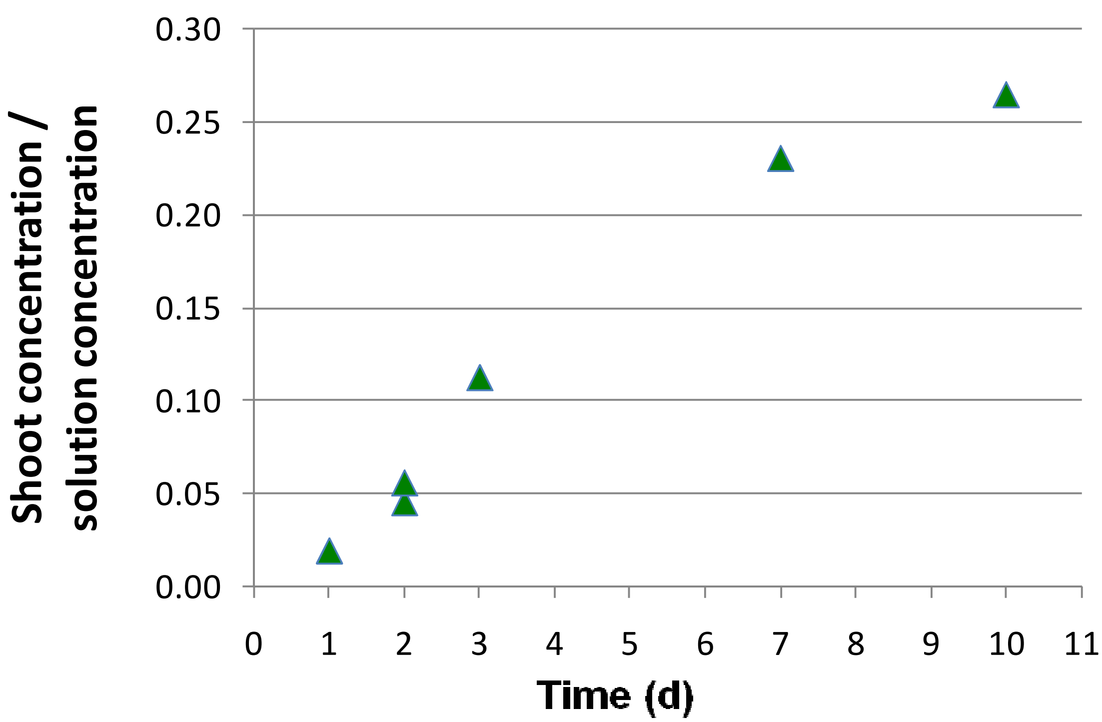

Figure 7.3 The ratios of shoot concentration to solution concentration are plotted versus exposure time. An increase in the ratios is seen with time, although the relative increase is smaller between 7 and 10d.

In Figure 7.4 the root CR_s data increase linearly 1 – 3d, however between 3d and 7d the increase is no longer linear and at 10d, the CR_s value is less than those at 3d and 7d. The time trend of the root CR_s data suggest that the roots may have become saturated with Pu between days 3 and 10. Comparing Figures 7.3 and 7.4, the time trends are similar; however, the root values are about 250-1000 times greater than those of the equivalent shoots. The translocation of Pu from the roots to the shoots continues to increase, albeit to a lesser degree. It is important to notice that in both Figures 7.3 and 7.4, the data from two different experimental sets of 2d exposures are consistent for the shoots and the roots.

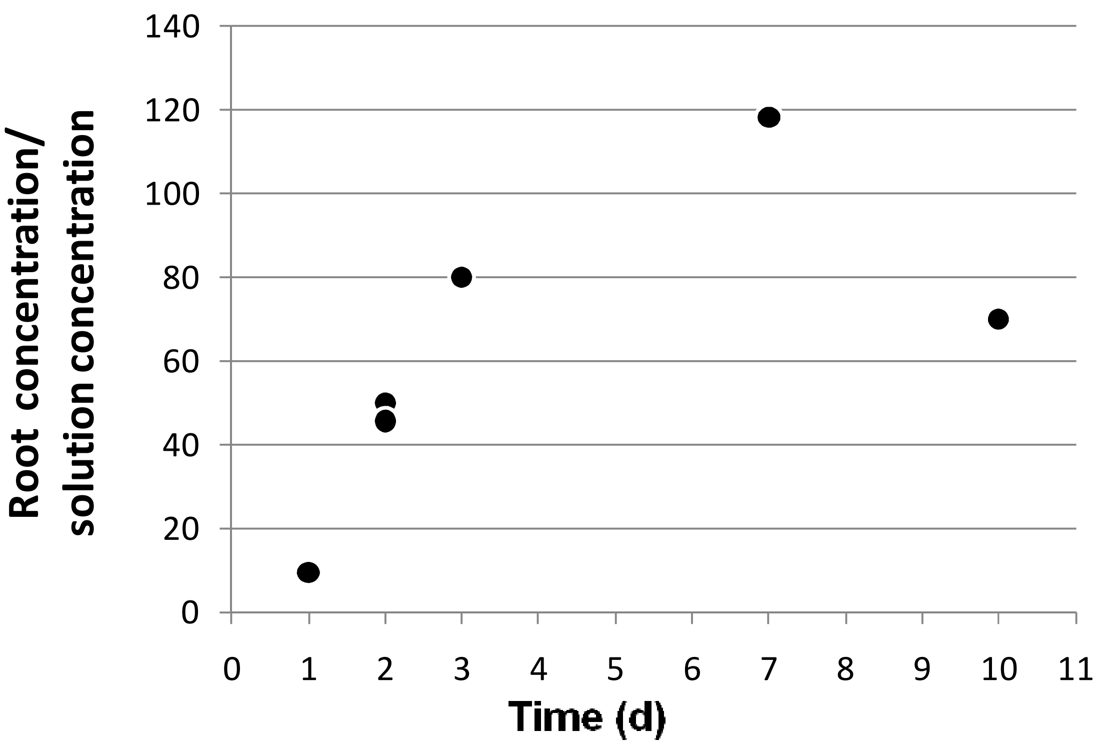

Figure 7.4 The root CR_S are plotted versus exposure time. Similar to the shoot CR_S data, the root CR_S are linear over the first three days. The rate of root CR_S increase is smaller between 3d and 7d, and by 10d, the root CR_S is less than the 7d value. This may indicate that Pu saturation occurred in the root tissues. The mean root masses of the 7 and 10d plants are very similar at 0.29 and 0.30 g.

7.2.2 Plant root data from other hydroponic studies of actinide uptake

Lee et al. (2002) transferred the hyperaccumulating plants Indian mustard (*Brassica juncea*) and sunflower (*Helianthus annuus*) into $^{239}Pu(NO_3)_4$ labeled nutrient solutions for 7 d beginning when the plants were ~10 cm in shoot height.

The objective of the study was to determine conditions which would maximize shoot uptake. Table 7.2 is adapted from their 35 Bq/mL data at various concentrations of DTPA. It shows the activity fractions and the concentrations in the shoots and roots. The maximum fraction of Pu activity in the shoots was about 73 and 67% for Indian mustard and sunflower, respectively. These compare with a shoot activity fraction average of 2.5% and maximum of <5% in corn. The corn data in Table 7.1 originated from uptake experiments of Pu complexed with DFOB at 9.8×10^{-5} M. Preliminary experiments of Pu complexed with 8×10^{-5} M DTPA or DFOB showed that shoot Pu uptake was 2-4 times greater with Pu complexed DFOB than with DTPA. The Lee et al. (2002) data indicate that maximal root uptake occurred at 0 DTPA concentrations in both plants.

Table 7.2 Pu tissue activity fraction and concentration data of Lee et al (2002)

Plant	DTPA (Mol/L)	fraction activity shoot	fraction activity root	Shoot (Bq/g)	Root (Bq/g)	CR_s / CR_r	Root / Root (0)
Indian mustard	0	0.025	0.975	94.6	24785	0.004	1.000
(Brassica juncea)	1.3E-05	0.283	0.717	731.1	7811	0.094	0.315
	2.5E-05	0.591	0.409	1699.1	6610	0.257	0.267
	1.3E-04	0.733	0.267	1305.4	4399	0.297	0.177
Sunflower	0	0.012	0.988	66.8	20612	0.003	1.000
(Helianthus annuus)	1.3E-05	0.474	0.526	255.8	1183	0.216	0.057
	2.5E-05	0.526	0.474	211.1	725.6	0.291	0.035
	1.3E-04	0.669	0.331	206.3	582.4	0.354	0.028

The ratio of the shoot concentration to the root concentration is presented as a qualitative way to compare different studies. A check between Tables 7.1 and

7.2 shows that under the conditions of the Lee et al. (2002) experiments, the Indian mustard and sunflower plants translocate much more Pu into their shoots than corn. Lee et al. (2002) selected those plants as hyperaccumulating species whereas in our study corn was selected because of its similarity to the annual grasses in the Savannah River Site lysimeters.

Ruggiero et al. studied hydroponic plant U uptake and distribution in barley (*Hordeum vulgare*). Table 7.3 shows their shoot and root concentrations and the ratio of shoot concentration to root concentration at three Fe concentrations. Irrespective of the Fe concentration, the ratio of shoot to root concentrations suggests that the vast majority of the U remained in the roots. Similarly, Laroche et al. (2005) studied the uptake and distribution of ^{233}U in the common bean (*Phaseolus vulgaris*) using short-term (5 h) and long-term (3 d) root exposure to labeled nutrient solutions at pH 4.9, 5.7, and 7.0. They varied the concentrations of U ligands and competitive ions and used speciation models to examine the solution chemistry in detail. They exposed bean plants as juvenile seedlings and at the flowering stage of development. Under all conditions, 99% of the U was found in the root tissue.

Table 7.3 Hydroponic Barley Uptake of U (adapted from Ruggiero et al. 2004)

Fe (ppm)	**Shoot (ppm)**	**Root (ppm)**	$\frac{CR_s}{CR_r}$
0	105	15000	0.0070
7.5	105	18500	0.0057
100	20	26000	0.0008

7.2.3 Field studies of Pu uptake in root vegetables

Root vegetable uptake studies may be helpful to understand how Pu transits the root tissues, even though those plants are dissimilar to grasses because root vegetables have taproots and grass plants have fibrous roots. Taproot plant roots are much thicker and have larger cortical areas than fibrous plant roots. The root vegetable studies discussed below were conducted with plants exposed to Pu in soil and grown to maturity. Corey et al. (1983) suggested that the adherence of surface particles accounted for ≥ 93% of Pu in carrots (*Daucus carota*), turnips (*Brassica rapa*), potatoes (*Solanum tuberosum*), and sweet potatoes (*Ipomoea batatas*). After peeling the vegetable samples, only turnips had detectable Pu concentrations in the root. A more detailed study by Adriano et al. (2000) focused on the influence of culinary preparation on the radionuclide content in root vegetables. The nuclides studied were ^{90}Sr, ^{137}Cs, ^{234}U, ^{238}U, and ^{239}Pu and the vegetables studied were red beet (*Beta vulgaris*), carrot (*Daucus carota*), and turnips (*Brassica rapa*). Vegetable samples were processed by light washing, scrubbing, or peeling to test the effect of different preparations on the radionuclide concentration in the foods. Light washing was defined as vigorous hand washing until the “surface cleanliness visually resembled those available in the supermarket”, scrubbing removed all surface particulates using a kitchen brush, and peeling removed the exodermis.

Table 7.4 shows the Pu concentration ratios of beet, carrot, and turnip under the various sample treatments of Adriano et al. (2000). The position of the Pu activity in the root vegetables can be approximated by comparing the data from different treatments and assuming that changes in the sample mass from the treatments are small relative to the total sample mass. Using light wash data as the total activity (the root sample includes the surface, exodermis, and interior), the approximate activity fractions due to the various treatments are calculated as:

- Interior = [peeled / total]
- Exodermis = [(scrubbed – peeled) / total]
- Exterior = [(total – scrubbed) / total]

Over a growing season, 3-9% of the Pu was transported into the interior root tissues. Roughly 4-15% of the Pu was found in the exodermis. The exterior fraction contained 76-93% of the Pu. Although this is not a precise quantitative way to compare Pu uptake, it is clear from the relative positions of Pu that most of it did not enter the root. For comparison, 70-90% of both ^{90}Sr and ^{137}Cs and ~10-50% of the U isotopes were found in the interior, respectively.

Table 7.4 Pu Root Vegetables CR from Adriano et al. (2000) and Approximate Pu Fractions of the Interior, Exodermis, and Exterior

Plant	Light Wash (Total)	Scrubbed	Peeled	Interior Fraction	Exodermis Fraction	Exterior Fraction
Beet	0.00230	0.00028	0.00006	.03	.09	.88
Carrot	0.00300	0.00020	0.00008	.03	.04	.93
Turnip	0.00058	0.00014	0.00005	.09	.15	.76

The light wash data are taken as total values with differences between scrubbed and light wash treatment termed surface Pu, and differences between peeled and scrubbed treatments termed exodermis.

With the exception of hyperaccumulating plants, most Pu does not completely transit the root and enter the xylem of the plants discussed. The amount of Pu which crosses through the root tissue is dependent upon the type of plant, the presence of complexing agents such as siderophores, possibly the availability of Fe in the soil, and other factors. The upward Pu transport in plants requires that Pu enter the xylem to be transported. In the reactive transport simulations of the SRS lysimeter study, Demirkanli et al. (2009) utilized an uptake efficiency variable and set the efficiency equal to one. Strictly speaking this means that all of the Pu intercepted by the roots would enter the xylem (although due to the retardation being greater than one, some of the Pu would sorb to the root and shoot xylem tissue as the water moved upward). Although our data were generated in short term experiments in comparison to a growing season, extrapolations of the corn shoot and root concentrations over a longer growth period (data not shown) still predict that the majority of the Pu would be located in the roots. Based on this, the uptake efficiency parameter should be adjusted; however, our data are applicable to too short of a growth period to suggest an appropriate uptake efficiency factor. A longer term study would be required to accurately determine uptake efficiency or a root exclusion factor. Since most studies are concerned with the resultant plant concentrations in food or hyperaccumulating plants, this level of detail at the root interface is not available in the literature.

7.3 Evaluation of Basic Upward Transport Models

7.3.1 Introduction

In Chapter 2, two zero-dimensional approximations - instantaneous partitioning and steady-state advection - were developed to describe the upward transport observed in the Savannah River Site lysimeters. They were based on a simple conceptual model in which the lysimeter system is represented by two homogeneous regions: a source zone where the soil is considered to be contaminated solely by the Pu source and a root zone where the soil is considered to be contaminated solely by transport through roots which penetrate the source zone. Both approximations provide a means of calculating the ratio of Pu concentration in the root zone to that in the source zone: C_s/C_0. In this section, the body of C_s/C_o data from the lysimeters is used to evaluate the efficacy of the approximations.

7.3.2 Instantaneous Partitioning Approximation

The instantaneous partitioning (Eqn. 2.5) is

$$\frac{C_s}{C_0} = N \cdot CR_r \cdot \frac{\rho_r}{\rho_b} \qquad \text{Eqn. 7.1}$$

For the lysimeters, N is11 years, ρ_r is 0.070 g/cm^3, and ρ_b is 1.5 g/cm^3. Root density is the geometric mean of calculated root densities for the SRS soil from 0-20 cm in 1 cm increments and bulk soil density is from Demirkanli et al. (2009). Root density results were obtained using Demirkanli et al. (2009) root density with depth equation [RD(z)]:

$$RD(z) = 0.136 \bullet e^{-0.06646 \bullet z} \qquad \text{Eqn. 7.2}$$

The sole transport parameter in this approximation is concentration ratio for roots. Presented in Table 7.5 are predictions of C_s/C_0 based on selected values of Pu concentration ratios from Table 2.2. Calculations are not shown for

Nisbet and Shaw (1994) cabbage plants because they indicated that the outer leaves may have been contaminated from the soil Pu and for Druteikiene et. al. (1999) because they sampled only the top shoots of the grass plant, which may have introduced bias into their results due to the relative increase in the concentration of Pu in upper shoots. Where a range of values are listed, the geometric mean values were used in the calculations.

Table 7.5 Pu Soil Transport Parameters Calculated from Concentration Ratios

Plant	**CR (literature)**	**C/C_0**	**$\log_{10} C/C_0$**
$bean_1$	3.60E-04	1.68E-05	-4.77
$corn_1$	2.90E-04	1.35E-05	-4.87
$beet_2$	2.30E-03	1.07E-04	-3.97
$turnip_2$	6.00E-04	2.80E-05	-4.55
$carrot_2$	3.00E-03	1.40E-04	-3.85
$carrot_3$	3.40E-03	1.59E-04	-3.80
barley $straw_3$	2.20E-04	1.03E-05	-4.99
$grass_4$	(0.005 – 0.03)	5.72E-04	-3.24
all $plants_5$	(0.003 – 0.17)	1.05E-03	-2.98
RAIS	5.00E-03	2.33E-04	-3.63
RESRAD	2.50E-04	1.17E-05	-4.93

Concentration ratio (data are on a dry mass basis) sources include 1-Whicker et al. (1999), 2-Adriano et al. (2000), 3-Nisbet and Shaw (1994), 4-Sokolik et al. (2004), and 5-Lux et al. (1995). Studies 1 and 2 were conducted over a single growing season. Study 3 was conducted over 5y and is averaged data of loamy and sandy soils. Study 4 determined “meadow grass” plant concentration ratios in the contamination zone 15y after the Chernobyl nuclear power plant accident. Study 5 is a compilation of different plant species sampled from contaminated forest soils 6y after the Chernobyl accident. The entries for RAIS (Risk Assessment Information System, U.S. EPA) and RESRAD (Residual Radiation Assessment Software Package) are composite values which were determined from the data of many Pu plant uptake studies.

The C_s/C_0 predictions are compared to the lysimeter data in Figure 7.5. The horizontal lines are the mean (black solid) and one standard deviation about the mean (black dashed) of the $\log_{10}$ transformed data from the top 20 cm of the SRS lysimeters. The predictions are in very good agreement with the data with two of eleven values lying outside one standard deviation from the mean. The mean of the predicted values shown as a bright green dashed line (-4.11) is quite similar to the mean of the data (-4.45). The cohesiveness of the predictions and the agreement between the predictions and the data are surprising given the diversity of the concentration ratios, which represent field studies of shoot and root vegetables (studies 1 – 3), native species (studies 4 and 5), and default values used for risk assessment. A possible implication of the agreement between the predictions and the data seen in Figure 7.5 is that Pu may interact similarly with many different plants even though the uptake, net transport, effective distances, and dynamics of translocation may differ greatly among different plants. However, even if this broader implication does not hold, the comparison in Figure 7.5 provides a basis for using Equation 2.5 in risk assessments involving the upward migration pathway.

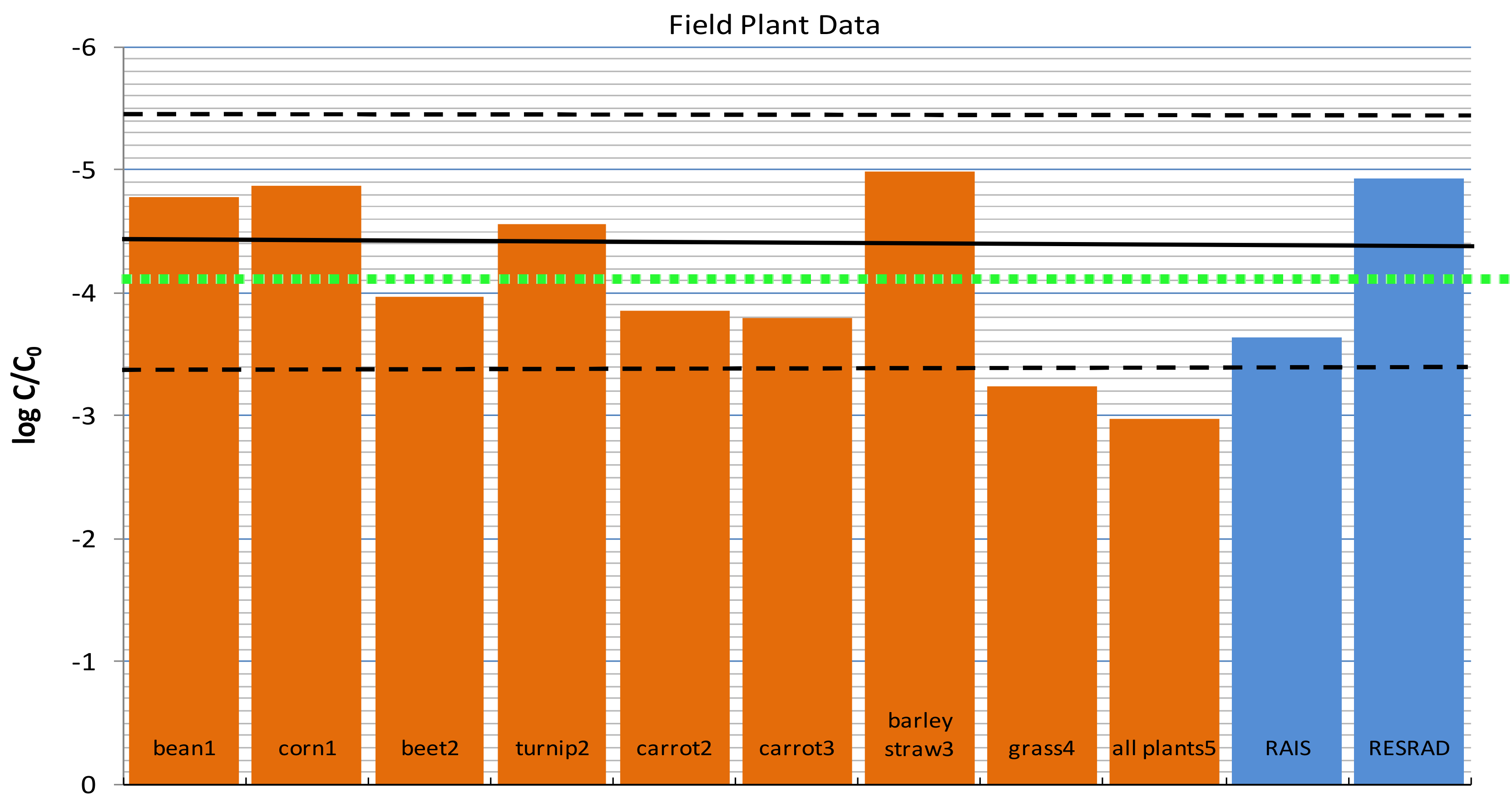

Figure 7.5 The logarithm$_{10}$ of SRS Pu C/C_0 data from the top 20 cm of lysimeter soil are plotted as the mean (solid black line) and 1 standard deviations about the mean (dashed black lines). Literature concentration ratio predictions of Pu C/C_0 (in Table 7.5) are plotted with the mean and standard deviations for the lysimeter soil. The field data include shoot and root vegetables, native grasses, and two reference composite values. The short dashed green line is the mean of the field C/C_0 predictions. The RAIS and RESRAD CR values are 5×10^{-3} and 2.5×10^{-4} respectively.

7.3.3 Steady-State Advection Approximation

The steady state advection (SSA) (Eqn. 2.15) is

$$\frac{C_s}{C_0} = N \frac{R_{Pu}}{K_{Ds}} \frac{\eta_x A_x}{\rho_b A_s} \qquad \text{Eqn. 7.4}$$

This equation has two transport parameters, Pu retardation factor in plants and soil-water distribution coefficient in the source zone. Measurement of retardation factor was one of the objectives of this dissertation (Chapter 4 & 5) and is treated as one of the known parameters in the right hand side of Equation 7.4. The known parameter values are given in Table 7.6. The Pu retardation factor in plants is an approximate midpoint value for the measured retardation discussed in Chapters 4 and 5. The exposure time is the lysimeter time in the field (Kaplan et al. (2006)), the xylem porosity and bulk soil density were obtained in Demirkanli (PhD Dissertation, Clemson University, Clemson, SC 2006), and the xylem area to soil area ratio is the geometric mean of the SRS soil sample depths from 0-20 cm in the lysimeters, calculated using:

$A_x/A_s = 0.000134 \bullet e^{-0.06646 \bullet z}$ Eqn. 7.5

Table 7.6 Parameters utilized for the calculation of K_{ds}

R_{Pu}	N	η_x	ρ_b	A_x/A_s (0-20)
3	10.75	0.6	1.5	6.24E-05

Since data that account for the effect of siderophores and other plant exudates on the availability of nutrients or contaminants sorbed to soil are not available, the soil distribution coefficient is treated as an unknown in Equation 7.4. Rather, values were back calculated from C/C_0 measurements for the top 20 cm of the lysimeters. Presented in Table 7.7 are the minimum and maximum K_d values along with the mean and standard deviation. These back calculated K_ds are less than those obtained in batch sorption experiments using SRS sediments in which 5950 is the best combined K_d value for reduced and oxidized Pu species (In Press, Daniel Kaplan, Savannah River National Laboratory, Aiken, SC). This is reasonable given the discussion above regarding the impact of plants on nutrient availability.

Table 7.7 K_{ds} Calculated from Lysimeter C/C_0 Data Using the Steady State Advection Model

Minimum	Mean	Maximum
0.10	23.0	1006

7.4 Plutonium Plant Distribution Coefficient Experiments

7.4.1 Introduction

A key transport parameter in advective models is the retardation factor of Pu in plants, R_{Pu}. The physical interpretation of retardation factor is the ratio of contaminant velocity to water velocity in a porous medium, and it quantifies the impact of contaminant sorption to the solid phase on its mobility. The measurements in this dissertation are based on the physical definition. However, the fundamental mathematical definition of retardation factor comes from the derivation of the reactive transport model, in which the distribution coefficient is used to account for partitioning of contaminant between the aqueous and solid phases. The mathematical definition (Equation 2.11) as applied to xylem is

$$R_{Pu} = 1 + \frac{\rho_x K_{dx}}{\eta_x} \qquad \text{Eqn. 7.6}$$

where ρ_x is xylem density [kg_x/m_x^3], K_{dx} is distribution coefficient for Pu in xylem [m_w^3/kg_x], and η_x is xylem porosity [m_w^3/m_x^3].

Thus, an alternative approach to obtaining Pu retardation factor in living plants is through batch sorption experiments of K_d. Consequently, short term batch sorption experiments were performed using plant xylem and cellulose contacted with Pu (IV) at pH 1.0 or 6.0 or pre-complexed $Pu_2(DTPA)_3$ or Pu(DFOB) at pH 6.0

Plant xylem is not commercially available, yet plant cellulose is. Thus the xylem must be collected from suitable sources. Grass species are unsuitable as xylem donors because their small xylem tissue size and vascular bundle distribution makes xylem collection highly impractical (Figure 5.6). The xylem in woody plants is much more distinct and convenient for collection than that of herbaceous plants. Cotton (*Gossypium hirsutum*) is a perennial shrub and an excellent xylem donor because its woody stem has a radial architecture with distinct tissues.

7.4.2 Materials

Clemson University grows cotton for crop research at Clemson University's Edisto Research Campus in Blackville, SC. Two dozen cotton plants

(*Gossypium hirsutum cv. Delta Pine 164 Bollgard II*) planted on May 19, 2008 were collected by Richard Reeves, Jr. in July 2008 when the plants were 50-60 cm tall and six weeks old. The fresh cotton plant samples were cleaned and placed in refrigerated storage at 4° C for eight weeks. They were stripped of their leaves, branches, and thick basal stalk leaving stem sections 25-30 cm long. Using a high speed rotary tool, the epidermis and cortical tissues were removed from the stem which was sectioned into ~5 cm pieces and split, exposing the pith. The pith was then removed with the rotary tool. Care was exercised to ensure the removal of all cortical and pith tissues from the xylem leaving woody xylem and phloem tissues. The pieces were then coarsely ground in a coffee grinder. The ground pieces were flash frozen with liquid nitrogen and reduced to a 20 mesh powder by cutting twice in a Wiley mill and drying at 75 ℃ for two days. Seventy-two g of unprocessed cotton stem tissue resulted in ~ 19 g of final product, henceforth described as xylem or xylem solid.

Cellulose procured from Ward Scientific (Rochester, NY) was manufactured by FMC Biopolymer (Newark, DE). As a plant-derived solid for comparison to cotton xylem, the cellulose manufactured and sold as Avicel® microcrystalline cellulose is a partially depolymerized alpha cellulose derived from softwood pulp, typically hemlock (*Tsuga sp*.) or spruce (*Picea sp*.). The product procured from Ward Scientific is advertised as bulk alpha-cellulose however their supplier states that the microcrystalline cellulose is a food grade product. This means it is processed to homogenize its particle size and mixing properties and to remove functional groups and other biological entities averse to human consumption.

7.4.3 Methods

The xylem samples were contacted with de-ionized water twice to reduce any ionic salts adsorbed to the xylem surface during drying, vacuum filtered with a Whatman #40 paper filter, and delivered into individual reaction vessels moist. The cellulose was processed in the same manner. The porosity was determined by measurement of wet and dry masses of 10 mL sample volumes. Moist solid phase samples equivalent to 0.1 – 0.25 g dry were transferred into the top sections of Pall MicroSep centrifugal chambers with a 3.5 mL total volume and a 30,000 molecular weight cut-off value. The chambers had been pre-conditioned with 0.5 mL of the applicable Pu solution to eliminate loss of Pu onto the separation device prior to contact with the solid phase. The pre-conditioning solution was discarded and 2.0 mL of Pu solution was pipetted into the top of the chambers with the weighed solids. Preliminary sorption tests spanning 1 – 24 h showed that a batch contact time of 6 h was sufficient to determine sorption. During contact, the samples were gently shaken at 30 cycles/ min. Samples were centrifuged at 7000 RPM for 20 min to separate the liquid and solid fractions. A minimum of duplicate samples were prepared for each treatment. Plutonium content was analyzed in 2 dram plastic scintillation vials with 1 mL sample added to 5 mL of Ultima Gold AB cocktail via liquid scintillation using a Wallac Model 1409 liquid scintillation counter.

The distribution coefficients were calculated by:

$$K_{d\,plant} = \frac{V*(C_0-C_t)}{M_s*C_t} \qquad \text{Eqn. 7.7}$$

where *V* is total solution volume (including the water in the wet solid), M_s is the dry solid mass, C_0 and C_t are the initial and final activities (Bq/mL) in the solution.

7.4.4 Results and Discussion

Table 7.8 lists the K_d and R data of Pu as Pu(IV), Pu(DFOB), and $Pu_2(DTPA)_3$ in contact with plant xylem or cellulose. In all solutions, the sorption of Pu to cellulose was much lower than its sorption to xylem. For both solid phases, the K_d data trend:

Pu(DFOB) > Pu(IV) @ pH 6.0 > Pu(IV) @ pH 1.0 > $Pu_2(DTPA)_3$

The Pu(IV) and Pu(DFOB) K_d values are approximately one to two orders of magnitude greater for xylem than for cellulose. For $Pu_2(DTPA)_3$, the xylem K_d is seven times the cellulose K_d. The retardation data follow the same trend as the K_d data. The bulk densities of the xylem and cellulose were 0.32 and 0.43 g/cm^3, respectively and their respective porosities were about 0.74 and 0.38.

Table 7.8 Distribution Coefficients and Retardation Factors of ^{238}Pu (IV) and complexed ^{238}Pu in Contact with Cotton Xylem or Cellulose

Batch Contact	pH	K_d	R
Xylem Pu (IV)	1.0	22.9	10.9
Xylem Pu (IV)	6.0	275	120
Xylem Pu(DFOB)	6.0	426	176
Xylem Pu(DTPA)	6.0	3.08	2.3
Cellulose Pu(IV)	1.0	2.77	4.1
Cellulose Pu(IV)	6.0	3.42	4.9
Cellulose Pu(DFOB)	6.0	14.2	17.1
Cellulose Pu(DTPA)	6.0	0.44	1.5

In nature, the Pu in plant xylem has been transported across the root and inside the plant in the transpiration fluid. It is not known whether sorption test results accurately represent the uptake and distribution behavior of Pu in living plants since the structure of xylem in live plants could be significantly altered in the excising, drying and tissue processing steps. Our retardation factors from live corn plants range from 1-10. In general retardation factors calculated from the cellulose K_d data are agree more closely with the live plant data than do the cotton xylem data. However, there are inconsistencies between our live plant data and these sorption test results. First, our live plant uptake experiments which compared the uptake of Pu complexed with DFOB and DTPA showed that Pu(DFOB) is taken up in greater concentrations than $Pu_2(DTPA)_3$ whereas the sorption results indicate that the retardation of Pu(DFOB) is one to two orders of magnitude greater than that of $Pu_2(DTPA)_3$. It is suggested that part of the effectiveness of a Pu complexant in increasing plant uptake is in its ability to transport Pu through the root tissues. In any case, the live plant Pu(DFOB) retardation factors are significantly less than those inferred from the equivalent sorption tests.

CHAPTER EIGHT

CONCLUSIONS

8.1 Significant research findings

This dissertation addresses the hypothesis that root uptake and transport in plants can influence the mobility of Pu in the vadose zone. The overarching goal was to provide experimental support for reactive transport modeling of root uptake and xylem transport and for a connection between Pu uptake and the plant's nutritional requirement for Fe. The objectives were to: (1) quantify complexed Pu retardation in graminaceous plants and to quantify complexed Pu sorption to plant xylem, (2) characterize the distribution and accumulation of complexed Pu in plants, and (3) compare correlations between plant uptake of complexed Pu and Fe. In addition, a couple of simple models for predicting Pu transport by roots were examined.

With respect to the first objective, the retardation factor of Pu in live plants was estimated experimentally to be 1-10, with the variability due mainly to water velocity uncertainty. This range is fairly consistent with a Pu retardation factor of 9 calculated from the Pu-plant K_d value reported in Demirkanli et al. (2009). The batch K_d experiments of Pu in contact with cotton vascular tissue and cellulose gave mixed results. Retardation factors from Pu-cellulose K_d data were 1.5 and 17 and the Pu-cotton xylem data were 2 and 176, with each pair representing $Pu_2(DTPA)_3$ and Pu(DFOB), respectively. The cellulose results were similar to those of living corn plants; however, the cotton xylem results differed by up to two orders of magnitude. Also, the K_d values are much larger for Pu(DFOB) than for $Pu_2(DTPA)_3$ which results in larger retardation factors (1 to 2 orders of magnitude larger for cellulose and cotton xylem, respectively). This finding is in opposition to uptake study results (Figure 5.2) which showed that the uptake of Pu in corn was greater as Pu(DFOB) than as $Pu_2(DTPA)_3$. The Pu retardation results from living plants are likely a better representation of plant interactions because sorption tests of Pu and materials removed from plants do not account for the natural physiology and structural differences between xylem in vivo and xylem or cellulose as an extracted plant material.

The Pu retardation factor from the live plant studies supports the case that upward Pu transport in the Savannah River Site lysimeters occurred through plants. Considering the lysimeter data, the transport simulation results, the isotopic measurements indicating that the surface Pu originated from the sources, and these Pu plant study results, a logical conclusion is that upward transport and redistribution of Pu occurred in the SRS lysimeter plants.

With respect to the second objective, analysis of the spatial distribution of Pu in corn indicated that discrimination occurs at the exodermis and in root tissues, most of the Pu in the plant was retained in the roots, and the fraction of Pu that entered the xylem was rapidly transported upward. In these experiments, an overall average of greater than 97% of the Pu was found in the roots with the remainder in the shoots. The maximum shoot activity fraction (the fraction of total plant activity found in the shoot) was approximately four per cent for plants exposed continuously for 10 d. The activity fraction in the shoots increased with increasing exposure time but did not reach a steady state during the relatively short exposure periods of this study. Profiles of Pu tissue concentration versus shoot length showed that Pu tended to concentrate in the upper shoots.

Analysis and comparison of the distribution of Pu in the roots and shoots in this and other studies suggest that the majority of Pu remains outside the xylem of most plants. This finding may be most applicable to phytoremediation efforts; however, transport modeling of Pu involving its uptake in plants should account for root exclusion. It is possible that Pu which becomes adsorbed to a root surface would be available for uptake by the roots of other plants at a later time.

With respect to the third objective, several findings are of interest. The averaged plant uptake of Pu remained unchanged for Fe: Pu ratios ranging from 0 - 2.2 x 10^5. Large changes in Fe concentrations did not inhibit or enhance plant uptake of Pu. Comparisons of the distribution profiles of Pu, ^{59}Fe, stable Fe, and several other nutrient elements showed that Pu was distributed very much like ^{59}Fe in the shoot. However six times as much Pu was found in the root than ^{59}Fe, and 40% more ^{59}Fe was found in the shoot than Pu. The shoot distribution data strongly suggest that upon entering the xylem, Pu and Fe are physiologically treated in a highly similar manner. Clearly, Pu is simultaneously taken up with Fe. These findings are consistent with the bacterial uptake and distribution study of John et al. (2001), which showed that more Fe was transported into the bacterial cells and that less Pu passed through the cell wall (analogous to the plant root tissue). This is the first study to report the plant uptake of Pu involving complexation with a siderophore which is produced to sequester Fe. These Fe and Pu correlations are consistent with a small but growing body of evidence that plants, bacteria, and possibly other organisms which require Fe can and do also incorporate Pu.

In addition, two simple transport approximations - instantaneous partitioning and steady-state advection - were developed to predict transport from the lysimeter source zone soil upward to the plant root zone soil. Using the instantaneous partitioning model, comparisons were remarkably consistent between the soil concentration data of the SRS lysimeters and predictions using concentration ratios derived from field studies involving different plants, soils, and experimental conditions. The steady-state advection model predicted K_d values for Pu and plant root zone soil that are much lower than batch sorption determinations. This is consistent with enhanced mobility of sorbed Pu by siderophores or other plant exudates.

8.2 Limits of the research

A logical way to demonstrate the impact plants have on the subsurface transport of Pu is to conduct controlled field experiments designed to quantify both the Pu distribution in soil and in discrete plant tissues. It is known that Pu is transferred from the soil to plants from field uptake studies, yet those studies were focused on the bulk transference of Pu from the soil into plants and not the movement and transport of Pu in the subsurface due to interactions with plants. The scope, costs, permissions and time required to execute such a study are not realistic for a single dissertation research topic.

In order to measure Pu retardation, the experimental design must introduce sufficient Pu to the plants in a controlled and quantifiable manner to allow for the measurement of Pu and of water which moved through the plants. Using pre-complexed Pu in solution is ideal for keeping Pu soluble and for accurate quantification of the Pu in the solution and the plants, however it does not allow for the process of desorption of Pu from the soil.

It is well known that plants, microbes, and fungi utilize several types of complexing agents, such as simple organic molecules and siderophores to gather metal nutrients. The use of the bacterial siderophore DFOB as a complexant instead of natively-produced phytosiderophores may affect the incorporation and final distribution of elements in the plants. Comparative studies of plant uptake of Fe complexed with different siderophores indicate that both the amount and rate of uptake is significantly influenced by the siderophore. Plants are more efficient at utilizing naturally-produced phytosiderophores than other substances.

8.3 Suggestions for future research

It would be convenient to measure Pu retardation through the simultaneous determination of Pu and the water in xylem. The availability of tracers which could be precisely conservative with water flow is problematic due to their volatility in the rigorous digestion process required for Pu analysis (i.e., labeled water would evaporate, Br or Cl would volatilize, and an element of heavier mass such as Rb would very likely not be conservative with water). In lieu of this, if desired, then more accurate estimation of the retardation can be obtained using the methods of this study with two adjustments. First, analogous to these Pu velocity experiments, plants could be exposed and collected at finer time intervals. Second, the xylem areas at more discrete intervals could be collected and measured to obtain a more accurate plant water velocity. As a word of caution, plant transpiration is highly sensitive to the environment, therefore to obtain accurate retardation data, the water velocity plants and the Pu velocity plants should be the same age, of similar size, and in precisely similar environments so that the resulting data can be correlated. Conducting these experiments in a growth chamber which is designed to minimize variations in experimental conditions may be helpful.

Soil uptake experiments (not designed for retardation) conducted at longer exposure times should allow quantification of desorption of Pu from soil, root uptake efficiency, and steady-state partitioning between roots and shoots. To quantify desorption from soil, well characterized homogenous Pu in soil could be presented to plant roots in an arrangement that would maximize the root contact yet permit the roots sufficient room for growth, allow for accurate determination of soil moisture, and allow for excellent separation of the root tissues and the soil after the contact period. Similarly, to perform a detailed examination of the root tissue, then the relative amounts of Pu in the root and external to the roots (surface Pu) could be characterized. Care should be taken to ensure that Pu adsorbed to the surface of roots, such as fine roots and root hairs is not included in the soil fraction. As discussed above, due to the bioaccumulation study designs, field plant roots and shoots have rarely, if ever, been carefully sampled to determine the total content in the entire root versus the shoot.

Research involving the use of natively-produced phytosiderophores with Pu may provide better insight into the relative amounts and the mechanisms of Pu transport into plants.

Appendix A. Liquid Scintillation Data

Guidance for liquid scintillation data tables: MP is midpoint distance of a particular shoot section, SQPE is Spectral Quench Parameter External (essentially constant efficiency above ~640), cpm is raw data in counts per minute (in the region of interest), net cpm is blank subtracted data, Bq & C and Bq/g & C are the activity and concentration data including control contributions, and (Pu or Fe) Bq and Bq/g are ^{238}Pu and ^{59}Fe activities and concentrations in each tissue section. Root data have negligible control activities, thus are uncorrected. For example, the activity and concentration data in the right section columns (Pu Bq, Fe Bq, etc.) were used to generate the graphs of activity or concentration versus shoot length throughout the dissertation.

Table A.1 LR9 Dual Labeled Pu and Fe

Plant Section Data	MP cm	section	mass (g)	SQPE	Pu cpm	net cpm	Bq & C	Bq/g & C	Pu Bq	Bq/g	Fe cpm	net cpm	Bq & C	Bq/g & C	Fe Bq	Bq/g
7 GNS Blank A				725.71	10.5						31.3					
7 GNS Blank B				729.18	9.2						28.1					
Mean					*9.85*	0	0.00				*29.7*	0	0.00			
PuFe 0.1 ml SSA				729.91	14754	14744	245.73				11536	11506	191.76			
PuFe 0.1 ml SSB				728.9	14727	14718	245.29				11478	11449	190.81			
Mean					14741	14731	245.51				11507	11477	191.29			
Exposure time (min)	1680															
PuFe A R0 (root)		18	0.29	702.6	47922.1	47912	798.54	**2754**			5619.8	5590	93.17	**321.27**		
PuFe A RS	**9**	18	0.0445	727.83	10.7	1	0.01	0.32			50.1	20	0.34	7.64		
PuFe A AR1	**NA**	NA	0.291	715.08	42	32	0.54	1.84			69.2	40	0.66	2.26		
PuFe A AR2	**NA**	NA	0.286	708.12	12.9	3	0.05	0.18			55.3	26	0.43	1.49		
PuFe A AR sum			0.577			35.2	0.59	1.02				65.1	1.09	1.88		
PuFeA S1	5	10	0.538	697.28	30.6	20.8	0.35	0.64	0.18	0.38	108.7	79	1.32	2.45	0.39	1.08
PuFeA S2	15	20	0.474	689.67	31.3	21.5	0.36	0.75	0.18	0.60	102.9	73.2	1.22	2.57	0.42	2.05
PuFeA S3	25	30	0.499	684.69	166.4	156.6	2.61	5.23	2.49	4.99	133.4	103.7	1.73	3.46	1.18	2.35
PuFeA S4	35	40	0.467	706.6	68.7	58.9	0.98	2.10	0.89	1.99	137.4	107.7	1.80	3.84	1.46	3.64
PuFeA S5	45	50	0.43	670.31	90.2	80.4	1.34	3.11	1.28	3.03	158.6	128.9	2.15	5.00	1.96	4.94
PuFeA S6	55	60	0.356	667.04	127.1	117.3	1.95	5.49	1.91	5.40	245.8	216.1	3.60	10.12	3.77	10.82
PuFeA S7	65	70	0.233	717.37	74.4	64.6	1.08	4.62	1.05	4.57	170.8	141.1	2.35	10.09	2.35	10.61
PuFeA S8	75	80	0.139	704.23	45.7	35.9	0.60	4.30	0.59	4.26	125.7	96	1.60	11.51	1.62	12.13
PuFeA S9	85.5	91	0.0571	710.03	19.3	9.5	0.16	2.76	0.16	2.75	65.5	35.8	0.60	10.45	0.59	11.22
PuFeA >40cm total		51	1.2151			307.5	5.12	4.22	4.99	4.15		617.9	10.30	8.48	10.29	8.87
Sum Shoot	91	91	3.1931			565.05	9.42	2.95	8.72	2.81		981.5	16.36	5.12	13.74	4.84
Sum Plant		109	4.6816			48,513	808.56	172.71	807.86	172.57		6,657	110.95	23.70	119.23	25.56

Table A.1 LR9 Dual Labeled Pu and Fe (continued)

Plant Section Data	MP cm	section	mass (g)	SQPE	Pu cpm	net cpm	Bq & C	Bq/g & C	Pu Bq	Bq/g	Fe cpm	net cpm	Bq & C	Bq/g & C	Fe Bq	Bq/g
Exposure time (min)	1680															
PuFe B R0		18	0.221	691.66	58746.6	58737	978.95	**4430**			12191.6	12162	202.70	**917.19**		
PuFe B RS			0.0209	703.55	53.7	44	0.73	34.97			71.2	42	0.69	33.09		
PuFe B AR1			0.353	693.37	18.9	9	0.15	0.43			52.6	23	0.38	1.08		
PuFe B AR2			0.28	705.3	19.1	9	0.15	0.55			53.2	24	0.39	1.40		
PuFe B AR sum			0.633			18.3	0.31	0.48				46.4	0.77	1.22		
PuFeB S1	5	10	0.587	699.77	41.1	31.3	0.52	0.89	0.35	0.63	102.7	73.0	1.22	2.07	0.28	0.67
PuFeB S2	15	20	0.495	715.92	29.3	19.5	0.32	0.65	0.15	0.50	94.3	64.6	1.08	2.18	0.26	1.60
PuFeB S3	25	30	0.458	688.18	37.7	27.9	0.46	1.01	0.35	0.77	93.3	63.6	1.06	2.31	0.43	2.58
PuFeB S4	35	40	0.417	691.77	48.8	39.0	0.65	1.56	0.56	1.45	104.2	74.5	1.24	2.98	0.85	2.67
PuFeB S5	45	50	0.337	666.28	67.2	57.4	0.96	2.84	0.90	2.75	108.2	78.5	1.31	3.88	1.02	3.69
PuFeB S6	55	60	0.273	706.2	98.1	88.3	1.47	5.39	1.42	5.30	150.8	121.1	2.02	7.39	2.00	7.78
PuFeB S7	65	70	0.168	695.86	98.8	89.0	1.48	8.82	1.46	8.77	181.4	151.7	2.53	15.05	2.55	16.14
PuFeB S8	76.5	83	0.0679	717.32	73	63.2	1.05	15.50	1.04	15.46	167.5	137.8	2.30	33.82	2.39	37.02
PuFeB >40cm total		43	0.8459			297.7	4.96	5.87	4.96	6.93		489.1	8.15	9.64	7.89	10.16
Sum Shoot	83	83	2.8029			415.2	6.92	2.47	6.78	2.42		764.8	12.75	4.55	9.71	4.20
Sum Plant		101	4.3108			59,232	987.21	229.01	986.51	228.85		13,015	216.91	50.32	237.39	55.24
Exposure time (min)	1680															
PuFe C R0 (root)		18	0.287	679.93	69625.8	69616	1160.27	**4043**			8855.6	8826	147.10	**512.54**		
PuFe C RS			0.0234	726.94	8.6	-1	-0.02	-0.89			37.3	8	0.13	5.41		
PuFe C AR1			0.395	624.42	9.8	0	0.00	0.00			55.4	26	0.43	1.08		
PuFe C AR2			0.297	685.04	34.2	24	0.41	1.37			50.2	21	0.34	1.15		
PuFe C AR sum			0.692			24.3	0.41	0.59				46.2	0.77	1.11		
PuFeC S1	5	10	0.719	682.57	119.5	109.7	1.83	2.54	1.66	2.28	135.4	105.7	1.76	2.45	0.88	1.09
PuFeC S2	15	20	0.482	677.91	59.7	49.9	0.83	1.72	0.65	1.57	118.8	89.1	1.49	3.08	0.72	2.61
PuFeC S3	25	30	0.463	694.5	64.6	54.8	0.91	1.97	0.79	1.73	113.2	83.5	1.39	3.01	0.80	3.35
PuFeC S4	35	40	0.391	678.71	80.8	71.0	1.18	3.02	1.09	2.91	136	106.3	1.77	4.53	1.44	4.41
PuFeC S5	45	50	0.446	668.56	153.6	143.8	2.40	5.37	2.34	5.29	210.8	181.1	3.02	6.77	2.93	6.91
PuFeC S6	55	60	0.362	673.74	207.1	197.3	3.29	9.08	3.24	9.00	279.7	250	4.17	11.51	4.40	12.37
PuFeC S7	65	70	0.266	684.41	202.8	193.0	3.22	12.09	3.19	12.04	289.6	259.9	4.33	16.28	4.56	17.52
PuFeC S8	75	80	0.157	704.51	152.3	142.5	2.37	15.12	2.36	15.08	219.8	190.1	3.17	20.18	3.36	21.80
PuFeC S9	84.5	89	0.0475	720.73	35.1	25.3	0.42	8.86	0.42	8.85	98.4	68.7	1.15	24.11	1.21	26.45
PuFeC >40cm total		49	1.2785			701.7	11.69	9.15	11.56	7.15		949.8	15.83	12.38	16.46	13.23
Sum Shoot	89	89	3.3335			986.9	16.45	4.93	15.75	4.73		1334.4	22.24	6.67	20.30	6.57
Sum Plant		107	5.0279			70625.9	1177.10	234.11	1176.40	233.97		10,214	170.24	33.86	185.34	36.89

Table A.1 LR9 Dual Labeled Pu and Fe (continued)

Plant Section Data	MP cm	section	mass (g)	SQPE	Pu cpm	net cpm	Bq & C	Bq/g & C	Pu Bq	Bq/g	Fe cpm	net cpm	Bq & C	Bq/g & C	Fe Bq	Bq/g
Mean Data (n=3 LR9 A,B,C)																
Exposure time (min)	1680															
PuFe R0 (root)		18	0.2660		58764.8	58755	979.25	**3681**			8855.6	8826	147.10	**553.00**		
PuFe RS			0.0296		24.3	14.5	0.24	8.16			52.9	23.2	0.39	13.04		
PuFe AR1			0.3463		23.6	13.7	0.23	0.66			59.1	29.4	0.49	1.41		
PuFe AR2			0.2877		22.1	12.2	0.20	0.71			52.9	23.2	0.39	1.34		
PuFe AR sum			0.6340	Rel Mass		25.9	0.43	0.68				52.6	0.88	1.38		
PuFe S1	5	10	0.6147	0.1966	63.7	53.9	0.90	1.36	0.73	1.10	115.6	85.9	1.43	2.32	0.52	0.94
PuFe S2	15	20	0.4837	0.1547	40.1	30.3	0.50	1.04	0.33	0.89	105.3	75.6	1.26	2.61	0.47	2.09
PuFe S3	25	30	0.4733	0.1514	89.6	79.7	1.33	2.74	1.21	2.50	113.3	83.6	1.39	2.93	0.80	2.76
PuFe S4	35	40	0.4250	0.1359	66.1	56.3	0.94	2.23	0.85	2.12	125.9	96.2	1.60	3.78	1.25	3.57
PuFe S5	45	50	0.4043	0.1293	103.7	93.8	1.56	3.77	1.51	3.69	159.2	129.5	2.16	5.22	1.97	5.18
PuFe S6	55	60	0.3303	0.1056	144.1	134.3	2.24	6.65	2.19	6.57	225.4	195.7	3.26	9.67	3.39	10.33
PuFe S7	65	70	0.2223	0.0711	125.3	115.5	1.92	8.51	1.90	8.46	213.9	184.2	3.07	13.81	3.16	14.76
PuFe S8	76	80	0.1213	0.0388	90.3	80.5	1.34	11.64	1.33	11.60	171.0	141.3	2.36	21.84	2.46	23.65
PuFe S9	85	89	0.0523	0.0167	27.2	17.4	0.29	5.81	0.29	5.80	82.0	52.3	0.87	17.28	0.90	18.84
PuFe >40cm total		49	1.1306	0.3615		441.4	7.36	6.51	7.22	6.44		703.0	11.72	10.36	10.64	9.84
Sum Shoot	88	76	3.1273	1.0000		661.5	11.02	3.53	10.33	3.39		1044.3	17.41	5.57	13.37	4.79
Sum Plant		94	4.6909	**AR rt**		59456.9	990.95	211.25	990.26	211.10		9,946	165.77	35.34	180.66	38.51
PuFe A R0		18	0.29	702.6	47922.1	47912	798.54	2753.58			5619.8	5590	93.17	321.27		
PuFe B R0		18	0.221	691.66	58746.6	58737	978.95	4429.62			12191.6	12162	202.70	917.19		
Pu Fe C R0		18	0.287	679.93	69625.8	69616	1160.27	4042.74			8855.6	8826	147.10	512.54		

Control Data (PuFe)	MP cm	section	mass (g)	SQPE	Pu cpm	net cpm	Bq	Bq/g	Fe cpm	net cpm	Bq	Bq/g
Exposure time (min)	0											
root		18										
CS1-2 (100)	5	10	0.656	686.41	9.7	10.2	0.17	0.26	62.2	58.1	0.97	1.48
CS2 (100)	15	20	1.14	683.66	15.4	10.6	0.18	0.15	84.8	50.4	0.84	0.74
CS3-2 (100)	25	30	0.495	693.2	8.4	7.1	0.12	0.24	54.9	40.4	0.67	1.36
CS4 (100)	35	40	0.832	683.49	10.3	5.5	0.09	0.11	63.4	29	0.48	0.58
Cs5 (100)	45	50	0.69	645.24	8.3	3.5	0.06	0.08	58	23.6	0.39	0.57
CS6 (100)	55	60	0.543	696.54	7.6	2.8	0.05	0.09	47.9	13.5	0.23	0.41
CS7 (100)	65	70	0.417	707.61	6.1	1.3	0.02	0.05	48.8	14.4	0.24	0.58
CS8 (100)	75	80	0.24	718.72	5.4	0.6	0.01	0.04	43.5	9.1	0.15	0.63
CS9 (100)	87	95	0.164	719.22	4.9	0.1	0.00	0.01	38.2	3.8	0.06	0.39
Ctl >40cm total		55	2.054			8.30	0.14	0.07		64.40	1.07	0.52
Sum Shoot	95	95	5.177			41.73	0.70	0.13		242.29	4.04	0.78
Sum Plant		113	5.177			41.73	0.70	0.13		242.29	4.04	0.78

Table A.2 Data for Pulse Shape Analysis of Dual Labeled Pu and Fe

The data are the results of series of simultaneous alpha and beta analyses performed at stated pulse shape discrimination settings. In general, lower settings adjust the pulse timing to favor maximizing beta counts and higher settings favor maximizing alpha counts. Optimum settings were 50 for beta only (^{59}Fe), 100 for both beta and alpha, and 150 for alpha only (^{238}Pu). Cross a to b means the alpha counts which were lost to the beta classification, similarly cross b to a means the beta counts which were lost and classified as an alpha count. The data/optimum refers to the factor or percentage difference between a particular count rate and the optimum rate as described above.

Sample ID	**PSA**	**Alpha cpm**	**Beta cpm**	**Cross a→b cpm**	**Cross b→a cpm**	**Alpha optimum**	**Beta optimum**
59Fe only mean	**25**	0.75	15255.7	NA	NA	0.1	101.5%
Fe only Optimum	**50**	13.95	15026.2	NA	0	1.0	100.0%
	75	93.2	14952.5	NA	74	6.7	99.5%
	100	467.15	14201.6	NA	825	33.5	94.5%
	125	1073.45	13019	NA	2007	76.9	86.6%
	150	1635.5	11673.9	NA	3352	117.2	77.7%
1:1 Fe:Pu	**25**	8.5	12253.3	6764	NA	0.1%	177.7%
	50	4479.35	8955.3	2293	NA	66.1%	129.9%
	75	6544.15	7221.95	229	NA	96.6%	104.8%
1:1 Fe:Pu Optimum	**100**	6772.8	6893.9	0	0	100.0%	100.0%
	125	7112.45	6278.85	NA	615	105.0%	91.1%
	150	7393.25	5682.9	NA	1211	109.2%	82.4%
1:1 Fe:Pu	**70**	6467.9	7237.8	336	NA	95.1%	106.0%
Finer PSA grid	**80**	6636.5	7096.55	167	NA	97.5%	103.9%
	90	6730.75	6992.7	73	NA	98.9%	102.4%
1:1 Fe:Pu Optimum	**100**	6803.95	6828.1	0	0	100.0%	100.0%
	110	6842.6	6520.75	NA	307	100.6%	95.5%
	120	7049.05	6306.2	NA	522	103.6%	92.4%
	130	7121.35	6093.85	NA	734	104.7%	89.2%
QC duplicates	**100**	6788.38	6861.00	Mean			
1:1 Fe:Pu		0.2%	0.5%	RPD			

Figure A.1 Spectra of ^{59}Fe and of ^{59}Fe and ^{238}Pu at PSA settings of 50, 100, and 150. Red data indicate alpha spectra and blue data indicate beta spectra.

Fe-59 only PSA 50
13 cpm alpha, 15070 cpm beta

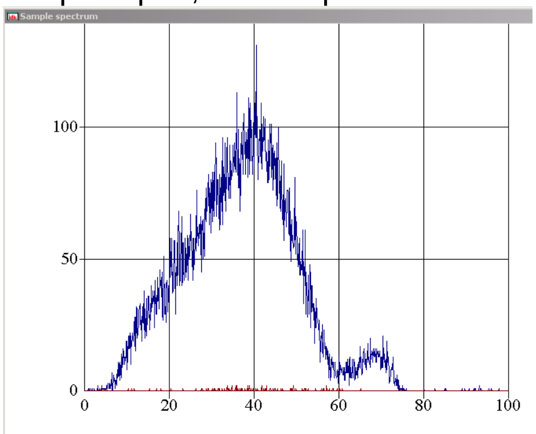

1:1 59Fe: 238Pu PSA 50
4440 cpm alpha, 8921 cpm beta

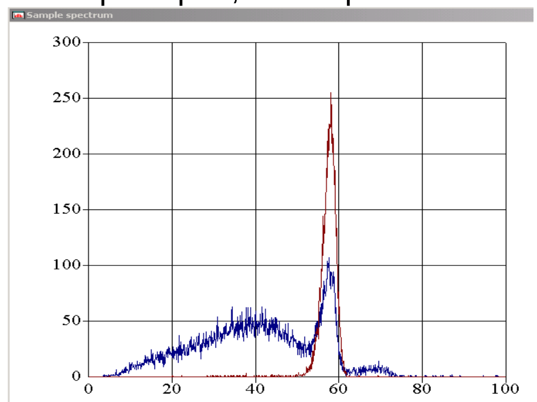

Fe-59 only PSA 100
441 cpm alpha, 14241 cpm beta

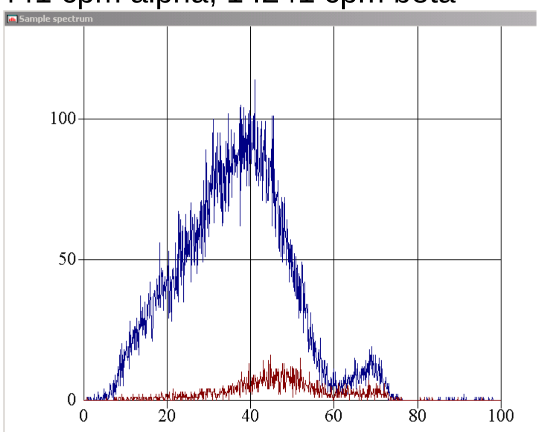

1:1 59Fe: 238Pu PSA 100
6813 cpm alpha, 6875 cpm beta

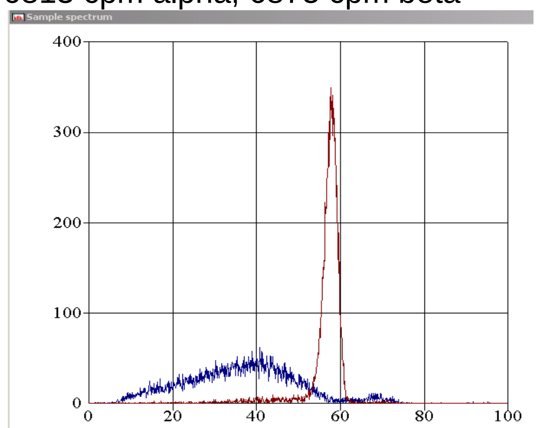

Fe-59 only PSA 150
1619 cpm alpha, 11709 cpm beta

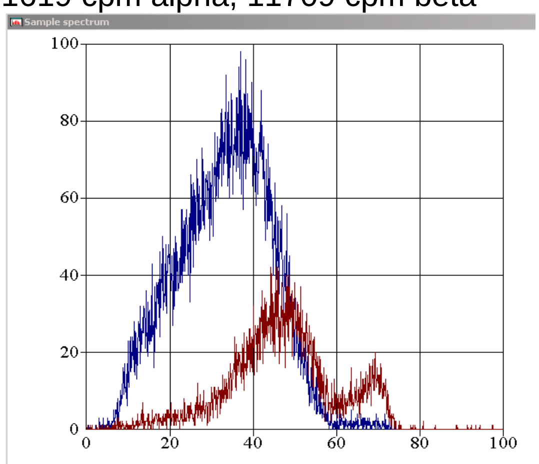

1:1 59Fe: 238Pu PSA 150
7448 cpm alpha, 5651 cpm beta

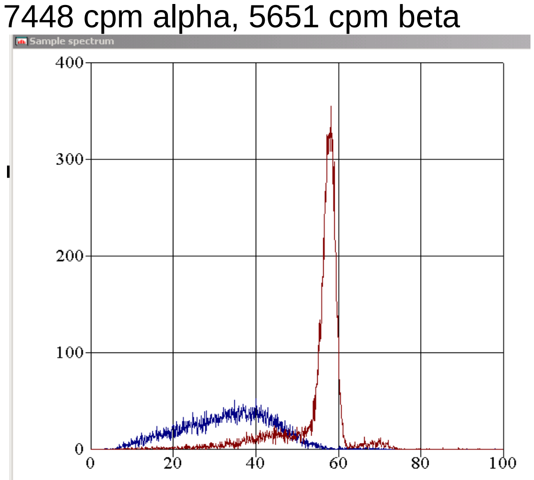

Figure A.2 Sample spectra of ^{59}Fe and ^{238}Pu analyzed using PSA setting of 100. Count rates are indicated for each spectrum.

Fe-59 and Pu-238 Sample Spectrum #1 235 cpm alpha, 360 cpm beta

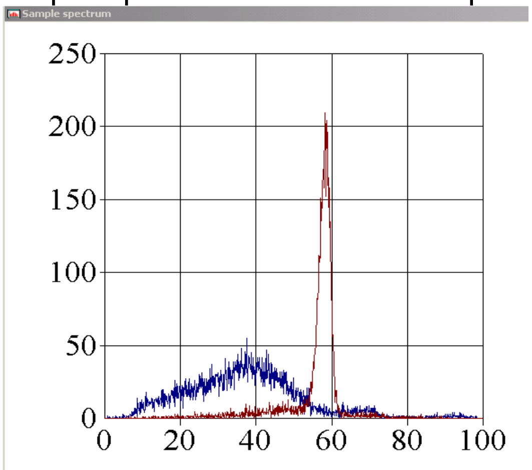

Fe-59 and Pu-238 Sample Spectrum #2 31 cpm alpha, 80 cpm beta

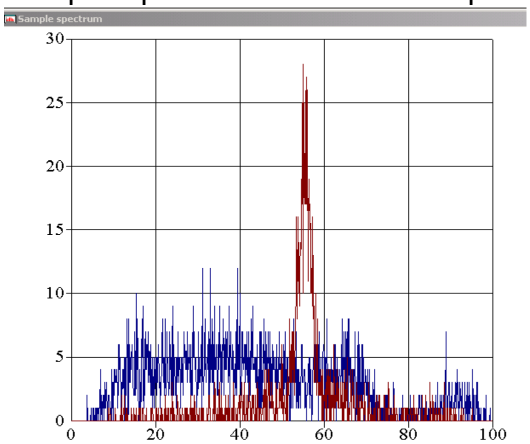

LSA Blank Sample Spectrum 5 cpm alpha, 36 cpm beta

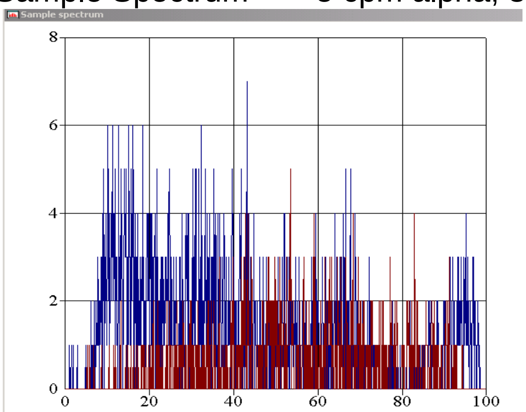

Table A.3 LR9 & LR8 Pu with 0x, 10x Fe in Solution

LR9 No (0x) Fe in GNS	MP cm	section	mass (g)	SQPE	Pu cpm	net cpm	Bq & C	Bq/g & C	Bq	Bq/g
0x Fe A * R0 (root)		18	0.14	717.71	88340.9	88330	1472.2	10515.4	1471.3	10511.2
0x FeA S1	5	10	0.495	681.25	54.6	43	0.7	1.5	0.4	1.0
0x FeA S2	15	20	0.413	685.5	78.5	67	1.1	2.7	0.8	2.3
0x FeA S3	25	30	0.341	669.78	105.5	94	1.6	4.6	1.3	4.3
0x FeA S4	35	40	0.262	682.05	134.2	123	2.1	7.8	1.8	7.5
0x FeA S5	45	50	0.188	701.24	219.5	208	3.5	18.5	3.3	18.1
0x FeA S6	57	64	0.106	716.53	172.8	162	2.7	25.4	2.6	25.2
0x Fe A >40cm total		24	0.294			370	6.2	21.0	5.9	20.1
Sum Shoot		64	1.805			698	11.6	6.4	10.3	5.7
Sum Plant		82	1.945			89028	1483.8	762.9	1482	762
0x Fe B * R0 (root)		18	0.0345	722.74	7234.3	7223	120.4	3489.4	119.5	3485.1
0x FeB S1	5	10	0.317	704.46	49.1	38	0.6	2.0	0.3	1.6
0x FeB S2	15	20	0.265	703.95	45.3	34	0.6	2.1	0.3	1.7
0x FeB S3	25	30	0.221	710.42	40.5	29	0.5	2.2	0.2	1.9
0x FeB S4	35	40	0.212	711.82	51.1	40	0.7	3.1	0.4	2.8
0x FeB S5	45	50	0.149	714.4	46.9	36	0.6	4.0	0.4	3.7
0x FeB S6	62	74	0.0757	719.72	50.2	39	0.7	8.6	0.6	8.4
0x Fe B >40cm total		34	0.2247			75	1.2	5.5	1.0	4.4
Sum Shoot		74	1.2397			216	3.6	2.9	2.2	1.8
Sum Plant		92	1.2742			7439	124.0	97.3	122	96

LR8 No (0x) Fe in GNS	MP cm	section	mass (g)	SQPE	Pu cpm	net cpm	Bq & C	Bq/g & C	Bq	Bq/g
0 Fe A * R0 (root)		18	0.385	726.04	8660	8649	144.1	374.4	143.3	370.1
0-Fe A S1	5	10	1.376	703.89	83.9	73	1.2	0.9	0.9	0.5
0-Fe A S2	15	20	1.002	706.99	59.7	49	0.8	0.8	0.5	0.4
0-Fe A S3	25	30	0.84	683.26	80.2	69	1.2	1.4	0.9	1.0
0-Fe A S4	35	40	0.781	701.47	92.4	81	1.4	1.7	1.1	1.4
0-Fe A S5	45	50	0.739	640.38	247.2	236	3.9	5.3	3.8	5.0
0-Fe A S6	55	60	0.58	704.68	381.2	370	6.2	10.6	6.1	10.4
0-Fe A S7	65	70	0.264	680.16	303.2	292	4.9	18.4	4.8	18.3
0-Fe A S8	78.5	87	0.164	707.05	119.8	109	1.8	11.0	1.8	10.9
0-Fe A >40cm total		47	1.747			1007	16.8	9.6	16.5	9.4
Sum Shoot		87	5.746			1278	21.3	3.7	19.9	3.5
Sum Plant		105	6.131			9927	165.4	27.0	163	27
0 Fe B * R0 (root)		18	0.381	727.05	25881	25870	431.2	1131.7	430.3	1127.4
0-Fe B S1	5	10	1.196	683.26	166.3	155	2.6	2.2	2.2	1.7
0-Fe B S2	15	20	0.771	692.06	68.6	57	1.0	1.2	0.7	0.8
0-Fe B S3	25	30	0.711	672.64	101.2	90	1.5	2.1	1.2	1.8
0-Fe B S4	35	40	0.53	708.28	91.4	80	1.3	2.5	1.1	2.2
0-Fe B S5	45	50	0.424	685.38	187.9	177	2.9	6.9	2.8	6.6
0-Fe B S6	55	60	0.243	708.12	175.4	164	2.7	11.3	2.7	11.1
0-Fe B S7	69	78	0.134	713.95	153.5	142	2.4	17.7	2.3	17.6
0-Fe B >40cm total		38	0.801			483	8.1	10.1	7.8	9.7
Sum Shoot		78	4.009			866	14.4	3.6	13.0	3.3
Sum Plant		96	4.39			26736	445.6	101.5	443	101
0 Fe C R0 (root)		18	0.653	694.22	60030	60019	1000.3	1531.9	999.5	1527.6
0-Fe C S1	5	10	1.002	713.62	68.6	57	1.0	1.0	0.6	0.5
0-Fe C S2	15	20	0.651	674.26	54	43	0.7	1.1	0.4	0.7
0-Fe C S3	25	30	0.67	694.96	69.6	58	1.0	1.5	0.7	1.1
0-Fe C S4	35	40	0.578	678.25	96.9	86	1.4	2.5	1.2	2.1
0-Fe C S5	45	50	0.536	678.37	166.9	156	2.6	4.8	2.4	4.5
0-Fe C S6	55	60	0.397	698.98	247	236	3.9	9.9	3.9	9.7
0-Fe C S7	65	70	0.269	702.48	182.1	171	2.8	10.6	2.8	10.4
0-Fe C S8	80	90	0.166	698.13	40.5	29	0.5	2.9	0.5	2.8
0-Fe C >40cm total		50	1.368			592	9.9	7.2	7.1	5.2
Sum Shoot		90	4.269			836	13.9	3.3	12.5	2.9
Sum Plant		108	4.922			60855	1014.3	206.1	1012	206

Table A.3 LR9 & LR8 Pu with 0x, 10x Fe in Solution (Continued)

LR9 10x Fe in GNS	MP cm	section	mass (g)	SQPE	Pu cpm	net cpm	Bq & C	Bq/g & C	Bq	Bq/g
10 Fe A (root)		18	0.108	709.86	31699.9	31689	528.15	4890	527.3	4886.0
10x FeA S1	5	10	0.353	714.07	33.7	23	0.38	1.1	0.0	0.6
10x FeA S2	15	20	0.329	705.98	46.8	36	0.59	1.8	0.3	1.4
10x FeA S3	25	30	0.275	717.76	71.2	60	1.00	3.6	0.7	3.3
10x FeA S4	35	40	0.189	706.03	84.4	73	1.22	6.5	1.0	6.1
10x FeA S5	45	50	0.0811	719.84	54.3	43	0.72	8.9	0.5	8.5
10x FeA S6	53	56	0.0131	729.85	12.3	1	0.02	1.4	-0.1	1.2
10x Fe A >40cm total		26	0.0942			44	0.7	7.8	0.5	5.2
Sum Shoot		56	1.3482			236	3.9	2.9	2.6	1.9
Sum Plant		74	1.3482			31924	532.1	394.7	530	393
10 Fe B (root)		18	0.108	711.65	41856.8	41846	697.43	6458	696.6	6453.4
10x FeB S1	5	10	0.453	691.32	47.6	36	0.61	1.3	0.3	0.9
10x FeB S2	15	20	0.325	713.95	59.6	48	0.81	2.5	0.5	2.1
10x FeB S3	25	30	0.302	698.7	78.6	67	1.12	3.7	0.9	3.4
10x FeB S4	35	40	0.23	692.23	120	109	1.81	7.9	1.6	7.6
10x FeB S5	45	50	0.103	708.9	94.6	83	1.39	13.5	1.2	13.2
10x FeB S6	58	66	0.0466	719.16	36.6	25	0.42	9.1	0.3	8.9
10x Fe B >40cm total		26	0.1496			109	1.8	12.1	1.6	10.5
Sum Shoot		66	1.4596			370	6.2	4.2	4.8	3.3
Sum Plant		84	1.5676			42215	703.6	448.8	701	447

LR8 10x Fe in GNS	MP cm	section	mass (g)	SQPE	Pu cpm	net cpm	Bq & C	Bq/g & C	Bq	Bq/g
10 Fe A (root)		18	0.305	722.46	39204	39193	653.22	2142	652.4	2137.4
10-Fe A S1	5	10	1.089	699.71	29.4	18	0.30	0.3	0.0	-0.1
10-Fe A S2	15	20	0.76	690.64	40.5	29	0.49	0.6	0.2	0.2
10-Fe A S3	25	30	0.675	681.94	44.6	33	0.56	0.8	0.3	0.5
10-Fe A S4	35	40	0.599	675.48	55.1	44	0.73	1.2	0.5	0.9
10-Fe A S5	45	50	0.527	713.06	78.9	68	1.13	2.1	1.0	1.8
10-Fe A S6	55	60	0.457	680.5	139.4	128	2.14	4.7	2.1	4.5
10-Fe A S7	65	70	0.328	708.9	161.4	150	2.50	7.6	2.5	7.5
10-Fe A S8	80	90	0.163	694.84	51.4	40	0.67	4.1	0.6	4.0
10-Fe A >40cm total		50	1.475			386	6.4	4.4	5	3.5
Sum Shoot	98	90	4.903			511	8.5	1.7	7	1
Sum Plant		108	4.903			39704	661.7	135.0	659	135
10 Fe B (root)		18	0.451	709.46	27942	27931	465.52	1032	464.7	1027.9
10-Fe B S1	5	10	0.981	673.1	71.1	60	1.00	1.0	0.7	0.6
10-Fe B S2	15	20	0.724	685.55	49.6	38	0.64	0.9	0.4	0.5
10-Fe B S3	25	30	0.669	676.58	66.7	56	0.93	1.4	0.7	1.0
10-Fe B S4	35	40	0.571	672	77.1	66	1.10	1.9	0.9	1.6
10-Fe B S5	45	50	0.548	693.2	179.5	168	2.81	5.1	2.6	4.8
10-Fe B S6	55	60	0.398	690.64	387.3	376	6.27	15.7	6.2	15.5
10-Fe B S7	65	70	0.207	705.08	305.7	295	4.91	23.7	4.9	23.6
10-Fe B S8	78	86	0.11	709.58	143.3	132	2.20	20.0	2.2	19.9
10-Fe B >40cm total		46	1.263			971	16.2	12.8	13	10.5
Sum Shoot		86	4.208			1191	19.8	4.7	18	4
Sum Plant		104	4.659			29122	485.4	104.2	483	104
10 Fe C (root)		18	0.618	721.35	60900	60889	1014.81	1642	1014.0	1637.8
10-Fe C S1	5	10	1.371	702.6	117.9	107	1.78	1.3	1.4	0.9
10-Fe C S2	15	20	1.044	691.49	132.2	121	2.02	1.9	1.7	1.5
10-Fe C S3	25	30	0.834	701.8	231.8	221	3.68	4.4	3.4	4.1
10-Fe C S4	35	40	0.74	698.36	401.5	390	6.51	8.8	6.3	8.5
10-Fe C S5	45	50	0.608	696.2	688.9	678	11.30	18.6	11.1	18.3
10-Fe C S6	55	60	0.573	726.38	891.7	881	14.68	25.6	14.6	25.4
10-Fe C S7	65	70	0.373	707.55	1632.3	1621	27.02	72.4	27.0	72.3
10-Fe C S8	80.5	91	0.206	715.69	277.4	266	4.44	21.5	4.4	21.4
10-Fe C >40cm total		51	1.76			3446	57.4	32.6	46	26.1
Sum Shoot		91	5.749			4284	71.4	12.4	70	12
Sum Plant		109	6.367			65173	1086.2	170.6	1084	170

Table A.3 LR9 & LR8 Pu with 0x, 10x Fe in Solution (Continued)

Averaged LR9 & 8 0x Fe Data	MP cm	section	mass (g)	SQPE	Pu cpm	net cpm	Bq & C	Bq/g & C	Bq	Bq/g
0 Fe Mean Root		18	0.3187	717.6	38029.3	38018.1	633.6	3408.6	632.8	3404.3
0-Fe S1	5	10.0	0.877	697.3	84.5	73.3	1.2	1.5	0.9	1.1
0-Fe S2	15	20.0	0.620	692.6	61.2	50.0	0.8	1.6	0.5	1.2
0-Fe S3	25	30.0	0.557	686.2	79.4	68.2	1.1	2.4	0.9	2.0
0-Fe S4	35	40.0	0.473	696.4	93.2	82.0	1.4	3.5	1.1	3.2
0-Fe S5	45	50.0	0.407	684.0	173.7	162.5	2.7	7.9	2.5	7.6
0-Fe S6	57	63.6	0.280	709.6	205.3	194.1	3.2	13.2	3.2	12.9
0-Fe S7	66	72.7	0.222	698.9	212.9	201.7	3.4	15.6	3.3	15.4
0-Fe S8	79	88.5	0.165	702.6	80.2	69.0	1.1	7.0	1.1	6.9
0-Fe >40cm total (large variance)		46.6	1.075			505.2	8.4	10.7	7.7	7.1
Sum Shoot		78.6	3.602			778.7	13.0	4.0	11.6	3.4
Sum Plant		96.6	3.920			38797	647	239	644	238

Averaged LR9 & 8 10x Fe Data	MP cm	section	mass (g)	SQPE	Pu cpm	net cpm	Bq & C	Bq/g & C	Bq	Bq/g
10 Fe Mean Root		18	0.318	714.96	40320.6	40309.4	671.8	3232.8	671.0	3228.5
10-Fe S1	5	10.0	0.849	696.16	59.9	48.7	0.81	1.0	0.5	0.6
10-Fe S2	15	20.0	0.636	697.52	65.7	54.5	0.91	1.5	0.6	1.1
10-Fe S3	25	30.0	0.551	695.36	98.6	87.4	1.46	2.8	1.2	2.4
10-Fe S4	35	40.0	0.466	688.82	147.6	136.4	2.27	5.3	2.1	4.9
10-Fe S5	45	50.0	0.373	706.24	219.2	208.0	3.47	9.6	3.3	9.3
10-Fe S6	55	60.4	0.298	709.31	293.5	282.3	4.70	11.3	4.6	11.1
10-Fe S7	65	70.0	0.303	707.18	699.8	688.6	11.48	34.6	11.4	33.3
10-Fe S8	80	89.0	0.160	706.70	157.4	146.2	2.44	15.2	2.4	15.1
10x Fe >40cm total		39.8	1.133			1068.3	16.5	13.9	13.3	11.2
Sum Shoot		77.8	3.636			1318.2	22.0	5.2	20.6	4.6
Sum Plant		95.8	3.954			47147	694	251	692	250

Table A.3 LR9 & LR8 Pu with 0x, 10x Fe in Solution (Continued)

Control Plant Data (Pu) LR9	MP cm	section	mass (g)	SQPE	Pu cpm	net cpm	Bq	Bq/g	(Compared to LR8)	
C R0		18	0.201	715.41	62.8	51.6	0.86	4.28		
C RS			0.0257	713.34	7.2	-4.0	-0.07	-2.59		
C AR			1.006	697.28	86.5	75.3	1.26	1.25	**Bq**	**Bq/g**
C S1	23	10	0.821	680.79	32.1	20.9	0.35	0.42	0.14	0.10
C S2	33	20	0.687	700.96	28.4	17.2	0.29	0.42	-0.20	-0.01
C S3	43	30	0.734	689.95	26.4	15.2	0.25	0.35	0.07	-0.03
C S4 total	53	40	0.668			13.2	0.22	0.33	-0.05	0.00
C S5	63	50	0.532	662.52	21.5	10.3	0.17	0.32	-0.03	0.03
C S6	73	60	0.375	702.93	15.9	4.7	0.08	0.21	-0.04	-0.02
C S7	86	70	0.215	714.52	13.1	1.9	0.03	0.15	-0.07	-0.10
C S8 Interpolated (for Transpirat	93	80					0.02	0.10		
C S9 Interpolated	103	90					0.01	0.05		
C S10 Interpolated	110	97					0.00	0.00		
C >40cm total		57	1.122			17	0.28	0.25	0	-0.1
Sum Shoot		97	5.038			159	2.65	0.53	0	0
Sum Plant		115	5.2647			206	3.44	0.65	0	0
C S4-1	53	40	0.394	689.72	19.3	8.1	0.14	0.34	0.14	0.34
C S4-2	53	40	0.274	698.41	16.3	5.1	0.09	0.31	0.09	0.31

Control Plant Data (Pu) LR8	MP cm	section	mass (g)	SQPE	Pu cpm	net cpm	Bq	Bq/g		
CS1-2 (150)	23	10	0.656	686.58	21.2	12.7	0.21	0.32		
CS2 (150)	33	20	1.14	684.35	37.6	29.1	0.48	0.42		
CS3-2 (150)	43	30	0.495	692.74	19.8	11.3	0.19	0.38		
CS4 (150)	53	40	0.832	684.29	25	16.5	0.27	0.33		
CS5 (150)	63	50	0.69	644.23	20.8	12.3	0.20	0.30		
CS6 (150)	73	60	0.543	696.37	15.9	7.4	0.12	0.23		
CS7 (150)	83	70	0.417	708	14.7	6.2	0.10	0.25		
CS8 (150)	93	80	0.24	718.72	11.6	3.1	0.05	0.21		
CS9 (150)	105	95	0.164	718.83	9.8	1.3	0.02	0.13		
C >40cm total		65	2.054			30	0.50	0.24	0	0.0
Sum Shoot		105	5.177			87	1.45	0.28	0	0
Sum Plant		123	5.177			99	1.66	0.32	0	0

Table A.4 LR9 3-10d Exposure Data

3 d Exposure	MP cm	section	mass (g)	SQPE	Pu cpm	net cpm	Bq & C	Bq/g & C	Bq	Bq/g	f Plt Act	f Tot Act	Total mL
3dA R0		18	0.196	681.82	27961.8	27950	465.8	2376.7	465.0	2372.5	0.98695	5.7E-02	500
3dA RS			0.031	729.24	10	-1	-0.02	-0.78	0.05	1.98	0.00010	5.7E-06	**Trans mL**
3dA AR1			0.426	706.6	20.8	9	0.16	0.37			0.00000	0.0E+00	130
3dA AR2			0.363	718.21	21.4	10	0.17	0.46			0.00000	0.0E+00	Bq Trans
3dA AR			0.789			19	0.32	0.41	-0.93	-0.84	-0.00197	-1.1E-04	2140
3dA S1	23	10	0.867	676.06	54.7	43	0.72	0.83	0.38	0.41	0.00080	4.6E-05	P Act/ BqTr
3dA S2	33	20	0.674	608.26	29.3	18	0.30	0.44	0.02	0.03	0.00003	1.8E-06	0.220
3dA S3	43	30	0.588	680.21	88.1	77	1.28	2.17	1.03	1.83	0.00218	1.2E-04	
3dA S4	53	40	0.451	671.65	167.3	156	2.60	5.76	2.39	5.44	0.00506	2.9E-04	
3dA S5	63	50	0.229	691.09	175.4	164	2.73	11.93	2.57	11.62	0.00544	3.1E-04	
3dA S6	73	60	0.054	718.83	55.5	44	0.73	13.60	0.66	13.40	0.00140	8.0E-05	Bq Eq/Trn Bq
3dA >40cm total		20	0.283			208	3.5	12.2	3.2	11.4	0.00685	3.9E-04	0.2173
Sum Shoot		60	2.863			502	8.4	2.9	7.0	2.5	0.01492	8.5E-04	0.0033
Sum Plant		78	4.668			28489	474.8	101.7	471	101	1.00000	5.7E-02	0.2202
3dB R0		18	0.247	722.97	7534.2	7523	125.4	507.6	124.5	503.4	0.98140	1.5E-02	**Total mL**
3dB RS			0.0208	727.67	22.1	11	0.18	8.53	0.25	11.29	0.00196	3.0E-05	500
3dB AR1			0.271	708.45	21	10	0.16	0.59			0.00000	0.0E+00	**Trans mL**
3dB AR2			0.196	712.44	18.9	7	0.12	0.63			0.00000	0.0E+00	162
3dB AR			0.467			17	0.28	0.61	-0.97	-0.64	-0.00763	-1.2E-04	Bq Trans
3dB S1	23	10	0.76	663.99	42.1	31	0.51	0.67	0.17	0.25	0.00131	2.0E-05	2666
3dB S2	33	20	0.554	696.77	47.6	36	0.60	1.09	0.32	0.68	0.00252	3.9E-05	P Act/ BqTr
3dB S3	43	30	0.434	675.83	54.7	43	0.72	1.66	0.47	1.32	0.00372	5.7E-05	0.048
3dB S4	53	40	0.357	693.42	63.2	52	0.86	2.42	0.65	2.10	0.00513	7.9E-05	
3dB S5	63	50	0.231	685.09	65.1	54	0.89	3.87	0.73	3.56	0.00573	8.8E-05	
3dB S6	75	65	0.121	700.79	60.5	49	0.82	6.76	0.74	6.56	0.00586	9.0E-05	Bq Eq/Trn Bq
3dB >40cm total		25	0.352			103	1.7	4.9	1.5	4.2	0.01159	1.8E-04	0.0467
Sum Shoot		65	2.457			265	4.4	1.8	3.1	1.3	0.02427	3.7E-04	0.0012
Sum Plant		83	3.6588			7832	130.5	35.7	127	35	1.00000	1.5E-02	0.0476
3dC R0		18	0.152	725.09	9817.8	9806	163.4	1075.3	162.6	1071.0	0.98512	2.0E-02	**Total mL**
3dC RS			0.0094	728.62	8.7	-3	-0.05	-4.88	0.03	-2.12	0.00015	3.0E-06	500
3dC AR1			0.309	721.29	30.4	19	0.32	1.02			0.00000	0.0E+00	**Trans mL**
3dC AR2			0.289	703.33	35.1	24	0.39	1.36			0.00000	0.0E+00	91
3dC AR			0.598			43	0.71	1.19	-0.54	-0.06	-0.00328	-6.6E-05	Bq Trans
3dC S1	23	10	0.524	710.64	50.5	39	0.65	1.24	0.31	0.82	0.00186	3.7E-05	1498
3dC S2	33	20	0.393	717.43	48.4	37	0.62	1.57	0.33	1.16	0.00202	4.1E-05	P Act/ BqTr
3dC S3	43	30	0.346	709.35	54.5	43	0.72	2.07	0.47	1.73	0.00284	5.7E-05	0.110
3dC S4	53	40	0.28	699.6	65.1	54	0.89	3.19	0.68	2.88	0.00414	8.3E-05	
3dC S5	63	50	0.163	703.78	65.3	54	0.90	5.51	0.73	5.19	0.00442	8.9E-05	
3dC S6	77	68	0.0649	710.76	42.9	31	0.52	8.08	0.45	7.88	0.00273	5.5E-05	Bq Eq/Trn Bq
3dC >40cm total		28	0.2279			85	1.4	6.2	1.2	5.2	0.00715	1.4E-04	0.1086
Sum Shoot		68	1.7709			258	4.3	2.4	3.0	1.7	0.01800	3.6E-04	0.0020
Sum Plant		86	3.1283			10147	169.1	54.1	165	53	1.00000	2.0E-02	0.1102
Averaged 3 d Data	MP cm	section	mass (g)	SQPE	Pu cpm	net cpm	Bq & C	Bq/g & C	Bq	Bq/g	f Plt Act	f Tot Act	Total mL
3d R0		18	0.1983	710	15105	15093	252	1320	251	1316	0.9856	3.0E-02	500
3d RS			0.0204	729	25.1	13.7	0.23	0.82	0.11	3.72	0.0004	1.3E-05	**Trans mL**
3d AR			0.6180			26.3	0.44	0.73	-0.81	-0.51	-0.0032	-9.9E-05	128
3d S1	23.0	10.0	0.7170	683.56	49.1	37.7	0.63	0.92	0.28	0.50	0.0011	3.4E-05	Bq Trans
3d S2	33.0	20.0	0.5403	674.15	41.8	30.3	0.51	1.03	0.22	0.62	0.0009	2.7E-05	2101
3d S3	43.0	30.0	0.4560	688.46	65.8	54.3	0.91	1.97	0.66	1.63	0.0026	8.0E-05	P Act/ BqTr
3d S4	53.0	40.0	0.3627	688.22	98.5	87.1	1.45	3.79	1.24	3.47	0.0049	1.5E-04	0.126
3d S5	63.0	50.0	0.2077	693.32	101.9	90.5	1.51	7.10	1.34	6.79	0.0053	1.6E-04	
3d S6	75.0	64.3	0.0800	710.13	53.0	41.5	0.69	9.48	0.62	9.28	0.0024	7.5E-05	Bq Eq/Trn Bq
3d >40cm total		24.3	0.288			132	2.2	7.6	1.96	6.8	0.0077	2.4E-04	0.1193
Sum Shoot		64.3	2.364			341	5.7	2.4	4.36	1.8	0.0171	5.3E-04	0.0021
Sum Plant		82.3	3.200			15475	257.9	80.6	254.35	79	1.0000	3.1E-02	0.1211

Table A.4 LR9 3-10d Exposure Data (Continued)

7 d Exposure	MP cm	section	mass (g)	SQPE	Pu cpm	net cpm	Bq & C	Bq/g & C	Bq	Bq/g	f Plt Act	f Tot Act	Total mL
7dA R0		18	0.107	696.77	27962	27950	465.8	4353.6	465.0	4349.4	0.98460	5.7E-02	1000
7dA RS			0.0471	725.93	108.4	97	1.62	34.31	1.69	37.06	0.00357	2.0E-04	**Trans mL**
7dA AR			0.6	681.19	32.9	21	0.36	0.60	-0.89	-0.65	-0.00189	-1.1E-04	245
7dA S1	23	10	0.639	648.14	57.8	46	0.77	1.21	0.43	0.79	0.00091	5.2E-05	Bq Trans
7dA S2	33	20	0.518	689.55	72.1	61	1.01	1.95	0.73	1.54	0.00154	8.9E-05	4032
7dA S3	43	30	0.503	685.21	93.4	82	1.37	2.72	1.12	2.38	0.00236	1.4E-04	P Act/ BqTr
7dA S4	53	40	0.423	676.17	121.8	110	1.84	4.35	1.63	4.03	0.00345	2.0E-04	0.117
7dA S5	63	50	0.248	685.55	108.1	97	1.61	6.50	1.44	6.18	0.00306	1.8E-04	
7dA S6	74	62	0.109	712.89	84	73	1.21	11.09	1.14	10.90	0.00240	1.4E-04	Bq Eq/Trn Bq
7d A >40cm total		22	0.357			169	2.8	7.9	2.6	7.2	0.00546	3.1E-04	0.1153
Sum Shoot		62	2.44			469	7.8	3.2	6.5	2.7	0.01372	7.9E-04	0.0016
Sum Plant		80	3.1941			28537	475.6	148.9	472	148	1.00000	5.7E-02	0.1171
7dB R0		18	0.316	709.18	12950	12938	215.6	682.4	214.8	678.1	0.96479	2.6E-02	**Total mL**
7dB RS			0.0333	717.93	108	97	1.61	48.32	1.68	51.08	0.00755	2.0E-04	1000
7dB AR1			0.266	707.22	71.2	60	1.00	3.74			0.00000	0.0E+00	**Trans mL**
7dB AR2			0.524	711.15	54	43	0.71	1.35			0.00000	0.0E+00	528
7dB AR			0.79			102	1.71	2.16	0.45	0.91	0.00204	5.5E-05	Bq Trans
7dB S1	23	10	0.77			32	0.54	0.69	0.19	0.28	0.00086	2.3E-05	8690
7dB S2	33	20	0.654	678.83	61.2	50	0.83	1.27	0.55	0.86	0.00246	6.6E-05	P Act/ BqTr
7dB S3	43	30	0.604	643.64	73.4	62	1.03	1.71	0.78	1.37	0.00352	9.5E-05	0.026
7dB S4	53	40	0.5	670.6	90.4	79	1.32	2.63	1.10	2.31	0.00496	1.3E-04	
7dB S5	63	50	0.394	641.69	122.2	111	1.85	4.68	1.68	4.37	0.00754	2.0E-04	
7dB S6	73	60	0.25	709.75	61.6	50	0.84	3.34	0.76	3.15	0.00342	9.3E-05	
7dB S7	85	74	0.093	698.41	51.5	40	0.67	7.18	0.64	7.05	0.00287	7.8E-05	Bq Eq/Trn Bq
7d B >40cm total		24	1.237			201	3.3	2.7	3.1	2.5	0.01384	3.7E-04	0.0247
Sum Shoot		74	3.265			424	7.1	2.2	5.7	1.7	0.02563	6.9E-04	0.0007
Sum Plant		92	5.1943			13663	227.7	43.8	223	43	1.00000	2.7E-02	0.0256
7dB S1-1	23	10	0.424	692.51	30.1	19	0.31	0.73					
7dB S1-2	23	10	0.346	692.57	24.9	13	0.22	0.65					
7dC R0		18	0.451	680.62	22082	22071	367.85	816	367.0	811.4	0.95898	4.5E-02	**Total mL**
7dC RS			0.04	727.5	215.2	204	3.40	84.90	3.47	87.65	0.00906	4.2E-04	1000
7dC AR1			0.464	701.41	25	14	0.23	0.49			0.00000	0.0E+00	**Trans mL**
7dC AR2			0.381	724.42	23.8	12	0.21	0.54			0.00000	0.0E+00	491
7dC AR			0.845			26	0.43	0.51	-0.82	-0.73	-0.00214	-1.0E-04	Bq Trans
7dC S1	23	10	0.821	677.04	74.3	63	1.05	1.28	0.70	0.86	0.00184	8.5E-05	8081
7dC S2	33	20	0.715	673.28	98	87	1.44	2.02	1.16	1.61	0.00303	1.4E-04	P Act/ BqTr
7dC S3	43	30	0.588	660.28	135.1	124	2.06	3.50	1.81	3.17	0.00473	2.2E-04	0.047
7dC S4	53	40	0.455	637.24	150	139	2.31	5.08	2.10	4.76	0.00548	2.5E-04	
7dC S5	63	50	0.321	676.98	228.2	217	3.61	11.25	3.45	10.94	0.00900	4.2E-04	
7dC S6	73	60	0.174	682.69	169.8	158	2.64	15.17	2.57	14.97	0.00670	3.1E-04	
7dC S7	83	70	0.048	716.7	89.1	78	1.29	26.96	1.27	26.83	0.00331	1.5E-04	Bq Eq/Trn Bq
7 d C>40cm total		30	0.543			453	7.5	13.9	7.3	13.4	0.01901	8.8E-04	0.0454
Sum Shoot		70	5.303			864	14.4	2.7	13.0	2.5	0.03410	1.6E-03	0.0016
Sum Plant		88	5.303			23191	386.5	72.9	383	72	1.00000	4.7E-02	0.0474
Averaged 7 d Data	MP cm	section	mass (g)	SQPE	Pu cpm	net cpm	Bq & C	Bq/g & C	Bq	Bq/g	f Plt Act	f Tot Act	Total mL
7d R0		18	0.2913	696	20998	20986	349.77	1950.55	349	1946	0.9714	4.2E-02	1000
7d RS			0.0401	724	144	132	2.21	55.84	2.28	58.60	0.0063	2.8E-04	**Trans mL**
7d AR			0.7450	681	33	50	0.83	1.09	-0.42	-0.16	-0.0012	-5.1E-05	421
7d S1	23.0	10.0	0.7433	663	66	47	0.79	1.06	0.44	0.64	0.0012	5.4E-05	Bq Trans
7d S2	33.0	20.0	0.6290	681	77	66	1.09	1.75	0.81	1.33	0.0023	9.9E-05	6934
7d S3	43.0	30.0	0.5650	663	101	89	1.49	2.64	1.24	2.30	0.0034	1.5E-04	P Act/ BqTr
7d S4	53.0	40.0	0.4593	661	121	109	1.82	4.02	1.61	3.70	0.0045	2.0E-04	0.063
7d S5	63.0	50.0	0.3210	668	153	141	2.36	7.48	2.19	7.16	0.0061	2.7E-04	
7d S6	73.3	60.7	0.1777	702	105	94	1.56	9.87	1.49	9.67	0.0041	1.8E-04	
7d S7	84.0	72.0	0.0705	708	70	59	0.98	17.07	0.95	16.94	0.0027	1.2E-04	Bq Eq/Trn Bq
7d >40cm total		25.3	0.248			294	4.9	19.7	4.31	17.4	0.0120	5.2E-04	0.0503
Sum Shoot		68.7	2.223			558	9.3	4.2	8.41	3.8	0.0234	1.0E-03	0.0012
Sum Plant		86.7	4.042			21774	362.9	89.8	359.19	89	1.0000	4.4E-02	0.0518

Table A.4 LR9 3-10d Exposure Data (Continued)

10 d Exposure	MP cm	section	mass (g)	SQPE	Pu cpm	net cpm	Bq & C	Bq/g & C	Bq	Bq/g	f Plt Act	f Tot Act	Total mL
10dA R0		18	0.384	714.24	18416.7	18405	306.8	798.8	305.9	794.6	0.95275	3.7E-02	1500
10dA RS			0.0353	727.95	37.1	26	0.43	12.11	0.50	14.87	0.00155	6.1E-05	**Trans mL**
10dA AR1			0.277	711.65	29	18	0.29	1.06			0.00000	0.0E+00	490
10dA AR2			0.286	711.99	26.6	15	0.25	0.88			0.00000	0.0E+00	Bq Trans
10dA AR			0.563			33	0.55	0.97	-0.71	-0.28	-0.00220	-8.6E-05	8064
10dA S1	23	10	0.87			136	2.27	2.60	1.92	2.18	0.00598	2.3E-04	P Act/ BqTr
10dA S2	33	20	0.685			135	2.24	3.27	1.96	2.86	0.00610	2.4E-04	0.040
10dA S3	43	30	0.509	714.63	185.4	174	2.90	5.70	2.65	5.36	0.00825	3.2E-04	
10dA S4	53	40	0.362	697.34	163.6	152	2.54	7.01	2.32	6.69	0.00724	2.8E-04	
10dA S5	63	50	0.266	691.49	213.8	202	3.37	12.68	3.21	12.36	0.00998	3.9E-04	
10dA S6	77	68	0.144	688.75	215.1	204	3.39	23.57	3.32	23.37	0.01034	4.0E-04	Bq Eq/Trn Bq
10dA >40cm total		28	1.281			406	6.8	5.3	6.5	5.1	0.02032	7.9E-04	0.0379
Sum Shoot		68	2.836			1003	16.7	5.9	15.4	5.4	0.04790	1.9E-03	0.0019
Sum Plant		86	4.3813			19499	325.0	74.2	321	73	1.00000	3.9E-02	0.0398
10dA S1-1	23	10	0.46	717.6	88.1	77	1.28	2.8	0.9	2.4			
10dA S1-2	23	10	0.41	723.53	70.7	59	0.99	2.4	0.7	2.0			
10dA S2-1	33	20	0.454	703.72	87	76	1.26	2.8	1.0	2.4			
10dA S2-2	33	20	0.231	720.67	70.4	59	0.98	4.3	0.8	3.9			
10dB R0		18	0.32	711.49	16436.8	16425	273.76	855	272.9	851.2	0.94520	3.3E-02	**Total mL**
10dB RS			0.0388	727.55	50	39	0.64	16.56	0.71	19.32	0.00247	8.7E-05	1500
10dB AR1			0.296	710.53	21	10	0.16	0.54			0.00000	0.0E+00	**Trans mL**
10dB AR2			0.312	694.5	25.6	14	0.24	0.76			0.00000	0.0E+00	639
10dB AR			0.608			24	0.40	0.65	-0.86	-0.59	-0.00296	-1.0E-04	Bq Trans
10dB S1	23	10	0.923	704.29	83.2	72	1.20	1.30	0.85	0.88	0.00295	1.0E-04	10517
10dB S2	33	20	0.759	703.78	87.2	76	1.26	1.66	0.98	1.25	0.00339	1.2E-04	P Act/ BqTr
10dB S3	43	30	0.626	705.53	154.2	143	2.38	3.80	2.13	3.46	0.00738	2.6E-04	0.027
10dB S4	53	40	0.504	667.04	210.7	199	3.32	6.59	3.11	6.27	0.01077	3.8E-04	
10dB S5	63	50	0.352	688.98	241.4	230	3.83	10.89	3.67	10.57	0.01269	4.5E-04	
10dB S6	73	60	0.204	690.18	201.3	190	3.16	15.51	3.09	15.31	0.01070	3.8E-04	
10dB S7	84	73	0.0905	715.13	141.4	130	2.17	23.93	2.14	23.80	0.00741	2.6E-04	Bq Eq/Trn Bq
10-Fe B >40cm total		33	0.6465			550	9.2	14.2	8.9	13.8	0.03080	1.1E-03	0.0259
Sum Shoot		73	3.4585			1039	17.3	5.0	16.0	4.6	0.05529	1.9E-03	0.0015
Sum Plant		91	5.0333			17551	292.5	58.1	289	57	1.00000	3.5E-02	0.0275
10dC R0		18	0.2	721.96	21817.5	21806	363.4	1817.2	362.6	1812.9	0.97744	4.4E-02	**Total mL**
10dC RS			0.025	728.23	33.9	22	0.37	14.97	0.45	17.72	0.00120	5.4E-05	1500
10dC AR1			0.684	575.41	14	3	0.04	0.06			0.00000	0.0E+00	**Trans mL**
10dC AR2			0.501	659.68	42.4	31	0.52	1.03			0.00000	0.0E+00	296
10dC AR			1.185			34	0.56	0.47	-0.69	-0.77	-0.00187	-8.4E-05	Bq Trans
10dC S1	23	10	0.916	704.06	70.9	59	0.99	1.08	0.65	0.66	0.00174	7.9E-05	4872
10dC S2	33	20	0.611	709.46	53.1	42	0.69	1.14	0.41	0.72	0.00111	5.0E-05	P Act/ BqTr
10dC S3	43	30	0.526	681.65	125.6	114	1.90	3.62	1.65	3.28	0.00446	2.0E-04	0.076
10dC S4	53	40	0.378	696.6	156.2	145	2.41	6.38	2.20	6.07	0.00593	2.7E-04	
10dC S5	63	50	0.212	703.1	174.4	163	2.72	12.81	2.55	12.50	0.00687	3.1E-04	
10dC S6	75	64	0.0713	711.21	85.3	74	1.23	17.26	1.16	17.06	0.00312	1.4E-04	Bq Eq/Trn Bq
10-Fe C >40cm total		24	0.2833			237	3.9	13.9	3.7	13.1	0.00999	4.5E-04	0.0744
Sum Shoot		64	2.7143			597	9.9	3.7	8.6	3.2	0.02323	1.0E-03	0.0018
Sum Plant		82	5.3093			22492	374.9	70.6	371	70	1.00000	4.5E-02	0.0761
Averaged 10 d Data	MP cm	section	mass (g)	SQPE	Pu cpm	net cpm	Bq & C	Bq/g & C	Bq	Bq/g	f Plt Act	f Tot Act	Total mL
10d R0		18	0.301	716	18890	18879	314.65	1157.17	313.79	1152.91	0.9599	3.8E-02	1500
10d RS			0.033	728	40	29	0.48	14.55	0.55	17.30	0.0017	6.7E-05	**Trans mL**
10d AR			0.785			30	0.50	0.70	-0.75	-0.55	-0.0023	-9.1E-05	475
10d S1	23.0	10.0	0.903	704		89	1.48	1.66	1.14	1.24	0.0035	1.4E-04	Bq Trans
10d S2	33.0	20.0	0.685	707		84	1.40	2.02	1.12	1.61	0.0034	1.4E-04	7818
10d S3	43.0	30.0	0.554	701	108	144	2.39	4.37	2.14	4.03	0.0066	2.6E-04	P Act/ BqTr
10d S4	53.0	40.0	0.415	687	141	165	2.76	6.66	2.54	6.34	0.0078	3.1E-04	0.048
10d S5	63.0	50.0	0.277	695	153	198	3.31	12.13	3.14	11.81	0.0096	3.8E-04	
10d S6	75.0	64.0	0.140	697	164	156	2.60	18.78	2.52	18.58	0.0077	3.1E-04	
10d S7	84.0	73.0	0.091	715	141	130	2.17	23.93	2.14	23.80	0.0065	2.6E-04	Bq Eq/Trn Bq
10d >40cm total		33	0.5069			484	8.1	15.9	6.37	12.6	0.0195	7.7E-04	0.0401
Sum Shoot		73	3.0633			966	16.1	5.3	13.32	4.3	0.0407	1.6E-03	0.0017
Sum Plant		91	4.1830			19904	331.7	79.3	326.91	78	1.0000	4.0E-02	0.0418

Table A.5 LR9 Transpiration Test Data

LR9 Transpiration - no fan	MP cm	section	mass (g)	SQPE	Pu cpm	net cpm	Bq & C	Bq/g & C	Bq	Bq/g	f Plt Act	f Tot Act	Total mL
T-A R0		18	0.462	726.77	12306.7	12293.8	204.90	443	204.0	439.2			500
T-A S1	23	10	1.154	700.62	99.1	86.2	1.44	1.24	1.09	0.82			**Trans mL**
T-A S2	33	20	0.758	711.09	60.7	47.8	0.80	1.05	0.51	0.63			156
T-A S3	43	30	0.656	687.27	62.5	49.6	0.83	1.26	0.57	0.92			Bq Trans
T-A S4	53	40	0.589	683.66	83.4	70.5	1.18	1.99	0.96	1.67			11355
T-A S5	63	50	0.492	696.54	99.7	86.8	1.45	2.94	1.28	2.62			P Act/ BqTr
T-A S6	73	60	0.402	695.47	152.8	139.9	2.33	5.80	2.25	5.59			0.019
T-A S7	83	70	0.298	709.97	205	192.1	3.20	10.74	3.17	10.60			
T-A S8	93	80	0.174	723.81	47.6	34.7	0.58	3.32	0.56	3.22			
T-A S9 (1)	105	95	0.055	718.72	58.4	45.5	0.76	13.79	0.75	13.74			
T-A >40 cm total		55	1.421			499	8.32	5.85	8.01	5.63	0.03720	2.2E-04	
Sum Shoot		95	4.578			753	12.55	2.74	11.13	2.43	0.05173	3.1E-04	
Sum Plant		113	5.04			13047	217.45	43.14	215.17	42.69	1.00000	5.9E-03	
													Total mL
T-B R0		18	0.406	707.22	8775.9	8763	146.05	360	145.2	355.5			500
T-B S1	23	10	0.841	718.21	22.4	9.5	0.16	0.19	-0.19	-0.24			**Trans mL**
T-B S2	33	20	0.729	707.95	36.6	23.7	0.40	0.54	0.11	0.12			177
T-B S3	43	30	0.701	709.8	38.9	26	0.43	0.62	0.18	0.27			Bq Trans
T-B S4	53	40	0.601	716.03	31.7	18.8	0.31	0.52	0.09	0.19			12883
T-B S5	63	50	0.564	708.73	55.1	42.2	0.70	1.25	0.53	0.92			P Act/ BqTr
T-B S6	73	60	0.466	691.77	79.6	66.7	1.11	2.39	1.03	2.18			0.012
T-B S7	83	70	0.375	704.57	133.2	120.3	2.01	5.35	1.97	5.20			
T-B S8	93	80	0.172	713.73	102.8	89.9	1.50	8.71	1.48	8.61			
T-A S9 (2)	106	96	0.093	720.4	25.4	12.5	0.21	2.24	0.20	2.19			
T-B >40 cm total		56	1.67			332	5.53	3.31	5.22	3.12	0.03463	1.4E-04	
Sum Shoot		96	4.542			410	6.83	1.50	5.41	1.19	0.03590	1.5E-04	
Sum Plant		114	4.948			9173	152.88	30.90	150.60	30.44	1.00000	4.1E-03	
LR9 Transpiration with fan	MP cm	section	mass (g)	SQPE	Pu cpm	net cpm	Bq & C	Bq/g & C	Bq	Bq/g	f Plt Act	f Tot Act	Total mL
T+A R0		18	0.239	720.12	13555.3	13542.4	225.71	944	224.8	940.1			500
T+A S1	23	10	0.952	712.89	101.4	88.5	1.48	1.55	1.13	1.13			**Trans mL**
T+A S2	33	20	0.707	702.82	67.2	37.3	0.62	0.88	0.34	0.46			79
T+A S3	43	30	0.676	709.41	95.9	34.1	0.57	0.84	0.32	0.50			Bq Trans
T+A S4	53	40	0.581	711.88	46.3	24	0.40	0.69	0.18	0.36			5750
T+A S5	63	50	0.485	702.31	125.5	31.8	0.53	1.09	0.36	0.77			P Act/ BqTr
T+A S6	73	60	0.417	719.56	125	25.4	0.42	1.02	0.35	0.81			0.040
T+A S7	83	70	0.244	702.48	142.9	25.9	0.43	1.77	0.40	1.62			
T+A S8	96	86	0.114	715.41	54.4	22.9	0.38	3.35	0.36	3.25			
T+A >40 cm total		46	1.26			106	1.77	1.40	1.47	1.16	0.00642	4.0E-05	
Sum Shoot		86	4.176			290	4.83	1.16	3.42	0.82	0.01499	9.4E-05	
Sum Plant		104	4.415			13832	230.54	52.22	228.27	51.70	1.00000	6.3E-03	
													Total mL
T+B R0		18	0.379	700.34	23447.1	23434.2	390.57	1031	389.7	1026.2			500
T+B S1	23	10	1.385	681.48	74.5	61.6	1.03	0.74	0.68	0.32			**Trans mL**
T+B S2	33	20	0.87	686.3	54.5	41.6	0.69	0.80	0.41	0.38			156
T+B S3	43	30	0.816	658.21	46.5	33.6	0.56	0.69	0.31	0.34			Bq Trans
T+B S4	53	40	0.745	708.96	39.7	26.8	0.45	0.60	0.23	0.27			11355
T+B S5	63	50	0.685	689.04	56.5	43.6	0.73	1.06	0.56	0.74			P Act/ BqTr
T+B S6	73	60	0.581	702.03	72.4	59.5	0.99	1.71	0.91	1.50			0.035
T+B S7	83	70	0.506	712.61	82	69.1	1.15	2.28	1.12	2.13			
T+B S8	93	80	0.334	698.07	132.6	119.7	2.00	5.97	1.98	5.87			
T+B S9	103	90	0.187	710.36	33.5	20.6	0.34	1.84	0.33	1.79			
T+B S10	118	110	0.072	725.26	12.8	-0.1	0.00	-0.02	0.00	-0.02			
T+B >40 cm total		70	2.365			312	5.21	2.20	4.90	2.07	0.01235	1.3E-04	
Sum Shoot		110	6.181			476	7.93	1.28	6.51	1.05	0.01644	1.8E-04	
Sum Plant		128	6.56			23910	398.50	60.75	396.22	60.40	1.00000	1.1E-02	

Table A.6 LR8 Dual Labeled Pu and Fe Scoping Test Data

Plant Section Data	MP cm	section	mass (g)	SQPE	Pu cpm	net cpm	cpm/g	minutes	cpm-cntl	conc-cntl	Fe cpm	net cpm	cpm/g	cpm-cntl	conc-cntl
PuFe A R0 (root)		18	0.479	711.54	15202	15193	**31718**				1478.6	1442	**3010**		
PuFeA S1-(1+2)	23	10	1.017	711.88	93.8	84.9	83.4				140.1	103.35	101.6		
PuFeA S1-(3)	23	10	0.442	722.46	44.1	35.2	79.5				87.9	51.15	115.7		
PuFeA S1 (total)	23	10	1.459			120.0	*82.2*		109.8	74.8		154.5	105.9	96.4	63.5
PuFeA S2	33	20	1.069	710.48	75.6	66.7	62.3		56.1	53.0	151.1	114.35	107.0	64.0	62.8
PuFeA S3	43	30	0.988	696.54	133.3	124.4	125.9		117.3	118.6	186.4	149.65	151.5	109.3	110.1
PuFeA S4	53	40	0.86	691.66	237.8	228.9	266.1		223.4	259.5	266.5	229.75	267.2	200.8	232.3
PuFeA S5	63	50	0.61	692.12	430.8	421.9	691.6		418.4	686.5	545.4	508.65	833.9	485.1	799.6
PuFeA S6	73	60	0.328	724.87	235.4	226.5	690.4		223.7	685.2	359.8	323.05	984.9	309.6	960.0
PuFeA S7	86	76	0.169	709.18	176.5	167.6	991.4		166.3	988.3	388.4	351.7	2080.8	337.3	2046.2
PuFeA >40cm total		36	1.107			815.9	737.0	1440	808.3	665.8		1183.4	1069.0	1131.9	1022.4
Sum Shoot	76	76	6.942		1427.3	1475.7	212.6	1440	1314.7	189.4		1831.6	263.8	1602.2	230.8
Sum Plant		94	7.421		16,629	16,669	2,246	1440	1314.7	177.2		3,273	441	1602.2	215.9
PuFe B R0		18	0.217	720.95	50743.3	50734	**233799**				2736.9	2700	**12443**		
PuFeB S1	23	10	1.13	671.82	20.5	11.6	10.2		1.3	2.8	123.8	87.1	77.0	28.9	34.7
PuFeB S2	33	20	0.859	715.47	18.2	9.3	10.8		-1.4	1.5	92.2	55.5	64.6	5.1	20.3
PuFeB S3	43	30	0.797	694.39	20.6	11.7	14.6		4.6	7.3	82.5	45.8	57.4	5.4	16.0
PuFeB S4	53	40	0.7	700.39	30.9	22.0	31.4		16.5	24.7	80.0	43.3	61.8	14.3	26.9
PuFeB S5	63	50	0.751	716.59	47.7	38.8	51.6		35.3	46.5	111.2	74.5	99.1	50.9	64.9
PuFeB S6	73	60	0.499	713.67	38.4	29.5	59.0		26.7	53.9	119.1	82.4	165.0	68.9	140.2
PuFeB S7	83	70	0.311	715.47	11.6	2.7	8.5		1.4	5.4	60.7	24.0	77.0	9.6	42.5
PuFeB >40cm total		50	1.561			70.9	45.4	1440	63.3	29.1		180.8	115.8	129.3	82.8
Sum Shoot	103	90	5.047		187.9	125.3	24.8	1440	84.2	16.7		412.3	81.7	182.9	36.2
Sum Plant		108	5.264		50,931	50,860	9,662	1440	84.2	16.0		3,112	591	182.9	34.7
PuFe A R0		18	0.479	711.54	15202	15193	**31718**				1478.6	1442	**3010**		
PuFe B R0		18	0.217	720.95	50743.3	50734	**233799**				2736.9	2700	**12443**		

Table A.7 LR8 Fe Velocity Data

Plant Section Data	MP cm	section	mass (g)	SQPE	Fe cpm	net cpm	cpm/g	min	cpm-cntl	conc-cntl	cpm-cntl	conc-cntl
root		18										
5 m S1	23	10	1.204	723.08	225.3	184.1	152.9		110.3	99.1	108.0	93.3
5 m S2	33	20	0.779	700.05	155.7	114.5	147.0		48.9	89.4	43.4	78.3
5 m S3	43	30	0.674	663.22	123.9	82.7	122.7		31.3	69.9	30.6	63.3
5 m S4	53	40	0.55	714.35	92.6	51.4	93.5		12.0	46.1	9.9	42.4
5 m S5	63	50	0.395	667.21	72.5	31.3	79.2		2.4	37.4	0.1	34.0
5 m S6	73	60	0.382	709.01	69.2	28.0	73.3		6.8	34.3	4.4	28.4
5 m S7	83	70	0.225	720.9	54.6	13.4	59.6		-9.5	4.6	-7.5	5.2
5 m S8	103	90	0.098	705.98	49.4	8.2	83.7		-4.3	31.6	-5.5	31.6
5 m >40cm total		50	1.1			72.7	**66.1**	**5**	-4.6	24.6	-8.4	22.6
Sum Shoot	103	90	**4.307**		**843.2**	**513.6**	**119.2**	**5**	**197.9**	**45.9**	**183.4**	**42.6**
root		18										
10 m S1	23	10	1.13	688.41	108	66.8	59.1		-7.0	5.3	-9.3	-0.5
10 m S2	33	20	0.859	669.67	99.1	57.9	67.4		-7.7	9.9	-13.2	-1.2
10 m S3	43	30	0.797	697.62	87.1	45.9	57.6		-5.5	4.7	-6.2	-1.8
10 m S4	53	40	0.7	696.37	77.5	36.3	51.9		-3.1	4.5	-5.2	0.8
10 m S5	63	50	0.751	693.2	76.4	35.2	46.9		6.3	5.0	4.0	1.6
10 m S6	73	60	0.499	689.04	63.4	22.2	44.5		1.0	5.4	-1.4	-0.4
10 m S7	83	70	0.311	726.6	56.5	15.3	49.2		-7.6	-5.7	-5.6	-5.1
10 m S8	103	90	0.167	715.92	50	8.8	52.7		-3.7	0.6	-4.9	0.6
10 m >40cm total		50	1.728			72.7	**42.1**	**10**	-4.0	0.6	-7.8	-0.5
Sum Shoot	103	90	**5.214**		**618**	**288.4**	**55.3**	**10**	**-27.3**	**-5.2**	**-41.8**	**-8.0**
root		18										
20 m S1	23	10	1.19	710.87	108.2	67.0	56.3		-6.8	2.5	-9.1	-3.3
20 m S2	33	20	0.883	715.24	98.4	57.2	64.8		-8.4	7.2	-13.9	-3.9
20 m S3	43	30	0.941	707.55	96.1	54.9	58.3		3.5	5.5	2.8	-1.0
20 m S4	53	40	0.709	693.82	81	39.8	56.1		0.4	8.8	-1.7	5.0
20 m S5	63	50	0.668	687.5	77.7	36.5	54.6		7.6	12.8	5.3	9.4
20 m S6	73	60	0.56	709.35	74.9	33.7	60.2		12.5	21.1	10.1	15.3
20 m S7	83	70	0.348	699.83	61.1	19.9	57.2		-3.0	2.3	-1.0	2.9
20 m S8	103	90	0.214	707.83	53.7	12.5	58.4		0.0	6.3	-1.2	6.3
20 m >40cm total		50	1.79			102.6	**57.3**	**20**	17.1	15.8	13.3	4.7
Sum Shoot	103	90	**5.513**		**651.1**	**321.5**	**58.3**	**20**	**5.8**	**1.1**	**-8.7**	**-1.6**
root		18										
40 m S1	23	10	1.081	690.07	123	81.8	75.7		8.0	21.9	5.7	16.1
40 m S2	33	20	0.783	684.01	112.5	71.3	91.1		5.7	33.5	0.2	22.4
40 m S3	43	30	0.802	687.55	111.3	70.1	87.4		18.7	34.6	18.0	28.0
40 m S4	53	40	0.708	683.95	106.9	65.7	92.8		26.3	45.4	24.2	41.7
40 m S5	63	50	0.588	663.69	101.3	60.1	102.2		31.2	60.3	28.9	57.0
40 m S6	73	60	0.449	718.32	119.1	77.9	173.5		56.7	134.5	54.3	128.6
40 m S7	83	70	0.329	689.27	112.4	71.2	216.4		48.3	161.5	50.3	162.1
40 m S8	103	90	0.239	688.18	93.2	52.0	217.6		39.5	165.5	38.3	165.5
40 m >40cm total		50	1.605			261.2	**162.7**	**40**	175.7	121.2	171.9	79.9
Sum Shoot	103	90	**4.979**		**879.7**	**550.1**	**110.5**	**40**	**234.4**	**47.1**	**219.9**	**44.2**
root		18										
80 m S1	23	10	1.23	666.39	114.6	73.4	59.7		-0.4	5.9	-2.7	0.1
80 m S2	33	20	1.021	683.2	101.6	60.4	59.2		-5.2	1.6	-10.7	-9.5
80 m S3	43	30	1.001	700.68	97.8	56.6	56.5		5.2	3.7	4.5	-2.8
80 m S4	53	40	0.867	675.25	99.4	58.2	67.1		18.8	19.8	16.7	16.0
80 m S5	63	50	0.619	690.75	86.8	45.6	73.7		16.7	31.8	14.4	28.4
80 m S6	73	60	0.417	661.34	108.5	67.3	161.4		46.1	122.3	43.7	116.5
80 m S7	83	70	0.204	710.76	67.8	26.6	130.4		3.7	75.5	5.7	76.1
80 m S8	103	90	0.041	721.46	49.2	8.0	195.1		-4.5	143.0	-5.7	143.0
80 m >40cm total		50	1.281			139.5	**108.9**	**80**	62.0	67.4	58.2	71.0
Sum Shoot	103	90	**5.4**		**725.7**	**396.1**	**73.4**	**80**	**80.4**	**14.9**	**65.9**	**12.2**

Table A.8 LR7 & LR6 Pu Velocity Data

Plant Section Data	MP cm	section	mass (g)	Pu cpm	net cpm	Bq & C	Bq/g & C	Bq	Bq/g
load data	**(root)**	18	1						
10A1	23	10	1.019	39.7	30.3	0.50	0.49	0.08	0.06
10A2	33	20	0.579	25.2	15.8	0.26	0.45	-0.07	0.03
10A3	43	30	0.438	21.5	12.1	0.20	0.46	-0.05	0.05
10A4	53	40	0.417	20	10.6	0.18	0.42	-0.02	0.11
10A >40cm total	72	82	0.664	22.9	13.5	0.22	0.34	-0.33	0.02
Sum Shoot	91	82	3.117	129.3	82.05	1.37	0.44	-0.39	0.07
Sum Plant		82	4.117	129.3	82.05	1.37	0.33	-0.39	-0.01
load data	**(root)**	18	1						
10B1	23	10	0.933	45.6	36.2	0.60	0.65	0.18	0.21
10B2	33	20	0.774	38.4	29.0	0.48	0.62	0.15	0.20
10B3	43	30	0.726	32.1	22.7	0.38	0.52	0.12	0.11
10B4	53	40	0.66	30.5	21.1	0.35	0.53	0.15	0.22
10B >40(a+b)	72		1.051	37.5	28.1				
10B >40(c+d)	72		0.806	30.3	20.9				
10B >40cm total	72	82	1.857		48.9	0.82	0.44	0.26	0.12
Sum Shoot	91	82	4.95	214.4	157.7	2.63	0.53	0.87	0.16
Sum Plant		82	5.95	214.4	157.7	2.63	0.44	0.87	0.10
*									
ST1R0	**(root)**	15.8	0.233	2350.8	2342.2				
ST1S1 LR6 10 min	20.8	10	0.574	32.5	23.9	0.40	0.69	-0.02	0.26
ST1S2	30.8	20	0.406	26.8	18.2	0.30	0.75	-0.02	0.32
ST1S3	40.8	30	0.359	21.3	12.7	0.21	0.59	-0.04	0.18
ST1S4	50.8	40	0.323	18.6	10	0.17	0.52	-0.03	0.21
ST1S > 40cm	63.3	55	**0.239**	14.9	6.3	0.11	0.44	-0.45	0.12
Sum Shoot		shoot	1.901	114.1	71.1	1.19	0.62	-0.57	0.26
Sum Plant		total	2.134	2464.9	2413.3	40.22	18.85	38.47	18.51
Mean 10 minute	MP cm	section	mass (g)	Pu cpm	net cpm	Bq & C	Bq/g & C	Bq	Bq/g
S1	22.3	10	0.842		30.1	0.50	0.60	0.08	0.16
S2	32.3	20	0.586333		21.0	0.35	0.60	0.02	0.17
S3	42.3	30	0.507667		15.8	0.26	0.52	0.01	0.11
S4	52.3	40	0.466667		13.9	0.23	0.50	0.03	0.19
> 40cm	69.1	55	0.92		22.9	0.38	0.41	-0.17	0.09

Table A.8 LR7 & LR6 Pu Velocity Data (Continued)

Plant Section Data	MP cm	section	mass (g)	Pu cpm	net cpm	Bq & C	Bq/g & C	Bq	Bq/g
load data	**(root)**	18	1						
20A1	23	10	0.903	45.4	36.0	0.60	0.66	0.18	0.23
20A2	33	20	0.641	41.2	31.8	0.53	0.83	0.20	0.40
20A3	43	30	0.592	36.1	26.7	0.44	0.75	0.19	0.34
20A4	53	40	0.511	28.9	19.5	0.32	0.63	0.13	0.33
20A >40(a+b)	72		0.809	50.6	41.2				
20A >40(c+d)	72		0.638	48.5	39.1				
20A >40cm total	72	82	1.447		80.2	1.34	0.92	0.78	0.60
Sum Shoot	91	82	4.094	250.7	194	3.23	0.79	1.48	0.42
Sum Plant		100	5.094	250.7	194	3.23	0.63	1.48	0.30
*									
load data	**(root)**	18	1						
20B1	23	10	0.861	54.4	45.0	0.75	0.87	0.33	0.43
20B2	33	20	0.781	42.3	32.9	0.55	0.70	0.22	0.28
20B3	43	30	0.646	39.1	29.7	0.49	0.76	0.24	0.35
20B4	53	40	0.69	42.4	33.0	0.55	0.80	0.35	0.49
20B >40(a+b)	72		0.876	53.2	43.8				
20B >40(c+d)	72		0.935	101.8	92.4				
20B >40cm total	72	82	1.811		136.1	2.27	1.25	1.72	0.93
Sum Shoot	91	82	4.789	333.2	276.5	4.61	0.96	2.85	0.60
Sum Plant		18	5.789	333.2	276.5	4.61	0.80	2.85	0.46
ST2R0	**(root)**	16	0.1187	1863.7	1855.1				
ST2S1 LR6 20 min	21	10	0.309	22	13.4	0.22	0.72	-0.20	0.28
ST2S2	31	20	0.244	19.2	10.6	0.18	0.72	-0.15	0.30
ST2S3	41	30	0.228	20.5	11.9	0.20	0.87	-0.06	0.46
ST2S4	51	40	0.213	18.5	9.9	0.17	0.77	-0.03	0.47
ST2S > 40 cm	63.5	55	**0.161**	18	9.4	0.16	0.97	-0.10	0.60
Sum Shoot		55	1.155	98.2	55.2	0.92	0.80	-0.84	0.43
Sum Plant		71	1.274	1961.9	1910.3	31.84	25.00	30.08	24.66
Mean 20 minute	MP cm	section	mass (g)	Pu cpm	net cpm	Bq & C	Bq/g & C	Bq	Bq/g
S1	22.3	10	0.691		31.4	0.52	0.76	0.10	0.32
S2	32.3	20	0.555		25.1	0.42	0.75	0.09	0.33
S3	42.3	30	0.489		22.7	0.38	0.78	0.13	0.36
S4	52.3	40	0.471		20.8	0.35	0.73	0.15	0.43
> 40cm	69.2	55	1.140		75.2	1.25	1.10	1.06	0.79

Table A.8 LR7 & LR6 Pu Velocity Data (Continued)

Plant Section Data	MP cm	section	mass (g)	Pu cpm	net cpm	Bq & C	Bq/g & C	Bq	Bq/g
load data	**(root)**	18	1						
40A1	23	10	0.987	53.3	43.9	0.73	0.74	0.31	0.30
40A2	33	20	0.918	47.9	38.5	0.64	0.70	0.31	0.28
40A3	43	30	0.799	28.3	18.9	0.31	0.39	0.06	-0.02
40A4	53	40	0.68	44.7	35.3	0.59	0.86	0.39	0.56
40A >40(a+b)	72		0.746	72.8	63.4				
40A >40(c+d)	72		0.8	106.9	97.5				
40A >40cm total	72	82	1.546		160.8	2.68	1.73	2.13	1.41
Sum Shoot	91	82	4.93	353.9	297.2	4.95	1.00	3.20	0.64
Sum Plant		18	5.93	353.9	297.2	4.95	0.84	3.20	0.50
*									
load data	**(root)**	18	1						
40B1-1	23	10	0.514	22.7	13.3				
40B1-2	23	10	0.704	25.1	15.7				
40B2-1	33	20	0.396	21.7	12.3				
40B2-2	33	20	0.379	22.2	12.8				
40B3-1	43	30	0.375	21.4	12.0				
40B3-2	43	30	0.402	24.9	15.5				
40B4-1	53	40	0.398	21.6	12.2				
40B4-2	53	40	0.391	19.9	10.5				
40B >40(a+b)	72		0.864	54.5	45.1				
40B >40(c+d)	72		1.093	64.4	55.0				
40B1 total	23	10	1.218	47.8	28.9	0.48	0.40	0.06	-0.04
40B2 "	33	20	0.775	43.9	25	0.42	0.54	0.09	0.12
40B3 "	43	30	0.777	46.3	27.4	0.46	0.59	0.20	0.18
40B4 "	53	40	0.789	41.5	22.6	0.38	0.48	0.18	0.17
40B >40cm total	72	82	1.957	118.9	100.0	1.67	0.85	1.11	0.53
Sum Shoot	91	82	5.516	298.4	203.9	3.40	0.62	1.64	0.25
Sum Plant		18	6.516	298.4	203.9	3.40	0.52	1.64	0.18
ST3R0	**(root)**	16.2	0.184	12483.5	12474.9				
ST3R1 LR6 40 min		8.1	0.0096	25.6	17				
ST3R2		8.1	0.0488	9.9	1.3				
ST3 EXTRA ROOT	**(root)**	16.2	0.0438	12.9	4.3				
ST3S1	21.2	10	0.46	36	27.4	0.46	0.99	0.03	0.55
ST3S2	31.2	20	0.354	33.7	25.1	0.42	1.18	0.09	0.76
ST3S3	41.2	30	0.327	38.2	29.6	0.49	1.51	0.24	1.10
ST3S4	51.2	40	0.296	48.9	40.3	0.67	2.27	0.47	1.96
ST3S > 40 cm	63.7	55	**0.296**	90.1	81.5	1.36	4.59	0.81	4.27
Sum Shoot		55	1.733	246.9	203.9	3.40	1.96	1.64	1.59
Sum Plant		71.2	2.019	12778.8	12701.4	211.69	104.84	209.93	104.50
Mean 40 minute	MP cm	section	mass (g)	Pu cpm	net cpm	Bq & C	Bq/g & C	Bq	Bq/g
S1	22.4	10	0.888		33.4	0.56	0.63	0.13	0.19
S2	32.4	20	0.682		29.5	0.49	0.72	0.16	0.30
S3	42.4	30	0.634		25.3	0.42	0.66	0.17	0.25
S4	52.4	40	0.588		32.7	0.55	0.93	0.35	0.62
> 40cm	69.2	55	1.266		114.1	1.90	1.50	1.65	1.13
ST4R0	**(root)**	16.5	0.192	3094.4	3085.8				
ST4R1 LR6 80 min		8.2	0.0067	36.5	27.9				
ST4R2		8.3	0.0285	10.7	2.1				
ST4S1	21.5	10	0.545	34.5	25.9	0.43	0.79	0.01	0.35
ST4S2	31.5	20	0.39	28.2	19.6	0.33	0.84	0.00	0.42
ST4S3	41.5	30	0.321	24.5	15.9	0.27	0.83	0.01	0.41
ST4S4	51.5	40	0.292	29.8	21.2	0.35	1.21	0.15	0.90
ST4S > 40 cm	64	55	**0.287**	26.2	17.6	0.29	1.02	-0.26	0.70
Sum Shoot		55	1.835	190.4	130.2	2.17	1.18	0.41	0.82
Sum Plant		71.5	2.062	3284.8	3216	53.60	25.99	51.84	25.65

Table A.9 LR7 Pu Velocity-Accumulation Data

Plant Section Data	MP cm	section	mass (g)	Pu cpm	net cpm	Bq & C	Bq/g & C	Bq	Bq/g
load data	**(root)**	18	1						
120A1	23	10	0.719	39.3	29.9	0.50	0.69	0.07	0.25
120A2	33	20	0.591	37.2	27.8	0.46	0.78	0.13	0.36
120A3	43	30	0.559	30.3	20.9	0.35	0.62	0.09	0.21
120A4	53	40	0.529	34.1	24.7	0.41	0.78	0.21	0.47
120A5	63	50	0.396	33.2	23.8	0.40	1.00	0.14	0.63
120A6	73	60	0.268	32.7	23.3	0.39	1.45	0.22	1.11
120A7	83	70	0.161	24.9	15.5	0.26	1.60	0.18	1.39
120A8	94.5	83	0.129	16.1	6.7	0.11	0.86	0.07	0.57
120A >40cm total	73.75	83	0.954		69.1	1.15	1.21	0.60	0.89
Sum Shoot	94.5	83	3.352	247.8	172.2	2.87	0.86	1.11	0.49
Sum Plant		101	4.352	247.8	172.2	2.87	0.66	1.11	0.32
	(root)	18	1						
120B1	23	10	0.694	43.5	34.1	0.57	0.82	0.14	0.38
120B2	33	20	0.534	33.4	24.0	0.40	0.75	0.07	0.33
120B3	43	30	0.527	41.3	31.9	0.53	1.01	0.28	0.60
120B4	53	40	0.487	52.3	42.9	0.71	1.47	0.52	1.16
120B5	63	50	0.414	69.4	60.0	1.00	2.41	0.74	2.04
120B6	73	60	0.277	81.4	72.0	1.20	4.33	1.03	3.99
120B7	83	70	0.151	47.2	37.8	0.63	4.17	0.55	3.95
120B8	95.5	85	0.045	14.3	4.9	0.08	1.80	0.04	1.50
120B >40cm total	74.25	85	0.887		174.5	2.91	3.28	2.36	2.96
Sum Shoot	95.5	85	3.129	382.8	307.2	5.12	1.64	3.36	1.27
Sum Plant		103	4.129	382.8	307.2	5.12	1.24	3.36	0.90
	(root)	18	1						
360A1	23	10	0.954	50.1	40.6	0.68	0.71	0.25	0.27
360A2	33	20	0.722	45.9	36.5	0.61	0.84	0.28	0.42
360A3	43	30	0.661	49.1	39.7	0.66	1.00	0.41	0.59
360A4	53	40	0.643	60.6	51.1	0.85	1.33	0.65	1.02
360A5	63	50	0.561	88.0	78.6	1.31	2.33	1.05	1.96
360A6	73	60	0.502	243.0	233.5	3.89	7.75	3.72	7.42
360A7	83	70	0.373	91.9	82.4	1.37	3.68	1.30	3.47
360A8	93	80	0.209	61.7	52.3	0.87	4.17	0.83	3.88
360A9	105.5	95	0.089	24.5	15.0	0.25	2.81	0.24	2.68
360A >40cm total	79.25	95	1.734		461.8	7.70	4.44	7.14	4.12
Sum Shoot	105.5	95	4.714	714.7	629.7	10.49	2.23	8.74	1.86
Sum Plant		113	5.714	714.7	629.7	10.49	1.84	8.74	1.50
	(root)	18	1						
360B1	23	10	1.313	50.2	40.8	0.68	0.52	0.26	0.08
360B2	33	20	1.022	58.3	48.9	0.81	0.80	0.49	0.37
360B3	43	30	0.879	50.2	40.8	0.68	0.77	0.43	0.36
360B4	53	40	0.7	65.5	56.1	0.93	1.33	0.74	1.03
360B5	63	50	0.376	36.2	26.8	0.45	1.19	0.19	0.81
360B6	74.5	63	0.111	16.5	7.1	0.12	1.06	-0.05	0.72
360B >40cm total	63.75	63	0.487		33.8	0.56	1.16	0.01	0.84
Sum Shoot	74.5	63	4.401	276.9	220.2	3.67	0.83	1.91	0.47
Sum Plant		81	5.401	276.9	220.2	3.67	0.68	1.91	0.34

Table A.9 LR7 Pu Velocity-Accumulation Data (Continued)

Plant Section Data	MP cm	section	mass (g)	Pu cpm	net cpm	Bq & C	Bq/g & C	Bq	Bq/g
	(root)	18	0.899						
1400A1	23	10	1.564	56.4	47.0	0.78	0.50	0.36	0.06
1400A2	33	20	0.1234	54.5	45.1	0.75	6.08	0.42	5.66
1400A3	43	30	1.067	77.5	68.1	1.13	1.06	0.88	0.65
1400A4	53	40	0.854	84.1	74.7	1.24	1.46	1.05	1.15
1400A5	63	50	0.67	142.9	133.5	2.22	3.32	1.97	2.95
1400A6	73	60	0.545	86.9	77.5	1.29	2.37	1.12	2.03
1400A7	83	70	0.404	261.3	251.9	4.20	10.39	4.12	10.18
1400A8	93	80	0.245	132	122.6	2.04	8.34	2.00	8.04
1400A9	105.5	95	0.111	54.5	45.1	0.75	6.76	0.74	6.63
1400A >40cm total	79.25	95	1.975		630.4	10.51	5.32	9.95	5.00
Sum Shoot	105.5	95	5.5834	950.1	865.1	14.42	2.58	12.66	2.22
Sum Plant		113	6.4824	950.1	865.05	14.42	2.22	12.66	1.89
	(root)	18	0.244						
1400B1	23	10	0.918	67.6	58.2	0.97	1.06	0.55	0.62
1400B2	33	20	0.706	40.1	30.7	0.51	0.72	0.18	0.30
1400B3	43	30	0.58	50.2	40.8	0.68	1.17	0.43	0.76
1400B4	53	40	0.458	38.3	28.9	0.48	1.05	0.28	0.74
1400B5	63	50	0.289	50.2	40.8	0.68	2.35	0.42	1.98
1400B6	73	60	0.173	33.8	24.4	0.41	2.35	0.24	2.01
1400B7	84	72	0.057	16.9	7.5	0.12	2.18	0.05	1.97
1400B >40cm total	68.5	72	0.519		72.6	1.21	2.33	0.66	2.01
Sum Shoot	84	72	3.181	297.1	231.0	3.85	1.21	2.09	0.84
Sum Plant		90	3.425	297.1	230.95	3.85	1.12	2.09	0.79
Control Plant Data	MP cm	section	mass (g)	Pu cpm	net cpm	Bq & C	Bq/g & C	Bq	Bq/g
LR7 and 6 (n=3)		**18**							
1	23	10	(0-40 sections All 3)		25.4	0.42	0.44	0.00	0.00
2	33	20			19.7	0.33	0.42	0.00	0.00
3	43	30			15.2	0.25	0.41	0.00	0.00
4	53	40			11.9	0.20	0.31	0.00	0.00
5	63	50	(50 + sections LR7)		15.3	0.25	0.37	0.00	0.00
6	73	60			10.2	0.17	0.34	0.00	0.00
7	83	70			4.7	0.08	0.21	0.00	0.00
8	95.3	80			2.5	0.04	0.29	0.00	0.00
9	104	90.5			0.5	0.01	0.13	0.00	0.00
Control Mn >40cm	72.417	50.5	1.727		33.2	0.55	0.32	0.00	0.00
Sum Shoot	104	90.5	4.790	0.0	105.4	1.76	0.37	0.00	0.00
Sum Plant	Max	108.5	5.205	0.0	105.4	1.76	0.34	0.00	0.00

Table A.10 LR6 Pu Accumulation Data

Plant Section Data	MP cm	section	mass (g)	Pu cpm	net cpm	Bq & C	Bq/g & C	Bq	Bq/g
1R0 DFOB 1d	**(root)**	17	0.0941	2744.7	2736.1	45.60	484.61	45	482
1S1 DFOB 1d	22	10	0.305	32.2	23.6	0.39	1.29	0.11	0.79
1S2	32	20	0.24	28.4	19.8	0.33	1.38	0.19	0.98
1S3	42	30	0.201	38.9	30.3	0.51	2.51	0.35	2.03
1S4	52	40	0.199	54.8	46.2	0.77	3.87	0.68	3.59
1S5	62	50	0.123	56.4	47.8	0.80	6.48	0.75	6.22
1S6	72	60	0.0572	33.9	25.3	0.42	7.37	0.40	7.11
Sum Shoot	72	60	1.1252	244.6	193	3.22	2.86	2.48	2.20
Sum Plant		60	1.2193	2989.3	2929.1	48.82	40.04	47.68	39.10
3R0 DFOB 2d		18	0.0707	4982.9	4974.3	82.91	1172.63	83	1170
3S1 DFOB 2d	23	10	0.409	37	28.4	0.47	1.16	0.19	0.66
3S2	33	20	0.28	33.2	24.6	0.41	1.46	0.27	1.07
3S3	43	30	0.275	62.6	54	0.90	3.27	0.74	2.79
3S4	53	40	0.242	106.2	97.6	1.63	6.72	1.54	6.44
3S5	63	50	0.164	87.2	78.6	1.31	7.99	1.27	7.73
Sum Shoot	63	50	1.37	326.2	283.2	4.72	3.45	4.00	2.92
Sum Plant		50	1.4407	5309.1	5257.5	87.63	60.82	86.51	60.04
5R0 DFOB 4d		17	0.1714	15369	15360.7	256.01	1493.65	256	1491
5S1 DFOB 4d	22	10	0.432	92	83.4	1.39	3.22	1.10	2.72
5S2	32	20	0.363	159.4	150.8	2.51	6.92	2.37	6.53
5S3	42	30	0.328	227.2	218.6	3.64	11.11	3.48	10.62
5S4	52	40	0.279	372.1	363.5	6.06	21.71	5.97	21.43
5S5	62	50	0.186	328.8	320.2	5.34	28.69	5.29	28.43
5S6	72	60	0.0774	258.6	250	4.17	53.83	4.15	53.57
Sum Shoot	72	60	1.6654	1438.1	1386.5	23.11	13.88	22.37	13.43
Sum Plant		77	1.8368	16807	16747.2	279.12	151.96	277.98	151.34
4R0 DTPA 1d		16.8	0.1579	2885.9	2877.3	47.96	303.70	48	302
4S1 DTPA 1d	21.8	10	0.318	33.9	25.3	0.42	1.33	0.14	0.83
4S2	31.8	20	0.222	26.5	17.9	0.30	1.34	0.16	0.95
4S3	41.8	30	0.213	31.9	23.3	0.39	1.82	0.23	1.34
4S4	51.8	40	0.183	38	29.4	0.49	2.68	0.40	2.40
4S5	61.8	50	0.0718	21	12.4	0.21	2.88	0.16	2.62
Sum Shoot	61.8	50	1.0078	151.3	108.3	1.81	1.79	1.09	1.08
Sum Plant		66.8	1.1657	3037.2	2985.6	49.76	42.69	48.64	41.73
C1R0 DTPA 2d		16.6	0.1367	5998.5	5989.9	99.83	730.30	99	728
C1S1 DTPA 2d	21.6	10	0.328	39.8	31.2	0.52	1.59	0.23	1.09
C1S2	31.6	20	0.242	32.7	24.1	0.40	1.66	0.26	1.26
C1S3	41.6	30	0.241	40.6	32	0.53	2.21	0.37	1.73
C1S4	51.6	40	0.193	58.2	49.6	0.83	4.28	0.74	4.00
C1S5	64.1	55	0.192	125	116.4	1.94	10.10	1.90	9.84
Sum Shoot	64.1	55	1.196	296.3	253.3	4.22	3.53	3.50	2.93
Sum Plant		71.6	1.3327	6294.8	6243.2	104.05	78.08	102.93	77.24
7R0 DTPA 4d		16	0.1016	9540.4	9531.8	158.86	1563.62	158	1561
7S1 DTPA 4d	21	10	0.326	24.9	16.3	0.27	0.83	-0.02	0.34
7S2	31	20	0.283	32.4	23.8	0.40	1.40	0.26	1.00
7S3	41	30	0.282	30.2	21.6	0.36	1.28	0.20	0.79
7S4	51	40	0.253	54.7	46.1	0.77	3.04	0.68	2.76
7S5	61	50	0.202	84.1	75.5	1.26	6.23	1.21	5.97
7S6	71	60	0.164	156.8	148.2	2.47	15.06	2.45	14.80
Sum Shoot	71	60	1.51	383.1	331.5	5.53	3.66	4.79	3.17
Sum Plant		76	1.6116	9923.5	9863.3	164.39	102.00	163.25	101.30
STC1R0 Control	**(root)**	16	0.186	32.6	24	0.40	2.15	0	0
STC1S1	21	10	0.578	25.8	17.2	0.29	0.50	0.00	0.00
STC1S2	31	20	0.357	17.1	8.5	0.14	0.40	0.00	0.00
STC1S3	41	30	0.331	18.2	9.6	0.16	0.48	0.00	0.00
STC1S4	51	40	0.309	13.8	5.2	0.09	0.28	0.00	0.00
*STC1*S5 (w 0.67)*	*61*	*50*	*0.16683*	*8.4*	*2.6*	0.04	0.26	0.00	0.00
*STC1*S6 (w 0.33)*	*63.5*	*55*	*0.08217*	*4.1*	*1.3*	0.02	0.26	0.00	0.00
STC1S > 40 cm	63.5	55	0.249	12.5	3.9	0.07	0.26	0.00	0.00
Sum Shoot	63.5	55	1.824	87.4	44.4	0.74	0.41		
Sum Plant		71	2.01	120	68.4	1.14	0.57		

Table A.11 LR5 Pu(DFOB) Characterization

LR5 Plant Data	MP cm	section	mass (g)	SQPE	Pu cpm	net cpm	Bq & C	Bq/g & C	Bq	Bq/g
DFOB by time										
Pu(DFOB) 2h	**(root)**	17.5								
(LR5) 1R0			0.162	726.6	838.8	831.7	13.9	85.6	13.47	84.32
1s1	22.5	10	0.465	680.33	69	61.9	1.03	2.22	0.60	1.54
1s2	32.5	20	0.351	719.72	62.2	55.1	0.92	2.62	0.52	1.75
1s3	42.5	30	0.38	708.9	31.1	24	0.40	1.05	0.12	0.33
1s5	57.5	50	0.362	719.72	49.9	42.8	0.71	1.97	0.52	1.34
1s7	77.5	70	0.233	716.42	34	26.9	0.45	1.92	0.35	1.33
1s8	92.5	80	0.16	716.53	19.6	12.5	0.21	1.30	0.14	0.59
1s9	102.5	90	0.0588	728.68	46.1	39	0.65	11.05	0.59	10.46
1s10	113.5	102	0.0305	726.27	46	38.9	0.65	21.26	0.61	20.44
Sum Shoot	113.5	102	2.0403			301.1	5.02	2.46	3.45	1.69
Sum Plant			2.2023			1132.8	18.88	8.57	16.92	7.68
Pu(DFOB) 4h (6.9Bq Eq., 3.8g)	**(root)**	17.5								
4s1-1		10	0.441	723.02	49.4	42.3		95.9		
4s1-2		10	0.346	698.87	54	46.9		135.5		
4s2-1		20	0.226	728.34	56.4	49.3		218.1		
4s2-2		20	0.336	705.7	37.5	30.4		90.5		
4R0			0.308	725.87	5168.8	5161.7	86.0	279.3	85.63	278.07
4S1 total	22.5	10	0.787		103.4	96.3	1.61	2.04	1.17	1.36
4S2 total	32.5	20	0.562		93.9	86.8	1.45	2.57	1.05	1.71
4s3	42.5	30	0.549	719.56	53.1	46	0.77	1.40	0.49	0.67
4s4	52.5	40	0.534	707.05	52.5	45.4	0.76	1.42	0.52	0.77
4s5	62.5	50	0.523	700.62	59	51.9	0.87	1.65	0.67	1.02
4s6	72.5	60	0.428	685.38	39.6	32.5	0.54	1.27	0.36	0.53
4s7	82.5	70		706.65	60.7	53.6	0.89		0.80	-0.60
4s8	92.5	80	0.228	706.99	57.6	50.5	0.84	3.69	0.78	2.98
4s9	102.5	90	0.104	710.7	40.3	33.2	0.55	5.32	0.50	4.72
4s10	115.25	105.5	0.0418	722.86	42.2	35.1	0.59	14.00	0.55	13.18
Sum Shoot	115.25	105.5	3.7568			531.3	8.86	2.36	6.87	1.83
Sum Plant			4.0648			5693.0	94.88	23.34	92.50	22.76
Pu(DFOB) 8h (7.3Bq Eq., 2.8g)	**(root)**	16.5								
2s1-1		10	0.335	683.15	69.9	62.8		187.5		
2s1-2		10	0.261	678.31	61.4	54.3		208.0		
2R0			0.262	722.8	2384.6	2377.5	39.6	151.2	39.23	150.00
2S1 total	21.5	10	0.596		131.3	124.2	2.07	3.47	1.64	2.79
2s2	31.5	20	0.505	660.63	79.8	72.7	1.21	2.40	0.81	1.53
2s3	41.5	30	0.505	706.2	51.3	44.2	0.74	1.46	0.46	0.73
2s4	51.5	40	0.46	677.79	55.6	48.5	0.81	1.76	0.57	1.11
2s5	61.5	50	0.372	696.71	114.5	107.4	1.79	4.81	1.59	4.18
2s6	76.5	70	0.315	715.92	121.5	114.4	1.91	6.05	1.73	5.31
2s8	93.5	84	0.0582	626.92	42.8	35.7	0.60	10.22	0.53	9.51
Sum Shoot	93.5	84	2.8112			547.1	9.12	3.24	7.32	2.61
Sum Plant			3.0732			2924.6	48.74	15.86	46.55	15.15

Table A.11 LR5 Pu(DFOB) Characterization (Continued)

LR5 Plant Data	MP cm	section	mass (g)	SQPE	Pu cpm	net cpm	Bq & C	Bq/g & C	Bq	Bq/g
Pu(DFOB) 12h	**(root)**	16.7								
3s1-1		10	0.508	718.83	47.2	40.1		78.9		
3s1-2 (projected)		10	0.539		50.1	42.5		78.9		
3s2-1		20	0.324	692.8	33.1	26		80.2		
3s2-2		20	0.265	716.36	23.7	16.6		62.6		
3s3-1		30	0.313	718.38	25.7	18.6		59.4		
3s3-2		30	0.261	716.08	41.7	34.6		132.6		
3R0			0.443	715.24	11791.1	11784	196.4	443.3	196.01	442.10
3S1 total	21.7	10	1.047		97.3	90.2	1.50	1.44	1.07	0.76
3S2	31.7	20	0.589		56.8	49.7	0.83	1.41	0.43	0.54
3S3	41.7	30	0.574		67.4	60.3	1.01	1.75	0.72	1.02
3s4	51.7	40	0.555	705.24	66.3	59.2	0.99	1.78	0.75	1.13
3s5	61.7	50	0.513	713.28	40.6	33.5	0.56	1.09	0.36	0.46
3s7	76.7	70	0.433	727.78	36.7	29.6	0.49	1.14	0.40	0.54
3s8	91.7	80	0.198	716.76	39.9	32.8	0.55	2.76	0.48	2.05
3s9	103.45	93.5	0.071	722.13	27.8	20.7	0.35	4.86	0.29	4.26
Sum Shoot	103.45	93.5	3.98			376.0	6.27	1.57	4.50	1.13
Sum Plant			4.423			12159.98	202.67	45.82	200.50	45.33
Pu(DFOB) 24h	**(root)**	15.9								
6s1-1		10	0.496	720.62	30.3	23.2		46.8		
6s1-2		10	0.571	727.83	38.3	31.2		54.6		
6s2-1		20	0.426	728.39	34	26.9		63.1		
6s2-2 (projected)		20	0.311		24.8	19.6		63.1		
6s3-1		30	0.368	728.9	39	31.9		86.7		
6s3-2 (projected)		30	0.36	723.36	38.2	31.2		86.7		
6s4-1		40	0.366	709.24	52.9	45.8		125.1		
6s4-2 (projected)		40	0.307	701.8	44.4	38.4		125.1		
6s5-1		50	0.268	706.93	47	39.9		148.9		
6s5-2 (projected)		50	0.341		59.8	50.8		148.9		
6R0 total			0.736		11454.7	11447.6	190.8	259.2	190.40	257.99
6s1 total	20.9	10	1.067		68.6	61.5	1.03	0.96	0.59	0.28
6S2 total	30.9	20	0.737		58.8	51.7	0.86	1.17	0.46	0.30
6S3 total	40.9	30	0.728		77.2	70.1	1.17	1.60	0.89	0.88
6S4 total	50.9	40	0.673		97.3	90.2	1.50	2.23	1.26	1.59
6S5 total	60.9	50	0.609		106.8	99.7	1.66	2.73	1.46	2.10
6s6	70.9	60	0.459	702.88	104.6	97.5	1.63	3.54	1.44	2.80
6s7	80.9	70	0.351	699.83	132.3	125.2	2.09	5.94	1.99	5.35
6s8	90.9	80	0.224	725.99	164.5	157.4	2.62	11.71	2.56	11.00
6s9	100.65	89.5	0.048	727.67	36.4	29.3	0.49	10.17	0.43	9.58
Sum Shoot	100.65	89.5	4.896			782.5	13.04	2.66	11.09	2.27
Sum Plant			5.632			12230.15	203.84	36.19	201.49	35.78

Table A.12 LR5 Pu(DTPA) Characterization

LR5 Plant Data	MP cm	section	mass (g)	SQPE	Pu cpm	net cpm	Bq & C	Bq/g & C	Bq	Bq/g
DTPA 4h a	**(root)**	17.2								
11s1-1		10	0.483	687.61	30	22.9		47.4		
11s1-2 (projected)		10	0.226		21.3	14.2		62.8		
11R0		17.2	0.258	675.36	3122.3	3115.2	51.9	201.2	51.53	200.00
11S1 total	22.2	10	0.709		51.3	44.2	0.74	1.04	0.30	0.36
11s2	32.2	20	0.495	692.4	35.5	28.4	0.47	0.96	0.08	0.09
11s3	42.2	30	0.542	675.83	32	24.9	0.42	0.77	0.13	0.04
11s4	52.2	40	0.506	647.43	40.5	33.4	0.56	1.10	0.32	0.46
11s5	62.2	50	0.45	645.42	26.5	19.4	0.32	0.72	0.13	0.09
11s6	72.2	60	0.325	692.91	28.8	21.7	0.36	1.11	0.18	0.37
11s7	82.2	70	0.207	716.98	21.6	14.5	0.24	1.17	0.14	0.57
11s8	92.2	80	0.0828	719.22	48.2	41.1	0.69	8.27	0.62	7.56
11s9	102.7	91	0.0243	731.31	10.1	3.0	0.05	2.06	-0.01	1.46
Sum Shoot	102.7	91	3.3411			230.6	3.84	1.15	1.89	0.57
Sum Plant			3.5991			3345.79	55.76	15.49	53.42	14.84
DTPA 4h b	**(root)**	17.7								
12s1-1		10	0.454	727.22	20.2	13.1		28.9		
12s1-2		10	0.497	699.21	26.1	19		38.2		
12s2-1		20	0.381	710.19	25.5	18.4		48.3		
12s2-2		20	0.22	694.16	20.9	13.8		62.7		
12s3-1		30	0.196	716.03	13	5.9		30.1		
12S3-2 (projected)		40	0.391			11.8		30.1		
12s4-1		40	0.387	708.34	22.6	15.5		40.1		
12S4-2 (projected)		40	0.193			7.7		40.1		
12s5-1		50	0.32	723.42	20.1	13		40.6		
12s5-2 (projected)		50	0.23			9.3		40.6		
12R0		17.7	0.494	698.7	1995.3	1988.2	33.1	67.1	32.74	65.84
12S1 total	22.7	10	0.951		46.3	39.2	0.65	0.69	0.22	0.01
12S2 total	32.7	20	0.601		46.4	39.3	0.66	1.09	0.26	0.22
12S3 total	42.7	30	0.587			17.7	0.29	0.50	0.01	-0.22
12S4 total	52.7	40	0.58			23.2	0.39	0.67	0.15	0.02
12S5 total	62.7	50	0.55			22.3	0.37	0.68	0.17	0.05
12s6	72.7	60	0.439	691.94	33.1	26.0	0.43	0.99	0.25	0.25
12s7	82.7	70	0.318	713.9	32.5	25.4	0.42	1.33	0.33	0.73
12s8	92.7	80	0.171	719.84	18.4	11.3	0.19	1.10	0.12	0.39
12s9	104.2	93	0.052	728.73	14.2	7.1	0.12	2.28	0.06	1.68
Sum Shoot	104.2	93	4.249			211.5	3.53	0.83	1.58	0.37
Sum Plant			4.743			2199.744	36.66	7.73	34.32	7.24
DTPA 8h a	**(root)**	16.8								
8S1-1		10	0.395	723.53	31.2	24.1		61.0		
8S1-2(projected)		10	0.359			21.9		61.0		
8R0		16.8	0.391	720.34	419.8	412.7	6.9	17.6	6.48	16.35
8s1 total	21.8	10	0.754		31.2	24.1	0.40	0.53	-0.03	-0.15
8s2	31.8	20	0.498	713.95	43.5	36.4	0.61	1.22	0.21	0.35
8s3	41.8	30	0.502	677.96	46	38.9	0.65	1.29	0.37	0.56
8s4	51.8	40	0.481	730.64	41.8	34.7	0.58	1.20	0.34	0.56
8s5	61.8	50	0.466	704.34	49.9	42.8	0.71	1.53	0.52	0.90
8s6	71.8	60	0.375	709.63	56.2	49.1	0.82	2.18	0.64	1.44
8s7	81.8	70	0.222	729.29	48.9	41.8	0.70	3.14	0.60	2.54
8s8	93.8	84	0.088	731.82	30.5	23.4	0.39	4.43	0.33	3.72
Sum Shoot	93.8	84	3.386			291.2	4.85	1.43	2.96	0.87
Sum Plant			3.777			703.9	11.73	3.11	9.45	2.50

Table A.12 LR5 Pu(DTPA) Characterization (Continued)

LR5 Plant Data	MP cm	section	mass (g)	SQPE	Pu cpm	net cpm	Bq & C	Bq/g & C	Bq	Bq/g
DTPA 8h b	**(root)**	16.5								
9s1-2		10	0.397	711.15	32.7	25.6		64.5		
9s1-1 (projected)		10	0.414		34.1	26.7		64.5		
9s2-2		20	0.175	729.97	26.8	19.7		112.6		
9s2-1 (projected)		20	0.453		69.4	51.0		112.6		
9s3-1		30	0.458	706.37	33.2	26.1		57.0		
9s3-2 (projected)		30	0.16		11.6	9.1		57.0		
9s4-1		40	0.41	691.43	33	25.9		63.2		
9S4-2 (projected)		40	0.174		14.0	11.0		63.2		
9R0		16.5	0.188	718.88	20992.5	20985.4	349.8	1860.4	349.36	1859.17
9S1 total	21.5	10	0.397		66.8	59.7	1.00	2.51	0.56	1.83
9S2 total	31.5	20	0.628		96.2	89.1	1.48	2.36	1.09	1.50
9S3 total	41.5	30	0.618		44.8	37.7	0.63	1.02	0.35	0.29
9S4 total	51.5	40	0.584		47.0	39.9	0.67	1.14	0.43	0.50
9s5	61.5	50	0.503	669.08	41.6	34.5	0.58	1.14	0.38	0.51
9s6	71.5	60	0.404	726.71	45.3	38.2	0.64	1.58	0.46	0.84
9s7	81.5	70	0.277	726.43	36.9	29.8	0.50	1.79	0.40	1.20
9s8	91.5	80	0.105	728.96	23.3	16.2	0.27	2.57	0.21	1.86
9s9	101.5	90	0.0201	729.29	22	14.9	0.25	12.35	0.19	11.76
Sum Shoot	101.5	90	3.5361			360.0	6.00	1.70	4.05	1.15
Sum Plant			3.7241			21345.38	355.76	95.53	353.41	94.90
DTPA 12h a	**(root)**	16.7								
10s1-1		10	0.487	707.72	28.2	21.1		43.3		
10S1-2 (projected)		10	0.436		25.2	18.9		43.3		
10s2-1		20	0.467	710.31	29.7	22.6		48.4		
10S2-2 (projected)		20	0.282		17.9	13.6		48.4		
10s3-1		30	0.479	714.4	29.4	22.3		46.6		
10S3-2 (projected)		30	0.241		14.8	11.2		46.6		
10s4-1		40	0.485	711.21	28.4	21.3		43.9		
10S4-2 (projected)		40	0.182		10.7	8.0		43.9		
10R0		16.7	0.384	724.59	4568.7	4561.6	76.0	198.0	75.63	196.74
10S1 total	21.7	10	0.923		53.4	46.3	0.77	0.84	0.34	0.16
10S2 total	31.7	20	0.749		47.6	40.5	0.68	0.90	0.28	0.04
10S3 total	41.7	30	0.72		44.2	37.1	0.62	0.86	0.34	0.13
10S4 total	51.7	40	0.667		39.1	32.0	0.53	0.80	0.29	0.16
10s5	61.7	50	0.532	644.17	40.3	33.2	0.55	1.04	0.36	0.41
10s6	71.7	60	0.432	618.6	57.4	50.3	0.84	1.94	0.66	1.20
10s7	81.7	70	0.303	680.39	37.3	30.2	0.50	1.66	0.41	1.06
10s8	91.7	80	0.128	716.98	19.1	12.0	0.20	1.56	0.14	0.85
10s9	103.7	94	0.0717	724.98	12.1	5.0	0.08	1.16	0.03	0.57
Sum Shoot	103.7	94	4.5257			286.6	4.78	1.06	2.83	0.63
Sum Plant			4.9097			4848.231	80.80	16.46	78.46	15.98
DTPA 12h b	**(root)**	16.2								
7s1-1		10	0.365	728.68	40.1	33		90.4		
7s1-2 (projected)		10	0.209		23.0	18.9		90.4		
7R0		16.2	0.262	713.62	24863.1	24856	414.3	1581.2	413.87	1579.93
7S1 total	21.2	10	0.574		63.1	56.0	0.93	1.62	0.50	0.95
7s2	31.2	20	0.385	717.99	41.9	34.8	0.58	1.51	0.18	0.64
7s3	41.2	30	0.401	707.44	41.2	34.1	0.57	1.42	0.29	0.69
7s4	51.2	40	0.376	727.39	37.3	30.2	0.50	1.34	0.27	0.70
7s5	61.2	50	0.329	691.43	36.6	29.5	0.49	1.49	0.29	0.86
7s6	71.2	60	0.283	730.53	35.5	28.4	0.47	1.67	0.29	0.93
7s7	81.2	70	0.203	728.68	37.7	30.6	0.51	2.51	0.41	1.92
7s8	91.2	80	0.0927	728.62	28.7	21.6	0.36	3.88	0.30	3.17
7s9	101.95	91.5	0.0311	730.13	23.4	16.3	0.27	8.74	0.22	8.14
Sum Shoot	101.95	91.5	2.6748			281.5	4.69	1.75	2.74	1.03
Sum Plant			2.9368			25137.46	418.96	142.66	416.61	141.86

Table A.13 LR4, LR5, and LR6 Control Data

Control Data	MP cm	section	mass (g)	SQPE	Pu cpm	net cpm	Bq & C	Bq/g & C	Bq	Bq/g	
Control (LR5)	**(root)**	17									
5S1-1		10	0.336	707.27	19	11.9	0.20	0.59			
5S1-2		10	0.401	681.82	21.9	14.8	0.25	0.62			
5R0		17	0.318	724.25	30.8	23.7	0.40	1.24			
5 S1 total	22	10	0.737		40.9	26.7	0.45	0.60			
5S2	32	20	0.46	669.78	31	23.9	0.40	0.87			
5S3	42	30	0.424	698.75	23.5	16.4	0.27	0.64			
5S4	52	40	0.395	689.15	21.6	14.5	0.24	0.61			
5S5	62	50	0.325	689.55	18.1	11	0.18	0.56			
5S6	72	60	0.208	716.59	14.9	7.8	0.13	0.63			
5S7	82	70	0.102	717.37	10.5	3.4	0.06	0.56			
5S8	93	82	0.026	728.23	9.3	2.2	0.04	1.41			
Sum Shoot	93	82	2.677			105.9	1.77	0.66			
Sum Plant											
Control (LR4)	**(root)**	15.3									
LR4 Control 10S1	20.3	10	0.538	705.92	32.4	25.3	0.42	0.78			
Missing 10S2											
10S3	40.3	30	0.349	698.07	24.4	17.3	0.29	0.83			
10S4	50.3	40	0.346	697.28	21.2	14.1	0.24	0.68			
10S5	60.3	50	0.305	684.06	19.9	12.8	0.21	0.70			
10S6	70.3	60	0.281	676.12	21	13.9	0.23	0.82			
10S7	80.3	70	0.225	666.16	15.4	8.3	0.14	0.61			
10S8	90.3	80	0.155	691.94	12.6	5.5	0.09	0.59			
10S9	100.3	90	0.095	703.67	10.4	3.3	0.06	0.58			
10S10	112.3	104	0.045	717.26	11.2	4.1	0.07	1.52			
Sum	112.3	104	2.339			79.3	1.32	0.57			
Mean Control	4, 5, & 6	29 d	mass (g)	SQPE	Pu cpm	net cpm	Bq	Bq/g			
5R0			0.318	724.25			0.40	1.24			
S1	21.77		0.638				0.43	0.68			
S2 LR5 only	32.50		0.460				0.40	0.87			
S3	41.77		0.387				0.28	0.73			
S4	51.77		0.371				0.24	0.64			
S5	61.77		0.315				0.20	0.63			
S6	71.77		0.245				0.18	0.74			
S7	81.77		0.164				0.10	0.60			
S8	92.10		0.091				0.06	0.71			
S9	103.28		0.095				0.06	0.60			
S10 LR4 only	112.30		0.045				0.04	0.81			
Sum	112.30										
Control (LR6)	(root)	18								**29 d Control Conc**	
Sample ID	MP cm	section	mass (g)	SQPE	Pu cpm	net cpm	Bq	Bq/g	aliquot	LR6	MP cm
1.0 mL NS				726.83	8.6					10 cm eq	
29 d Control Conc										**Bq/g**	(root)
6S1	20.5	5	0.717	699.38	23.4	14.8	0.25	0.34	1.000	0.31	23
6S2*	25.5	10	0.537	725.26	16.6	9.1	0.15	0.28	0.875	0.37	33
6S3	30.5	15	0.455	715.86	18.9	10.3	0.17	0.38	1.000	0.27	43
6S4*	35.5	20	0.446	726.15	17.1	9.7	0.16	0.36	0.875	0.28	53
6S5	40.5	25	0.459	713.79	18.6	10.0	0.17	0.36	1.000	0.23	63
6S6*	45.5	30	0.446	730.86	13.5	5.6	0.09	0.21	0.875	0.22	73
6S7	50.5	35	0.421	707.1	16.8	8.2	0.14	0.32	1.000	0.16	83
6S8*	55.5	40	0.378	709.58	13.3	5.4	0.09	0.24	0.875	0.12	93
6S9	60.5	45	0.376	699.88	14.5	5.9	0.10	0.26	1.000	-0.02	106.25
6S10*	65.5	50	0.357	704.4	12.5	4.5	0.07	0.21	0.875		
6S11*	73	60	0.519	711.88	14.7	7.0	0.12	0.22	0.875		
6S12*	83	70	0.412	725.09	12	3.9	0.06	0.16	0.875		
6S13	93	80	0.236	714.85	10.3	1.7	0.03	0.12	1.000		
6S14	106.25	96.5	0.0726	726.99	8.5	-0.1	0.00	-0.02	1.000		
Sum	106.25	96.5	5.8316			95.9	1.60	0.27			

Figure A.3 23 d Control Plant Shoot Concentration Data

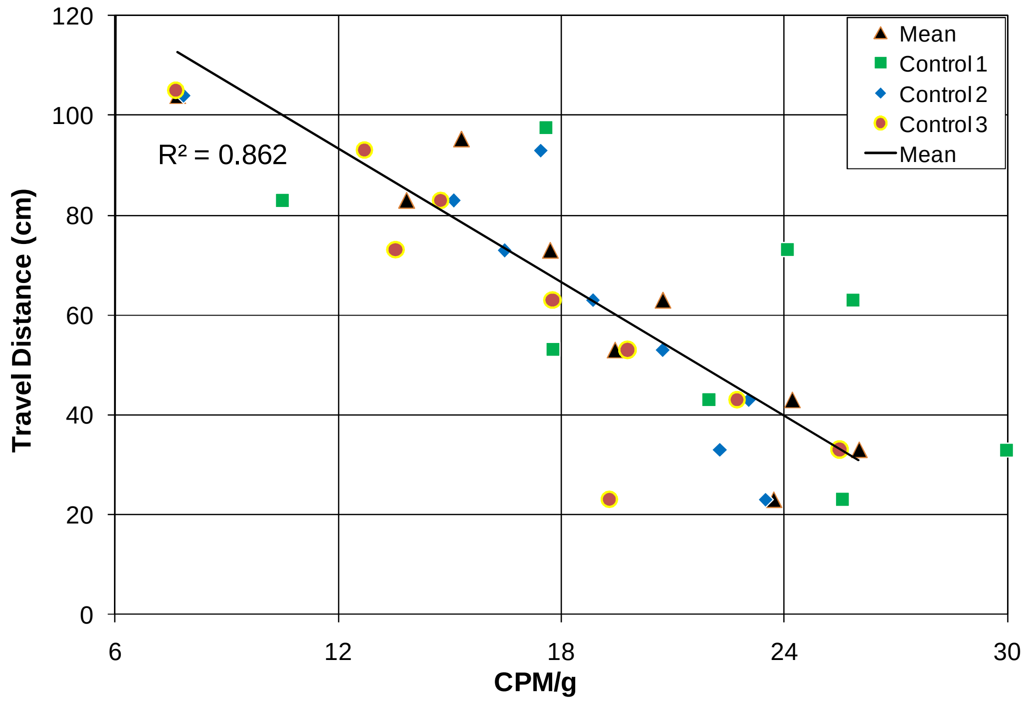

Figure A.4 23, 28, and 29 d Control Plant Shoot Concentration Data

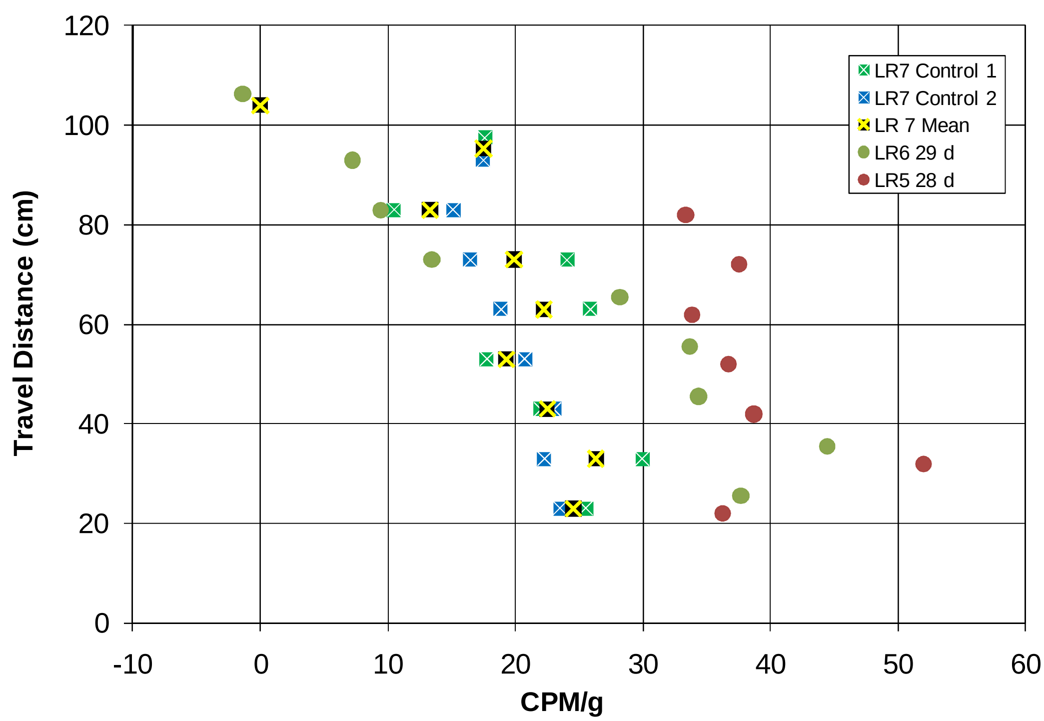

Appendix B. Plant Water and Transpiration Data

Table B.1 LR9 Plant Water and Transpiration Data

	Top solution watering volumes (all plants)																				
Date	10-Sep	12-Sep	14-Sep	16-Sep	18-Sep	21-Sep	23-Sep			**Total mL**											
Vol (mL)	50	50	60	60	70	80	100			**470**											
	Vol (mL) for each plant from reservoir																				
Exper. Group	**Root/shoot 10 d**			**Root/shoot 7 d**			**Root/shoot 3 d**			**Pu Fe Dual**			**Pu with 0 Fe, 10 Fe**				**Transpiration**				**Control**
Plant Number	**1**	**2**	**3**	**4**	**5**	**7**	**7**	**8**	**11**	**18**	**19**	**20**	**21**	**C1**	**17**	**14**	**9**	**15**	**12**	**16**	**10**
Plant ID	**10d A**	**10d B**	**10d C**	**7d A**	**7d B**	**7d C**	**3d A**	**3d B**	**3d C**	**PuFe A**	**PuFe B**	**PuFe C**	**0 Fe A**	**0 Fe B**	**10 Fe A**	**10 Fe B**	**T - A**	**T - B**	**T + A**	**T + B**	**Control**
Plant FW (g)	**27.5**	**29.0**	**17.0**	**19.0**	**26.5**	**26.5**	**21.5**	**22.5**	**13.0**	**28.5**	**26.0**	**32.0**	**13.5**	**10.5**	**8.0**	**10.5**	**37.0**	**38.0**	**34.0**	**55.0**	**39.5**
Shoot cm	**68**	**73**	**64**	***62***	**74**	**70**	**60**	**65**	**68**	**91**	**83**	**89**	**64**	**74**	56	66	**95**	**96**	**86**	**110**	**76**
Exposure Date	**14-Sep**	**14-Sep**	**14-Sep**	**17-Sep**	**17-Sep**	**17-Sep**	**21-Sep**	**21-Sep**	**21-Sep**	**22-Sep**	**22-Sep**	**22-Sep**	**22-Sep**	**22-Sep**	**22-Sep**	**22-Sep**	**23-Sep**	**23-Sep**	**23-Sep**	**23-Sep**	**23-Sep**
Exposure Time	**18:45**	**18:45**	**18:45**	**17:30**	**17:30**	**17:30**	**16:30**	**16:30**	**16:30**	**15:45**	**15:45**	**15:45**	**14:45**	**14:45**	**14:45**	**14:45**	**11:00**	**11:00**	**11:00**	**11:00**	**11:00**
11-Sep	26	4	6	24	39	7	2	22	27	7	19	19	20	30	16	23	6	6	17	13	6
14-Sep	24	82	38	46	55	32	26	18	30	22	34	63	36	31	12	33	28	37	42	51	46
17-Sep	87	112	75	61	116	82	71	72	31	59	84	112	46	26	13	26	81	100	70	108	78
21-Sep	223	266	164	140	258	279	230	181	98	188	170	215	147	57	22	81	242	244	117	201	128
22-Sep										56	32	56	25	8	2	18					
9/24/2009 '23 d old	180	261	57	105	270	212	130	162	91	77	102	98	52	30	18	49					
25-Sep																	211	177	170	294	172
9/26/2009 '25 d old																	*156*	*177*	*79*	156	*128*
Subtotal (n=21)	540	725	340	376	738	612	459	455	277	409	441	563	326	182	83	230	724	741	495	823	558
& Top	470	470	470	470	470	470	470	470	470	470	470	470	470	470	470	470	470	470	470	470	470
Sum Total	1010	1195	810	846	1208	1082	929	925	747	879	911	1033	796	652	553	700	1194	1211	965	1293	1028
Difference Mean	*118*	*303*	*82*	*46*	*316*	*190*	*37*	*33*	*145*	*13*	*19*	*140*	*96*	*240*	*339*	*192*	*56*	*73*	*173*	*155*	*110*
Percent Diff	*28%*	*72%*	*-19%*	*-11%*	*75%*	*45%*	*9%*	*8%*	*-34%*	*-3%*	*4%*	*33%*	*-23%*	*-57%*	*-80%*	*-46%*	*8%*	*11%*	*-26%*	*23%*	*-16%*
Rank (nearest Mn)	*8*	*14*	*6*	*5*	*15*	*11*	*4*	*3*	*10*	*1*	*2*	*9*	*7*	*13*	*16*	*12*	*1*	*2*	*5*	*4*	*3*
Condition	Pu(DFOB) ~8284 Bq/plant									1:1 Pu:Fe Activity			**Smaller Plants 37000 Bq/plant**				**25 d old plants: 9,10,12,15,16**				
										Total Transpiration Figure											
LR9 23 d plants	**Mean**	**min**	**max**	**1 SD**	**1SD/Mn**					**Mean**	**min**	**max**	**1 SD**	**1SD/Mn**	**LR9 25 d plants**		**Mean**	**min**	**max**	**1 SD**	**1SD/Mn**
Reservoir total	**422**	**83**	**738**	**185**	**44%**					**319**	**83**	**563**	**166**	**52%**	**Reservoir total**		**668**	**495**	**823**	**136**	**20%**

Table B.2 LR8 Plant Water and Transpiration Data

	Top solution watering volumes (all plants)													
Date	13-Jul	15-Jul	17-Jul	19-Jul	21-Jul	23-Jul	25-Jul	27-Jul		**Total mL**				
Vol (mL)	50	50	60	60	80	80	80	90		**550**				
	Vol (mL) for each plant from reservoir						**Abnormal Growth**							
Exper. Group	**24 h Pu, No-Fe**			**24 h Pu, 10X-Fe**			**24 h Pu +^{59}Fe**		**^{59}Fe Velocity (No Pu)**					
Plant Number	**10**	**13**	**15**	**9**	**18**	**20**	**2**	**19**	**21**	**14**	**16**	**12**	**11**	**17**
Plant FW (g)	**42.0**	**34.5**	**34.0**	**33.0**	**29.0**	**40.0**	**48.5**	**20.5**	**38.0**	**43.5**	**46.5**	**42.5**	**46.5**	**46.5**
Shoot cm	**87**	**78**	**90**	***90***	**86**	**91**	**76**	**74.5**						**95**
Date _ Start Times	**10:33**	**10:34**	**10:36**	**10:40**	**10:42**	**10:44**	**10:12**	**10:14**	**12:27**	**12:27**	**12:27**	**12:27**	**12:27**	**12:27**
17-Jul	32	17	23	43	129	68	33	32	167	95	107	69	126	29
20-Jul	71	42	57	45	75	83	64	60	152	139	126	96	139	69
23-Jul	121	90	162	95	120	156	87	31	206	213	215	230	228	197
27-Jul	235	255	340	221	182	291	373	211	366	446	440	362	444	435
29-Jul	213	135	128	152	156	213	237	105	213	225	300	217	240	281
Use during 24 h *	*248*	*147*	*136*	*164*	*184*	*251*	*139*	*54*	*NR*	*NR*	*NR*	*NR*	*NR*	*300*
Subtotal (n=16)	672	539	710	556	662	811	794	439	1104	1118	1188	974	1177	1011
& Top	550	550	550	550	550	550	550	550	550	550	550	550	550	550
Sum Total	**1222**	**1089**	**1260**	**1106**	**1212**	**1361**	**1344**	**989**	**1654**	**1668**	**1738**	**1524**	**1727**	**1561**
Difference Mean	*168*	*301*	*130*	*284*	*178*	*29*	*46*	*401*	*264*	*278*	*348*	*134*	*337*	*171*
Percent Diff	*-20%*	*-36%*	*-15%*	*-34%*	*-21%*	*-3%*	*-5%*	*-48%*	*31%*	*33%*	*41%*	*16%*	*40%*	*20%*
Rank (nearest Mn)	*5*	*11*	*3*	*10*	*7*	*1*	*2*	*14*	*8*	*9*	*13*	*4*	*12*	*6*
Plant ID	**0X Fe A**	**0X Fe B**	**0X Fe C**	**10X Fe A**	**10X Fe B**	**10X Fe C**	**PuFe A**	**PuFe B**	**5 min**	**10 min**	**20 min**	**40 min**	**80 min**	**Control**
Treatment Group	0 Fe in GNS			1.07 E-4 M Fe in GNS			1:1 Pu:Fe Activity		2 MicroCurie /plant					No Fe, Pu
LR8 23 d plants	**Mean**	**min**	**max**	**1 SD**	**1SD/Mn**									
Reservoir total	**840**	**439**	**1188**	**254**	**30.29%**									
** During exposure lights were the entire 24 h = 1440 minutes. NR - Not Recorded*														
10X Fe C had second root . All 10X Fe solutions slight orange tinge on preparation Fe & DFOB, All Bright Yellow after exposure to plants.														
	24 h Pu, No-Fe			**24 h Pu, 10X-Fe**			**24 h Pu +^{59}Fe**			**Transpiration During Exposure**				
Trans while exposed	248	147	136	164	184	251	139	54		**Mean**	**min**	**max**	**1 SD**	**1SD/Mn**
Plant FW mass	**42.0**	**34.5**	**34.0**	**33.0**	**29.0**	**40.0**	**48.5**	**20.5**		**188**	**136**	**251**	**50**	**27%**

Table B.3 LR7 Plant Water and Transpiration Data

	Top solution watering volumes (all plants)															
Date	3-May	5-May	7-May	9-Mar	11-Mar	13-May	15-May	17-May		**Total mL**						
Vol (mL)	50	50	60	60	60	70	70	80		**500**						
	Vol (mL) for each plant from reservoir												short		Big Ctl	short
Plant Number	**10***	**13**	**12**	**4**	**6**	**1**	**15**	**8***	**11**	**7**	**2**	**9***	**3**	**18**	**5**	**19***
Plant FW (g)	**40.0**	**45.5**	**23.5**	**43.0**	**40.0**	**43.0**	**43.0**	**48.5**	**33.0**	**31.0**	**38.5**	**31.5**	**47.5**	**19.5**	**47.5**	**47.5**
Sht Length (cm)	**89**	***92***							**83**	**85**	**95**	**63**	**95**	72	**83.5**	NA
Date (ID)	**Control 1**	**Control 2**	**10A**	**10B**	**20A**	**20B**	**40A**	**40B**	**120A**	**120B**	**360A**	**360B**	**1400A**	**1400B**	**Alternate**	**Alternate**
6-May	57	13	7	29	74	33	27	24	53	38	114	23	29	43	69	10
8-May	45	16	11	33	49	25	40	38	37	39	52	18	56	32	64	19
11-May	173	88	70	146	105	108	196	243	123	99	205	100	179	94	238	111
14-May	187	225	160	228	183	171	208	254	139	127	231	121	286	89	267	158
17-May	248	272	356	355	310	270	364	315	144	155	325	241	391	138	374	176
18-May	130	129	55	168	127	144	114	167	74	65	129	50	118	16	138	56
									12	8	68	28	142	35		
Subtotal (n=16)	840	743	659	959	848	751	949	1041	570	523	1056	553	1059	412	1150	530
& Top	500	500	500	500	500	500	500	500	500	500	500	500	500	500	500	500
Sum Total	**1340**	**1243**	**1159**	**1459**	**1348**	**1251**	**1449**	**1541**	**1070**	**1023**	**1556**	**1053**	**1559**	**912**	**1650**	**1030**
Difference Mean	*50*	*47*	*131*	*169*	*58*	*39*	*159*	*251*	*220*	*267*	*266*	*237*	*269*	*378*	*360*	*260*
Percent Diff	*6.3%*	*-6.0%*	*-16.6%*	*21.4%*	*7.3%*	*-5.0%*	*20.1%*	*31.7%*	*-27.9%*	*-33.8%*	*33.6%*	*-30.0%*	*34.0%*	*-47.9%*	*45.5%*	*-32.9%*
Rank (near Mn)	*3*	*2*	*5*	*7*	*4*	*1*	*6*	*10*	*8*	*13*	*12*	*9*	*14*	*16*	*15*	*11*
Plant ID	**Control 1**	**Control 2**	**10A**	**10B**	**20A**	**20B**	**40A**	**40B**	**120A**	**120B**	**360A**	**360B**	**1400A**	**1400B**	**Alternate**	**Alternate**
LR7 23 d plants	**Mean**	**min**	**max**	**1 SD**	**1SD/Mn**		**LR7 Transpiration During Exposure Is Not Comparable Due to the Wide Variation In Time**									
Reservoir total	790	412	1150	231.32	29%											
LR7 Transpiration by Mass Measurement				**Transpiration Rates (g/d)**						**Water Loss Rates (through air portal) (g/d)**					**Loss Fraction**	
Plant ID	**10***	**13**	**Time**	**10***		**13**		**Mn Rate**		ID	Loss 1		Loss 2		**0.00195**	
5/18/09 10:20	1491.9	1462.6	0	mass	rate	mass	rate	**239.8**		5/15/09 14:15	625.0		632.6			
5/19/09 10:20	1266.2	1208.8	0:00:00	225.7	225.7	253.8	253.8	RPD		5/17/09 11:54	622.8		631.1			
								5.9%		**Time (d)**	Loss 1		Loss 2			
										0	mass	rate	mass	rate	**Mn Rate**	RPD
										1.90	2.2	1.2	1.5	0.8	**1.0**	18.9%

Table B.4 LR6 Plant Water and Transpiration Data

	Top solution watering volumes (all plants)								*29 d Control*				
Date	28-Feb	1-Mar	3-Mar	7-Mar	9-Mar	11-Mar	**Total mL**		13-Mar	**Total mL**			
Vol (mL)	50	50	60	70	70	80	**380**		80	**460**			
	Vol (mL) for each plant from reservoir												
	Vel Cntl	**DFOB-Pu**				**DFOB-Pu**			**DTPA-Pu**			***28 d Control***	
Plant FW (g)						**10.5**	**11**	**17**	**10.5**	**12.5**	**14.5**	***51***	***47.5***
Date	**Control1**	**ST 10 min**	**ST 20 min**	**ST 40 min**	**ST 80 min**	**1d**	**2d**	**4d**	**1d**	**2d**	**4d**	**#6**	**C2**
4-Mar	27	62	53	18	24	12	9	11	6	7	12	27	22
7-Mar	43	47	55	34	36	15	26	37	11	28	40	91	66
10-Mar	117	115	67	107	136	75	83	41	55	66	23	142	166
11-Mar						25			31				
12-Mar	77	92	55	61	112	16	64	159	22	64	136		
13-Mar												202	347
16-Mar												231	269
Subtotal	264	316	230	220	308	143	182	248	125	165	211	693	870
& Top	380	380	380	380	380	380	380	380	380	380	380	460	460
Sum Total	**644**	**696**	**610**	**600**	**688**	**523**	**562**	**628**	**505**	**545**	**591**	**1153**	**1330**
LR6 23 d plants	**Mean**	**min**	**max**	**1 SD**	**SD/Mn (%**	**23 d plant**	**Mean**	**min**	**max**	**1 SD**	**SD/Mn (%)**		
Reservoir total	219	125	316	62.67	29%	**FW (g)**	12.7	10.5	17.0	2.62	21%		
LR6 23d : LR5 28d	**solution**	**0.309**	**total wate**	**0.454**	**FW**	**0.363**							
LR5 Transpiration by Mass Measurement					**Transpiration Rates (g/d)**								
Plant ID	**2**	**5**		**Time**	**2**		**5**		**Mn Rate**				
2/4/09 9:35	1524.5	1591.6		0	mass	rate	mass	rate	**137.9**				
2/4/09 17:16	1475.3	1554.1		7:41:00	49.2	153.7	37.5	117.1	RPD				
2/5/09 9:21		1470.7		23:46:00	-		120.9	122.1	11.5%				

Table B.5 LR5 Plant Water and Transpiration Data

	Top solution watering volumes (all plants)											
Date	18-Jan	19-Jan	21-Jan	23-Jan	26-Jan	28-Jan	30-Jan	2-Feb	Total mL			
Vol (mL)	50	50	50	50	80	70	70	80	500			
	Vol (mL) for each plant from reservoir											
	DFOB-Pu						DTPA-Pu					
Date	1	2	3	4	5	6	7	8	9	10	11	12
19-Jan	73	68	76	78	6	57	55	45	53	15	43	8
22-Jan	37	62	80	79	53	77	32	57	72	51	45	40
26-Jan	82	96	122	172	105	137	43	80	132	157	78	108
29-Jan	49	112	170	195	133	149	77	131	117	232	140	132
2-Feb	132	191	353	310	251	271	178	247	236	303	186	308
2/4/2009 *	80	78	142	112	110	141	83	72	120	121	92	167
Subtotal	453	607	943	946	658	832	468	632	730	879	584	763
& Top	500	500	500	500	500	500	500	500	500	500	500	500
Sum Total	953	1107	1443	1446	1158	1332	968	1132	1230	1379	1084	1263
LR5	**Mean**	**min**	**max**	**1 SD**	**SD/Mn (%)**							
Reservior total	**708**	**453**	**946**	**176.96**	**25%**							
Plant FW (g)	26.5	29	40.5	40.5	27.5	43.5	28	30	38.5	40	32.5	39
Shoot length (cm)	102	84	93.5	105.5	82	89.5	91.5	84	90	94	91	93
Plant FW (g)	**Mean**	**min**	**max**	**1 SD**	**SD/Mn (%)**	**Shoot length (cm)**		**Mean**	**min**	**max**	**1 SD**	**SD/Mn (%)**
	35	**27**	**44**	**6.25**	**18%**			**92**	**82**	**106**	**6.93**	**7.6%**

Appendix C. Corn Xylem Dimensional Data

Table C.1 First Corn Xylem Area Data from LR6

S Thompson	**LR6 Corn Experimental data**	
Corn Xylem area to Total Area measurement with Ian Stocks, Clemson Entomology		
samples	**n**	
(mm2)	**9**	
0.037	mean	
0.031	**0.0357**	
0.037	1 stdev	
0.031	**0.0073**	
0.038	area SD	
0.045	**20.5%**	
0.037	xylem/bundle	
0.044	**0.3**	
0.021	xylem mm^2	
	0.0107	
Bundles	**xylem area**	**Total Area**
55	**0.5885**	**32.32**
	Xylem/Total	
	0.0182	

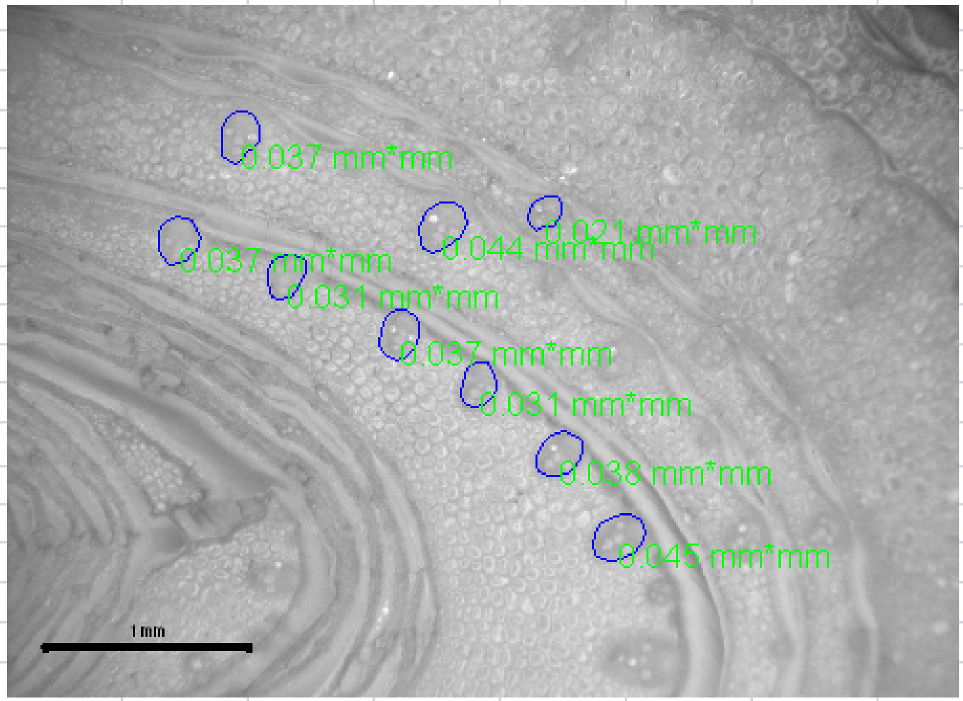

Table C.2 Second Corn Xylem Area Data from LR7

S Thompson		**5/28/2009**			**LR7 Corn xylem dimension measurement data**				
Plant	Section	Diam (cm)	Area (cm2)		Vascular Bundle Dimensions and Stats				
Control 1	20 cm	ND	1.016		**C1 at 20 cm**	Area (mm2)	Proportion	bundle area	
	5cm	ND	ND			n=7	20 per 0.25	(mm2)	
	root top	0.1434	0.016151			0.019	80	0.019	mean
	root bot mn	0.0812	0.005178			0.023	Bundle Area	0.006	std dev
	bottom 1	0.0904				0.022	1.5164	0.3163	1 sd/mn
	bottom 2	0.072				0.025			
						0.009			
Transpire (cc/h)	mass t0	1491.6				0.022			
24	mass t24	1266.2				0.013			
	net	225.4			Mean	0.019			
					Min	0.009			
					Max	0.025			
					Sum	0.133			
					Std.Dev.	0.006			
Control 2	20 cm	ND	0.767		**C2 at 5 cm**	Area (mm2)	Proportion	bundle area	
	5cm	ND	1.078			n=8	30 per 0.25	(mm2)	
	root top	0.1215	0.011594			0.042	120	0.041	mean
	root bot mn	0.085	0.005675			0.042	Bundle Area	0.008	std dev
	bottom 1	0.0794	bottom			0.046	4.9391	0.1913	1 sd/mn
	bottom 2	0.0906	bottom			0.049			
						0.025			
Transpire (cc/h)	mass t0	1462.6				0.037			
24	mass t24	1208.8				0.041			
	net	253.8				0.049			
					Mean	0.041			
					Min	0.025			
					Max	0.049			
					Sum	0.329			
					Std.Dev.	0.008			
					C2 at 20 cm		Proportion		
							21 per 0.25		

Appendix D. ICP-MS Data

Table D.1 ICP-MS of Dual Labeled Pu and Fe

ID	mass (g)	cm	24Mg	39K	44Ca	56Fe	96Mo	98Mo	mass fraction	24Mg f	39K f	44Ca f	56Fe f	96Mo f
10dA R0	0.384		1.11E+07	1.85E+07	6.03E+07	1.22E+05	1.04E+04	1.04E+04	39.1%	74.8%	16.7%	84.2%	10.5%	35.1%
10dA RS	0.0353		1.01E+06	9.44E+06	1.86E+06	2.55E+05	8.12E+03	1.01E+04	3.6%	6.8%	8.5%	2.6%	21.9%	27.6%
10dA AR	0.277		1.32E+06	4.02E+07	4.55E+06	3.38E+05	4.22E+03	4.45E+03	28.2%	8.9%	36.4%	6.4%	29.0%	14.3%
10dA AR	0.286		1.40E+06	4.24E+07	4.89E+06	4.49E+05	6.79E+03	6.90E+03	29.1%	9.4%	38.3%	6.8%	38.6%	23.0%
Σ root	0.98		1.48E+07	1.11E+08	7.16E+07	1.16E+06	2.95E+04	3.19E+04	100.0%	100.0%	100.0%	100.0%	100.0%	100.0%
PFA R0	0.29		9.91E+04	2.80E+05	4.02E+05	2.88E+03	5.03E+01	5.74E+01	33.4%					
PFA AR1	0.291		2.75E+03	2.20E+05	1.06E+04	3.45E+02	5.13E+01	2.92E+01	33.6%					
PFA AR2	0.286		1.28E+06	4.42E+07	4.62E+06	3.59E+05	6.62E+03	6.79E+03	33.0%					
Σ root	0.87		1.38E+06	4.47E+07	5.03E+06	3.63E+05	6.72E+03	6.87E+03	100.0%					
PFA S1	0.538	5	3.77E+06	7.00E+07	7.60E+06	5.33E+04	2.49E+03	2.50E+03	1.5164	1.3751	1.4191	1.0584	0.4772	0.3868
PFA S2	0.474	15	2.36E+06	7.50E+07	4.39E+06	5.50E+04	2.75E+03	2.73E+03	1.3360	0.8596	1.5192	0.6115	0.4923	0.4270
PFA S3	0.499	25	2.38E+06	5.66E+07	4.66E+06	7.16E+04	3.64E+03	3.71E+03	1.4065	0.8677	1.1462	0.6493	0.6411	0.5647
PFA S4	0.467	35	2.34E+06	5.07E+07	5.37E+06	9.43E+04	4.41E+03	4.47E+03	1.3163	0.8514	1.0281	0.7480	0.8437	0.6837
PFA S5	0.43	45	2.73E+06	4.28E+07	6.44E+06	1.31E+05	5.93E+03	5.99E+03	1.2120	0.9950	0.8682	0.8972	1.1735	0.9189
PFA S6	0.356	55	2.23E+06	3.79E+07	6.71E+06	1.36E+05	6.93E+03	7.01E+03	1.0034	0.8126	0.7686	0.9335	1.2125	1.0747
PFA S7	0.233	65	2.33E+06	3.76E+07	6.31E+06	1.12E+05	7.48E+03	7.70E+03	0.6567	0.8474	0.7623	0.8784	0.9981	1.1608
PFA S8	0.139	75	2.97E+06	3.54E+07	8.93E+06	1.40E+05	8.98E+03	9.39E+03	0.3918	1.0834	0.7178	1.2430	1.2528	1.3924
PFA S9	0.0571	84.5	3.59E+06	3.80E+07	1.42E+07	2.13E+05	1.54E+04	1.64E+04	0.1609	1.3078	0.7706	1.9806	1.9088	2.3911
Σ Shoot	3.19		2.47E+07	4.44E+08	6.46E+07	1.01E+06	5.80E+04	5.99E+04	1.0000	9.0000	9.0000	9.0000	9.0000	9.0000
Mean	9		2.74E+06	4.93E+07	7.18E+06	1.12E+05	6.45E+03	6.66E+03	1.0000	1.0000	1.0000	1.0000	1.0000	1.0000

Table D.1 ICP-MS of Dual Labeled Pu and Fe (Continued)

ID	mass (g)	cm	24Mg	39K	44Ca	56Fe	96Mo	98Mo	mass fraction	24Mg f	39K f	44Ca f	56Fe f	96Mo f
PFB R0	0.221		5.03E+06	4.76E+07	2.15E+07	4.02E+05	4.91E+03	5.61E+03	25.9%					
PFB AR1	0.353		1.26E+06	4.27E+07	5.04E+06	1.51E+05	3.63E+03	3.80E+03	41.3%					
PFB AR2	0.28		1.35E+06	3.95E+07	6.01E+06	3.47E+05	5.70E+03	5.88E+03	32.8%					
Σ root	0.85		7.63E+06	1.30E+08	3.25E+07	9.00E+05	1.42E+04	1.53E+04	100.0%					
PFB S1	0.587	5	2.14E+06	6.64E+07	7.14E+06	4.65E+04	2.34E+03	2.31E+03	1.6754	1.3411	1.4080	1.0466	0.3504	0.3800
PFB S2	0.495	15	1.62E+06	6.25E+07	6.20E+06	5.08E+04	2.54E+03	2.51E+03	1.4128	1.0132	1.3237	0.9094	0.3829	0.4131
PFB S3	0.458	25	1.24E+06	5.48E+07	5.08E+06	8.04E+04	3.36E+03	3.35E+03	1.3072	0.7778	1.1619	0.7451	0.6055	0.5455
PFB S4	0.417	35	1.42E+06	4.94E+07	6.52E+06	1.25E+05	5.39E+03	5.47E+03	1.1902	0.8854	1.0469	0.9561	0.9402	0.8764
PFB S5	0.337	45	1.38E+06	4.23E+07	5.39E+06	1.30E+05	5.69E+03	5.77E+03	0.9619	0.8611	0.8974	0.7908	0.9808	0.9252
PFB S6	0.273	55	1.31E+06	3.29E+07	5.99E+06	1.29E+05	6.35E+03	6.51E+03	0.7792	0.8206	0.6968	0.8774	0.9706	1.0325
PFB S7	0.168	65	1.61E+06	3.54E+07	8.06E+06	2.79E+05	1.02E+04	1.04E+04	0.4795	1.0042	0.7509	1.1814	2.0978	1.6517
PFB S8	0.0679	76.5	2.07E+06	3.37E+07	1.02E+07	2.22E+05	1.34E+04	1.41E+04	0.1938	1.2966	0.7144	1.4933	1.6717	2.1755
Σ Shoot	2.80		1.28E+07	3.78E+08	5.46E+07	1.06E+06	4.92E+04	5.04E+04	1.0000	8.0000	8.0000	8.0000	8.0000	8.0000
Mean	8		1.60E+06	4.72E+07	6.82E+06	1.33E+05	6.15E+03	6.30E+03	1.0000	1.0000	1.0000	1.0000	1.0000	1.0000

ID	mass (g)	cm	24Mg	39K	44Ca	56Fe	96Mo	98Mo	mass fraction	24Mg f	39K f	44Ca f	56Fe f	96Mo f
PFC R0	0.287		5.29E+06	4.21E+07	2.78E+07	4.39E+05	3.07E+03	3.60E+03	29.3%					
PFC AR1	0.395		1.34E+06	3.66E+07	5.57E+06	5.14E+05	5.06E+03	5.14E+03	40.3%					
PFC AR2	0.297		1.49E+06	3.46E+07	6.14E+06	3.00E+05	4.56E+03	4.68E+03	30.3%					
Σ root	0.98		8.12E+06	1.13E+08	3.96E+07	1.25E+06	1.27E+04	1.34E+04	100.0%					
PFC S1	0.719	5	2.85E+06	6.66E+07	7.43E+06	7.24E+04	2.60E+03	2.47E+03	1.9412	1.8199	1.2634	1.1491	0.4188	0.4273
PFC S2	0.482	15	1.69E+06	7.97E+07	5.46E+06	6.40E+04	2.42E+03	2.26E+03	1.3013	1.0766	1.5118	0.8445	0.3701	0.3987
PFC S3	0.463	25	1.56E+06	6.62E+07	4.82E+06	7.15E+04	2.67E+03	2.53E+03	1.2500	0.9943	1.2566	0.7452	0.4136	0.4389
PFC S4	0.391	35	1.35E+06	5.76E+07	4.90E+06	1.06E+05	3.35E+03	3.42E+03	1.0556	0.8615	1.0934	0.7571	0.6152	0.5513
PFC S5	0.446	45	1.32E+06	5.10E+07	5.75E+06	1.60E+05	4.67E+03	4.69E+03	1.2041	0.8435	0.9675	0.8888	0.9263	0.7681
PFC S6	0.362	55	1.23E+06	4.03E+07	5.84E+06	2.02E+05	5.89E+03	5.91E+03	0.9774	0.7856	0.7648	0.9027	1.1710	0.9686
PFC S7	0.266	65	1.32E+06	3.76E+07	6.97E+06	2.38E+05	7.50E+03	7.65E+03	0.7182	0.8438	0.7141	1.0785	1.3752	1.2347
PFC S8	0.157	75	1.48E+06	3.85E+07	9.49E+06	2.59E+05	1.02E+04	1.04E+04	0.4239	0.9474	0.7310	1.4678	1.5014	1.6727
PFC S9	0.0475	85.5	1.29E+06	3.68E+07	7.54E+06	3.82E+05	1.54E+04	1.64E+04	0.1282	0.8273	0.6975	1.1663	2.2085	2.5396
Σ Shoot	3.33		1.41E+07	4.74E+08	5.82E+07	1.56E+06	5.47E+04	5.58E+04	1.0000	9.0000	9.0000	9.0000	9.0000	9.0000
Mean	9		1.57E+06	5.27E+07	6.47E+06	1.73E+05	6.08E+03	6.20E+03	1.0000	1.0000	1.0000	1.0000	1.0000	1.0000

Table D.1 ICP-MS of Dual Labeled Pu and Fe (Continued)

Mean PuFe LR9 Data					Concentration							Concentration Fraction		
ID	mass (g)	cm	24Mg	39K	44Ca	56Fe	96Mo	98Mo	mass fraction	24Mg f	39K f	44Ca f	56Fe f	96Mo f
PuFe R0	0.266													
PuFe AR	0.346													
PuFe AR	0.297													
Σ root														
PuFe S1	0.615	5.0	2.92E+06	6.77E+07	7.39E+06	5.74E+04	2.48E+03	2.42E+03	1.7110	1.5121	1.3635	1.0847	0.4155	0.3980
PuFe S2	0.482	15.0	1.69E+06	7.97E+07	5.46E+06	6.40E+04	2.42E+03	2.26E+03	1.3013	1.0766	1.5118	0.8445	0.3701	0.3987
PuFe S3	0.473	25.0	1.73E+06	5.92E+07	4.85E+06	7.45E+04	3.22E+03	3.20E+03	1.3212	0.8799	1.1882	0.7132	0.5534	0.5164
PuFe S4	0.425	35.0	1.70E+06	5.26E+07	5.60E+06	1.08E+05	4.38E+03	4.45E+03	1.1874	0.8661	1.0561	0.8204	0.7997	0.7038
PuFe S5	0.404	45.0	1.81E+06	4.54E+07	5.86E+06	1.40E+05	5.43E+03	5.49E+03	1.1260	0.8999	0.9110	0.8589	1.0268	0.8708
PuFe S6	0.330	55.0	1.59E+06	3.70E+07	6.18E+06	1.56E+05	6.39E+03	6.48E+03	0.9200	0.8063	0.7434	0.9045	1.1181	1.0253
PuFe S7	0.222	65.0	1.75E+06	3.69E+07	7.11E+06	2.09E+05	8.38E+03	8.57E+03	0.6181	0.8985	0.7424	1.0461	1.4904	1.3491
PuFe S8	0.121	75.5	2.18E+06	3.59E+07	9.54E+06	2.07E+05	1.08E+04	1.13E+04	0.3365	1.1091	0.7211	1.4014	1.4753	1.7469
PuFe S9	0.052	85.00	2.44E+06	3.74E+07	1.09E+07	2.97E+05	1.54E+04	1.64E+04	0.1446	1.0675	0.7340	1.5735	2.0586	2.4653
Σ Shoot	3.11		1.72E+07	4.32E+08	5.91E+07	1.21E+06	5.40E+04	5.54E+04	1.0000	8.6667	8.6667	8.6667	8.6667	8.6667
Mean	9		1.97E+06	4.97E+07	6.82E+06	1.39E+05	6.23E+03	6.38E+03	1.0000	1.0000	1.0000	1.0000	1.0000	1.0000
Molar			7.16E-04	1.11E-02	1.34E-03	2.16E-05	5.62E-07	5.65E-07						
Ratio			6.5E-02	1.0E+00	1.2E-01	1.9E-03	5.1E-05							

Appendix E. Plant Growth and Tissue Processing Information

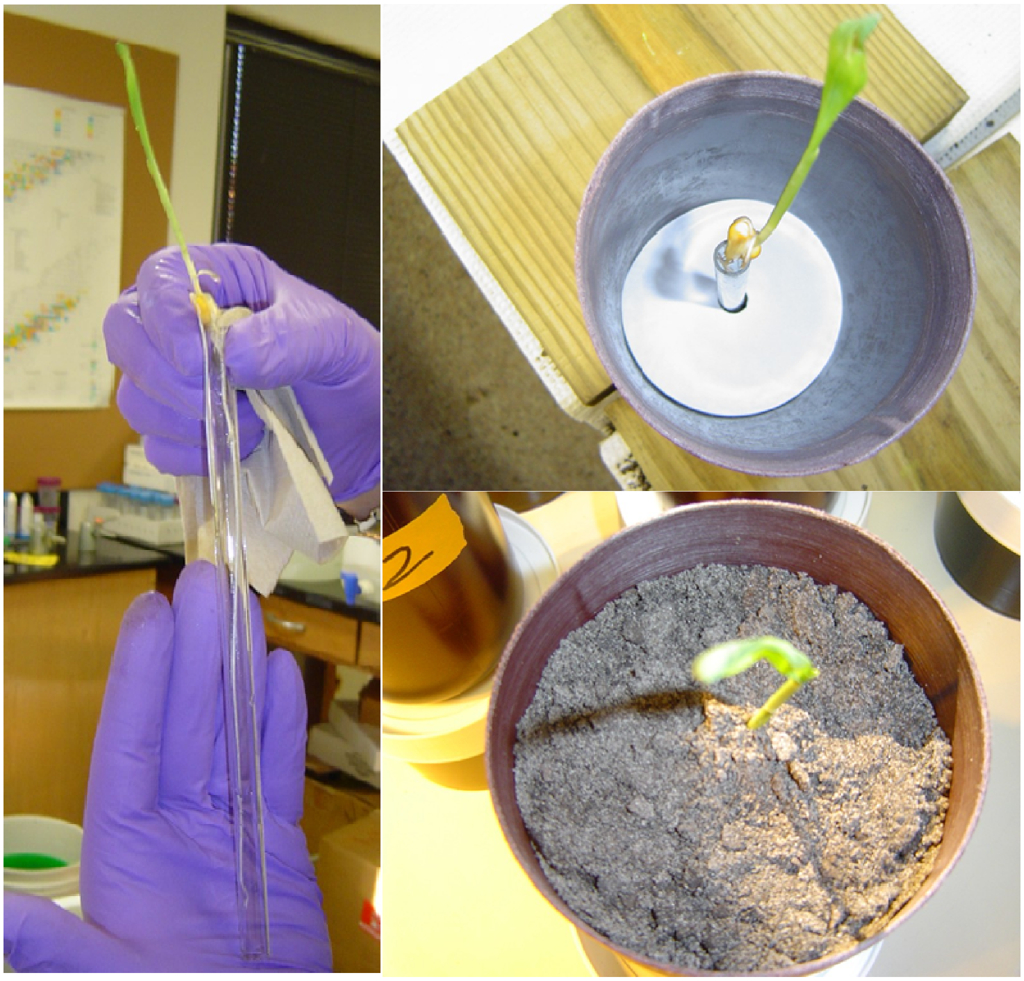

Figure E.1 Transfer of the seedling from germination paper to the long root growing system. The image at left shows a corn seedling that was grown for 7d in germination paper until the root was longer than 15 cm. The seedling root was inserted into the tube under running water, and then the tube and a paper filter were placed at the bottom of a soil pot. The tube was held in place while potting soil was placed in the pot around the tube, wetted and compressed, and filled nearly to the top. While holding the seedling, the tube was withdrawn through a hole in the bottom of the pot. The soil was gently packed around the seedling, additional soil was added at the top, the plant was watered, and the root was inspected prior to placing the potted plant on top of a nutrient solution container. If the root was broken or damaged, then the plant was discarded. Once transferred, the plants were arranged under the lights and aerated continuously.

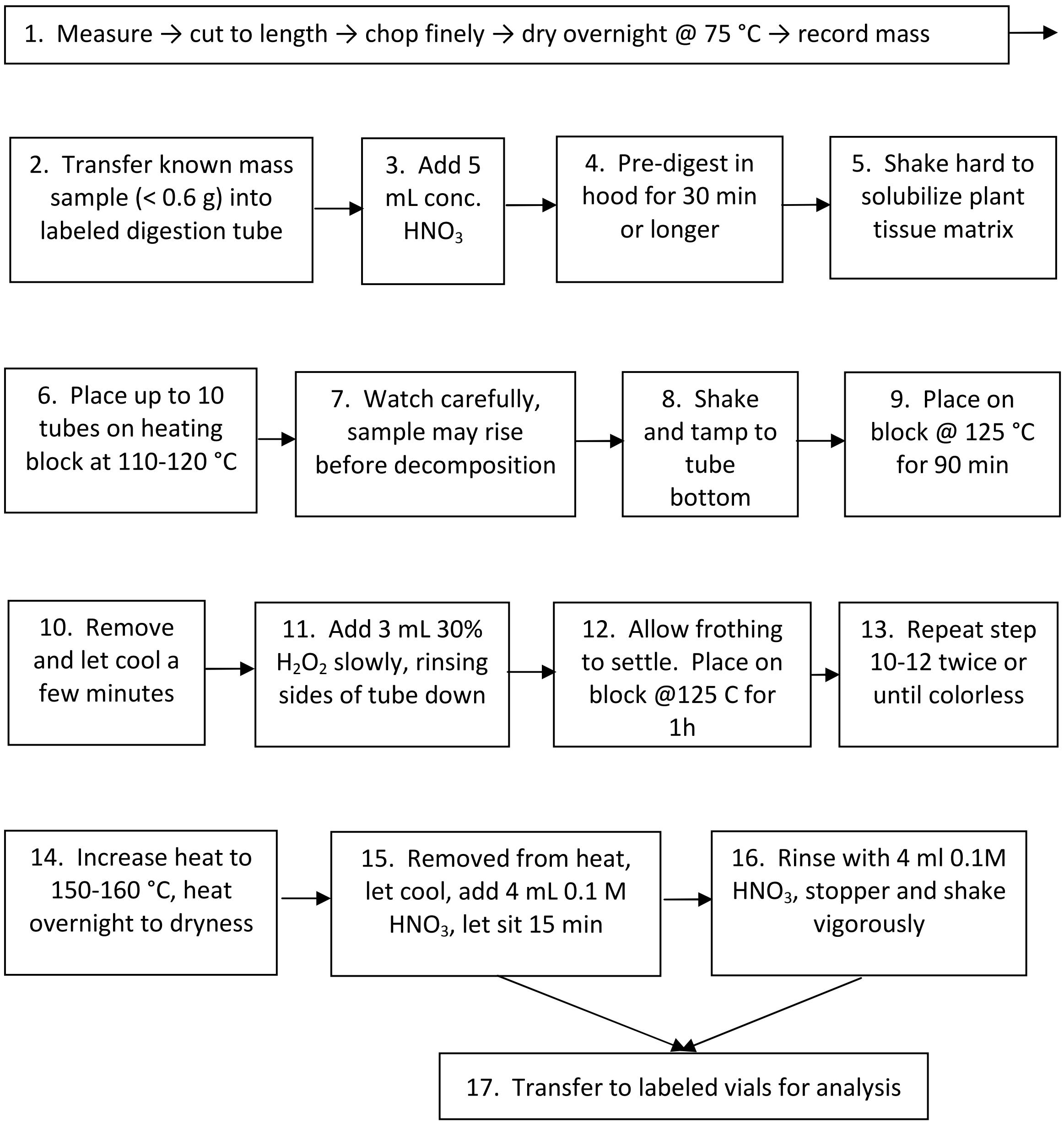

Figure E.2 A flow diagram showing plant tissue digestion steps for the analysis of P, K, Ca, Mg, Zn, Mn, Cu, Fe, S, Mo and Pu. The digested tissue samples are suitable for analysis via liquid scintillation or ICP-MS.

REFERENCES

1. Adriano, D. C., McLeod, K. W., Ciravolo, T. G. (1986). "Long-Term Availability of Cm and Pu to Crop Plants." Health Physics 50(5): 647-651.

2. Adriano, D. C., Doswell, A. C., Ciravolo, T. G., Pinder, J. E., McLeod, K. W. (2000). "Radionuclide content of selected root vegetables as influenced by culinary preparation." J. of Environ Radioactiv. 49, 307-317.

3. Ardon, O., Nudelman, R., Caris, C., Libman, J., Shanzer, A., Chen, Y. N. Hadar, Y. (1998). "Iron uptake in Ustilago maydis: Tracking the iron path." Journal of Bacteriology 180(8): 2021-2026.

4. Ashworth, D. J., Shaw, G. (2006) "Soil migration, plant uptake and volatilization of radio-selenium from a contaminated water table." Science of the Total Environment 370(2-3): 506-514.

5. Bar-Ness, E., Hadar, Y., Chen, Y., Shanzer, A., Libman, J. (1992). "Iron uptake by plants from microbial siderophores." Plant Physiology 99: 1329-1335.

6. Beck, C. S. (2005). An Introduction to Plant Structure and Development: Plant Anatomy for the 21st Century. Cambridge, UK, Cambridge University Press.

7. Bergeron, R. J., Wiegand, J., Brittenham, G. M. (2002). "HBED ligand: preclinical studies of a potential alternative to deferoxamine for treatment of chronic iron overload and acute iron poisoning." Blood 99(8): 3019-3026.

8. Bernstein, J. (2007). Plutonium: a history of the world's most dangerous element. Washington, D.C., Joseph Henry Press.

9. Bollard, E. G. (1960). "Transport in the Xylem." Annual Review Plant Physiology 11: 141-166.

10. Boukhalfa, H., Reilly, S. D., Neu, M. P. (2007). "Complexation of Pu(IV) with the natural siderophore desferrioxamine B and the redox properties of Pu(IV)(siderophore) complexes." Inorganic Chemistry 46(3): 1018-1026.

11. Brown, J. C. (1978). "Mechanism of iron uptake by plants." Plant, Cell and Environment 1: 249-257.

12. Buesseler, K. O. (1997). "The isotopic signature of fallout plutonium in the North Pacific." Journal of Environmental Radioactivity 36(1): 69-83.

13. Cataldo, D. A., McFadden, K. M., Garland, T. R., Wildung, R. E. (1988). "Organic-Constituents and Complexation of Nickel(Ii), Iron(Iii), Cadmium(Ii), and Plutonium(Iv) in Soybean Xylem Exudates." Plant Physiology 86(3): 734-739.

14. Choppin, G. R., A. H. Bond, P. M. Hromadka (1997). "Redox speciation of plutonium." Journal of Radioanalytical and Nuclear Chemistry 219(2): 203-210.

15. Choppin, G., J.O. Liljenzin, J. Rydberg (2001). Radiochemistry and nuclear chemistry. London, UK, Butterworth-Heinemann, Ltd.

16. Cleveland, J. M. (1970). The chemistry of plutonium. New York, N.Y., Gorden and Breach, Science Publishers, Inc.

17. Cochran, T. (1997). Safeguarding Nuclear Weapon-Usable Materials in Russia. International Forum Illegal Nuclear Traffic: Risks, Safeguards and Countermeasures. Como, Italy, NATURAL RESOURCES DEFENSE COUNCIL, INC.

18. Crowley, D. E. (2006). Microbial siderophores in the plant rhizosphere. Iron nutrition in plants and rhizospheric microorganisms. Barton, L. L. and Abadia, J. Amsterdam, Netherlands, Springer: 169-198.

19. Curie, C., Briat, J. F. (2003). "Iron transport and signaling in plants." Annual Review of Plant Biology 54: 183-206.

20. Curie, C., Cassin, G., Couch, D., Fanchon, D, Higuchi, K., Le Jean, M. Misson, J., Schikora, A., Czernioc, P., Mari, S. (2009). "Metal movement within the plant: contribution of nicotianamine and yellow stripe 1-like transporters." Annals of Botany 103: 1-11.

21. Curtis, D., Fabryka-Martin, J., Dixon, P., Cramer, J. (1999). "Nature's uncommon elements: plutonium and technetium." Geochimica Et Cosmochimica Acta 63(2): 275-285.

22. Demirkanli, D. I., Molz, F. J., Kaplan, D. I., Fjeld, R. A. (2009). "Soil-root interactions controlling upward plutonium transport in variably saturated soils." Vadose Zone Journal 8(3): 574-585.

23. Demirkanli, D. I., Molz, F. J., Kaplan, D. I., Fjeld, R. A. (2008). "A fully transient model for long-term plutonium transport in the Savannah River Site vadose zone: Root water uptake." Vadose Zone Journal 7(3): 1099-1109.

24. Demirkanli, D. I., Molz, F. J., Kaplan, D. I., Fjeld, R. A., Serkiz, S. M. (2007). "Modeling long-term plutonium transport in the Savannah River Site vadose zone." Vadose Zone Journal 6(2): 344-353.

25. DOE (1996). Closing the circle on the splitting of the atom: The environmental legacy of nuclear weapons production and what the department is doing about it. EM-0266. Office of Environmental Management, U.S. Department of Energy.

26. DOE (1997). Linking legacies: connecting the Cold War nuclear weapons production processes to their environmental consequences. EM-0319. Management, Office of Environmental Management, U.S. Department of Energy.

27. Druteikiene, R., Luksiene, B., Holm, E. (1999). "Migration of ^{239}Pu in soluble and insoluble forms in soil." Journal of Radioanalytical and Nuclear Chemistry 242(3): 731-737.

28. Duckworth, O. W., Sposito, G. (2005). "Siderophore-manganese(III) interactions II. Manganite dissolution promoted by desferrioxamine B." Environmental Science & Technology 39(16): 6045-6051.

29. Duckworth, O. W., Sposito, G. (2007). "Siderophore-promoted dissolution of synthetic and biogenic layer-type Mn oxides." Chemical Geology 242(3-4): 497-508.

30. Ehlken, S., Kirchner, G. (2002). "Environmental processes affecting plant root uptake of radioactive trace elements and variability of transfer factor data: a review." Journal of Environmental Radioactivity 58(2-3): 97-112.

31. EPA (1999). Understanding variation in partition coefficient, K_d, values, Volume 1: The K_d model, methods of measurement, and application of chemical reaction codes. EPA 402-R-99-004A, Office of Air and Radiation, U. S. Environmental Protection Agency.

32. Epstein, E., Norlyn, J. D. (1973). "The velocities of ion transport into and through the xylem of roots." Plant Physiology 52: 346-349.

33. Falck, W. E. (2004). Remediation of sites with dispersed radioactive contamination. Technical Reports Series, ISSN 0074-1914; no. 424. Vienna, Austria, IAEA.

34. Fjeld, R. A., DeVol, T. A., Goff, R. W., Blevins, M. D., Brown, D. D., Ince, S. M., Elzerman, A. W. (2001). "Characterization of the mobilities of selected actinides and fission/activation products in laboratory columns containing subsurface material from the Snake River Plain." Nuclear Technology 135(2): 92-108.

35. Fjeld, R. A., Serkiz, S. M., McGinnis, P. L., Elci, A., Kaplan, D. I. (2003). "Evaluation of a conceptual model for the subsurface transport of plutonium involving surface mediated reduction of Pu(V) to Pu(IV)." Journal of Contaminant Hydrology 67(1-4): 79-94.

36. Fried, S., Friedman, A. M., Hines, J. J., Atcher, R. W., Quarterman, L. A., Volesky, A. (1976). The migration of Plutonium and Americium in the lithosphere. American Chemical Society. New York, NY, ACS.

37. Garland, T. R., Cataldo, D. A., Wildung, R. E. (1981). "Absorption, Transport, and Chemical Fate of Plutonium in Soybean Plants." Journal of Agricultural and Food Chemistry 29(5): 915-920.

38. Garland, T. R.; Cataldo, D. A.; McFadden, K. M.; Wilding, R. E. (1987) Factors affecting absorption, transport, and form of Pu in plants. Environmental Research on Actinide Elements: Conference-841142, U. S. Department of Energy, Office of Health and Environmental Research (DE86008713), 83-95.

39. Gerzabek, M. H., Strebl, F., Temmel, B. (1998). "Plant uptake of radionuclides in lysimeter experiments." Environmental Pollution 99(1): 93-103.

40. Gobran, G. R., Wenzel, W. W., Lombi, E. (2001). Trace elements in the rhizosphere. Boca Raton, FL, CRC Press.

41. Gregory, P. (2006). Plant Roots: growth, activity, and interaction with soils. Oxford, UK, Blackwell Publishing.

42. Hainsworth, J. M., Aylmore, L. A. G. (1986). "Water Extraction by Single Plant-Roots." Soil Science Society of America Journal 50(4): 841-848.

43. Hecker, S. S. (2000). "Plutonium in use." Los Alamos Science Challenges in Plutonium Science (26): 10-16.

44. Henner, P., Colle, C., Morello, M. (2005). "Retention and translocation of foliar applied ^{239}Pu, ^{240}Pu and ^{241}Am, as compared to ^{137}Cs and ^{85}Sr, into bean plants (Phaseolus vulgaris)." Journal of Environmental Radioactivity 83(2): 213-229.

45. Hill, K. A., Lion, L. W., Ahner, B. A. (2002). "Reduced Cd accumulation in Zea mays: A protective role for phytosiderophores?" Environmental Science & Technology 36(24): 5363-5368.

46. Hiradate, S., Inoue, K. (2000). "Dissolution of iron by mugineic acid from soils and comparison with DTPA soil test." Soil Science and Plant Nutrition 46(3): 673-681.

47. Hoffman, D. C., Lawrence, F. O., Mewherte, J. l., Rourke, F. M. (1971). "Detection of ^{244}Plutonium in Nature." Nature 234(5325): 132-**.

48. Holgye, Z., Maly, M. (2000). "Sources, vertical distribution, and migration rates of ^{239}Pu, ^{240}Pu, ^{238}Pu, and ^{137}Cs in grassland soil in three localities of central Bohemia." Journal of Environmental Radioactivity 47(2): 135-147.

49. Hore-Lacey, I. (2008). "The Encyclopedia of Earth." Retrieved September 9, 2008, from http://www.eoearth.org/article/Plutonium.

50. Hossner, L. R., Loeppert, R. H., Newton, R. J., Szanoszlo, P. J., Attrep, M. J. (1998). Literature Review: Phytoaccumulation of Chromium, Uranium, and Plutonium in Plant Systems, Amarillo National Resource Center for Plutonium.

51. Huheey, J. E. (1978). Inorganic Chemistry. New York, NY, Harper & Row.

52. Hulse, S. E., Ibrahim, S. A., Whicker, F. W., Chapman, P. L. (1999). "Comparison of ^{241}Am, ^{239}Pu, ^{240}Pu and ^{137}Cs concentrations in soil around rocky flats." Health Physics 76(3): 275-287.

53. Jeong, J., Cohu, C., Kerkeb, L., Pilon, M., Connolly, E. L., Guerinot, M. L. (2008). "Chloroplast Fe(III) chelate reductase activity is essential for seedling viability under iron limiting conditions." Proceedings of the National Academy of Sciences of the United States of America 105(30): 10619-10624.

54. Jia, G. G., Triulzi, C., Marzano, F. N., Belli, M., Vaghi, M. (2000). "The fate of plutonium, ^{241}Am, ^{90}Sr and ^{137}Cs in the Antarctic ecosystem." Antarctic Science 12(2): 141-148.

55. John, S. G., Ruggiero, C. E., Hersman, L. E., Tung, C. S., Neu, M. P. (2001). "Siderophore mediated plutonium accumulation by Microbacterium flavescens (JG-9)." Environmental Science & Technology 35(14): 2942-2948.

56. Jones, C. A. (1985). C4 grasses cereals: growth, development, and stress response. New York, N.Y., John Wiley and Sons.

57. Jones, J. B.; Wallace, A. Sample preparation and determination of iron in plant tissue samples. J. Plant Nutr. 1992, 15, 2085-2108.

58. Jungk, A. (2001). "Root hairs and the acquisition of plant nutrients from soil." Journal of Plant Nutrition and Soil Science 164: 121-129.

59. Kaplan, D. I., Demirkanli, D. I., Gumapas, L., Powell, B. A., Fjeld, R. A., Molz, F. J., Serkiz, S. M. (2006). "Eleven-year field study of Pu migration from PuIII, IV, and VI sources." Environmental Science & Technology 40(2): 443-448.

60. Kaplan, D. I., Powell, B. A., Demirkanli, D. I., Fjeld, R. A., Molz, F. J., Serkiz, S. M., Coates, J. T. (2004). "Influence of oxidation states on plutonium mobility during long-term transport through an unsaturated subsurface environment." Environmental Science & Technology 38(19): 5053-5058.

61. Kaplan, D. I., Powell, B. A., Duff, M. C., Demirkanli, D. I., Denham, M., Fjeld, R. A., Molz, F. J. (2007). "Influence of sources on plutonium mobility and oxidation state transformations in vadose zone sediments." Environmental Science & Technology 41(21): 7417-7423.

62. Kaplan, D. I. (2010). (In press) Geochemical Data Package for Performance Assessment Calculations Related to the Savannah River Site. Aiken, SC. SRNL.

63. Kim, C. K., Kim, C. S., Chang, B. U., Choi, S. W., Chung, C. S., Hong, G. H., Hirose, K., Igarashi, Y. (2004). "Plutonium isotopes in seas around the Korean Peninsula." Science of the Total Environment 318(1-3): 197-209.

64. Koide, M., Griffin, J. J., Goldberg, E. D. (1975). "Records of Plutonium Fallout in Marine and Terrestrial Samples." Journal of Geophysical Research 80(30): 4153-4162.

65. Kraemer, S. M., Crowley, D. E., Kretzschmar, R. (2006). “Geochemical aspects of phytosiderophore-promoted iron acquisition by plants.” Advances in Agronomy, Vol 91. 91: 1-46.

66. Kudo, A. (2001). "An opportunity for the millennium: investigating Nagasaki plutonium." Journal of Environmental Radioactivity 57: 81-85.

67. Ladouceur, A., Akiha, F., Kawai, S. (2008). "Effect of supplied phytosiderophore on ^{59}Fe absorption and translocation in Fe-deficient barley grown hydroponically in low phosphorus media." Soil Science and Plant Nutrition 54(4): 560-565.

68. Lauchli, A., Arthur R. Spurr, Emanual Epstein (1971). "Lateral Transport of Ions into the Xylem of Corn Roots." Plant Physiology 48: 118-124.

69. Lee, J. H., Hossner, L. R., Attrep, M., Kung, K. S. (2002). "Comparative uptake of plutonium from soils by Brassica juncea and Helianthus annuus." Environmental Pollution 120(2): 173-182.

70. Lee, J. H., Hossner, L. R., Attrep, M., Kung, K. S. (2002). "Uptake and translocation of plutonium in two plant species using hydroponics." Environmental Pollution 117(1): 61-68.

71. Lee, M. H., Clark, S. B. (2005). "Activities of Pu and Am isotopes and isotopic ratios in a soil contaminated by weapons-grade plutonium." Environmental Science & Technology 39(15): 5512-5516.

72. Little, C. A., Whicker, F. W., Winsor, T. F. (1980). "Plutonium in a Grassland Ecosystem at Rocky Flats." Journal of Environmental Quality 9(3): 350-354.

73. Livens, F. R., Horrill, A. D., Singleton, D. L. (1994). "The Relationship between Concentrations of Plutonium and Americium in Soil Interstitial Waters and Their Uptake by Plants." Science of the Total Environment 155(2): 151-159.

74. Loring, J. S., Simanova, A. A., Persson, P. (2008). "Highly mobile iron pool from a dissolution-readsorption process." Langmuir 24(14): 7054-7057.

75. Lux, D., Kammerer, L., Ruhm, W., Wirth, E. (1995). "Cycling of Pu, Sr, Cs, and other long living radionuclides in forest ecosystems of the 30-km zone around Chernobyl." Science of the Total Environment 173(1-6): 375-384.

76. Maas, E., V., Leggett, J. E. (1968). "Uptake of ^{86}Rb and K by Excised Maize Roots." Plant Physiology 43: 2054-2056.

77. Maas, E. V., Ogata, G. (1972). "Radial transport of sodium and chloride into tomato root xylem." Plant Physiology 50: 64-68.

78. Mahara, Y., Kudo, A. (1995). "Plutonium released by the Nagasaki A-bomb: Mobility in the Environment." Applied Radiation and Isotopes 46(11): 1191-1201.

79. Manthey, J. A., Tisserat, B., Crowley, D. E. (1996). "Root responses of sterile-grown onion plants to iron deficiency." Journal of Plant Nutrition 19(1): 145-161.

80. Marschner, H. (1995). Mineral Nutrition of Higher Plants. London, UK, Academic Press Limited.

81. MARSSIM (2001). Multi-Agency Radiation Surveys and Site Investigation Manual (MARSSIM). DOD, DOE, EPA and NRC, National Technical Information Service (NTIS). NTIS Reference Number: PB97-117659.

82. McConnell, J. W., Rogers, R. D., Jastrow, J. D., Cline, S. R., Findlay, M. W., Davis, E. C., Wickliff Hicks, D. S., Sanford, W. E., Sullivan, T. M., Neilson, R. M., Brey, R. R., Fuhrmann, M., Larson, I. L., Rogers, J. W., Hilton, L. D. (1998). Low-Level Data Base Development Program, NRC.

83. McIntyre, P. F. (1987). 1987 Monitoring Report for the Defense Waste Lysimeters. Aiken, SC, Savannah River Laboratory.

84. Milyukova, M. S. G., N.I.; Sentyurin, L.G.; Sklyarenko, I.S. (1969). Analytical chemistry of plutonium. Ann Arbor, MI, Ann Arbor-Humprhrey Science Publishers.

85. Mori, S., Kiyomiya, S., Nakanishi, H., Ishioka, N. S., Watanabe, S., Osa, A., Matsuhashi, S., Hashimoto, S., Sekine, T., Uchida, H., Nishiyama, S., Tsudaka, H., Tsuji, A. (2000). "Visualization of ^{15}O-Water Flow in Tomato and Rice in the Light and Dark Using a Positron-Emitting Tracer Imaging System (PETIS)." Soil Sciences and Plant Nutrition 46(4): 975-979.

86. Neu, M. P. (2000). "Siderophore-mediated chemistry and microbial uptake of plutonium." Los Alamos Science(26): 416-418.

87. Neu, M. P., C. E. Ruggiero, A. J. Francis. 2002. Bioinorganic Chemistry of Plutonium and Interactions of Plutonium with Microorganisms and Plants. In. D. C. Hoffman, pp. 169-211. Advances in Plutonium Chemistry, 1967–2000., LaGrange Park, IL, Am. Nucl. Soc, Amarillo, TX University Research Alliance.

88. Neu, M. P., Matonic, J. H., Ruggiero, C. E. and Scott, B. L. (2000). "Structural characterization of a plutonium(IV) siderophore complex: Single-crystal structure of Pu-desferrioxamine E." Angewandte Chemie-International Edition 39(8): 1442.

89. Nisbet, A. F., Shaw, S. (1994). "Summary of a 5-Year Lysimeter Study on the Time-Dependent Transfer of ^{137}Cs, ^{90}Sr, ^{239}Pu, ^{240}Pu and ^{241}Am to Crops from 3 Contrasting Soil Types .2. Distribution between Different Plant-Parts." Journal of Environmental Radioactivity 23(2): 171-187.

90. Nitsche, H., Silva, R. J. (1996). "Investigation of the carbonate complexation of Pu(IV) in aqueous solution." Radiochimica Acta 72(2): 65-72.

91. Ohnuki, T., Yoshida, T., Ozaki, T., Kozai, N., Sakamoto, F., Nankawa, T., Suzuki, Y., Francis, A. J. (2007). "Chemical speciation and association of plutonium with bacteria, kaolinite clay, and their mixture." Environmental Science & Technology 41(9): 3134-3139.

92. Ohya, T., Tanoi, K., Hamada, Y., Okabe, H., Rai, H., Hojo, J., Suzuki, K., Naknishi, T. M. (2008). "An Analysis of Long Distance Transport in the Soybean Stem Using $H_2{}^{15}O$." Plant Cell Physiology 49(5): 718-729.

93. P. Wadey, G. Shaw, Bell, J. N. B.. "Radionuclide Transport above a Near-Surface Water Table: III. Soil Migration and Crop Uptake of Three Gamma-Emitting Radionuclides, 1990 to 1993." Journal of Environmental Quality (2001) 30(4): p. 1341-1353.

94. Pentreath, R. J. (1995). "The analysis of Pu in environmental samples: a brief historical perspective." Applied Radiation and Isotopes 46(11): 1279-1285.

95. Peuke, A. D., Rokitta, M., Zimmermann, U., Schreiber, L., Haase, A. (2001). "Simultaneous measurement of water flow velocity and solute transport in xylem and phloem of adult plants of Ricinus communis over a daily time course by nuclear magnetic resonance spectrometry." Plant Cell and Environment 24(5): 491-503.

96. Pinder, J. E., McLeod, K. W., Adriano, D. C., Corey, J. C., Boni, A. L. (1990). "Atmospheric Deposition, Resuspension, and Root Uptake of Pu in Corn and Other Grain-Producing Agroecosystems near a Nuclear-Fuel Facility." Health Physics 59(6): 853-867.

97. Pinton, R., Zeno Varanini, Paolo Nannipieri, Ed. (2007). The Rhizosphere: Biochemistry and Organic Substances at the Soil-Plant Interfaces. Boca Raton, FL, CRC Press.

98. Price, K. R. (1974). Tumbleweed and Cheatgrass Uptake of Transuranium Elements Applied to Soil as Organic Complexes. Richland, WA, Battelle Pacific Northwest Laboratory.

99. Reichard, P. U., Kretzschmar, R., Kraemer, S. M. (2007). "Dissolution mechanisms of goethite in the presence of siderophores and organic acids." Geochimica Et Cosmochimica Acta 71(23): 5635-5650.

100. Rhodes, R. (1986). The making of the atomic bomb. New York, NY, Simon & Schuster.

101. Romheld, V., Marschner, H. (1986). "Evidence of specific uptake system for iron phytosiderophores in roots of grasses." Plant Physiology 80: 175-180.

102. Ruggiero, C. E., Matonic, J. H., Reilly, S. D., Neu, M. P. (2002). "Dissolution of plutonium(IV) hydroxide by desferrioxamine siderophores and simple organic chelators." Inorganic Chemistry 41(14): 3593-3595.

103. Ruggiero, C. E., Twary, S., Deladurantaye, E., Gordon, J., Duran, B. (2004). Phytosiderophore effects on subsurface actinide contaminants: potential for phytostabilization and phytoextraction, LANL [PowerPoint presentation] Pu Futures, US Department of Energy, Office of Biological and Environmental Research.

104. Ruggiero, C. E.; Matonic, J. H.; Reilly, S. D.; Neu, M. P. Dissolution of plutonium(IV) hydroxide by desferrioxamine siderophores and simple organic chelators. Inorg. Chem. 2002, 41(14), 3593-3595.

105. Salbu, B., Skipperud, L., Germain, P., Guegueniat, P., Strand, P., Lind, O. C., Christensen, G. (2003). "Radionuclide speciation in effluent from La Hague reprocessing plant in France." Health Physics 85(3): 311-322.

106. Salt, D. E., Blaylock, M., Kumar, N., Dushenkov, V., Ensley, B. D., Chet, I., Raskin, I. (1995). "Phytoremediation - a Novel Strategy for the Removal of Toxic Metals from the Environment Using Plants." Bio-Technology 13(5): 468-474.

107. Sanford, W. E., Larsen, I. L., McConnell, J. W., Rogers, R. D. (1998). "Upward migration of radio-cesium and strontium in a sand-filled lysimeter." Journal of Environmental Radioactivity 41(2): 147-162.

108. Schaaf, G., Ludewig, U., Erenoglu, B. E., Mori, S., Kitahara, T., von Wiren, N. (2004). "ZmYS1 functions as a proton-coupled symporter for phytosiderophore- and nicotianamine-chelated metals." Journal of Biological Chemistry 279(10): 9091-9096.

109. Smith, D. K., Williams, R. W. (2005). "The dynamic movement of plutonium in an underground nuclear test with implications for the contamination of groundwater." Journal of Radioanalytical and Nuclear Chemistry 263(2): 281-285.

110. Sokolik, G. A., Ivanova, T. G., Leinova, S. L., Ovsiannikova, S. V., Kimlenko, I. M. (2001). "Migration ability of radionuclides in soil-vegetation cover of Belarus after Chernobyl accident." Environment International 26(3): 183-187.

111. Sokolik, G. A., Ovsiannikova, S. V., Ivanova, T. G., Leinova, S. L. (2004). "Soil-plant transfer of plutonium and americium in contaminated regions of Belarus after the Chernobyl catastrophe." Environment International 30(7): 939-947.

112. Sperry, J. S., Stiller, V., Hacke, U. G. (2003). "Xylem hydraulics and the soil-plant-atmosphere continuum: Opportunities and unresolved issues." Agronomy Journal 95(6): 1362-1370.

113. Steudle, E. (2000). "Water uptake by roots: effects of water deficit." Journal of Experimental Botany 51(350): 1531-1542.

114. Suzuki, M., Takahashi, M., Tsukamoto, T., Watanabe, S., Matsuhashi, S., Yazaki, J., Kishimoto, N., Kikuchi, S., Nakanishi, H., Mori, S., Nishizawa, N. K. (2006). "Biosynthesis and secretion of mugineic acid family phytosiderophores in zinc-deficient barley." Plant Journal 48(1): 85-97.

115. Suzuki, M., Tsukamoto, T., Takahashi, M., Nakanishi, H., Mori, S., Nishizawa, N. (2006). "The contribution of Mugineic acids in transport and absorption of Zn in graminaceous plants - Tracer Experiments using PETIS method." Plant and Cell Physiology 47: S156-S156.

116. Thomas, R., W., Healy, J. W. (1976). An appraisal of available information on uptake by plants of transplutonium elements and neptunium. Los Alamos, NM, LANL.

117. Thompson, J. L. (1989). "Actinide behavior on crushed rock columns." Journal of Radioanalytical and Nuclear Chemistry 130(2): 353-364.

118. Thompson, S. W.; Molz, F. J.; Fjeld, R. A.; Kaplan, D. I. (2009). “Plutonium uptake velocity in *Zea mays* (corn) and implications for plant uptake of Pu in the root zone.” Journal of Radioanalytical and Nuclear Chemistry 282, 439-442.

119. Uren, N. C. (2007). Types, amounts, and possible functions of compounds released into the rhizosphere by soil-grown plants. The Rhizosphere: Biochemistry and Organic Substances At The Soil Plant Interface. Pinton, R. Boca Raton, FL, CRC Press.

120. Von Wiren, N., Romheld, V., Morel, J. L., Guckert, A.; Marschner, H. (1993). "Influence of microorganisms on iron acquisition in maize." Soil Biology and Biochemistry 25(3): 371-376.

121. Vyas, B. N., Mistry, K. B. (1981). "Influence of Clay Mineral Type and Organic-Matter Content on the Uptake of ^{239}Pu and ^{241}Am by Plants." Plant and Soil 59(1): 75-82.

122. Walker, F. W., Parrington, J. R., Feiner, F. (1989). Nuclides and Isotopes. San Jose, CA, General Electric Company.

123. Walter, A., Romheld, V., Marschner, H., Crowley, D. E. (1994). "Iron Nutrition of Cucumber and Maize - Effect of Pseudomonas-Putida Yc-3 and Its Siderophore." Soil Biology & Biochemistry 26(8): 1023-1031.

124. Wang, Y., Brown, H. N., Crowley, D. E., Szaniszlo, P. J. (1993). "Evidence for Direct Utilization of a Siderophore, Ferrioxamine-B, in Axenically Grown Cucumber." Plant Cell and Environment 16(5): 579-585.

125. Ward, J. W., Brett Lahner, Elena Yakubova, David E. Salt, Kashchandra G. Ragothama (2008). "The Effect of Iron on the Primary Root Elongation of Arabidopsis during Phosphate Deficiency." Plant Physiology 147: 1181-1191.

126. Wenzel, C. L., Margaret E. McCully, Martin J. Canny (1989). "Development of Water Conducting Capacity in the Root Systems of Corn and Some Other C4 Grasses." Plant Physiology 89: 1094-1101.

127. WGBH (1999). Race for the Superbomb: Nuclear Weapons Test Map. THE AMERICAN EXPERIENCE Tovares, J., PBS.

128. Whicker, F. W., Hinton, T. G., Orlandini, K. A., Clark, S. B. (1999). "Uptake of natural and anthropogenic actinides in vegetable crops grown on a contaminated lake bed." Journal of Environmental Radioactivity 45(1): 1-12.

129. Wildung, R. E., Garland, T. R. (1974). "Influence of Soil Plutonium Concentration on Plutonium Uptake and Distribution in Shoots and Roots of Barley." Journal of Agricultural and Food Chemistry 22(5): 836-838.

130. Wolff-Boenisch, D., Traina, S. J. (2007). "The effect of desferrioxamine B on the desorption of U(VI) from Georgia kaolinite KGa-1b and its ligand-promoted dissolution at pH 6 and 25 degrees C." Chemical Geology 242(1-2): 278-287.

131. Wolff-Boenisch, D., Trama, S. J. (2006). "A comparative study of the effect of desferrioxamine B, oxalic acid, and Na-alginate on the desorption of U(VI) from goethite at pH 6 and 5 degrees C." Geochimica Et Cosmochimica Acta 70(17): 4356-4366.

132. Yehuda, Z., Shenker, M., Romheld, V., Marschner, H., Hadar, Y., Chen, Y. N. (1996). "The role of ligand exchange in the uptake of iron from microbial siderophores by graminaceous plants." Plant Physiology 112(3): 1273-1280.

133. Yoder, C. K., Nowak, R. S. (1999). "Hydraulic lift among native plant species in the Mojave Desert." Plant and Soil 215: 93-102.

134. Yoshida, S., Muramatsu, Y., Yamazaki, S., Ban-Nai, T. (2007). "Distribution of nuclear bomb Pu in Nishiyama area, Nagasaki, estimated by accurate and precise determination of $^{240}Pu/^{239}Pu$ ratio in soils." Journal of Environmental Radioactivity 96(1-3): 85-93.